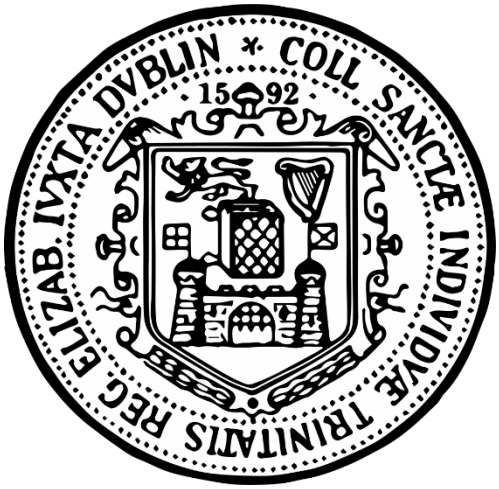

Jennifer Gansau, B.Sc., M.Sc.

On the Effect of Primed Cellular Microcapsules and pH Neutralizing Biomaterials to Augment Regeneration of the Intervertebral Disc

---

Trinity College Dublin, 2020

A thesis submitted to the University of Dublin in partial fulfilment of the requirements for the degree of

Doctor in Philosophy

Supervisor: Professor Conor T. Buckley

Internal examiner: Professor Triona Lally

External examiner: Dr. Stephen Richardson

DECLARATION

I declare that this thesis has not been submitted as an exercise for a degree at this or any other university and is entirely my own work. I agree to deposit this thesis in the University's open access institutional repository or allow the library to do so on my behalf, subject to Irish Copyright Legislation and Trinity College Library conditions of use and acknowledgement.

_____

Jennifer Gansau

Dublin, 2020

SUMMARY

One of the most common topics of research worldwide for medical health care is low back pain (LBP). It is widely accepted that LBP is associated with degeneration of the intervertebral disc (IVD), the shock absorbent soft tissue between the vertebral bodies. Degenerative discs disease (DDD) is characterised by increased cell death and loss in structural extracellular matrix (ECM) molecules within the nucleus pulposus (NP) tissue, the highly hydrated gelatinous tissue in the centre of the IVD. Being an avascular structure, the nutrient supply within the IVD is limited, resulting in a compromised microenvironment with limited oxygen and glucose, and a low pH. These can drop even lower during the progression of disc degeneration resulting in further cell death and loss of structural integrity. Cell-based therapy has been proposed to re-establish the natural cell population within the disc and subsequentially re-produce matrix molecules for a healthy IVD. Some success has been made using NP cells, yet shortcomings for a long-term solution remain such as poor cell yield post-isolation, limited matrix forming capacities, and cell death and leakage during re-injections. The overall objective of this thesis was to develop an injectable biomaterial that successfully delivers cells into the disc while preserving their capability to sustain the harsh microenvironment characteristic of degenerative disc. Specifically, this thesis investigates i) technical challenges associated with intradiscal injections of cells (i.e. cell damage due to shear forces) by establishing a material for consistent delivery into the disc and ii) a strategy to overcome the microenvironmental limitations found in degenerated disc, with specific focus on the acidic pH.

The thesis began by characterizing the electrohydrodynamic spraying (EHDS) technology for microencapsulation of cells into ionically crosslinked alginate hydrogels. Adjusting the operation settings, injectable microcapsules (μCaps) were successfully fabricated with entrapped cells in an optimised seeding density for matrix accumulation. These were further capable to sustain shear stress during injection through a needle. Thereafter, a viscous bulking agent was developed using a fibrin-hydrogel base to enhance μCap delivery into the highly pressurized IVD. A fibrin-hyaluronic acid (HA) blend was found to induce increased proliferation

and matrix deposition of cells, making the advantages of the bulking agent two-fold: i) enhanced μCap delivery into the disc and ii) promoted disc-like tissue formation for better regeneration potential.

The thesis continued by exploring a way to improve cellular response to the acidic environment of the IVD. Three different pH conditions (pH 7.1, 6.8 and 6.5), representative for different stages of disc degeneration, were investigated using articular chondrocytes (AC) and bone marrow-derived stem cells (BMSC) with and without priming using TGF-β3. By priming the cells, the detrimental pH effect observed on cells without priming was overcome with significantly improved viability and ECM levels for both cell types in all pH levels investigated. Finally, the challenging acidic microenvironment was altered using pH neutralizing antacids. After applying EHDS to fabricate antacid microcapsules, efficient pH increase was found using $CaCO_3$ nanoparticles inside alginate μCaps with a slow release kinetics for long lasting neutralization effects. Exploring the established hybrid-hydrogel containing EHDS fabricated cellular μCaps (AC or BMSC) and $CaCO_3$ μCaps within the fibrin-HA bulking gel, within a disc explant model, elevation of core pH was successfully established. Moreover, improved matrix retention within the disc tissue was accomplished with both cell types, AC and BMSC.

To conclude, this thesis describes a novel approach to develop an injectable material for minimally invasive treatment of the degenerated IVD. A hybrid hydrogel was established containing i) μCaps with primed cells to deposit *de novo* matrix into the acidic microenvironment of the disc and aid resident cells to re-establish their potential by paracrine signalling, ii) μCaps containing $CaCO_3$ nanoparticles to elevate local pH and subsequentially enhance cell viability and matrix accumulation of resident cells and iii) a fibrin-HA bulking agent to facilitate μCap deposition into the IVD while promoting cell proliferation and disc-like matrix accumulation.

ACKNOWLEDGEMENTS

The past 5 years of my life have been a difficult but exciting, confusing but enlightening and long but fast journey. As much demanding it was scientifically, it was probably even more challenging emotionally/mentally, where many people were a great support in one way or another.

First of all:

To my always supporting supervisor Professor Conor Buckley:

Thank you so much for your guidance and mentorship during this time. I know it has not always been easy and cheerful with me, but you kept your faith in me even at times where I lost it myself and I will always be grateful for this. Your enthusiasm and passion for the research was always inspiring (and annoying at times….) and made me a better researcher. I can't even put into words how thankful I am for your patience and support during some dark days. But this encouragement carried me over the finish line in the end. I couldn't have asked for a better supervisor and mentor.

To my 'PhD mommy' at early days Dr. Masooma Naqvi

You have probably been the most important part during the first stage of my PhD. You taught me how to walk, in the kindest and most patient way possible and welcomed me into the lab with all your heart. Thank you for all the hours of solving problems, discussing ideas and listening when I was near another breaking point. You have guided me through the first year and made me strong enough for the years that followed.

To current and past Buckley Lab members

I also want to express my gratitude to the whole Buckley lab (past and current) for all their help. With a special thank you to i) Chiara Borrelli- you are some woman! Head strong and enthusiastic about science! Thank you for all your help in the lab, the stimulating discussions, deliberating cursing and swearing and enjoyable laughs! ii) Dr. Leyla Žilić – your mental support and long chats were such a huge help at difficult times. Thanks for listening and cheering me up! Iii) Emily McDonnell- you are an incredible person with a lot of talent! Thank you so much for your help during my last stage of this thesis. Without your design skills, fast learning capabilities and readiness (while always smiling), I definitely wouldn't have been able to finish this. I am so grateful for everything you have done for me and hope I can return this somehow someday.

To the best 'Squad' someone could wish for doing a PhD- Dr. Dinorath Olvera- Ramos and Dr. Susan Critchley

You two have always been able to brighten the day in and outside the lab. I am so grateful that we spend almost the whole time together, fighting for survival, sharing good and bad moments to lift each other up. Thank you, Susan, your sarcasm was always a reason to laugh even tho I didn't always get it. But sure look. And my dearest Dinorath: You have become my best friend of all times. The chats with you are always stimulating, inspiring, enjoyable and funny. Your optimism, happy spirits and endless amount of positive energy always give me a boost even when you don't even notice it. You have seen me at my highest highs and lowest lows and were always there with good advice to save the situation, eventually pulling me out of that dark place. Without you, I would have often stayed lost for so much longer. Thank you for just being you.

To my favourite couple and housemates (soon to be Dr) Julia Fernández-Pérez and Stefan Scheurer

Living with you guys has been (and still is) one of the luckiest things that happened to me in Dublin. Getting on with people you live AND work, therefore spending a lot of time together, without killing each other is a scary thing and can go quite wrong. But it didn't. Thank you for all the refreshing discussions at lunch in TBSI and later over dinner at home (or at breakfast in the morning). Having a healthy home-environment is so important to recover from a long day at work. Especially thank you to Julia. You helped me out in the lab multiple times as well as you were always my "emergency contact" (literally speaking as well as metaphorically). You have probably seen my tears the most often and were always right there for a big, warm Spanish hug. Wouldn't have wanted anyone else as my roomies.

To all my great friends from the 'other labs'

My greatest gratitude to the people, who laughed with me, researched with me, travelled with me and simply made my PhD life such and enjoyable experience at most times. Thank you to Dr. Tommy, (soon to be Dr) Pedro, Dr Andy and Ian. You were a source of inventiveness to solve any problem and could fill the days with funny anecdotes inside and outside the walls of TBSI.

To my amazing sharp proof-readers who spend hours bringing my English up to the next level

Thank you, Dr. Leyla Žilić! I really appreciate all the time you spend on my literature review! Thank you to Dr. Emma Fitzpatrick! Not only for proofreading sections of this work but also for becoming such a good friend! Your support in the last years was invaluable and I really miss our early morning tea + chats. They gave me a good mentally push into the day. My greatest gratitude also to Dr. Simon Carroll. You are the person I know the longest in this lab. Getting to know you better and listening to some of your interesting points of views towards life in general has often left me thinking. Project "FJL" has been a life saviour at times. And while you not only

a remarkable friend, you are also an amazing colleague. Thank you for always being available to help with whatever it is! Being it a small fix of screwing something, a bigger fix of an oven or solving biggest computer issues. You always take time to help and get people back on track. You are awesome! Thank you for all your help and support over the years!

To the most incredible Volleyball team

You guys have welcomed me into our midst from my year one onwards. The training and matchdays were always able to get my mind off and just focus on another love of my life: Volleyball. A special thank you to Dr. Stephany Micallef (Steph) and Katie Ward for supporting me on court as well as off court. You guys always listened to the stuff I brought in, made me forget about it and helped me to move on. Thanks to all of ye guys for being a small family to me and keeping me sane.

To my "friends over in Parsons"

Thank you for the fun times, running in the evenings and racing, cycling or surfing at weekends. A special thanks to Dr. Nicolas Baudin (Nico), who fixed my electrosprayer several times and was always up for some laughs. To Dr. Maeve O'Neill and Dr. Jason Botha, who kept pushing the running, keeping us fit – ish always smiling. Thank you, guys, for providing me refuge in your office to write this thesis in times of great need.

To my closest and furthest of all- my mom, dad and sis

Thank you for all your endless support not only the last five years but also before. I know, seeing the "baby of the family" growing its own wings and fly off to another country has not been easy (especially to you, mom). But despite being 1302.05km apart, you have always given me the feeling of comfort and safety. Thank you for being the greatest family!

In German:

An meine Nächsten und doch am weitesten entfernten von allen – meine Mama, mein Papa und meine Schwester

Danke für eure unendliche Unterstützung nicht nur während der letzen fünf Jahre, sondern noch davor. Mir ist bewusst, dass zu zu sehen, wie dem Nesthäckchen Flügel wachsen und in ein anderen Land fliegt, war nicht leicht (vor allem nicht für dich, Mama). Aber auch wenn 1302,05 km von einander entfernt, habt ihr mir immer ein Gefühl von Geborgenheit und Sicherheit gegeben. Danke ´, dass ihr die krasseste, super mega, geilste Familie seid.

THANK GOD, IT'S DONE!

TABLE OF CONTENT

LIST OF FIGURES

LIST OF TABLES

NOMENCLATURE

µCap	microcapsule
AC	Articular chondrocytes
ADCT	autologous disc cell transplantation
ADSCs	adipose-derived mesenchymal stem cells
AF	Annulus Fibrosus
AmpB	amphotericin B
ANC	acid-neutralizing capacity
ASIC	acid sensing ion channel
ATP	adenosine triphosphate
bFGF	basic fibroblast growth factor
BMP	Bone morphogenetic protein
BMSC	bone marrow-derived stem cells
BSA	bovine serum albumin
CaSR	calcium-sensing receptor
CDM	chemically defined medium
CEP	cartilaginous endplates
Col1	collagen type I
Col2	collagen type II
DAPI	4′,6-diamidino-2-phenylindole
DDD	degenerative disc disease
DMEM	Dulbecco's Modified Eagles Medium
DMMB	dimethylmethylene blue dye-binding assay
DNA	Deoxyribonucleic acid
ECM	extracellular matrix
EHDS	Electrohydrodynamic spraying
EP	endplates
EthD-1	ethidium homodimer-1
F	fibrin
FBS	foetal bovine serum
FC	fibrin–collagen blend
FCH	fibrin–collagen–hyaluronic acid blend
FH	Fibrin-hyaluronic acid blend
FH-2.5	Fibrin-hyaluronic acid blend with 2.5 mg/mL HA content
FH-5	Fibrin-hyaluronic acid blend with 5 mg/mL HA content
GCR	glucose consumption rates
GDF	growth and differentiation factor
HA	hyaluronic acid
hg-DMEM	High glucose Dulbecco's Modified Eagles Medium
HIF	hypoxia-inducible factor
HMW	High molecular weight
IDCT	injectable discogenic cell therapy
ITS	insulin-transferrin-selenium
IVD	Intervertebral Disc
LacA	Lactic acid / Lactate
LBP	Low Back Pain
lg-DMEM	low glucose Dulbecco's Modified Eagles Medium
LPR	lactate production rate
MMP	matrix metalloproteinase
MSCs	Mesenchymal stem cells
NAD+	Nicotinamide adenine dinucleotide
NC	notochordal cells
nd	not detectable
NP	Nucleus Pulposus
NPMSC	Nucleus Pulposus Mesenchymal stem cells
OA	osteoarthritis
OCR	Oxygen consumption rate
PBS	phosphate buffered saline
PCM	pericellular matrix
PEG	Polyethylene glycol
PEG	polyethylene glycol
PFA	paraformaldehyde
PGs	proteoglycans
SCDM	supplemented chemically defined medium
SD	standard deviation
sGAG	Sulphated glycosaminoglycans
TCA	tricarboxylic acid

TGF	transforming growth factor
TonEBP	tonicity enhancer-binding protein
UPW	ultra-pure water

PUBLICATIONS

First author publications

- **GANSAU, J**., KELLY, L. & BUCKLEY, C. T. 2018. *Influence of key processing parameters and seeding density effects of microencapsulated chondrocytes fabricated using electrohydrodynamic spraying*. Biofabrication, 10, 035011.

- **GANSAU, J**. & BUCKLEY, C. T. 2018. *Incorporation of Collagen and Hyaluronic Acid to Enhance the Bioactivity of Fibrin-Based Hydrogels for Nucleus Pulposus Regeneration*. J Funct Biomater, 9.

Under Review

- **GANSAU, J**. & BUCKLEY, C. T. (submitted 2019) *Priming as a means to mitigate acidic pH effects on bone marrow-derived stem cells and articular chondrocytes cultured under intervertebral disc-like conditions.* J Tissue Eng Regen Med

Co-author publications

- NAQVI, S. M., VEDICHERLA, S., **GANSAU, J**., MCINTYRE, T., DOHERTY, M. & BUCKLEY, C. T. 2016. *Living Cell Factories - Electrosprayed Microcapsules and Microcarriers for Minimally Invasive Delivery*. Adv Mater, 28, 5662-71.

- NAQVI, S. M., **GANSAU, J**. & BUCKLEY, C. T. 2018. *Priming and cryopreservation of microencapsulated marrow stromal cells as a strategy for intervertebral disc regeneration.* Biomed Mater, 13, 034106.

- NAQVI, S. M., **GANSAU, J**., GIBBONS, D. & BUCKLEY, C. T. 2019. *In vitro co-culture and ex vivo organ culture assessment of primed and cryopreserved stromal cell microcapsules for intervertebral disc regeneration*. Eur Cell Mater, 37, 134-152.

Conference abstracts

- GANSAU, J. & BUCKLEY, C. T., *Injectable Biomimetic Hydrogels for Nucleus Pulposus Regeneration*, 21st Annual Conference of the Section of Bioengineering of the Royal Academy of Medicine in Ireland, January 2015, Dublin, Ireland

- GANSAU, J. & BUCKLEY, C. T., *Modulating fibrinogen concentration to enhance nucleus pulposus-like tissue formation of articular chondrocytes*, 22nd Annual Conference of the Section of Bioengineering of the Royal Academy of Medicine in Ireland, January 2016, Galway, Ireland.

- GANSAU, J. & BUCKLEY, C. T., *Effect of fibrin concentration on matrix deposition capacity of articular chondrocytes for nucleus pulposus regeneration*, Tissue Engineering and Regenerative Medicine International Society (TERMIS), European Chapter, June 2016, Uppsala, Sweden

- GANSAU, J. & BUCKLEY, C. T., *Biomimetic Fibrin-Based Hydrogels for Intervertebral Disc Regeneration*, 3rd Annual Matrix Biology Ireland Meeting (MBI), November 2016, Galway, Ireland

- GANSAU, J. & BUCKLEY, C. T., *Electrohydrodynamic Spraying – Investigation of key processing parameters for fabrication of injectable cellular microcapsules*, 1st European Society of Engineering and Medicine (ESEM) Web Conference, December 2016

- GANSAU, J. & BUCKLEY, C. T., *Chondrocyte-loaded microcapsules for minimally invasive regeneration of the nucleus pulposus*, 23rd Annual Conference of the Section of Bioengineering of the Royal Academy of Medicine in Ireland, January 2017, Belfast, U.K.

- GANSAU, J. & BUCKLEY, C. T., *Injectable Cell- Loaded Microcapsules as a Potential Strategy for Nucleus Pulposus Regeneration*, 6th International Congress on Biotechnologies for Spinal Surgery (BioSpine 6), April 2017, Berlin, Germany

- GANSAU, J. & BUCKLEY, C. T., *Survival and Matrix Accumulation of Nucleus pulposus, chondrocytes and stem cells in a low pH intervertebral disc-like Microenvironment*, 24th Annual Conference of the Section of Bioengineering of the Royal Academy of Medicine in Ireland, January 2018, Dublin, Ireland

- GANSAU, J. & BUCKLEY, C. T., *Investigation of Various Cell Types for Intervertebral Disc Repair under Disc Degenerative Culture Conditions*, 8th World Congress of Biomechanics (WCB), July 2018, Dublin, Ireland

- GANSAU, J. & BUCKLEY, C. T., *The Effect of Priming on Matrix Accumulation and Metabolism of Stem Cells and Chondrocytes in altered Intervertebral Disc- like pH Conditions*, 26th European Orthopaedic Research Society (EORS), September 2018, Galway, Ireland

- GANSAU, J., MCDONNELL, E. E. & BUCKLEY, C. T., *Altering the Local Acidic Microenvironment of the Degenerated Intervertebral Disc using Injectable Antacid Microcapsules*, ORS PSRS 5th International Spine Research Symposium, November 2019, Skytop, Pennsylvania, USA

CHAPTER 1
INTRODUCTION

1.1. Intervertebral disc degeneration – a burden of modern society

IVD degeneration often manifests itself as pain in the lumbar region of the spine. Naturally, disc degeneration can occur with age, but risk factors including smoking, obesity and injuries can accelerate the degenerative process. Consequentially the majority of the population will be affected, with 70% experiencing LBP at least once during their life (Bogduk et al., 2013, Wilkens et al., 2013). Annual costs of $500 billion in the US and £12 billion in the UK, makes LBP one of the most expensive disorders worldwide, indicating evidently the clinical need for a more sufficient therapy (Dieleman et al., 2016, Maniadakis and Gray, 2000).

The IVD is composed of three main compartments: the central NP, a highly gelatinous, collagen type II (Col2)-rich tissue (Inoue, 1981); the annulus fibrosus (AF), a fibrocartilaginous tissue which wraps around the NP in concentric rings, and the cartilaginous endplates (CEP), which form the interface on the top and bottom between the soft tissue and the vertebral bodies within the spine. Water imbibing proteoglycans (PGs) such as aggrecan and biglycan maintain the hydration of the NP causing the high osmotic pressure occurring within the IVD (Singh et al., 2009). As disc degenerating progresses, the PG content diminishes and results in subsequentially critical disc dehydration and disc height loss. Moreover, nutritional deprivation during disc degeneration is a critical issue. Nutrient supply into the central NP occurs predominantly by diffusion through the AF and blood vessels, which originate in the vertebral body and traverse the superficial region of the CEPs. Yet, during disc degeneration, osmotic pressure decreases due to the loss of PGs, and their water imbibing properties result in inhibited nutrient diffusion. Additionally, CEPs calcify, reducing the number of blood vessels, furthermore limiting nutrient flow (Boos et al., 2002, Benneker et al., 2005). As a result, not only does nutrient deficiency occur, but results in the accumulation of cellular waste products such as lactic acid (LacA) (Huang et al., 2014). With reduced availability of two key nutrients (oxygen and glucose), and a decrease

in extracellular pH due to the accumulation of LacA, the metabolic activity of the cells decreases (Katz et al., 1986, Urban et al., 1982). It has been shown previously that a drop in glucose levels below 0.5 mmol/L, even for a short period of time, can initiate cell death. Equally, a pH below 6.4 can have detrimental effects on cell viability (Bibby and Urban, 2004, Horner and Urban, 2001). In addition, it has been demonstrated that under oxygen conditions below 5%, cellular activity and matrix depositing capacities are drastically inhibited (Horner and Urban, 2001, Ishihara and Urban, 1999). The impaired cell number in combination with increased release of catabolic enzymes leads to an imbalance of matrix anabolism vs. catabolism (the ratio of which causes a disruption of tissue integrity and stability within the disc tissue) (Kadow et al., 2015). Due to the reduction of important structure molecules such as collagens and PGs along with disc dehydration and decreasing disc heights, the mechanical loading on the discs increase (Raj, 2008). If the load exceeds a critical threshold, the tissue collapses and starts to form fissures and tears within the AF. This can cause disc herniation, which is characterised by leakage of NP tissue, followed by a prolapse and NP extrusion, where the NP tissue breaks through the AF and eventually pressurises the adjacent spinal nerve cord, called sequestration (Figure 1-1 A and B). Within MRI images, mild disc degeneration is recognized by a grey to black structure within the IVD region with a bulging region towards the spinal cord (Figure 1-1 C). Conventional treatments such as physiotherapy or pain medication are a short-term solution for many patients, yet the origin of the pain, disc degeneration, is a long-term problem and cannot be resolved by this approach. Other strategies used when severe disc degeneration with bulging disc tissue is diagnosed, involve invasive surgical mid-term solutions such as nucleotomy, spinal fusion or total disc replacement. These approaches do not restore natural biomechanical function and have been found to risk further degeneration of adjacent disc due to elevated mechanical stress (Lee and Choi, 2015). Therefore, it is evident that an alternative approach is needed to promote a long-term solution, perhaps through the avenue of disc regeneration. Cell-based therapies are one such strategy and have been proposed previously to restore disc integrity, and subsequentially promote relief from LBP.

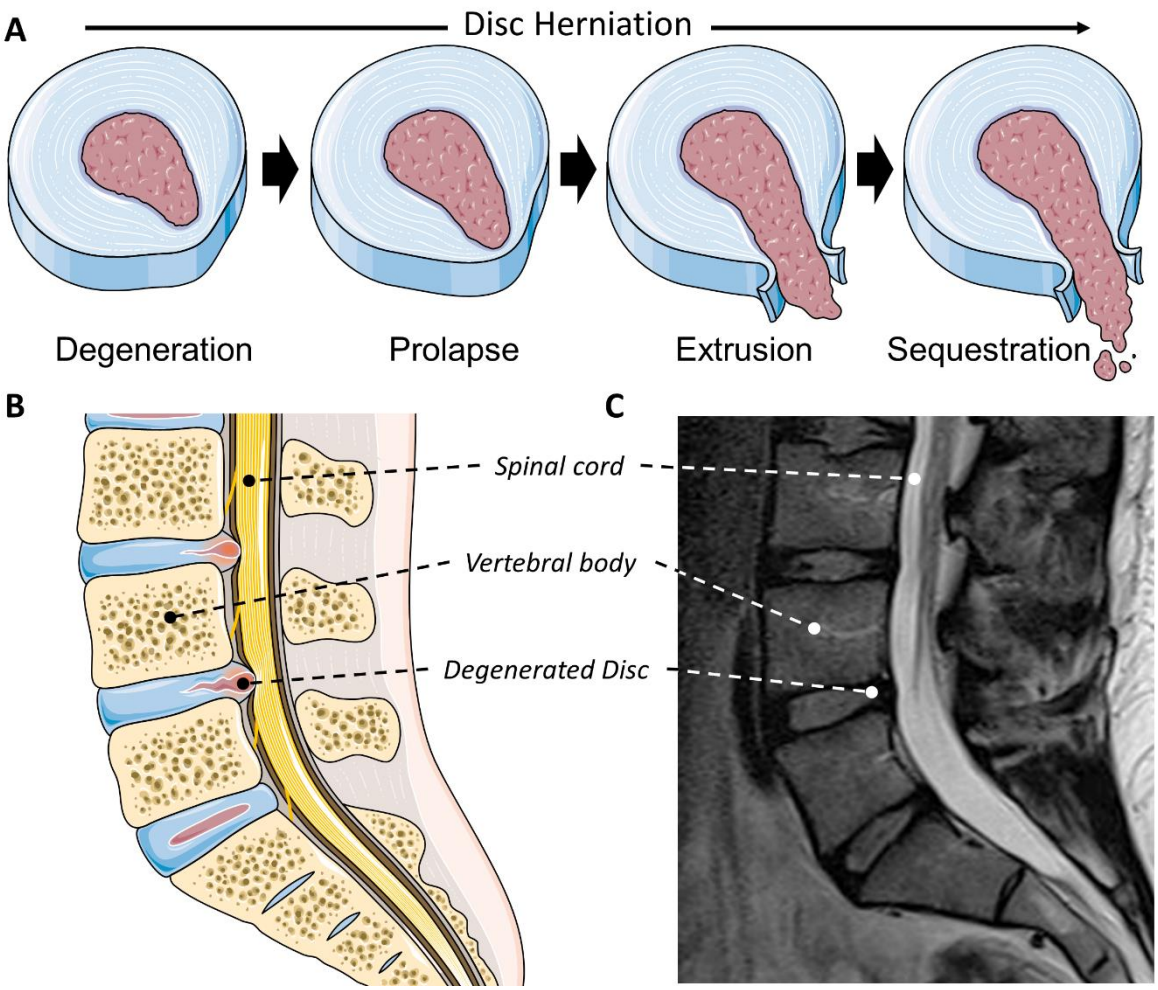

Figure 1-1: Disc degeneration (A) schematic overview of disc herniation progress **(B)** schematic illustration of disc degeneration and the pressurized spinal cord **(C)** MRI image of IVD with mild disc degeneration (personal image of author's spine)

1.2. Cell-based therapies – a promising approach for tissue repair

Cell-based therapy has been suggested for regeneration of several tissue types including cartilage (Park et al., 2018), bone (Hernigou et al., 2016) or cardiac tissue (Zwetsloot et al., 2016). It aims to enhance matrix anabolism by implanting healthy autologous cells inside the diseased tissue and subsequentially restoring tissue function. Autologous isolated cells can be 2D expanded to increase cell number, and consequentially produce a greater amount of total *de novo* matrix. The cell source proposed is highly dependent on the diseased target tissue. For disc regeneration, cells from the NP seem an obvious choice and have been shown to delay

degenerative disc changes after re-implantation in animal models (Okuma et al., 2000, Gruber et al., 2002). However, several limitations are associated with using culture expanded autologous NP cells, including poor cell yield after isolation, limited 2D expansion capacities and risks of tissue damage at the harvest site during cell isolation (Richardson and Hoyland, 2008, Wu et al., 2014, Nomura et al., 2001). Different cell types including ACs and BMSCs have been proposed for NP regeneration (Vedicherla and Buckley, 2017a, Urits et al., 2019). As fully differentiated primary cells, AC show some phenotypical differences to NP cells. However, they are easily accessible and capable of matrix deposition similar to NP tissue, which makes them attractive candidates to be considered for IVD repair. Also, BMSCs possess a high potential for IVD repair and have gained a lot of attention due to their versatility, translatability and accessibility. Moreover, they can differentiate towards a discogenic phenotype in response to microenvironmental or biological cues (Murphy et al., 2013, Richardson et al., 2006).

1.3. Microencapsulation to facilitate minimally invasive cell delivery into the intervertebral disc

Minimally invasive injections through the AF for cell delivery into the NP are also the most obvious approach to minimizing tissue damage during treatment. However, cellular injections are currently accompanied by a number of challenges, such as cell damage due to shear forces, cell leakage during injection and limited control over the target site (Li et al., 2014a, Vadala et al., 2012). One strategy to overcome some of these limitations is the use of biomaterials as a delivery vehicle. Hydrogels are highly hydrated polymers and are therefore suitable for NP regeneration approaches. Moreover, hydrogels provide a 3D network, which support a more natural cell assembly, and have the advantage of biomimetic modifications for improved cellular stimulus (biomechanical or biological) (Vermonden et al., 2008). Two naturally derived biomaterials widely used for biomedical applications include alginate and fibrin. Alginate is a natural anionic and unbranched polysaccharide with mild ionic crosslinking properties using divalent cations such as Ca^{2+}. It is biocompatible and supports the entrapment of different cell

types including NP cells (Chou et al., 2009, Gantenbein-Ritter et al., 2011, Leone et al., 2008) and MSCs (Xu et al., 2008, Ma et al., 2003) where it promotes a rounded, chondrocyte-like cell shape due to a lack of binding sites for cells (Rowley et al., 1999, Andersen et al., 2015). Fibrin, a viscoelastic polymer, naturally formed by an enzymatic reaction of fibrinogen and thrombin, the most important proteins involved in blood clotting. It allows cell-matrix interaction, promotes cell proliferation and migration within the 3D network (Greiling and Clark, 1997, Makogonenko et al., 2002). It has been investigated for disc repair, comparing juvenile chondrocytes with MSCs entrapped within the polymer in a porcine *in vivo* study (Acosta et al., 2011). Despite advantages associated with biomaterials, *in situ* gelling remains a challenge with respect to intradiscal injection (Zeng et al., 2015). Therefore, microencapsulation has been proposed, which involves the entrapment of cells (or different targets) into micron- sized polymeric spheres, which can be injected through a small needle lumen, and is ideal for minimally invasive delivery into the IVD. The advantage of polymer crosslinking prior to injection is three-fold: (i) the crosslinking reaction can be easily tailored before implanting, (ii) the polymer provides a protective shield against shear forces during injection and (iii) it allows more efficient cell delivery to the target site. EHDS is a versatile, one-step approach for microencapsulation (Bock et al., 2012a). During EHDS, a cell laden polymer passes through a small lumen sized needle, which is subjected to a high voltage and consequently positively charges the polymer, which disperses into small droplets (Eagles et al., 2006). Due to an applied potential difference between the needle and collector dish filled with a crosslinking agent, the droplets are drawn towards this crosslinking solution and solidify instantly upon hitting its surface, entrapping cells inside.

1.4. The challenging microenvironment of the degenerated disc and approaches to targeting it for enhanced cell-based therapy

As described above, cell-based therapy for IVD regeneration has huge potential to improve degenerative disc tissue and subsequentially provide a long-term solution for LBP. However, the microenvironment of a degenerated disc is highly compromised (i.e. low O_2, low

glucose, low pH), which inhibits its success. A steep nutrition gradient occurs from the AF towards the NP, resulting in elevated levels of LacA within the central NP. This causes higher matrix acidity, which has been found to be lethal for cells (Bibby and Urban, 2004). This is critical, not only for resident disc cells, but also for any of the cell types suggested for tissue regeneration. BMSCs are highly affected by matrix acidity which results in significant cell death (Wuertz et al., 2009) unless pre-treated using growth factors to initiate differentiation (Grunhagen et al., 2006, Naqvi et al., 2018). Driving BMSC towards a chondrogenic phenotype using TGF-β has been demonstrated to improve matrix deposition and enhance cell viability in a disc like environment (Dashtdar et al., 2011, Naqvi et al., 2019). Nevertheless, the compromised microenvironment remains, affecting resident cells and inhibiting the regeneration progress. Acidity appears to be one of the main challenges, whereby it reduces viability and matrix anabolism. Increasing the local pH therefore may improve cellular capacities and aid in the enhancement of ECM deposition. Multicomponent salts with pH neutralizing properties are called antacids, and are conventionally used against hyper-acidic gastric fluids (Sontag, 1990). They are frequently based on aluminium hydroxide, magnesium hydroxide, calcium carbonate or a combination of these. They typically dissolve in acidic fluids and initiate a neutralization reaction. Microencapsulating of these pH neutralizing salts allows controlled release kinetics for prolonged functionality (Chen et al., 2018). Using antacids to enhance the local microenvironment within the NP may benefit both the resident NP cells and injected cells for autologous cell therapy.

1.5. Objectives

The global objective of this thesis is to develop a suitable biomaterial with properties specifically designed to challenge the microenvironmental difficulties in a degenerated intervertebral disc. Therefore, aiding the regeneration of damaged NP tissue as well as providing cellular support. An overview of the proposed strategy is illustrated in Figure 1-2.

The specific objectives of this thesis are to

i. Explore key processing parameters of EHDS technology in order to minimize microcapsule size and optimize microcapsule shape.
ii. Investigate how altered parameters affect cell viability and what effect seeding density has on cell proliferation and matrix accumulation under *in vitro* culture conditions.
iii. Develop a biomimetic fibrin-based – hydrogel containing ECM derived molecules such as collagen and hyaluronic acid that can be used as a bulking agent to enhance delivery of μCaps into the IVD.
iv. Explore different cell types (ACs and BMSC) in degenerative disc like pH conditions (pH 7.1, 6.8 and 6.5) and their survival capacity as well as matrix accumulation capabilities and assess whether priming using TGF-β3 can mitigate the pH effect on cells.
v. Compare different antacids (such as aluminium hydroxide, calcium carbonate and magnesium hydroxide) in terms of pH neutralization capacities, cytotoxicity and matrix inhibition properties as potential supplement for cell-based therapy of the intervertebral disc.
vi. Verify the *in vitro* findings (from objective i-v) in a disc explant model using caudal bovine discs tissue in simulated degenerative disc conditions (i.e. low O_2, low glucose, high osmolarity and low pH), and compare two proposed cell types for their suitability.

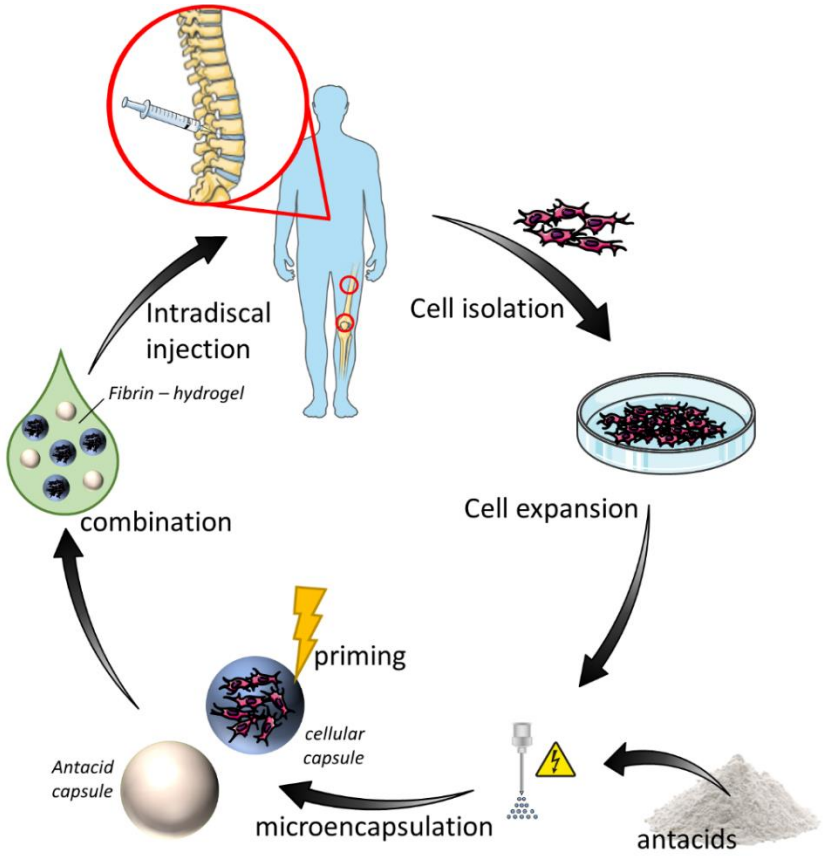

Figure 1-2: Strategy to approach DDD proposed in this thesis. Autologous cells from the bone marrow or the knee joint are isolated and 2D culture expanded. Next, cells and pH neutralizing antacids are encapsulated using EHDS technology to fabricate microcapsules. Cellular µCaps are primed using TGF-β3 to enhance sustainability and matrix accumulation. Lastly, a hybrid gel containing primed cells, antacids and a fibrin-HA blend are injected into the degenerated IVD to promote disc regeneration.

CHAPTER 2
LITERATURE REVIEW

2.1. The anatomy of the intervertebral disc

The IVD is a soft, fibrocartilaginous tissue which is located between two spinal vertebral bodies. It is composed of three main tissues; the NP, AF and CEP (Figure 2-1 A). Each region has a specific composition and therefore contributes to the mechanical function of the spine, such as load transmission and flexibility. The central region of the IVD, the NP, is a highly hydrated gelatinous tissue (Figure 2-1 B), which is composed of water (70-85% of total weight), PGs (30-50% of dry weight) and collagen (20% of dry weight) (Adams and Muir, 1976, Eyre, 1979). The most abundant PG of the NP is aggrecan, but smaller PGs such as biglycan, lumican and decoring can also be found (Roughley, 2004, Feng et al., 2006, Whatley and Wen, 2012). Aggrecan interacts with HA, resulting in the formation of long molecules, which are entrapped between collagen networks. The negatively charged HA binds Na^+ ions creating an increased number of cations inside the NP. This generates an imbalance of charge between the NP and surrounding environment which is responsible for the osmotic pressure within the NP and its water imbibing characteristics (the effect of osmolarity on IVD cells was recently reviewed by Sadowska *et al.* (Sadowska et al., 2018)). Located around the NP is the AF which has a fibrous cartilaginous ring structure. Similar to the NP, it is mainly composed of PGs and collagen. The healthy AF contains 50% water, approximately 70% collagen (dry weight) and 10% PGs (10% of dry weight). The high amount of collagen in the AF is critical to withstand both tensile and compressive stress during physiological loading. Because of the different function of AF and NP, the collagen structure also differs in both tissue types. This can be seen in distinct gradients of collagen type I (Col1) and Col2 between both AF and NP with a more organised Col1 structure observed in AF and a more randomised, long network of Col2 fibres in the NP. The third component of the IVD are the CEPs which form the interface between the NP and AF with the vertebral bodies at the top and bottom of the soft disc tissue. The main function of the CEP is to prevent extrusion of the

NP into the vertebral body and to provide a transport route for nutrients into the central disc tissue as well as the removal of cellular waste products. Nevertheless, only 1% of the IVD tissue is represented by cells: chondrocytic-like cells in the NP and AF which have an average density of 2200 ± 640 cells/mm^3 in the NP and fibroblastic-like cells in the outer AF with an average reported cell density of 1600 ± 580 cells/mm^3 of population between 30 and 60 years.. The cell population of the NP, however, may change with age and species (Roughley, 2004, Liebscher et al., 2011).

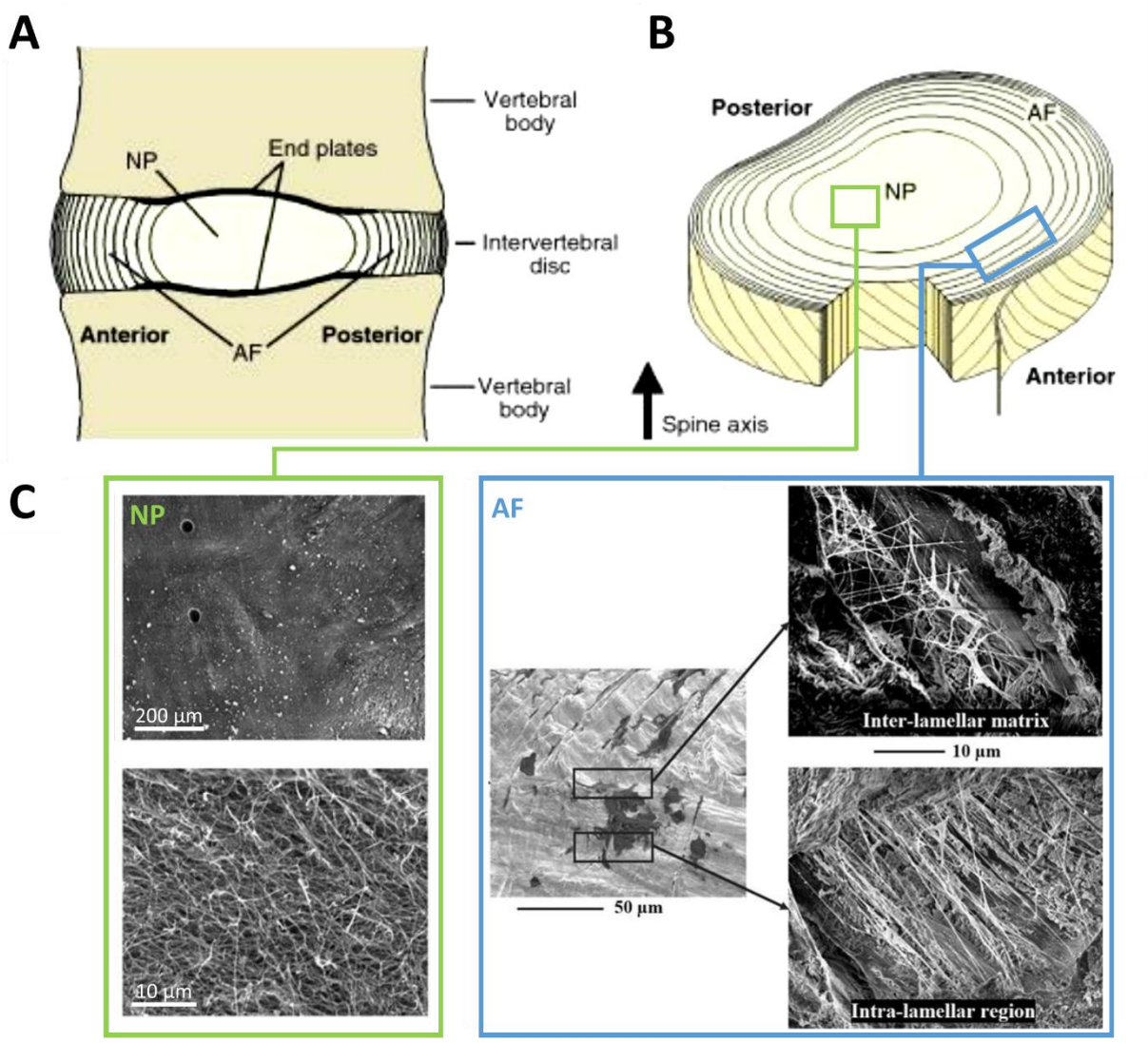

Figure 2-1: Schematic of the IVD. **(A)** The central NP tissue is surrounded by fibrous cartilaginous ring structured AF tissue. On top and bottom of these structures, **CEP** is located. **(B)** The AF tissue surrounds the NP tissues in multiple layers of lamellae structures (Smith et al., 2011). **(C)** SEM images of the NP (left), showing a randomised structure of fibres within the tissue and AF (right), demonstration more aligned fibres within a lamellae. (adapted from (Caldeira et al., 2017, Tavakoli et al., 2017))

The cell number within the IVD is controlled by the limited nutrition supply to the central region of the tissue. The IVD is the largest avascular tissue in the human body and receives its oxygen and nutrient supply primarily through the CEP via diffusion. As a result, a low oxygen and nutrient concentration exists within the nucleus pulposus, activating the anaerobic metabolic pathway of the cells (Bartels et al., 1998) which highlights the hypoxic nature of the disc. Cell metabolism and survival strongly correlates with hypoxia-inducible factor (HIF) (Semenza, 1994, Agrawal et al., 2007, Schipani et al., 2001), which regulates expression of molecules connected with glycolysis, activity of the tricarboxylic acid (TCA, also known as the citric acid cycle or Krebs cycle) cycle and oxidative phosphorylation. Furthermore, the IVD exhibits increased osmolarity due to the water imbibing properties of negatively charged PGs. NP cells respond to osmolarity by upregulation of transcription factor tonicity enhancer-binding protein (TonEBP), which is the only known factor that activates in response to osmolarity changes (Tsai et al., 2006).

2.2. The Microenvironment of the Intervertebral Disc

The IVD is a complex structure with the NP in the centre surrounded by AF fibres in concentric layers; providing a challenging microenvironment for cells. Nutrient and oxygen supply into the NP occurs primarily by diffusion through the CEPs or the AF tissue (Figure 2-2 A) with a decreasing gradient of oxygen (5.46%-0.27%), glucose (4.5 mM-0.5 mM) and increasing LacA concentration (1.2 mM – 4.4 mM) towards the centre (Holm et al., 1981, Selard et al., 2003, Bartels et al., 1998) (Figure 2-2 C). Hence the regenerative potential of transplanted cells may be limited by this low oxygen, low glucose and low pH tissue niche. Another important characteristic of the IVD niche is the elevated osmolarity, due to the negatively charged ECM. Combined together, this characteristic niche is important in the unique phenotype expression within cell populations as well as facilitating NP cells to maintain matrix turnover (Mwale et al., 2011).

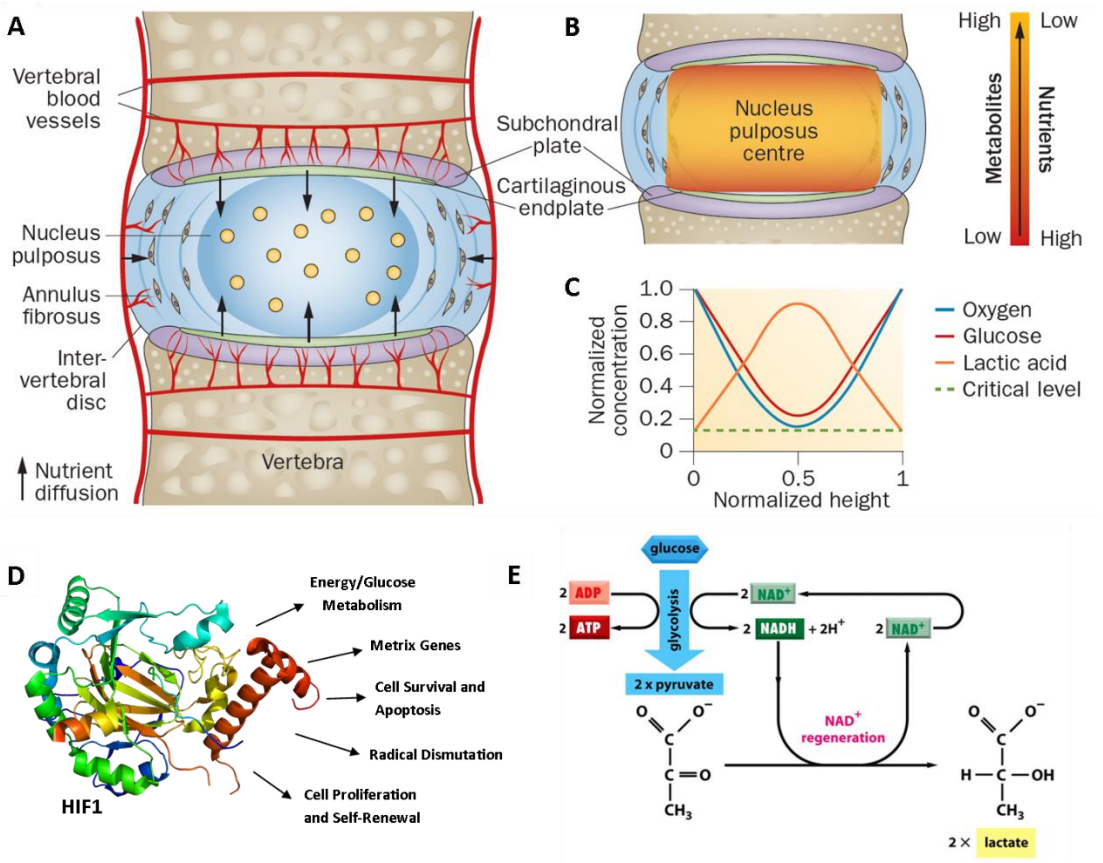

Figure 2-2: Different microenvironmental effects on the IVD. **(A)** Main nutrient supply for NP and inner AF cells occurs via diffusion through blood vessels located in the vertebrae. Cells from the outer AF are supplied with nutrients through capillaries of the surrounding soft tissue. **(B)** Nutrient gradients are present in the disc with the lowest nutrient (e.g. oxygen, glucose) levels located in the centre with high levels of metabolites (e.g. lactic acid). **(C)** Schematic showing normalised concentration gradients of glucose, oxygen and LacA across the NP from endplate to endplate (Huang et al., 2014). **(D)** Molecular structure of HIF-molecule and its regulating effect on cells including energy metabolism, apoptosis and proliferation. **(E)** Fermentation pathway under low oxygen conditions producing 2 lactate molecules from one glucose molecule under regeneration of the energy molecule Nicotinamide adenine dinucleotide (NAD^+) (Alberts et al., 2008)

2.2.1 Effect of oxygen-level in IVD

Oxygen is a vital nutrient, which plays a key role as an electron acceptor in the mitochondrial respiratory chain to generate adenosine triphosphate (ATP), the main energy source for cells, as well as being involved in several developmental processes. In the IVD, the physiological oxygen tension ranges from 4-7% and can decrease to 1% in a severely degenerated disc (Mwale et al., 2011, Ishihara and Urban, 1999, Bartels et al., 1998). Cell metabolism and survival strongly correlate with HIF, which is involved in the translation of hypoxic effects on

cellular function. It regulates expression of molecules connected with glycolysis, the activity of TCA cycle and oxidative phosphorylation (Figure 2-2 B) as well as being involved in regulating angiogenesis, cell survival, matrix synthesis, proliferation, apoptosis, self-renewal and differentiation (Oegema, 1993). HIF is a heterodimer of the helix-loop-helix family and composed of a constitutively expressed α-subunit and β-subunit (Figure 2-2 D). In most cells, the molecule and its subunits form a stable complex, however, with increasing oxygen level HIF-1 starts to degrade (Sakai, 2008, Wang et al., 1995). When activated, HIF-1α promotes expression of glycolytic enzymes and therefore enables cells to switch from aerobic to anaerobic glycolysis by inhibiting oxidative phosphorylation and increases the formation of lactate (Zigler et al., 2007, Gruber et al., 2002) (Figure 2-2 E). In chondrocytes it has been shown that HIF-1α degrades under normoxic conditions (20% O_2) (Okuma et al., 2000), however when HIF-1 is inhibited, the aggrecan expression is reduced indicating the correlation between oxygen supply, HIF-1 expression and matrix accumulation (Zhang et al., 2008). Therefore, when considering cell-based therapy for IVD repair, it is important to realise the effect and behaviour of the chosen cell type to manage the typically low oxygen conditions found *in vivo*.

Each tissue type inside the living body exhibits a unique oxygen gradient which is important to consider in tissue engineering and regenerative medicine approaches. These gradients play an important role in maintaining tissue phenotype and matrix synthesis in their distinct and unique environment (Malda et al., 2003). Grimshaw and Mason have shown that anoxia ($O_2 < 0.1\%$) has detrimental effects on matrix accumulation of bovine ACs, whereas higher levels of oxygen –physioxia (5 and 10%) result in an increase in matrix synthesis, followed by decreasing levels in normoxic conditions (20%) (Grimshaw and Mason, 2000). It has also been demonstrated that sustained hypoxia at 2% O_2 enhances articular cartilage matrix synthesis and chondrocyte viability in 3D culture (Malda et al., 2004). The authors observed enhanced levels of PG synthesis as early as 1 day after exposure to low oxygen, as measured by 35s-sulfate incorporation. Sulphated glycosaminoglycans (sGAG) and type II collagen synthesis have also been shown to be enhanced for human ACs under low oxygen tension (Scotti et al., 2012). These

findings highlight that intracellular pathways of cells subjected or exposed to a low oxygen environment are specifically designed for the individual needs of the associated tissue to provide their functionality.

2.2.2 The importance of glucose in the intervertebral disc

Glucose is a simple sugar composed of 6 carbon atoms and an important source of energy during cellular respiration. Given that glycolysis is the main energy-generating pathway in the disc, diffusion of sugars into and removal of the LacA by-product from the disc is essential. The physiological concentration of glucose in the IVD is approximately 5 mM (Bibby et al., 2005b). However, the reduction of glucose concentration below 0.05 mM even for three days demonstrates a detrimental effect on cell viability (Horner and Urban, 2001, Urban et al., 2004). Moreover, during the progression of disc degeneration, the endplates begin to calcify further limiting the diffusion of molecules between the disc and capillaries located in the CEPs, which have a distance of 7-8 mm in the centre of the disc (Urban et al., 2004). Therefore, while cell activity and even viability may be impaired with decreasing nutrient supply, enzyme activity remains constant creating an imbalance between matrix anabolism and catabolism which can contribute to further disc degeneration. Previous work investigating the effect of glucose concentrations on disc cells *in vitro*, confirm the critical effect of glucose on cell metabolism. In a study by Richardson *et al.* the authors observed changes of glucose transporters in the membrane of NP cells present in degenerative tissue suggesting that there are molecular adaptions to compensate for the reduced glucose concentrations (Richardson et al., 2008). However, for cell-based therapies, it is essential that both the host cells and transplanted cells, which are intended to repair or regenerate the damaged tissue can withstand the harsh environment of the IVD. In addition, the number of cells introduced for tissue regeneration needs to be considered, as a high number of cells may not be capable of withstanding the harsh environment of the IVD as well as competing for limited resources of glucose and oxygen which may exacerbate the degenerative problems rather than repair the damage. Naqvi *et al.* compared mesenchymal stem cells (MSCs) and NP cells cultured under IVD-like microenvironmental conditions with various

glucose concentrations and reported differential effects due to altered metabolic activities. NP cells were found to have a lower glucose consumption rate and exhibited higher viability in very low glucose concentration (1 mM glucose) and 5% external oxygen concentration compared to MSCs (Naqvi and Buckley, 2015c). Another study by Stephan *et al.* cultured bovine NP cells in alginate beads without glucose or under high glucose conditions and demonstrated that NP cell proliferation and survival are influenced by the availability of glucose (Stephan et al., 2011), with larger cluster formation of NP cells and increased levels of apoptotic and senescent cells under glucose deprivation. Bibby *et al.* investigated the effect of an IVD-like microenvironment on bovine NP cells and reported that 5 mM glucose and 5% oxygen enhanced NP-like matrix accumulation suggesting that low oxygen and low glucose conditions are preferable for matrix synthesis of disc cells (Bibby and Urban, 2004). Given, that chondrocytic-like cells have a low metabolism as well and appear to be able to sustain the harsh microenvironment of the disc, suggests that AC may be an attractive source for disc repair.

2.2.3 The role of acidic effects in the intervertebral disc

Within the human body, a variety of different acidities can be found. The lowest pH exists in the gastric fluid of the stomach with a pH ranging from 1.5-3.5 (Marieb and Hoehn, 2008). The human skin has a pH of approximately 4.7 with blood having a neutral pH of 7.4 (Lambers et al., 2006). However, the acidity may hinder cell survival and matrix synthesis capacity with changes in pH. Within a healthy IVD, the average pH has been reported to be 7.1 (Nachemson, 1969, Diamant et al., 1968). With the onset of degeneration, the pH within the NP drops to approximately 6.7-6.9 and can decrease further to 6.5 in severely degenerated IVD (Urban, 2002, Nachemson, 1969). Wuertz *et al*. demonstrated that matrix acidity has detrimental effects on BMSC behaviour with decreasing cell proliferation, lower cell viability and inhibited anabolic gene expression (Wuertz et al., 2009). When investigating pH effects in 3D alginate hydrogels, Naqvi *et al.* found that with decreasing pH, increased death of BMSCs was observed. Furthermore, matrix accumulation was found to be negatively affected by a lower pH environment (Naqvi and Buckley, 2016). When investigating the acidity effect on disc cells, it

was found that when disc-chondrocytes were cultured in nutrient-deprived conditions, viability is compromised at a pH of 6.2 (Bibby et al., 2005b). In a similar study, it was discovered that below a pH of 6.8 the accumulation of sGAG, a key component of disc tissue, was inhibited (Ohshima et al., 1992, Razaq et al., 2003). Uchiyama *et al.* investigated the acid-sensing ion channel 3 (ASIC3) in NP cells and demonstrated that they were expressed on disc cells, indicating their adaptive phenotype to an acidic environment (Uchiyama et al., 2007). ASICs are proton-gated sensitive channels of Na^+ and Ca^{2+} ions (Cuesta et al., 2014, Zhou et al., 2015b, Sun et al., 2013). Once activated by a low pH microenvironment, ions enter the intracellular space and trigger ion-dependent proteases, which subsequently alter the cellular gene expression, resulting in a number of effects such as cellular apoptosis (Yuan et al., 2016).

2.3. Degenerated Disc Disease (DDD) leads to microenvironmental structural changes

DDD is believed to be strongly associated with LBP (Luoma et al., 2000, Cheung, 2010). Different risk factors accelerate the tissue degeneration, such as age, lifestyle, injury or genetic predisposition (Luoma et al., 2000, Battie et al., 2009). Per definition, disc degeneration is the decrease in PG production whilst production of matrix-degrading proteins is elevated (Weiler et al., 2002, Le Maitre et al., 2004a). Furthermore, there is an increased number of senescent NP cells and cell death (Gruber et al., 2007). During the ageing process, a decline in nutritional supply occurs, resulting in a change in cell metabolism, which is believed to be one of the primary causes for age-related DDD (Holm et al., 1981). Nutrient flux naturally occurs through the endplates as well as diffusion across the matrix from the periphery of the AF into the central part of the NP. With a reduction in disc height and decrease in blood vessel density within the end plates, the ability for nutrient and waste product diffusion is diminished. This results in low oxygen and an acidotic microenvironment with a pH of around 6.8 in a mildly degenerated disc, and a change of the NP structure toward a more fibrotic appearance and the lamellae structure of the AF becoming more disorganised. Increased cell proliferation occurs with cluster formation and

increased cell death, necrosis and apoptosis in aged disc tissue (Gruber and Hanley, 1998, Johnson et al., 2001). Additionally, the remaining cells synthesise less matrix with age, resulting in an imbalance between matrix degradation and deposition. With a drop in matrix accumulation and continuation of aggrecan catabolism, a significant loss of PGs can occur (Lyons et al., 1981, Buckwalter et al., 1985) causing a decreased capacity for water imbibement and a decrease in osmotic pressure (Erwin et al., 2015). The disorganised structure of the tissue occurs due to collagen degradation, PG reduction followed by disc dehydration leads into a reduction in disc heights which has a critical influence on the mechanical properties of the tissue (Raj, 2008). These structural changes may result in tears occurring in the AF tissue and bulging of NP tissue, exerting pressure on the adjacent nerve roots, which manifests as LBP. A schematic overview of different states in disc degeneration and the cellular and environmental differences is depicted in Figure 2-3.

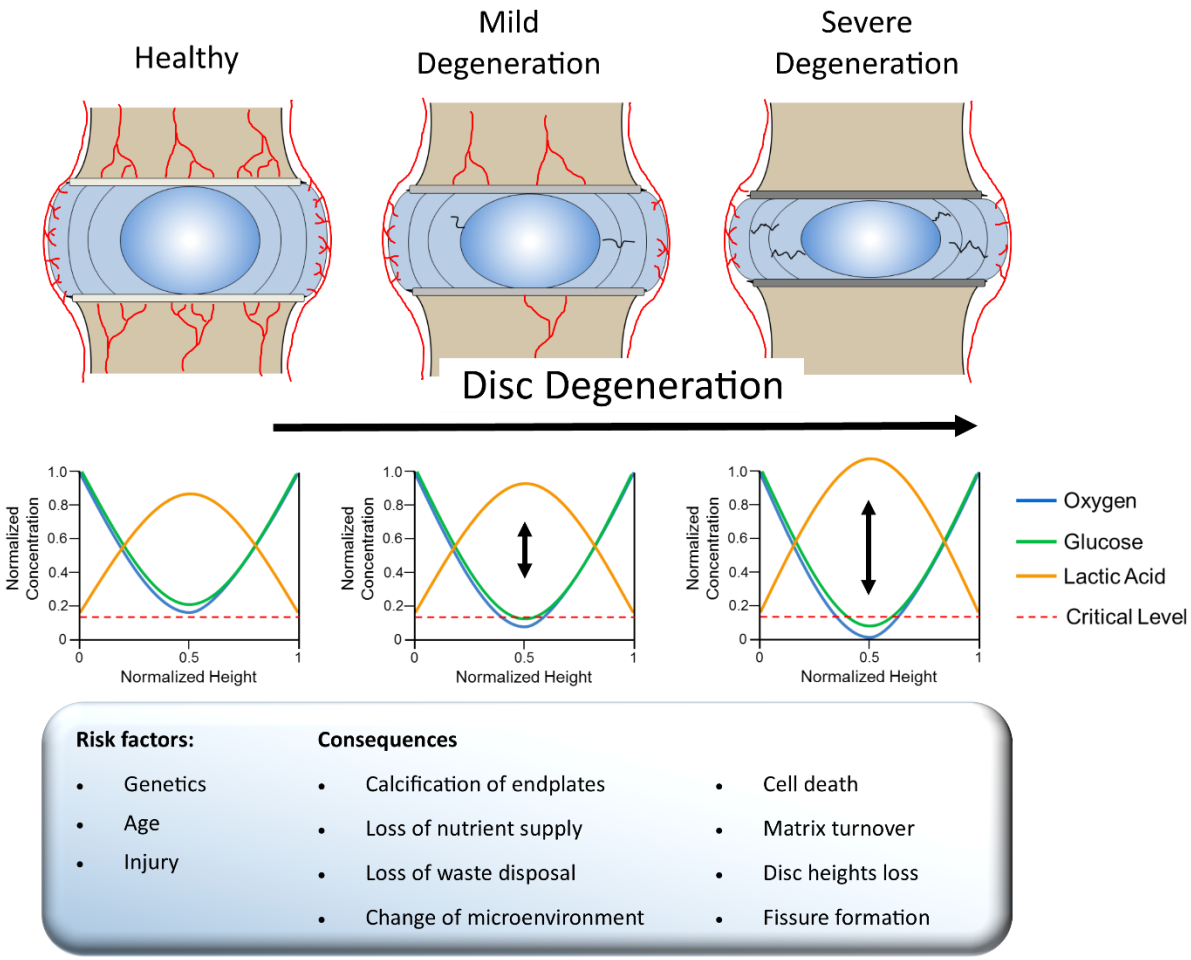

Figure 2-3: Different stages which occur during DDD. Degeneration of the IVD is indicated by a decrease in nutrient supply due to endplate calcification, matrix disorganization followed by fissure formation and disc height loss (top). The disc microenvironment changes its profile with decreasing levels of oxygen and glucose below a critical level and an increase of lactate resulting in a more acidic microenvironment.

2.4. Cell-based and advanced nucleus pulposus regeneration strategies

At present, the gold standard treatments for LBP includes conservative strategies such as physiotherapy and pain management (Gilbert et al., 2013). These treatments attempt to alleviate pain rather than treat the underlying cause of degeneration. When no further improvements can be achieved using these conventional approaches, surgical techniques such as microdiscectomy, spinal fusion and total disc replacement are performed. These treatments provide symptomatic relief but neglect to include the biological origin to restore disc function. Disc heights can be

compromised followed by limitations of anatomical flexibility and reduced mechanical load-bearing capabilities. In addition, these procedures are highly invasive and can result in surgical complications for patients as well as accelerated disc degeneration in adjacent segments (Hilibrand and Robbins, 2004, Lee and Choi, 2015). Therefore, the use of various cell types as therapeutic agents has received increased attention, with the specific aim to repopulate the NP and restore the natural function of the IVD. After cellular injection, these transplanted cells should ideally be able to proliferate and produce new matrix to replace the degenerated tissue. However, practical issues such as accessibility, abundance and safety concerns need to be considered for cell-based therapies. Potential cell types for these therapies need to reproduce tissue-specific matrix-molecules as well as being able to sustain the harsh microenvironment of the IVD. In the case of disc tissue, the most important ECM molecules that need to be accumulated are PGs such as aggrecan and HA as well as Col2. Another factor that needs to be considered using cell-based therapy for IVD repair is the avascular nature of the IVD along with its limited nutrient supply. The introduction of a new cell population may cause a higher imbalance of nutrient supply versus nutrient demand and can lead to further cell death and matrix catabolism (Huang et al., 2014). Disc cells and chondrocytes, therefore, are obvious candidates for disc regeneration as they are inherently programmed to produce these matrix proteins under optimal conditions. MSCs have also been widely used for cell-based therapies since they are easily accessible and have the ability to differentiate towards several cell lineages, including a disc-like phenotype (Risbud et al., 2004, Stoyanov et al., 2011, Caplan, 1991, Caplan, 2009).

Advanced approaches are currently being investigated including biological- cell- and gene-based therapies. Thompson *et al.* demonstrated that implantation of growth factors such as transforming growth factor β3 (TGF- β3) and insulin-transferrin-selenium (ITS) have the potential to increase matrix deposition up to five-fold in IVD cells (Thompson et al., 1991, Osada et al., 1996). However, sustained *in vivo* growth factor delivery is essential to prolong beneficial effects. This has motivated investigations into gene therapy strategies whereby a gene of interest, such as TGF-β, is transfected into a cell which increases the expression and release of TGF-β into

the microenvironment (Nishida et al., 1999). Gene therapy, however, is still far from clinical use as critical parameters such as safety; gene delivery vectors and choice of therapeutic genes still need to be fully elucidated.

2.4.1 Therapy using disc-derived cells

IVD cells have been proposed as a potential cell source for cell therapy of the NP. The cells are primed to the specific niche and can survive under the harsh circumstances present in the NP (limited supply of oxygen and glucose). Furthermore, adult NP cells can produce important ECM molecules such as aggrecan and Col2 (Roughley, 2004). Additionally, research has shown that NP cells continuously produce HIF1α, independently in the surrounding oxygen level, supporting anaerobic glycolysis to overcome the challenge of reduced nutrient availability (Risbud et al., 2006, Risbud et al., 2010). Moreover, there is evidence to suggest a link between HIF1α release and NP-specific ECM accumulation (Gogate et al., 2011), further endorsing the use of NP cells for disc regeneration.

In vivo studies on rabbit and canine models have shown improved disc heights, sGAG content (Feng et al., 2011) as well as an improvement in cell viability and pain score (Meisel et al., 2007) after the injection of autologous NP cells into the defect site of the IVD. This autologous disc cell transplantation (ADCT) approach has been tested clinically in human (Co.don®, Berlin, Germany) with cells isolated from the degenerated disc (see Table 2-1). An overview of ADCT is shown in Figure 2-4. Also, DiscGenics Inc. made some progress in the development of a cell-based therapy for IVD regeneration. They proposes the use of IDCT (injectable discogenic cell therapy), a mixture of specialized therapeutic progenitor cells engineered from donated adult disc tissue in combination with a viscous carrier gel and could demonstrate some success *in vivo* (Hiraishi et al., 2018). Their approach is currently under human clinical trials, evaluating safety and efficacy of their product (Table 2-1). However, the use of NP cells from degenerated discs is questionable as they seem to be damaged by the disc degeneration process. This is shown by their decreased Col2 accumulation capacities and increased rate of senescence (Roberts et al., 2006, Park et al., 2001). Moreover, cell yield from NP tissue is very low (density between 2000-5000

cells/mm^3 (Maroudas et al., 1975, Liebscher et al., 2011)) as well as the additional risk in isolating from a mixed population of NP cells, AF cells and cells from the cartilaginous endplate during surgical tissue removal (Brock et al., 1992, Yasuma et al., 1993, Schmid et al., 2004), making the procedure less reproducible and damaging the IVD tissue. In addition to the challenges raised during cell harvesting, the expansion of herniated disc cells has also proven to be difficult due to the limited expansion capacity of the cells, which may be as a result of dedifferentiation effects which in turn has an impact on ECM accumulation capacities (Gruber and Hanley, 2000, Ciapetti et al., 2012, Le Maitre et al., 2009). Given these limitations of ADCT, the need for an alternative cell type for disc regeneration is evident.

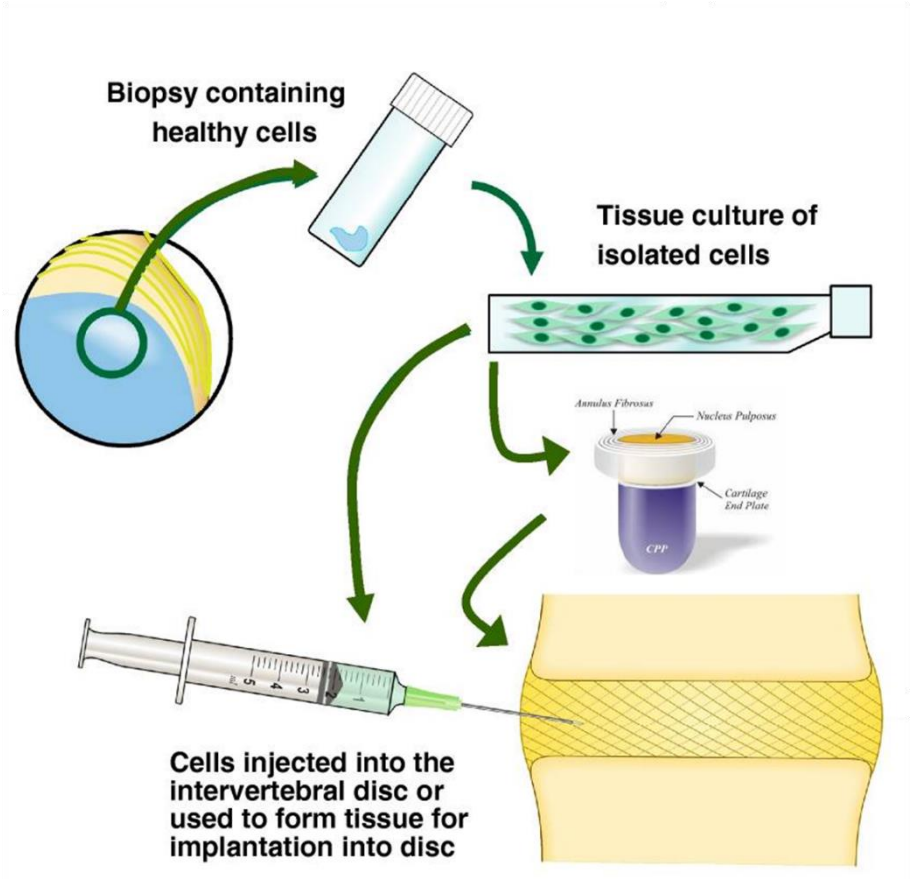

Figure 2-4: Schematic overview of ADCT, whereby a biopsy of healthy cells is isolated, expanded and re-injected into the degenerated IVD by simple needle injection or in form of a tissue engineered construct – indicated as CPP (Kandel et al., 2008)

2.4.2 Therapy using cartilage-derived cells

Chondrocytes are phenotypically very similar to NP cells and are found only in cartilaginous tissue. Both types are derived from load-bearing tissues that are avascular and hypocellular (Ganey et al., 2003). Chondrocytes have been isolated from different sources such as articular cartilage (Garcia and Knight, 2010), human auricular (van Osch et al., 2001) and nasal tissue (Kafienah et al., 2002, Vedicherla and Buckley, 2017b). However, isolation of chondrocytes from an articular cartilage biopsy is intrinsically associated with cellular dedifferentiation during monolayer cell culture (Benya and Shaffer, 1982). This is characterised by a shift of collagen synthesis from Col2 to Col1, such as in tendon or skin (Freyria and Mallein-Gerin, 2012). For example, it has been demonstrated that during monolayer expansion on tissue culture plastic to a higher passage, chondrocytes can lose their natural shape and metabolic profile (Velikonja et al., 2001, Lee et al., 2007b). This highlights the challenge using these cells for autologous cell therapy: the ability of chondrocyte expansion without dedifferentiation. An approach to overcome this obstacle may be re-differentiation, to induce matrix synthesis by using growth factor supplementation, such as TGF-β or BMP-2 (Hautier et al., 2008, Bobick et al., 2009) (See paragraph 2.5.1 “Priming (pre-differentiation) of cells”, page 28). Further, the chondrogenic capacity of isolated chondrocytes is highly variable and is dependent on factors such as biopsy site, culture medium supplements, expansion time and donor variability (Waldman et al., 2003, Jakob et al., 2001, Barbero et al., 2004). However, in 3D culture, chondrocytes have been shown to synthesise matrix without supplemented growth factors and are capable of maintaining their phenotype when cultured within scaffolds or hydrogels (Galois et al., 2006, Roche et al., 2001, Vedicherla and Buckley, 2017a). It has also been demonstrated that NP cells and chondrocytes have a similar gene expression profile, however with some differences in the quantitative expression of specific genes (Lee et al., 2007a, Rutges et al., 2010, Power et al., 2011, Minogue et al., 2010b). Both cell types demonstrate a similar pattern of SOX 9 (Takahashi et al., 1998) and matrix metalloproteinase (MMP) gene expression (Cui et al., 2010). Additionally, chondrocytes are able to accumulate an ECM with high levels of aggrecan and Col2 (Roughley,

2004), which contributes to beneficial properties, making them an attractive source for autologous cell transplantation therapy to regenerate the IVD.

2.4.3 Therapy using bone marrow-derived stem cells

Due to their ability to differentiate into different lineages and cell-types, adult mesenchymal stem cells (MSCs) have been widely used in tissue engineering applications including cartilage, bone, muscle and IVD repair (Bosnakovski et al., 2006, Arinzeh, 2005, Dezawa et al., 2005, Bertolo et al., 2015). They can be isolated from different sources such as bone marrow and adipose tissue and can be maintained undifferentiated *in vivo* as well as *in vitro*. Their characteristic includes the expression of surface markers such as CD44, CD71, CD90, CD105, CD120a and CD124 but they are negative for several hematopoietic lineage markers (Campagnoli et al., 2001). In addition, MSCs have been shown to secrete distinct cytokines including interleukin and leukaemia inhibitory factor for paracrine signalling (Majumdar et al., 1998).

For IVD regeneration, chondrogenesis is critical. Activation and maintenance of the differentiation pathway are only possible under the presence of growth factors, mainly from the transforming growth factor family (Freyria and Mallein-Gerin, 2012). However, these cues can also lead to hypertrophy, calcification and endochondral ossification (Dickhut et al., 2009, Farrell et al., 2011). In addition to the use of growth factors, 3D cultures were also found to increase the expression of chondrogenic markers in MSCs when compared to the traditional 2D cell culture (Minogue et al., 2010a). However, the use of MSCs always includes the risk of inappropriate differentiation post-implantation. For example, Vadala *et al.* observed a differentiation towards an osteogenic phenotype post injection, signifying unwanted side-effects and demonstrating the challenges that come with this approach (Vadala et al., 2012). Nevertheless, it has also been demonstrated that MSCs used in a co-culture system with NP cells were able to promote the release of intrinsic factors and improve cell viability and matrix accumulation of NP cells (Mochida et al., 2015, Naqvi and Buckley, 2014, Naqvi et al., 2019). These regenerative changes of disc tissue using MSCs have also been demonstrated *in vivo* (Hee et al., 2010, Goldschlager et

al., 2010). Despite the beneficial effect MSCs seem to have on the disc cell population, they still carry the risk of an adverse event due to unwanted differentiation. Furthermore, they also show limited ability to survive the disc conditions (microenvironmental factors such as pH, limited nutrients and osmolarity) (Bibby et al., 2005b, Acosta et al., 2011, Wuertz et al., 2008). For instance, Wuertz *et al.* reported an inhibiting effect from the expression of chondrogenic markers such as aggrecan and Col1, as well as the MMP inhibitor TIMP-3 when MSCs were cultured under acidic conditions (Wuertz et al., 2009). Moreover, a decrease in cell proliferation and viability were also observed as well as a change of MSC morphology. This highlights serious limitations for using this cell type as a cell source for disc regeneration in an undifferentiated stage.

Table 2-1: Current clinical trials using cell-based therapy for IVD regeneration.(found and summarised from **https://clinicaltrials.gov/)**

Time	Phase	Identifier	cells used	Sponsor	Publications
2018 -2021	1-2	NCT03347708	Discogenic cells	DiscGenics, Inc.	(Hiraishi et al., 2018)
2012 -2018	1-2	NCT01640457	Autologous Disc Chondrocyte Transplantation System (ADCT)	Tetec AG	(Tschugg et al., 2016)
2017-2018	n/a	NCT03709901	cellular allograft nucleus pulposus matrix	Vivex Biomedical, Inc.	
2013 -2017	1-2	NCT01860417	Allogenic Mesenchymal Stem Cells	Red de Terapia Celular	(Orozco et al., 2011) (Noriega et al., 2017)
2018 -2021	1	NCT03692221	Autologous Bone Marrow Derived Mesenchymal Stem Cells	Salim M Hayek	
2011 -2012	1-2	NCT02440074	Autologous Bone Marrow Derived Mesenchymal Stem Cells	Red de Terapia Celular	
2010-2017	1-2	NCT01513694	Autologous Bone Marrow Derived Mesenchymal Stem Cells	Red de Terapia Celular	
2018 -2020	1	NCT03461458	Autologous, Culture-Expanded Mesenchymal Stromal Cells	Mayo Clinic	
2018 -2020	2-3	NCT03737461	allogeneic BM-MSC	University Hospital, Montpellier	
2011 -2013	2	NCT01290367	adult, allogenic Mesenchymal Precursor Cells	Mesoblast, Ltd.	
2015-2020	3	NCT02412735	Allogeneic Mesenchymal Precursor Cells (Rexlemestrocel-L)	Mesoblast, Ltd.	
2015 -2017	1	NCT02338271	Autologous Adipose Derived StemCells	Inbo Han	(Kumar et al., 2017)
2014 -2017	n/a	NCT02097862	Adipose Stem Cells	Bioheart, Inc.	(Comella et al., 2017)
2013 -2020	2	NCT01771471*	juvenile chondrocytes, delivered in fibrin carrier	ISTO Technologies, Inc	* terminated-change in clinical strategies)

Despite the utilisation of numerous different cell types for delivery into the site of interest, there still remains a critical concern as well as certain shortcomings. In the case of cell delivery into the intervertebral disc, injection appears to be the most obvious choice. Nevertheless, cell leakage during intradiscal delivery is a major challenge. In addition, there is limited control over cell fate and undesired differentiation which can result in migration to sites other than the target region, as described earlier (Wang et al., 2012, Bayoussef et al., 2012).

2.4.4 Regeneration by altering the IVD acidic microenvironment

Besides approaches to regenerate the damaged tissue of the IVD using cell-based therapy, the underlying challenge of the microenvironment often becomes a secondary priority. However, an acidic environment can be detrimental for newly introduced cells. Therefore, the use of chemical agents to alter the pH opens a new path to approach IVD repair.

One group of such chemicals are antacids, a group of one or multiple component salts, available over the counter in pharmacies for several years. The active ingredients are suitable for treatment against symptoms such as heartburn and dyspepsia, which have been found to be associated with hyper-acidic gastric fluids (Sontag, 1990). They have rapid and effective pH neutralising properties in combination with the ability to inhibit the conversion of gastric pepsinogen into its active form pepsin, which is thought to be involved in tissue injury in ulcer disease (Gennaro and Remington, 2000). Their active component is usually based on aluminium hydroxide ($Al(OH)_3$), magnesium hydroxide ($Mg(OH)_2$), sodium bicarbonate ($NaHCO_3$), calcium carbonate ($CaCO_3$) or different combinations. They typically dissolve in the acidic environment resulting in neutralization reaction:

Equation 1:elementary neutralization reaction

$$Acid + Base \rightarrow Salt + Water$$

The exact neutralisation reaction, however, depends on the antacid being used. The effectiveness of neutralization reaction of an antacid can be determined by the acid-neutralizing capacity (ANC), which is defined by the total amount of acid neutralised in 1h at 37°C, the rate of neutralization and the time in which the pH remains above pH 3 (Grinshpan et al., 2008).

Aluminium hydroxide ($Al(OH)_3$) is a white, insoluble amorphous powder, which is widely used in pharmaceutical and personal care products such as stomach antacid or buffered analgesics ((ATSDR), 2008). Research in rodents and canine models have shown when taken orally, the aluminium content of $Al(OH)_3$ can be adsorbed and be found in the brain after a 5-month treatment (Arieff et al., 1979). However, an increase of gastric pH could be achieved from

pH 2.09 to 5.78 of a human patient post-surgery using a dosage of 30 mg/kg $Al(OH)_3$ (Krewski et al., 2007). When in an acidic environment, it behaves like a base and reacts according to the equation above followed by neutralization of pH (Equation 1). In some cases, $Al(OH)_3$ is complexed with sucrose octasulfate to form sucralfate. However, this complex did not show significant neutralization capacities, an effect on pepsin activity or on the production of gastric acids (Schucker and Ward, 2005, Tarnawski et al., 1995), therefore it has different beneficial properties. $Al(OH)_3$ is often combined with magnesium-complexes for better pH neutralizing efficiency.

Calcium Carbonate ($CaCO_3$) is the carbonic salt of calcium. It appears naturally as an odourless and tasteless powder or crystal and is used therapeutically as a phosphate buffer in haemodialysis as an antacid in gastric hyperacidity for temporary relief of indigestion and heartburn, and as a calcium supplement for preventing and treating osteoporosis. It is practically insoluble in water, at low pH however, it breaks down to Ca^{2+} and CO_2, which have been used recently to fabricate drug delivery vehicles. For instance, Dong, *et al.* combined $CaCO_3$ nanoparticles with polyethylene glycol (PEG) as a drug carrier for cancer treatment, whereby the particles stay intact at a neutral pH but breaks down at the acidic microenvironment around cancer cells, releasing the encapsulated drugs (Dong et al., 2016). This strategy of a pH-responsive drug delivery system has been proposed in numerous chemotherapeutics or nucleic acids for cancer treatment (Shi et al., 2015, Chen et al., 2012, Zhao et al., 2015, Wang et al., 2014, Shafiu Kamba et al., 2013). The use of $CaCO_3$ as a direct therapeutic has shown that the oral administration of 2g $CaCO_3$ can stimulate gastric acid secretion (Levant et al., 1973). An overdose of $CaCO_3$ antacid tablets, however, has been associated with hypercalcaemic crisis in pregnant women (Kleinman et al., 1991), indicating that the amount of antacid used as therapeutic can be critical.

Magnesium hydroxide ($Mg(OH)_2$), as with $CaCO_3$ and $Al(OH)_3$ appears as a white, odourless, water-insoluble powder. As an antacid, it dissolves in acidic conditions and reacts with hydrochloric acid of the stomach and forms magnesium chloride and water (Equation 2) to increase the gastric pH. It has been found to act as a strong base in gastric fluid and increases the

pH from 1.5 to 9.1 within 30 minutes, where it stabilizes (Mariadi et al., 2015). In order to alter the release kinetics, Chen *et al.* proposed to encapsulate $Mg(OH)_2$ into 0.8% alginate beads, which had an average size of 300-1600 µm (Chen et al., 2018). The authors demonstrated that the antacid release was stunted by 27% when encapsulated into alginate compared to non-encapsulation, and that both bead size and alginate concentration influenced release kinetics.

Equation 2: Chemical neutralization reaction of hydrochloric acid and magnesium hydroxide

$$2\,HCl + Mg(OH)_2 \leftrightarrow MgCl_2 + 2\,H_2O$$

Overall antacids appear to have the potential to be used not only for hyper-acidic gastric fluids and as a carrier for drugs but also as a system to treat the low pH in different areas of the human body, such as the IVD. The fact that the release kinetics can be altered using a hydrogel highlights the multifunctionality of this approach. A combination of these antacids and cells may open avenues of new therapeutic strategies for various tissue engineering challenges.

2.5. Approaches to enhance cell-based therapies

As outlined in the previous section, using cell-based therapies to regenerate the IVD comes with a number of limitations such as cell leakage during the injection phase and through fissures of the damaged tissue. Furthermore, isolated and expanded cells can de-differentiate when cultured on tissue culture plastic, diminishing subsequent ECM accumulation. There are a number of strategies to overcome some of these challenges including using an *in-situ* crosslinking carrier system during the injection phase or through pre-conditioning the cells with biochemical cocktails.

2.5.1 Priming (pre-differentiation) of cells

Considering the hostile environment of the degenerated IVD, using undifferentiated MSCs or de-differentiated primary cells (due to 2D cell expansion) can diminish potential outcomes of the cell therapy. In particular, several studies have shown MSCs to have limited capabilities in an undifferentiated stage for IVD repair (Holzwarth et al., 2010, Naqvi and Buckley, 2016, Wuertz et al., 2008). Therefore, priming (or pre-differentiation or pre-culturing

or pre-conditioning) has been investigated previously to induce the differentiation of MSCs towards a specific phenotype including cardiomyocyte-like cells (Carvalho et al., 2013, Shim et al., 2004), hepatocyte–like cells (Aurich et al., 2009), neuronal differentiation, (Chen et al., 2006) and towards an osteogenic lineage (Castano-Izquierdo et al., 2007, Grayson et al., 2010). Chondrogenically primed MSCs have also been demonstrated as an efficient treatment for osteoarthritis (OA) (Lam et al., 2014, Zscharnack et al., 2010) Regarding pre-differentiation towards a chondrocyte-like phenotype, it has been demonstrated that TGF-β is an effective cytokine. For example, Noth *et al.* revealed greater chondrogenesis of Col1 hydrogel encapsulated MSCs with prior exposure to TGF-β1 (Noth et al., 2007). When comparing different sub-groups of the TGF-β family, Mueller *et al.* demonstrated higher levels of chondrogenesis with pre-differentiated MSCs using TGF-β3 compared to TGF-β1 (Mueller et al., 2010). Priming of MSCs using TGF-β3 to promote cartilage-like cell differentiation can also enhance mechanical properties of MSCs constructs, when simultaneously exposed to dynamic loading the cells deposit greater levels of ECM molecules into the surrounding matrix (Huang et al., 2010). Dashtdar *et al.* demonstrated improved cartilage repair using TGF-β3 primed MSCs in a rabbit bilateral full thickness cartilage defect model (Dashtdar et al., 2011). TGF-β is a cytokine and belongs to the transforming growth factor beta superfamily which includes the TGF-β family, bone morphogenetic proteins (BMPs), growth and differentiation factors (GDFs), inhibins and activins. The TGF-β / BMP signal transduction pathway includes SMAD transcription mediated pathway and non-SMAD pathways, which both result in different cell responses such as cell cycle arrest, differentiation and ECM deposition (Figure 2-5). Numerous reviews discussing the TGF-β cell signalling pathway have been published previously (Kitisin et al., 2007, Horbelt et al., 2012, Weiss and Attisano, 2013, Schmierer and Hill, 2007).

For IVD regeneration specifically, it has been demonstrated that priming of MSCs using TGF-β3 promoted higher levels of sGAG and collagen deposition and supported survival of cells exposed to simulated IVD degenerative conditions (Naqvi and Buckley, 2015a, Naqvi et al., 2018, Naqvi et al., 2019). Additionally, Malonzo *et al.* showed that pre-conditioning of MSCs

using growth factors suitable for differentiation towards a disc-like phenotype could enhance NP-like matrix accumulation (Malonzo et al., 2015). They demonstrated the differentiation towards a chondrocyte-like phenotype, analysing the gene expression profile after 16 days of growth-factor stimulation. Similar findings were made by Naqvi *et al.*, who showed improved regeneration of an NP defect using TGF-β3 primed, alginate microencapsulated MSC in an *ex vivo* organ culture model (Naqvi et al., 2019).

In summary, pre-differentiation of cells, MSCs, in particular, has demonstrated significant potential for repair of several tissue types which may help overcome some of the microenvironmental challenges associated with IVD regeneration.

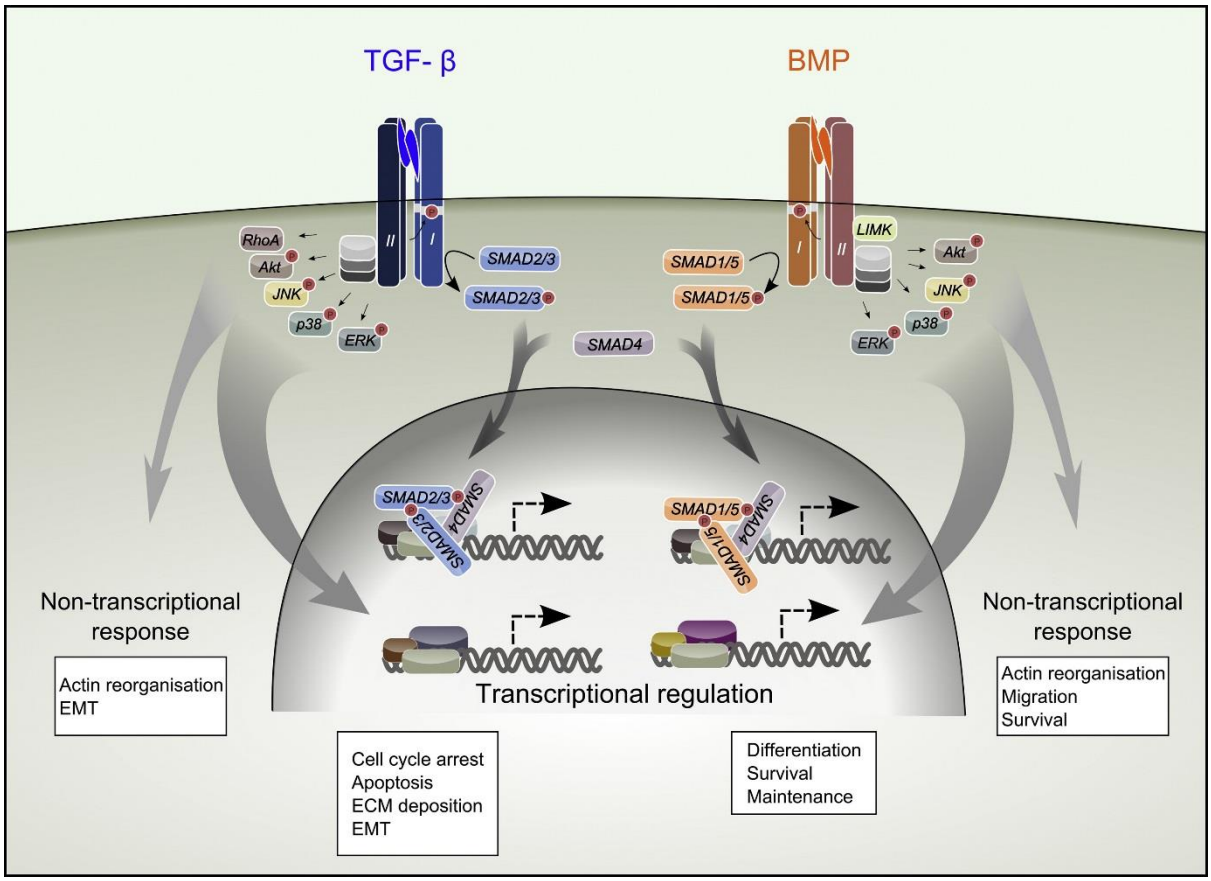

Figure 2-5: TGF-β and BMP intracellular pathways and cellular responses through SMAD and Non-SMAD pathways (Horbelt et al., 2012)

2.5.2 Naturally Derived Biomaterials for Disc Repair

Many of the aforementioned limitations of cell delivery and leakage can be overcome through the use of biomaterials. In addition, biomaterials can act as an extra component for cell-transplantation to ultimately augment the microenvironment such as pH, nutrient supply or waste product degradation as well as providing a protective shield against the host immune system. These attributes are highly attractive in disc regeneration approaches as the microenvironment primarily consists of a low pH and compromised nutrient supply. Recent approaches for IVD repair have demonstrated some success with allogeneic juvenile chondrocyte implantation (Acosta et al., 2011). In this approach, cryo-banked juvenile chondrocytes are injected with a fibrin glue into the early-stage degenerated NP tissue. However, the microenvironment of a degenerated disc is still challenging for healthy cells which may limit their regeneration potential and success in restoring the biomechanical function of the IVD. Using biomaterials, cells can grow in a more natural 3D environment which can activate intracellular pathways due to intrinsic material molecules or surrounding cells. These stimuli can further increase the accumulation of the tissue-specific ECM molecules and therefore tissue specific regeneration. Different biomaterials have been used to enhance cell performance and to facilitate cell delivery. Natural hydrogel biomaterials such as alginate, chitosan, collagen, fibrin and HA have been widely used in tissue engineering and regenerative medicine applications. For NP regeneration, injectable hydrogels are favourable since they can be delivered via a needle in a minimally invasive manner through a 25G needle, which is used clinically (Yang et al., 2014, Yang and Li, 2009).

Hydrogels are 3D hydrophilic, crosslinked polymeric networks stabilised through ionic or covalent bonding. They are capable of absorbing significant levels of water or biological fluids. They can be tailored to contain factors and biomolecules to influence cellular behaviours such as migration, proliferation, differentiation (Vermonden et al., 2008) and matrix deposition as well as providing a semi-permeable structure for nutrient, oxygen and growth factor diffusion (Uludag et al., 2000). Furthermore, hydrogels offer other essential properties such as biocompatibility, permeability and biodegradability.

Alginate has also been shown to fulfil many of these criteria as well as maintaining further cell viability during delivery, by protecting cells during needle-injection (Kong et al., 2003). Alginate is a natural anionic and unbranched polysaccharide derived from the cell walls of brown algae. The chemical structure of alginic acid is built in homopolymeric ionically liked blocks of (1-4)-linked β-D-mannuronate (M) and its C-5 epimer α-L-guluronate (G) residues, respectively (Figure 2-6 top-right). Different functional properties are due to its monomer composition (M/G- ratio) and sequence (Lee et al., 2003). Kong *et al*. demonstrated the influence of alginate concentration on cell viability, with more viable cells observed when using lower concentrations and lower molecular weights (Kong et al., 2003). Ionic crosslinking by divalent cations, such as Ca^{2+} to carboxylic acid moieties on the polymer result in a crosslinked network (Figure 2-6 bottom). *In vivo*, these networks degrade by an exchange of divalent ions with monovalent cations, such as Na^{+}. Alginate is a versatile material and has found numerous clinical applications in the treatment of heartburn and acid reflux (*e.g.* Gaviscon®, Bisodol®, Asilone™) and wound dressing materials (*e.g.* Algicell®, AlgiSite M™). In the context of tissue regeneration, alginate has been widely used for cell encapsulation. Entrapping cells promotes a rounded, chondrocyte-like cell shape due to a lack of binding sites for cells that would cause an elongated, fibroblast-like morphology (Rowley et al., 1999, Andersen et al., 2015). If required, cell attachment can be achieved by modifying alginate using RGD peptides, which induce binding sites into the crosslinked structure.

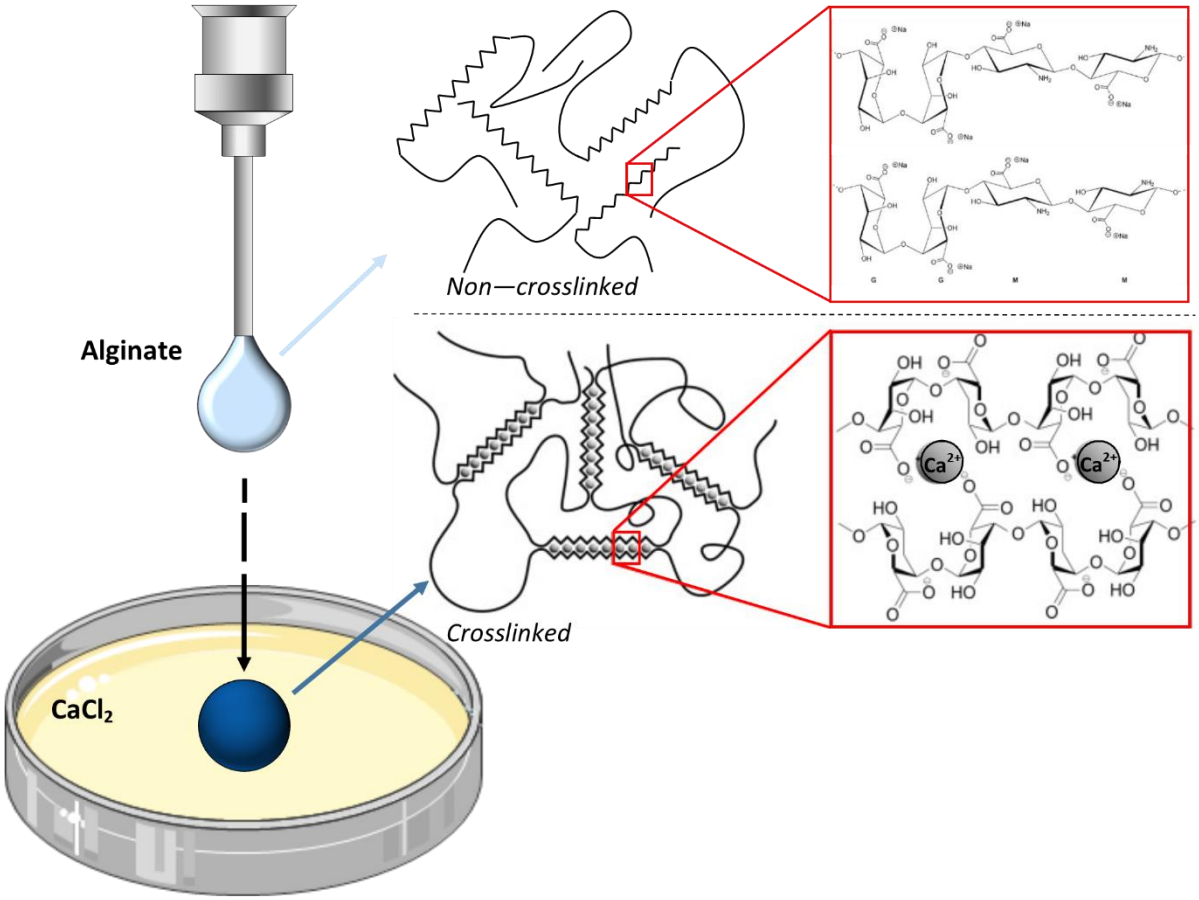

Figure 2-6: Chemical structure of alginate and ionically crosslinking reaction. Due to the presence of divalent cations such as Ca^{2+}, a crosslinking reaction occurs by diffusion of these to carboxylic acid moieties on the polymer resulting into a stable gel-like matrix (Bruchet and Melman, 2015).

Fibrin, another commonly used material in biomedical engineering applications is a viscoelastic polymer. It is formed by an enzymatic reaction of fibrinogen and thrombin, the most important proteins involved in blood clotting (Figure 2-7). It has the capacity to bind matrix proteins, such as fibronectin which enable cells to bind, proliferate and migrate within the material (Makogonenko et al., 2002, Greiling and Clark, 1997). Fibrin has the capacity to bind a variety of growth factors such as basic fibroblast growth factor (bFGF) and TGF-β which can provide the necessary cues to augment cell proliferation and differentiation of encapsulated MSCs (Sahni et al., 1998, Fava and McClure, 1987). Fibrin is currently being used clinically as an adjunct therapy to stem bleeding and to replace structures in certain applications such as skin graft adhesion (Mittermayr et al., 2006) and has shown to enhance healing and minimize scarring

(Santoro et al., 2007). For cartilage repair, fibrin has been shown to support chondrocyte viability and therefore cartilage regeneration (Dare et al., 2009). Eyrich *et al*. demonstrated enhanced Col2 and sGAG synthesis while inhibiting Col1 deposition by primary or MSC-derived chondrocytes (Eyrich et al., 2007), which was further enhanced through the addition of HA to the gel (Park et al., 2005). In terms of disc regeneration, fibrin was tested for the delivery of chondrocytes as part of the NuQu™ (ISTO Tech) technology. NuQu™ was investigated in a randomized controlled trial of 44 patients with mildly degenerated discs and has shown promising results. The trial, however, has been terminated recently (Smith et al., 2018). Nevertheless, this approach showed good potential for disc repair, as demonstrated by Acosta *et al.* , who compared juvenile chondrocytes with MSCs entrapped inside a fibrin hydrogel in a porcine *in vivo* study (Acosta et al., 2011) demonstrating deposition of NP-like matrix of juvenile chondrocytes within the fibrin hydrogel in a porcine disc model.

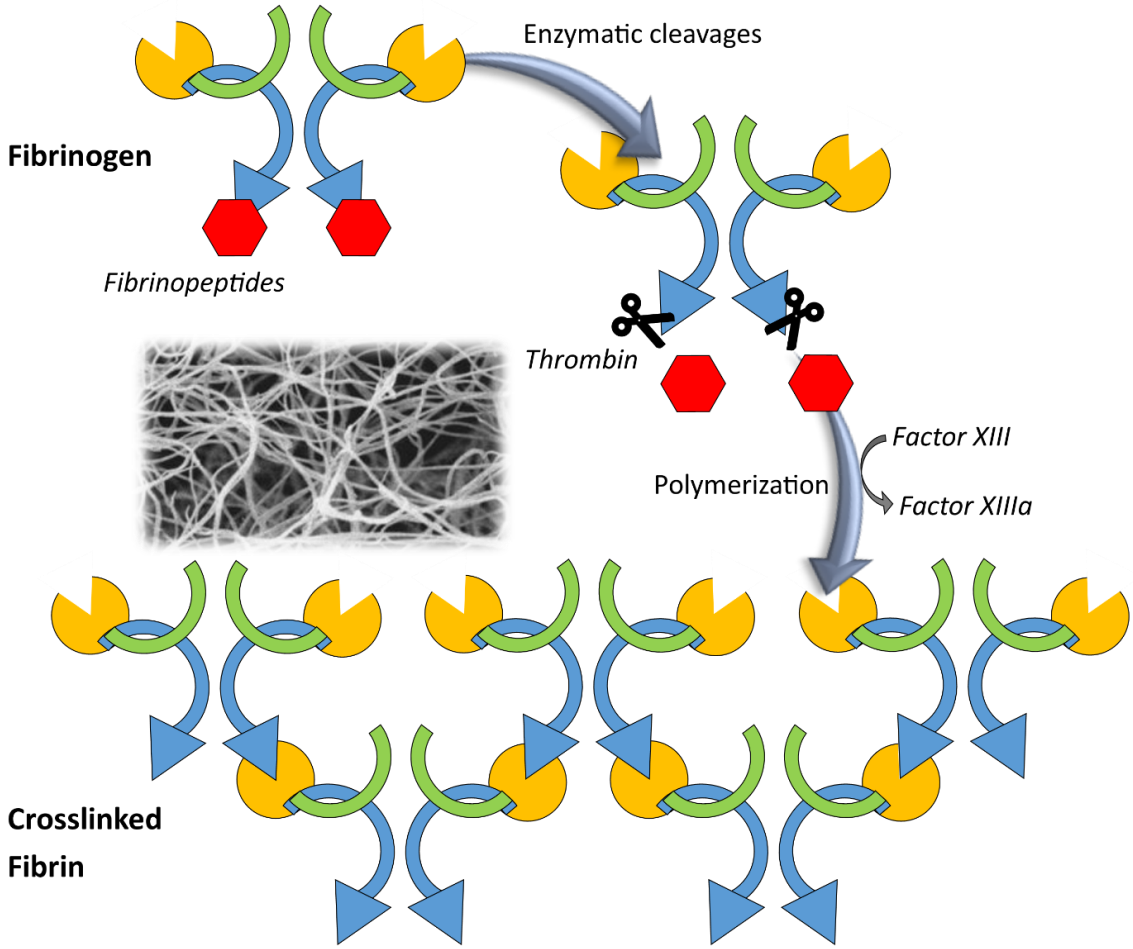

Figure 2-7: Structure and the crosslinking reaction of fibrin. Clotting is initiated after an enzymatic reaction from fibrinogen with thrombin which then follows a reaction cascade resulting in a stable fibrin clot. SEM image shows the fibrous structure of fibrin (Collet et al., 2005).

The incorporation of ECM derived components (e.g. collagen, HA) is advantageous to mimic the specific microenvironment of cells with preserved endogenous ligands. ECM components provide specific binding sites for interaction between matrix and cells enhancing cell attachment, proliferation, matrix production and phenotype expression (Hernández et al., 2010). Collagen is the most abundant protein of mammalian ECM with more than 90% of the extracellular protein in bone and tendon being composed of collagen (Friess, 1998). It promotes tissue stability in organs and maintains their structure. The common characteristic of all members of the collagen family is a right-handed supercoiled triple helix composed of three α-helices. The most important collagen types for disc, cartilage and bone repair are Col1 and Col2 as they are the most dominant types in these tissues contributing to 80% of total collagens in disc tissue (Eyre

and Muir, 1976). They provide torsional stability and tensile strength which gives the tissue its stability and integrity (Nedresky and Singh, 2020).

Collagen has been widely used in biomedical applications, including wound dressing, drug and gene delivery due to its biocompatibility, biodegradability and weak antigenicity (Maeda et al., 1999). Collagen can also store and deliver local growth factors and cytokines and offers cell adhesion molecules which are key for tissue development and wound healing (Lee et al., 2001). Its inherent ability to form strong and stable fibres through self-aggregation and cross-linking as well as the ability to tailor the grade of crosslinking and therefore the strength using chemical agents or physical crosslinking methods renders collagen a versatile biomaterial. Collagen can also be combined with a range of different biomaterials such as alginate or chitosan, combining the benefits of different materials for functionalisation. These composite materials can be used to imitate native tissues in terms of composition to generate a more native microenvironment for cells and promoting differentiation and matrix deposition.

HA is another commonly used material for tissue engineering. It is a linear non-sulphated GAG and binds to aggrecan. It is highly abundant in the NP, attracting water by osmosis which ensures its highly hydrated properties. HA is biocompatible, non-toxic, non-immunogenic and non-inflammatory (Park et al., 2005). It has several beneficial properties such as promoting cell condensation, differentiation as well as supporting the phenotypic expression of tissues *in vivo* (Collins and Birkinshaw, 2013). The most important HA receptor is CD44 which plays an important role in cell adhesion to ECM and is also implicated in the promotion of aggregation, proliferation, migration and angiogenesis (Isacke and Yarwood, 2002). Chondrocytes express an isoform of CD44 receptors which helps facilitate cell-matrix interactions and has been shown to promote chondrogenesis (Cavallo et al., 2010). In the context of disc-tissue engineering, Halloran *et al*. used a Col-HA cross-linked scaffold to maintain cell viability and promote the proliferation of embedded bovine NP cells. This composite biomaterial promoted retention of PGs with low elution of sGAG into the culture medium over 7 days (Halloran et al., 2008).

Considering the attractive properties of the mentioned naturally derived biomaterials for IVD regeneration, this project will focus on this class of biomaterials as carriers for an injectable cell delivery system.

2.5.3 Microencapsulation

Whilst hydrogels are highly attractive for cell delivery, there are some associated limitations including difficulty in controlling *in situ* gelation kinetics (Zeng et al., 2015). In addition, the delivery strategy of materials can also vary depending on the material itself and the approach. With regards to injection, *in situ* gelling of the material is often necessary. Many materials require an additional initiator during or post injection such as heat or UV light (Thirumala et al., 2013, Rowland et al., 2013, Kim et al., 2015). The ability to perform biomaterial crosslinking reactions prior to injection delivery to fabricate micro-sized hydrogels is highly advantageous.

To overcome some of these challenges, microencapsulation can be utilised. Cellular encapsulation involves the entrapment of cells into a polymeric solution and offers a powerful technique for controlled delivery systems as well as a providing a protective niche to prevent an immune response once implanted in the body (Paul et al., 2009, Antosiak-Iwariska et al., 2009). Cell microencapsulation can mask surface marker expression of cells to activate the immune system as well as permitting nutrient and waste product transport through the polymeric material. Encapsulation can also involve the immobilisation of cells or drugs in biomaterials in micron-sized hydrogels that can be implanted into the site of interest via injection. The small size of the spherical shaped particles has been shown to be durable, difficult to disrupt and advantageous in terms of mass transport due to the large surface-to-volume ratio which is important in terms of maintaining cell viability (Uludag et al., 2000, Vos et al., 2006).

Different techniques have been used to entrap cells into micron-sized beads, such as microfluidics, emulsion, stereo/photolithography, extrusion (Ringeisen et al., 2006). The method that is implemented in this project is EHDS. The encapsulation of cells into a biomaterial offers a beneficial microenvironment that can direct cell differentiation towards a desired lineage and

allows secretion of certain bioactive molecules for intercellular interactions (Nogués et al., 2013a, Murua et al., 2008). Regarding mass diffusion through the polymeric membrane, the size of a µCap should not be greater than 300-400 µm (Renken A., 1998, Sugiura et al., 2005). Furthermore, it has been demonstrated that smaller µCaps result in less of adverse immune response (Sakai et al., 2006). This isolation from the immune systems may offer significant potential in the use of allogeneic cell lines as well as genetically modified cells.

2.5.3.1. Technologies for microencapsulation

As mentioned above, numerous different strategies have been developed to fabricate µCaps and to entrap therapeutics such as drugs, growth factors or cells inside.

One such strategy is the microencapsulation using emulsion. This is a two-step consisting of polymer dispersion and hardening of the created capsules. Dispersion is achieved either by extrusion of the polymer or by emulsification (Groboillot et al., 1994). Using the extrusion method, the polymer suspension is dispersed through a nozzle, forming the spheres and falling into a crosslinking solution. Alternatively, the polymer in combination with the target (aquatic phase) is dispersed into an organic phase (such as oil), resulting in a water in oil emulsion. Using a stirrer, small droplets form, which can be stabilized in the crosslinking step by either cooling or an additional gelling/crosslinking agent, creating µCaps (Figure 2-8 A). In a final step, the organic phase is removed, and the capsules are washed. Baimark *et al.* evaluated crosslinking of alginate capsules using this technology and found an average size of capsules >100 µm as well as a delayed drug release kinetics (Baimark and Srisuwan, 2014) which can be useful for slow but sustained medication of certain diseases, such as diabetes. Furthermore, it has been demonstrated that encapsulated cells achieve a viability of 60-80% using this technique (Franco et al., 2011). However, the multiple step procedure limits the attractiveness of this approach compared to alternative techniques.

Spray drying is a technique, frequently used in the food industry. During this procedure, the target material is dispersed into a polymer solution, forming an emulsion or dispersion. The mixture is homogenised and atomized into a drying chamber (Jackson and Lee, 1991). Within the

drying chamber, the solvent (water) evaporates, resulting in the formation of matrix type microcapsules (Figure 2-8 B). Using this technique, a very small average size of particles can be achieved (>10 µm) (O'riordan et al., 2001). Whilst it is easy to operate and can be simply upscaled, the high temperatures within the drying chamber are detrimental for cells and therefore impractical for cell encapsulation, nonetheless this technology may be useful in the manufacture of injectable micro-scaffolds which can then be utilized as cell-carrier system.

Extrusion is probably the most common technique for microcapsule fabrication and is often combined with different strategies. During the process, the polymeric solution is projected through a nozzle at high pressure resulting in controllable droplet formation. Different variations can enhance size control to create smaller capsules. One such variation is the centrifugal extrusion. Here, the nozzle is located at the outer part of a centrifuge and centrifugated while the polymer passes through. As the system rotates, the liquid breaks into small droplets, which can then be collected. This technology is often used in food-industry to produce capsules with a specific coating. The size of these particles ranges from 150 to 2000 µm in diameter (Schlameus, 1995, Desai and Jin Park, 2005), which is a very large range for injectable microcapsules. A different variation of the extrusion is the use of a vibration nozzle, whereby the nozzle or the liquid exhibits vibrational force. This needs to be performed in resonance with the Rayleigh instability to generate very uniform droplets (Figure 2-8 C). Mazzitelli *et al.* characterised this technology in 2008 in terms of technical parameters and cell viability post-encapsulation. After combining low flow rates with a high frequency of vibration, the authors were able to obtain alginate capsules with an average size of 100 µm with a narrow size distribution (Mazzitelli et al., 2008). After encapsulation of neonatal porcine islet, they found good viability and functional properties of cells, showing the potential of this technology. This method also allows the use of a variety of polymers and can produce capsules with a diameter between 20-1000 µm, depending on polymer properties and technical settings of the equipment.

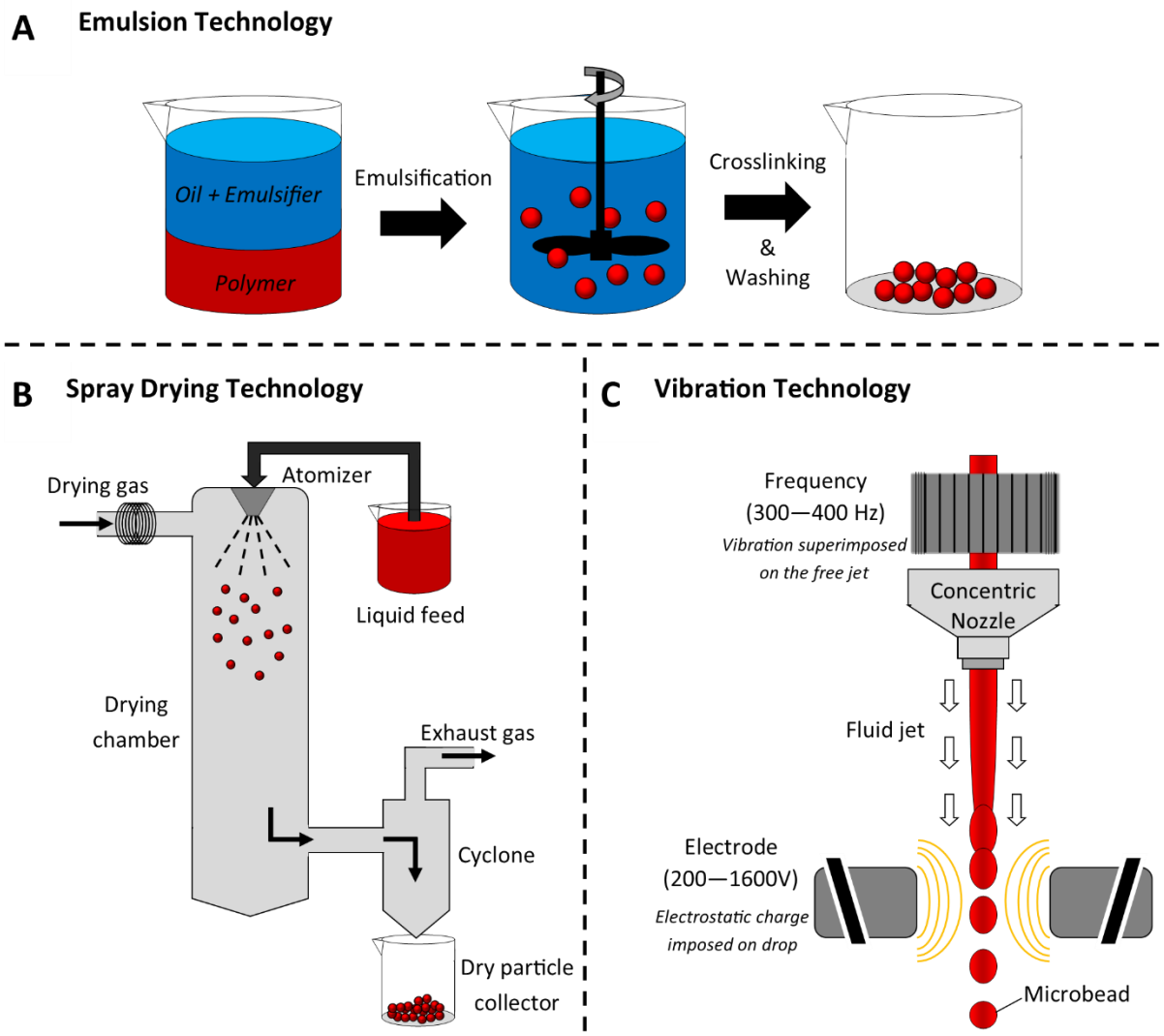

Figure 2-8: Different strategies for microcapsule fabrication. (A) Emulsion technology, which uses an aquatic and an organic phase to create capsules after hardening. **(B)** Spray drying technology extrudes the polymer into a drying chamber to form small capsules, which can be collected after passing through a cyclone. **(C)** Using the vibration technology, the polymer is guided through a nozzle, which exhibits vibrational force, breaking the fluid into droplets. An electrostatic charge facilitates the formation of uniform microbeads

Furthermore, EHDS technology, which is investigated and used in this work belongs to the category of extrusion-based microencapsulation strategies. It is a versatile and low-cost technique that can create micro-sized spheres in a one-step approach (Bock et al., 2012a). In this process, a polymeric solution or any other liquid is charged using a high voltage supply to several thousand volts and passed through an emitter needle where it is dispersed into small droplets (Figure 2-9 ai) (Eagles et al., 2006). The voltage required depends on the chemical and physical properties of the solution such as conductivity and viscosity. With increasing voltage, the liquid

undergoes deformation through different stages to form a conical shape, known as a Taylor cone (Figure 2-9 aii). Important parameters which can influence the size of µCaps formed include applied voltage, inner needle diameter as well as flow rate (Figure 2-9 aiii). By using a polymeric solution containing a target solution that reacts with the polymer to induce sol-gel transition and cells (or other encapsulates such as growth factors, drugs or ECM molecules), the droplets start to gel with entrapped cells/drugs inside to form µCaps (Figure 2-9 b). The fabrication of multi-layered structures using a coaxial needle containing an inner and an outer lumen can provide controllable core-shell compositions of different targets in each compartment, which increases the potential this technique offers. For instance, different cell types can be entrapped in different layers of these µCaps, generating an injectable and structured type of co-culture system (Figure 2-9 c). This technique has been used to entrap cells as well as several molecules using different polymers including chitosan, poly(lactic acid) and alginate (Bertolo et al., 2015, Gasperini et al., 2013a, Xu and Hanna, 2008). For example, Sahoo *et al*. demonstrated that MSCs remain viable after spraying with high voltages up to 30 kV, with cells still retaining the ability to proliferate not losing their differentiation potential (Sahoo et al., 2010a). The EHDS process is not limited to the encapsulation of cells and has also been used to entrap signalling molecules such as cytokines, growth factors or other chemicals that may be beneficial for cells and/or microenvironment (Xu and Hanna, 2008). As these particles can be produced on a micro-sized scale, they are easily injectable through a needle in a minimally invasive manner. Depending on the properties of the delivery material and the encapsulated target, controlled drug release is possible (Naqvi et al., 2016b). Hereby, a target site, such as the IVD or the knee joint is treated with tailored µCaps containing drugs or signalling molecules (Figure 2-9 d-i). Depending on the material being used, an external signal (i.e. heat or ultrasonication) can be used to initiate the release of the entrapped molecules, allowing very specific treatment of target site(Figure 2-9 d-ii and iii).

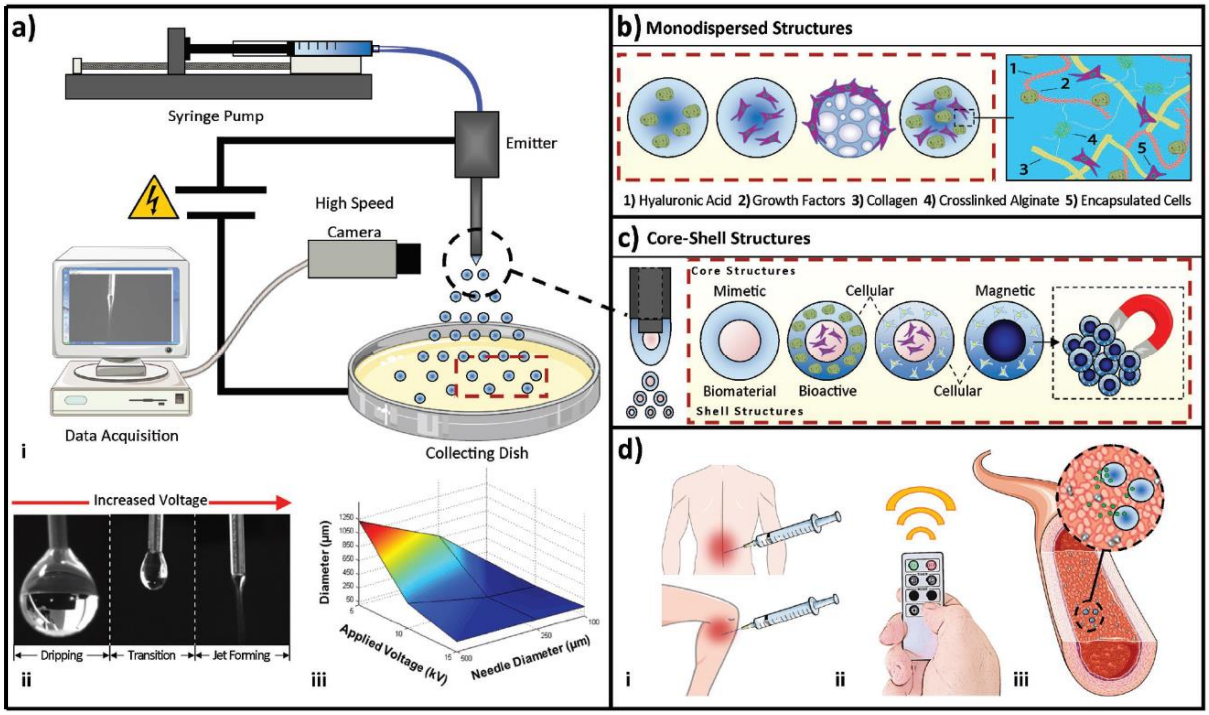

Figure 2-9: Principle and potential of EHD spraying technology a) (i) Schematic illustrating single needle arrangement for production of **µCaps** and microcarriers of uniform size using electrohydrodynamic (EHD) technology. **(ii)** Taylor cone formation with increasing applied voltage illustrating dripping zone (applied voltages have not overcome the effects of surface tension) transition zone (partial or intermittent jet formation) and jet forming zone. **(iii)** Influence of applied voltage and needle diameter on microcapsule size. **b)** Schematic representations of **µCaps** and microcarrier morphologies formed with various constituent configurations in monodispersed spraying mode. **c)** Coaxial spraying and different combinations and conformations of core-shell microcapsules. **d)** Potential application areas of **µCaps** and microcarriers **(i)** Injectable regenerative therapies **(ii)** Remote activation devices such as heat or ultrasonication **(iii)** Controlled spatiotemporal drug or cell release. (Naqvi et al., 2016b)

2.6. IVD model systems to assess the therapeutic potential

For any cell and biomaterial-based therapy being pursued, suitable models are required to fully assess their clinical potential prior to translation. *In vitro* models are beneficial for initial investigations as they allow high throughput of many different variables such as culture conditions, material type, and influence of biomolecules or cell densities in a small scale and comparable low budget. However, they do not clearly represent physiological conditions and cannot recapitulate the complex cell-tissue interactions accurately. There are many different aspects that need to be considered when choosing a suitable model to study the mechanical or biochemical conditions of human IVD. Firstly, humans are bipedal and therefore have unique

physical forces on the spine with an upright position. Furthermore, human discs are significantly larger in size than most discs found in common animal models such as mice, rabbits or rat. Besides the mechanical differences between large and small discs, nutrient diffusion also differs between different species. To overcome some of these limitations, large animal studies have been used including sheep, goats, pigs and dogs (Wilke et al., 1997, Huang et al., 2016). However, these models require strict ethical and regulatory approval and are also very costly. Therefore, these types of studies are more appropriate for late-stage investigations.

A viable and widely accepted approach to assess potential therapeutics for IVD regeneration in a more complex and translatable environment is through the use of *ex vivo* full organ culture models. Using bovine tail IVD explants is the most common model used for full organ culture, which has the advantage of higher throughput of different conditions being investigated compared to an *in vivo* model and further provides more accurate mechanical and structural environment compared to *in vitro* conditions. It has been shown that IVDs from bovine are very similar to human discs in terms of aspect ratios, nutrient transport distances and biochemical composition (Demers et al., 2004). In summary, organ culture systems permit the investigation of cellular and structural changes within the IVD in response to different biochemical signals and stimuli and serve as an essential preclinical tool prior to using large *in vivo* animal models. However, despite the advantages an *ex vivo* full organ culture provides, there are still limitations using this approach, including the creation of a consistent disc defect to evaluate regeneration approaches or precise analysis options such as biochemical analysis.

A more simplified version of the full organ culture is the explant model. Hereby, a section of the tissue is taken, modified or treated and evaluated in a smaller and more controllable scale. This reductionist approach allows individual aspects such as cell types to be assessed, inflammatory factors or microenvironmental cues and their different effects on cells, which is important for a better understanding of disc regeneration. It provides for an accessible means to interrogate individual aspects and serves as an intermediary between *in vitro* experiments and more complex *ex vivo* full organ culture models. It maintains many of the inherent advantages of

the full organ culture model such as the ability to conserve cells in their native tissue-structure environment, cellular composition and cell-cell configurations. For these reasons, the model has been used for various tissue types including bone (Chan et al., 2009, Staines et al., 2019), cartilage (Sah et al., 1989, Vinardell et al., 2009, Secretan et al., 2010, Vainieri et al., 2018), meniscus (Steinert et al., 2007, Grogan et al., 2013) and cornea tissue engineering (Foreman et al., 1996, Sabater et al., 2013, Zhou et al., 2015a, Castro et al., 2019). From a technical perspective using a scaled-down explant model has the added advantage of providing a consistent defect model as well as maintaining a known microenvironment with a minimal gradient across the disc tissue. Despite limitations associated with the explant model compared to *ex vivo* models, including loss of overall structure of the IVD and change the mechanical environment, it has the advantage to investigate the effect of different stimuli (i.e. microenvironment) on disc cells as well as on therapeutic cells due to defined separation of both compartments: disc ring and core gel.

Few studies have investigated the IVD in a smaller scale explant model. However, it was demonstrated that tissue swelling and PG loss due to the high osmotic pressure within the NP is one of the major challenges for this culture technique (van Dijk et al., 2011). Le Maitre *et al.* proposed to use a confined ring around the NP tissue to prevent swelling during culture and could successfully retain PGs within the tissue (Le Maitre et al., 2004b). Similar to bone or cartilage tissue, also in disc tissue the disc cells are directly attached to their surrounding matrix via integrins (Du et al., 2017, Bridgen et al., 2013). Integrins are transmembrane proteins that connect the intracellular cytoskeleton to fibronectin of the surrounding ECM. Using an explant model preserves these connections of the disc cells with their surroundings, which is essential for their functionality and facilitates signal transmission with neighbouring cells. Some tissue engineering approaches using the injection of BMSCs with or without a biomaterial into an NP explant have also been performed, demonstrating differentiation of BMSCs towards a chondrocyte like NP cells and matrix deposition (Figure 2-10) (Le Maitre et al., 2009, Thorpe et al., 2017). These results highlight the potential of explant models and their promising bridge between *in vitro* experiments and *ex vivo* studies before moving towards large *in vivo* models.

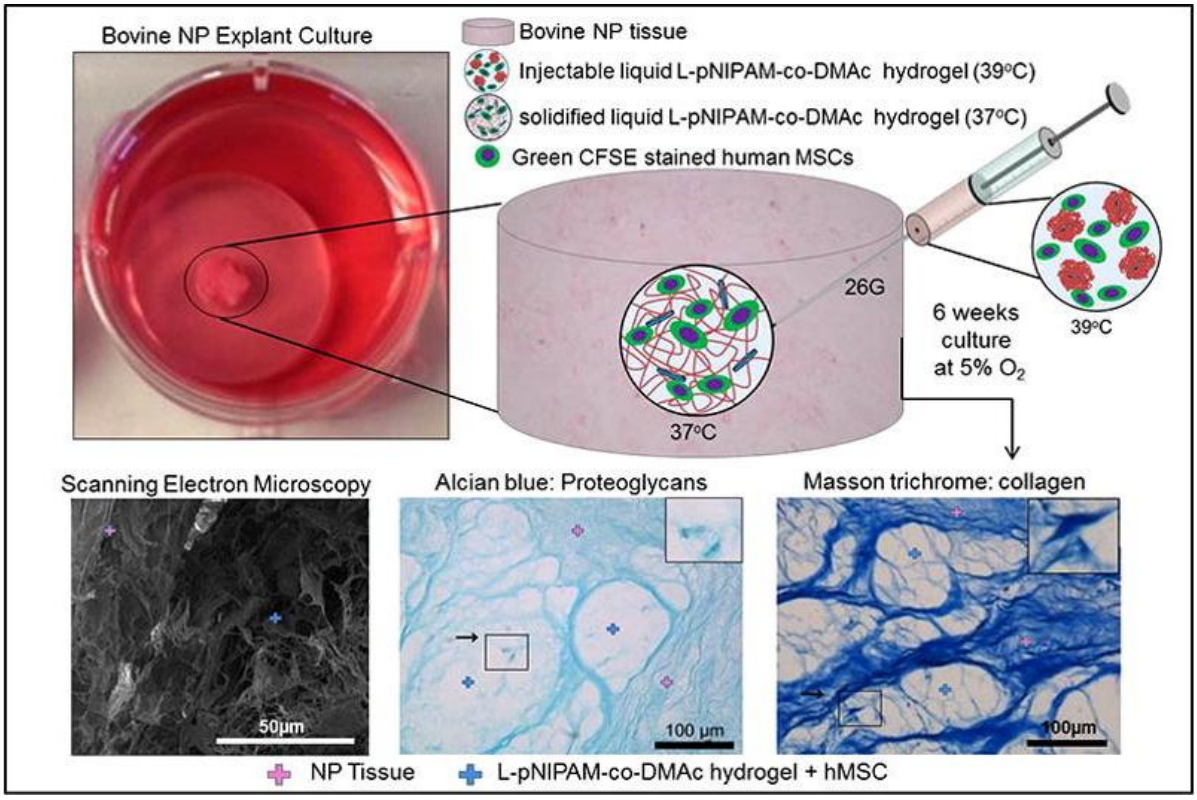

Figure 2-10: Use of NP explant model to investigate the matrix deposition capacities of BMSCs within a thermoresponsive hydrogel (Thorpe et al., 2017)

2.7. Summary

Current approaches for treatment of degenerative IVDs is predominantly focused on the symptoms, i.e. LBP. Yet, these therapies only allow short – to mid-term solutions with poor prospective of a long-term pain relief. This highlights the clinical need for alternative approaches for a long-lasting therapy and the overall improvement for a pain-free and active lifestyle. Strategies of regenerative medicine and tissue engineering have great potential to fill that gap. Using biomaterials in combination with metabolic active cells have been investigated in several clinical trials and demonstrated some improvements for treatment of DDD. However, further research is required for more sufficient success. Several challenges are associated with a good therapeutic for IVD repair. One of the main criteria for a good therapeutic is the invention of material, which can be injected in minimally invasive manner and prevents cell leakage during the injection procedure as well as allows efficient materials and cell deposition within the tissue,

which therefore enhances sustainability within the harsh disc environment (i.e. low oxygen, low glucose, low pH).

Therefore, this thesis designed and established an injectable, minimally invasive hydrogel that matches these requirements. Using EHDS, cells were entrapped into alginate µCaps, preventing cell leakage during injection. It was hypothesised that by using a viscous, bioactive bulking agent, the deposition of these cellular capsules could be maximised while improving matrix metabolism of cells within the tissue. Furthermore, this thesis aimed to improve the cellular response to the hostile acidic environment. Priming therapeutic cells for pre-differentiation and to initiate matrix deposition, it was conjectured that cells would improve their sustainability within the compromised disc conditions. Lastly this thesis considered using antacids to neutralize the local pH. Different models can be used to explore the potential of the suggested therapy strategy. With this novel approach of a hybrid hydrogel to target multiple challenges, a disc explant model seemed to be an appropriate choice as it allowed multiple aspects to be precisely examined in a higher throughput.

2.7.1 Specific aims

The previous sections highlight the challenges associated with regeneration of the IVD and different strategies to address them. In this work, the focus is on the use of an injectable cell-based therapy to restore matrix composition which could lead to reduce LBP in the future.

The overall aim of this thesis was to develop and investigate a minimally invasive material for cell-based therapies of the degenerated IVD. Specifically, two key challenges associated with this approach were addressed: (i) technical obstacles related to cell delivery into the highly pressurized disc and (ii) microenvironmental challenges associated with the acidity of the degenerated NP.

Technical obstacles are addressed in the first two results chapters of this work (chapter 4 and 5). Hereby EHDS technology was investigated and characterised in order to find optimal processing parameters for cellular microencapsulation. Specifically, the parameters were

optimized to minimize μCaps size with minimum cell damage. Furthermore, the aims were to find the optimal cell seeding density within these capsules to maximise matrix deposition for IVD repair (chapter 4). In chapter 5, the aim was to develop a biomimetic biomaterial that could enhance delivery of μCaps into the IVD as well as provide a matrix that could positively impact cells by incorporated ECM molecules (chapter 5).

The last two experimental chapters (chapter 6 and 7) aim to address the microenvironmental challenges with focus on the low pH levels found in degenerated IVD. Hereby, it was hypothesised that by using growth factor exposure prior to low pH conditions, cells would show enhanced sustainability compared to direct low pH culture. Therefore, in chapter 6 the intention was to maximize the cell viability and matrix deposition in acidic culture conditions. Lastly, chapter 7 focuses on the improvement of the local acidic environment overall, in order to aid therapeutic cells as well as resident cells to further increase matrix deposition and consequently regenerate IVD tissue.

CHAPTER 3
GENERAL METHODS

3.1. Cell isolation and monolayer expansion

Intervertebral discs (IVDs) were harvested from the lumbar region of the spine of porcine donors (3-4 months, 20-30 kg) within three hours of sacrifice. Under aseptic conditions, IVDs were carefully exposed and the gelatinous NP tissue removed from the central section of the disc (Naqvi and Buckley, 2015a). To confirm the absence of bacterial growth, dissected tissue was cultured overnight at 37°C, 5% CO_2 in a humidified atmosphere in serum-free low-glucose Dulbecco's Modified Eagles Medium (lg-DMEM, 1g/L D-glucose) supplemented with 100 U/mL penicillin, 100 μg/mL streptomycin. NP tissue was enzymatically digested in 2.5 mg/mL pronase solution for 1 hour followed by 2 hours in 0.5 mg/mL collagenase solution at 37°C under constant rotation. The digest was subjected to physical agitation cycles at the start, and every 30 min thereafter, using a Gentlemacs tissue dissociator (Miltenyi Biotech). Digested tissue/cell suspension was passed through a 100 μm cell strainer to remove tissue debris followed by 70 μm and 40 μm cell strainers to separate notochordal cells (NC) from the desired NP cells as previously described (Spillekom et al., 2014). Cells were then washed three times by repeated centrifugation at 650G for 5 minutes. NP cells were cultured to confluence in T-75cm^2 flasks with lg-DMEM, supplemented with 10% foetal bovine serum (FBS), 100 U/mL penicillin, 100 μg/mL streptomycin, 0.25 μg/mL amphotericin B (AmpB), 5 ng/mL FGF-2 (PeproTech, UK) at 37°C in a humidified atmosphere containing 5% CO_2, and expanded to passage 2 (P2) with medium exchanges performed every 3 days.

Porcine BMSCs were isolated and maintained as previously described (Naqvi and Buckley, 2015a). Briefly, mononuclear cells were isolated from the femora of 3-month-old porcine donors (~50 kg) within 2 hours of sacrifice and plated at 2.5×10^6 cells in 100 mm petri dishes to allow for colony formation. BMSCs were maintained in high-glucose DMEM (4.5 mg/mL D-Glucose, 200 mM L-Glutamine; hg-DMEM) supplemented with 10% FBS,

penicillin (100 U/mL)-streptomycin (100 µg/mL) (all GIBCO, Invitrogen, Dublin, Ireland) and AmpB (0.25 µg/mL, Sigma-Aldrich, Arklow, Ireland). Cultures were washed in Dulbecco's phosphate buffered saline (PBS) after 72 hrs. When passaged, BMSCs were plated at 5×10^3 cells/cm^2 and expanded to passage two (P2) in a humidified atmosphere at 37°C and 5% CO_2.

Juvenile porcine ACs were isolated from cartilage of the knee joint. Tissue was washed with PBS and finely minced. For cell isolation, minced tissue was digested with concentrations of 3000 U/mL collagenase type II (Gibco, Ireland) for ~2.5 h under constant rotation at 37°C in serum-free hg-DMEM, (4.5 mg/mL D Glucose, 200 mM L-Glutamine;) containing antibiotic/antimycotic (100 U/mL penicillin, 100 mg/mL streptomycin) (all Gibco, Invitrogen) and AmpB (0.25 µg/mL, Sigma-Aldrich). The digest was subjected to physical agitation cycles at the start, and every 30 min thereafter, using a Gentlemacs tissue dissociator (Miltenyi Biotech). The digested tissue/cell suspension was passed through a 100 µm cell strainer to remove tissue debris and washed three times by repeated centrifugation at 650 g for 5 min. Cell viability was determined with a haemocytometer and trypan blue exclusion. Cells were seeded at an initial density of 5×10^3 cells/cm^2 in media consisting of lg-DMEM (1 mg/mL D-Glucose, Sigma) supplemented with 10% FBS, penicillin (100 U/mL)-streptomycin (100 µg/mL) (all GIBCO, Invitrogen, Dublin, Ireland) and AmpB (0.25 µg/mL, Sigma-Aldrich, Arklow, Ireland) at 37°C and 5% CO_2 and cultured until passage 1 (~14 days).

3.2. Assessment of cell viability

Cell viability was assessed using the LIVE/DEAD® viability/cytotoxicity assay kit (Invitrogen, Ireland). Constructs were removed from culture, cut in half and incubated in phenol free DMEM media containing 2 µM calcein AM and 4 µM ethidium homodimer-1 (EthD-1) (both from Cambridge Bioscience, Cambridge, UK) for one hour at 37°C. Following incubation, constructs were imaged with a Leica SP8 scanning confocal microscope at 515 and 615 nm channels and analysed using Leica Application Suit X (LAS X) Software.

3.3. Cell shape analysis

µCaps were fixed with 4% paraformaldehyde (PFA), thoroughly washed in PBS and permeabilised using 0.5% Triton-X. Fluorescent dyes were prepared in 1.5% bovine serum albumin (BSA) solution (Rhodamine Phalloidin dilution 1:40; 1:1000 dilution for DAPI) and incubated with samples in the dark at room temperature (1h Rhodamine Phalloidin, 10 minutes for DAPI). Stained samples were subsequently imaged with a Leica SP8 scanning confocal at 358/524 and 540/565 nm channels and assessed using Leica Application Suit X (LAS X) Software.

3.4. Quantitative Biochemical Analysis

Samples were digested with papain (125 µg/mL) in 0.1 M sodium acetate, 5 mM L-cysteine HCl, 0.05 M EDTA and sodium citrate (55 mM) (Sigma-Aldrich, Ireland) at 60°C under constant agitation for 18 hours followed by an additional incubation with 1 M sodium citrate under constant rotation for 1h to disrupt the alginate-calcium crosslinks. DNA content of each sample was quantified using the Hoechst Bisbenzimide 33258 dye assay, with a calf thymus DNA standard. PG content was estimated by quantifying the amount of sulphated glycosaminoglycan (sGAG) in constructs using the dimethylmethylene blue dye-binding assay (DMMB Blyscan, Biocolor Ltd., Northern Ireland, UK), with a chondroitin sulphate standard. Total collagen content was determined by measuring the hydroxyproline content. Samples were hydrolysed at 110°C for 18 hours in concentrated HCl (38%) and assayed using a chloramine-T assay (Kafienah and Sims, 2004), using a hydroxyproline-to-collagen ratio of 1:7.69 (Ignat'eva et al., 2007).

3.5. Histological and Immunohistochemical Analysis

At each time point, samples were fixed in 4% PFA overnight at 4°C, followed by repeated washings in PBS. Fixed samples were dehydrated in a graded series of ethanol (70% to 100%), embedded in paraffin wax, sectioned at 6 µm, and affixed to microscope slides. Sections were stained with 1% alcian blue 8GX in 0.1 M HCL (alcian blue / aldehyde fuchsin for alginate –

based samples) to assess sGAG content and picrosirius red to assess collagen distribution (all from Sigma-Aldrich).

Collagen types I and II were evaluated using a standard immunohistochemical technique. Briefly, sections were treated with peroxidase, followed by treatment with chondroitinase ABC (Sigma-Aldrich) in a humidified environment at 37°C to enhance permeability of the ECM. Sections were incubated with goat serum to block non-specific sites and Col1 (ab90395, 1:400; 1 mg/mL, mouse monoclonal, Abcam, Cambridge, UK) or Col2 (sc-52658, 1:400; 1 mg/mL, mouse monoclonal, Santa Cruz, Dallas, USA) primary antibodies were applied for 18 hr at 4°C. Next, the secondary antibody (Anti-Mouse IgG biotin conjugate, 1.5:200 for Col1 and 1:300 for Col2; 2.1 mg/mL, B7151, Sigma-Aldrich) was added for 1 h followed by incubation with ABC reagent (Vectastain PK-400, Vector Labs, Peterborough, UK) for 45 min. Finally, sections were developed with DAB peroxidase (Vector Labs) for 5 min. Positive and negative controls were included in the immunohistochemistry staining protocol for each batch.

CHAPTER 4
INFLUENCE OF KEY PROCESSING PARAMETERS AND SEEDING DENSITY EFFECTS OF MICROENCAPSULATED CHONDROCYTES FABRICATED USING ELECTROHYDRODYNAMIC SPRAYING

The first research chapter addressed the first two objectives of this thesis and explores the EHDS technology and how it can be used for encapsulation of cells into µCaps of controlled size and shape.

4.1. Introduction

As described in chapter 2, IVD degeneration includes several changes including loss in a viable cell population and associated cell senescence. Cellular repopulation strategies such as ADCT have been proposed as a potential treatment for IVD degeneration (Hohaus et al., 2008, Meisel et al., 2006, Meisel et al., 2007). A major challenge with treating the NP of the IVD relates to it being an encapsulated region posing significant challenges for delivery and retention of transplanted cells especially cell leakage from the target site during needle injection (Vadala et al., 2012, Li et al., 2014a). For example, it has previously been demonstrated that injecting a cell suspension into the lumbar IVDs of rabbits resulted in a 90% loss of the injected cells within the first 30 minutes (Bertram et al., 2005). In addition, the needle diameter employed can have a significant impact with larger diameters responsible for inducing damage in the AF, the concentric ring structured tissue around the NP, and thus accelerating disc degeneration (Michalek et al., 2010).

Cell microencapsulation and delivery of microcapsules or micro-hydrogels is a promising and attractive approach to repair damaged tissue in a minimally invasive manner (Wang et al.,

2013, Wang and Stegemann, 2011, Wise et al., 2014) augmenting cellular retention and permitting targeted delivery. Specifically microencapsulation provides (i) a tailored 3D cellular niche environment to direct specific cellular differentiation and function (ii) protection from shear forces during delivery via injection (iii) targeted site delivery and (iv) high surface to volume ratio thereby minimising mass transfer limitations (Nogués et al., 2013b).

Several microencapsulation techniques have been established, as outlined in Chapter 2, Paragraph 2.5.3 “Microencapsulation”, page 37. In this chapter, the focus is on

a microfluidic based process, which involves the passing of a cell-polymer solution through a small aperture such as a needle/nozzle into a solution that contains the cross-linking agent, which in turn stabilizes the bead/capsule (Kang et al., 2014). One such technology that can be used to microencapsulate cells is EHDS, also known as electrohydrodynamic atomisation, which is a single step process requiring no additional solvents other than those usually present in suspension and can be performed under ambient conditions (Sahoo et al., 2010b). Using this versatile technique, micron sized capsules can be fabricated by subjecting a polymer/cell solution through a nozzle which is connected to a high voltage power supply followed by subsequent crosslinking (Gasperini et al., 2013b). During EHDS, a high electric potential difference between the source of flow (usually from a needle tip) and an earthed substrate (such as a crosslinking solution) is applied. Depending on the physicochemical properties of the solution, as the potential is increased the imposed electrical forces overcome the effects of surface tension when a critical charge is reached, deforming the flowing polymer into a conical shape, known as a Taylor cone from which a fine jet develops breaking up into charged droplets that are attracted towards the earthed substrate (Gasperini et al., 2013b, Workman et al., 2014, Enayati et al., 2011a). By using an aqueous polymer, such as alginate, in combination with cells, encapsulation into micron sized capsules can be performed (Workman et al., 2014). Most importantly, it facilitates fabricating µCaps from the micrometre to millimetre scale with a narrow size distribution (Enayati et al., 2011a). As such, it is a scalable technology that may have potential for application in the field of cell microencapsulation for minimally invasive tissue repair. With respect to disc repair strategies

desirable criteria of cell laden μCaps would include i) spherical shaped to facilitate nutrient transport and ii) maximum diameter of ~250 μm to be compatible with injecting through a small-bore needle typically used for intradiscal injections to avoid AF damage during this process.

Therefore, the primary objective of this work was to ascertain the effects of key processing parameters (applied voltage, needle diameter, applied flow rate and viscosity of the encapsulating polymer) to regulate the size and shape of alginate μCaps and subsequent viability of microencapsulated chondrocytes (Study 1). Additional *in vitro* experiments were performed for optimized parameters at three different seeding densities (5, 10 and $20x10^6$ cells/ml) to determine the development of ECM when cultured in disc-like conditions of low glucose and low oxygen (Study 2).

4.2. Methods

4.2.1 Experimental design

Study 1: Effects of key processing parameters on microcapsule size, shape and cell viability

For stage 1, acellular alginate μCaps were fabricated using EHDS at various applied voltages (0 kV 5 kV, 10 kV and 15 kV) and emitter needle diameters (with 21G; internal diameter 0.51 mm, 26G; internal diameter 0.26 mm and 30G; internal diameter 0.16 mm) while the alginate concentration (1% w/v in PBS), applied flow rate (100 μL/min) and working distance (50 mm) were maintained constant. For stage 2, μCaps were fabricated at flow rates of 50, 100, 250 and 500 μL/min with 1, 2 and 3% alginate solutions, while applied voltage (10 kV) and needle gauge (30G) were maintained constant. In stage 3, ACs were encapsulated in alginate (1, 2 and 3% w/v in PBS) to assess the effect of needle gauge (21G, 26G, 30G) using an applied voltage of 10 kV and flow rate of 100 μL/min (3.1). In addition, the effect of flow rate (50, 100, 250 and 500 μL/min) was investigated when using a 3% alginate solution (3.2). The assessment was performed in terms of cell viability within 1hr post fabrication and after seven days of culture. In stage 4, the effect of applied voltage (5 kV, 10 kV and 15 kV) on cell viability was investigated

(1% alginate, needle gauge: 30G; flow rate of 100 µL/min). A summary of stages and parameters investigated is provided in Table 4-1.

Table 4-1: Key parameters investigated using electro hydrodynamic spraying (EHDS) process for stages 1-4.

Stage	Cellular	Voltage (kV)	Needle Gauge	Flow Rate (µL/min)	Alginate Conc. (%)
1	No	**0 5 10 15**	**21G 26G 30G**	100	1
2	No	10	30G	**50 100 250 500**	**1 2 3**
3.1	Yes	10	**21G 26G 30G**	100	**1 2 3**
3.2	Yes	10	30G	**50 100 250 500**	3
4.	Yes	**5 10 15**	30G	100	1

Study 2: Effect of seeding density on chondrocyte viability and subsequent matrix synthesis

µCaps containing ACs were fabricated under optimized processing parameters determined from study 1 (applied voltage: 10 kV, 30G; inner needle diameter: 0.16 mm, flow rate: 100 µL/min and 1% alginate) at three seeding densities: $5x10^6$ cells/mL, $10x10^6$ cells/mL and $20x10^6$ cells/mL. µCaps were cultured for 28 days in low oxygen (5% O_2) and low glucose (5 mM) conditions. At day 0 and day 28 µCaps were assessed in terms of cell viability, biochemical content (sGAG, collagen) and histologically.

4.2.2 Rheology of the sodium alginate solutions of different concentrations

The rheological properties of different alginate concentrations (1, 2 and 3% w/v in PBS) were assessed using a Discovery HR-1 rheometer (TA Instruments, USA), at 25ºC with a 40 mm

steel plate as test geometry. Solutions were tested for their shear thinning behaviour (viscosity as a function of shear rate) under a steady state flow protocol, performed from 100-4000 s^{-1}. Each sample was dispensed onto the rheometer plate in liquid state. The geometry was lowered to the desired gap height and excess liquid was discarded prior to the applied testing sequence.

4.2.3 Electrohydrodynamic spraying process

A Spraybase® electrosprayer (Profector Life Sciences, Dublin, Ireland) was used for all experiments. This is an integrated system consisting of a high voltage generator, collecting dish and camera (Figure 4-1 A). The working distance which is the distance from the needle tip to the collecting dish was maintained at 50 mm for all experiments (Figure 4-1 B). A syringe containing alginate solution (Pronova UP LVG, FMC NovaMatrix, Norway) was placed into a syringe pump (KD Scientific, Gemini 88, Holliston, USA) and delivered at a constant flow rate (50, 100, 250 or 500 µL/min). Simultaneously the voltage was increased to the desired level (0, 5, 10 and 15 kV) to induce Taylor cone formation (Figure 4-1 C). Microcapsules were collected in a dish containing 100 mM calcium chloride ($CaCl_2$) to ionically crosslink the alginate hydrogel (5 minutes) and subsequently washed with ultra-pure water (UPW).

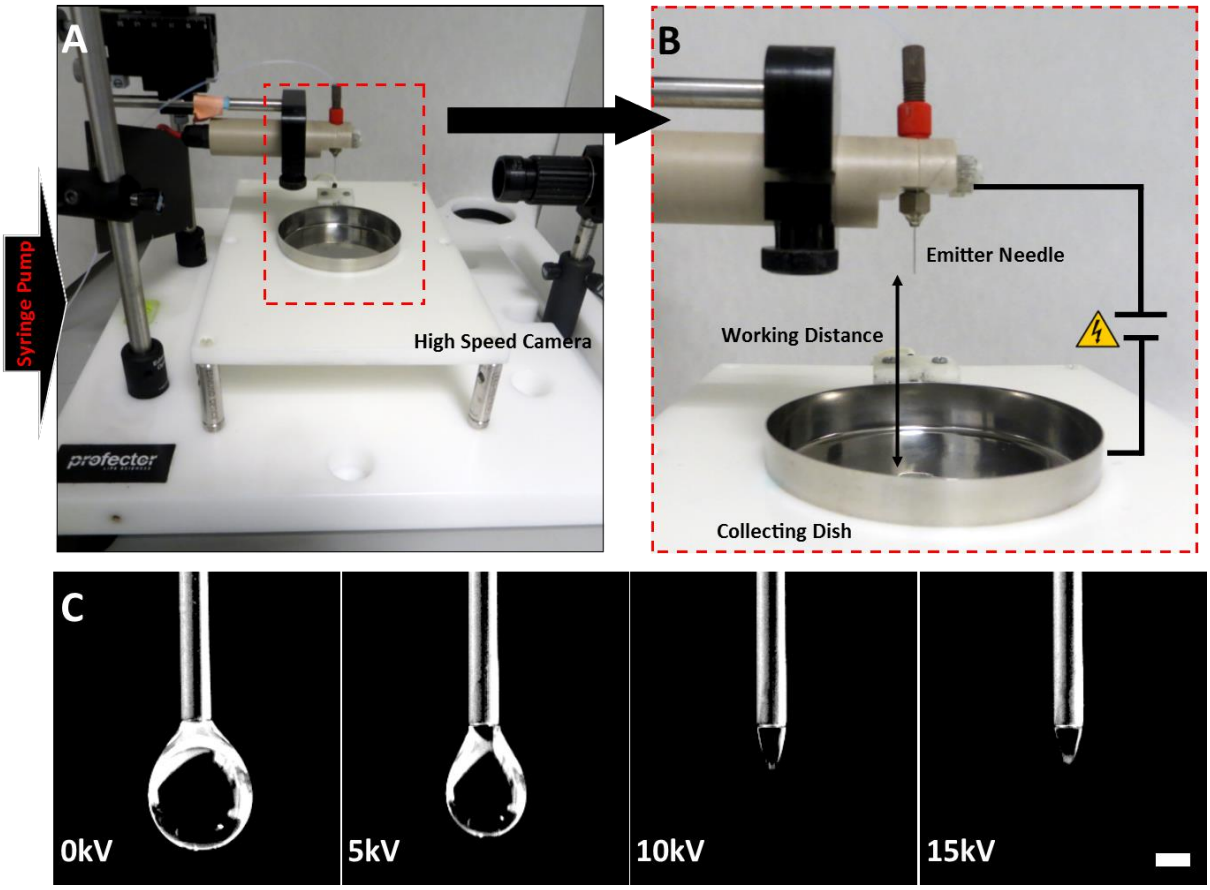

Figure 4-1: EHDS experimental arrangement (A) Assembled integrated Spraybase® system **(B)** Housed 30G needle and grounded collecting dish **(C)** Captured images demonstrating the effect of increasing applied voltage on Taylor cone formation for a 1% alginate solution and 26G needle. Scale bar= 1 mm.

4.2.4 Microcapsule image analysis

To facilitate visualisation, fabricated µCaps were stained in 1% alcian blue (8GX, Sigma Aldrich, Ireland) in 0.1 M HCl for 5 minutes and then washed thoroughly with UPW. Microcapsules were imaged using light microscopy and microcapsule diameters were determined using image analysis software (ImageJ, National Institutes of Health, and Bethesda, Maryland).

4.2.5 Cellular microencapsulation

For study 1, cells were trypsinised and re-suspended in media and combined with sterile alginate solution (Pronova UP LVG, FMC NovaMatrix, Norway) at a 1:1 ratio to yield the desired concentration (1, 2 or 3%) and a final seeding density of $10x10^6$ cells/mL. The alginate/cell

solution was electrosprayed into 100 mM $CaCl_2$, pH 7.2. For each batch, µCaps were crosslinked for 5 minutes and rinsed thoroughly with PBS.

For study 2 all processing parameters were maintained constant (30G needle, 10 kV applied voltage, 100 µL/mL flow rate, 50 mm working distance, 1% final alginate concentration) and µCaps were fabricated at three seeding densities (5, 10 and $20x10^6$ cells/mL). Microcapsules were cultured in 5 mL tubes with 100 µL of µCaps per tube in 2 mL of chemically defined medium (CDM) consisting of lg-DMEM, (1 mg/mL D-Glucose) supplemented with penicillin (100 U/mL)-streptomycin (100 µg/mL), (both from GIBCO, Invitrogen, Ireland), 0.25 µg/mL AmpB, 40 µg/mL L-proline, 1.5 mg/mL BSA, 4.7 µg/mL linoleic acid, 1× insulin–transferrin–selenium, 50 µg/mL L-ascorbic acid-2-phosphate and 100 nM dexamethasone (all Sigma-Aldrich, Ireland). All cultures were maintained in a low oxygen environment (5% O_2) to mimic native disc conditions (Naqvi and Buckley, 2015b). Half of the media was changed twice weekly.

4.2.6 Statistical analysis

Statistical analysis was performed using GraphPad Prism (version 6) with 3 samples analysed for each experimental group of 3 individual experiments of different porcine donors. Two-way ANOVA was used for analysis of variance in study 1 with Tukey's multiple comparison tests to compare between groups. One-way ANOVA was used for analysis of variance in study 2 with Tukey's multiple comparisons to test between groups. Numerical and graphical results are displayed as mean ± standard deviation (SD). Significance was accepted at a level of $p < 0.05$.

4.3. Results

4.3.1 Increasing applied voltage and decreasing needle size reduces microcapsule size

Results show that applied voltage had a significant effect on microcapsule diameter with higher voltages resulting in smaller µCaps being formed (Figure 4-2). For example, a 21G needle

(inner diameter = 0.508 mm) operating at 0 kV, 5 kV, 10 kV and 15 kV yielded microcapsule diameters ranging from 2959 ± 261.9 µm at 0 kV, to 2241.9 ± 242.3 µm at 5 kV, 494.1 ± 217.4 µm at 10 kV, and 235 ± 142.8 µm at 15 kV respectively (Figure 4-2 A). Needle gauge also had an effect on microcapsule diameter. However, for larger needle diameters, the voltage appeared to have a greater influence on microcapsule size. For example, a 21G needle under operation at 10 kV and flow rate of 100 µL/min generated µCaps with a mean diameter of 494.1 ± 217.4 µm, a 26G needle (inner diameter 0.250 mm) under these same operating parameters resulted in µCaps of diameter 212.5 ± 102.9 µm and the smallest microcapsule diameter was observed with a 30G needle (inner diameter 0.108 mm) at this voltage (151.6 ± 63 µm). Figure 4-2 B illustrates the influence of voltage and needle gauge on capsule size demonstrating that voltage is more influential than needle size overall.

In general, µCaps with a spherical morphology were observed (Figure 4-2 C). However, it is evident that for some processing parameter combinations, broad distributions of microcapsule sizes were obtained. Another observation was the formation of two distinct populations of sizes for different settings. For example, it can be seen in the histogram of 30G and 15 kV- settings, two different peaks at around 75 µm and 220 µm.

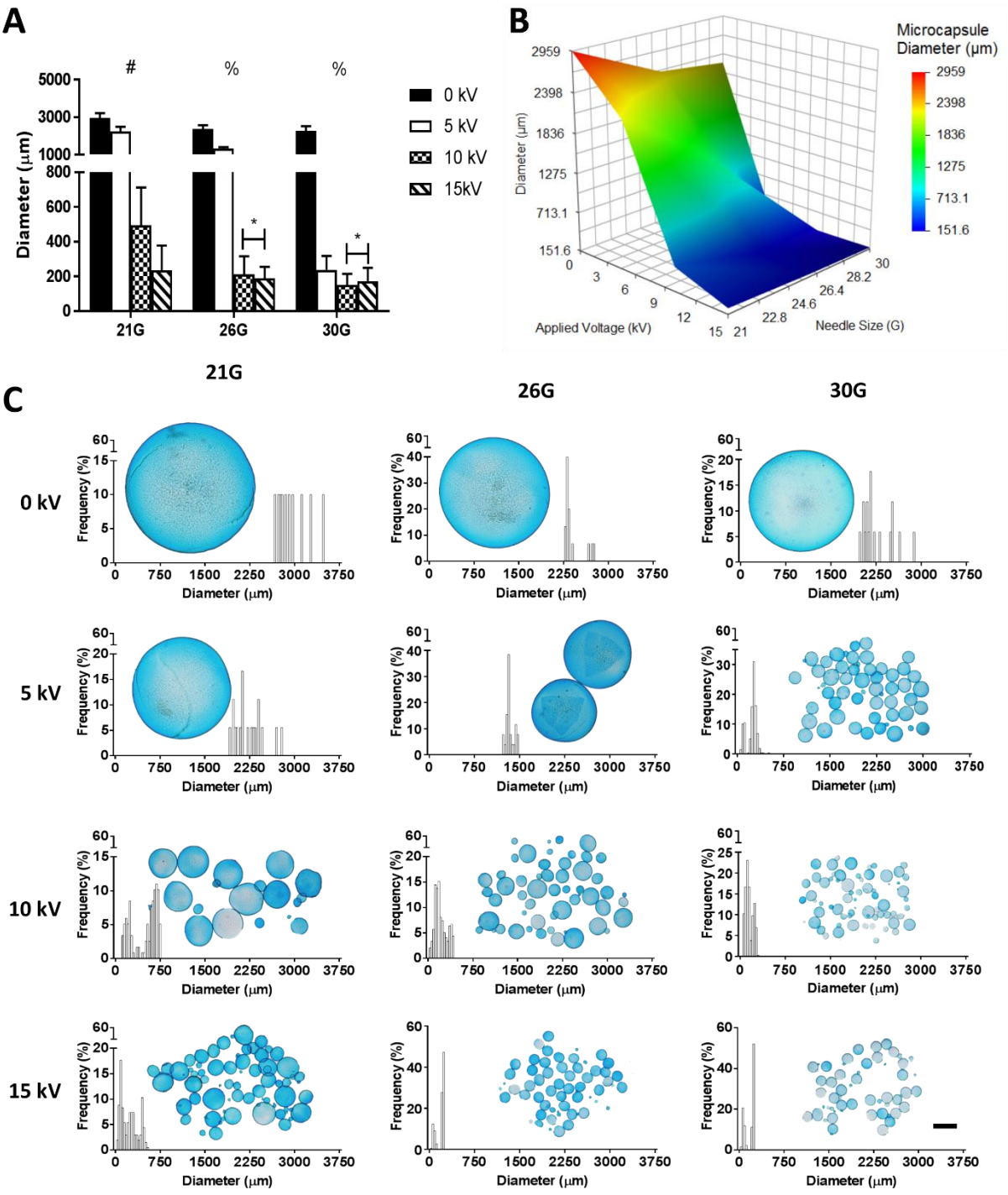

Figure 4-2: Effect of key processing parameters of applied voltage and needle gauge on alginate microcapsule diameter (A) Effect of voltage (0, 5, 10 and 15 kV) and needle gauge (21G, 26G and 30G) on microcapsule diameter of acellular alginate. # indicates significant difference between all voltages at 21G ($p<0.0001$), % indicates significant difference between all voltages with given needle, except 10 and 15 kV ($p<0.0001$), ! indicates significant difference between 21G and all other needle gauges at 15 kV ($p<0.0001$) and * indicates significant difference between 10 and 15 kV ($p<0.05$) **(B)** Contour map illustrating the influence of applied voltage and needle diameter on microcapsule size. **(C)** Visual assessment of microcapsule size. Histogram inserts demonstrate the population distributions of µCaps obtained for different applied voltages and needle gauges. Scale bar=500 µm.

4.3.2 Hydrogel concentration and applied flow rate effects on microcapsule size and morphology

Increasing the concentration of the polymeric solution alginate and therefore the viscosity resulted in changes in microcapsule size from 167.9 ±77.1 µm (1%) to 333.5 ±165.2 µm (3%) (Figure 4-3 A & B). On measuring viscosity of the different alginate solutions, shear thinning was observed for all groups when increasing the shear rate with an overall higher viscosity for higher concentrations (Figure 4-3 C). All data shown were fabricated with a constant flow rate of 50 µL/min as a representative group. Overall, µCaps produced at higher flow rates were larger in size with increasing alginate concentration (Appendix 1, page xxiii).

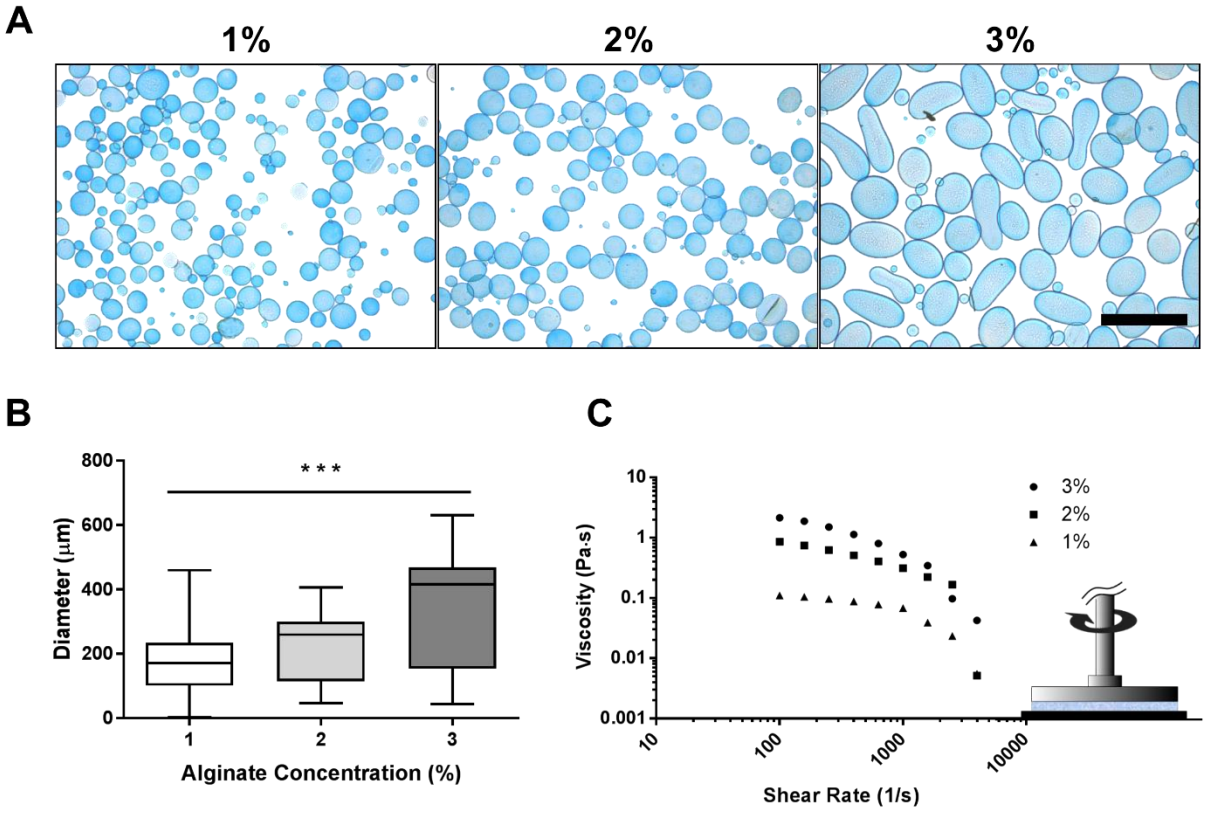

Figure 4-3: Effect of key processing parameters of alginate concentration (1, 2, 3%) on microcapsule size and viscosity. (A) Visual assessment of change in microcapsule size with changing concentrations for a flow rate of 50 µL/min. Scale bar =1000 µm. **(B)** Distribution of diameters depending on concentration. *** ($p<0.0001$) indicates difference between all groups **(C)** Effect of shear rate on viscosity of different alginate concentrations investigated.

With increasing alginate concentration, and thus the viscosity of the solution, flow rate had an effect with larger (flow rate of 50 µL/min) and ellipsoidal shaped (flow rate of 250 µL/min) µCaps formed with 3% alginate concentration solutions (Figure 4-4 A and B). Further, when investigating cell viability at the same parameters (high viscosity and different flow rates), a high percentage of live cells was observed for all groups with no significant differences observed between different flow rates (Figure 4-4 A and C).

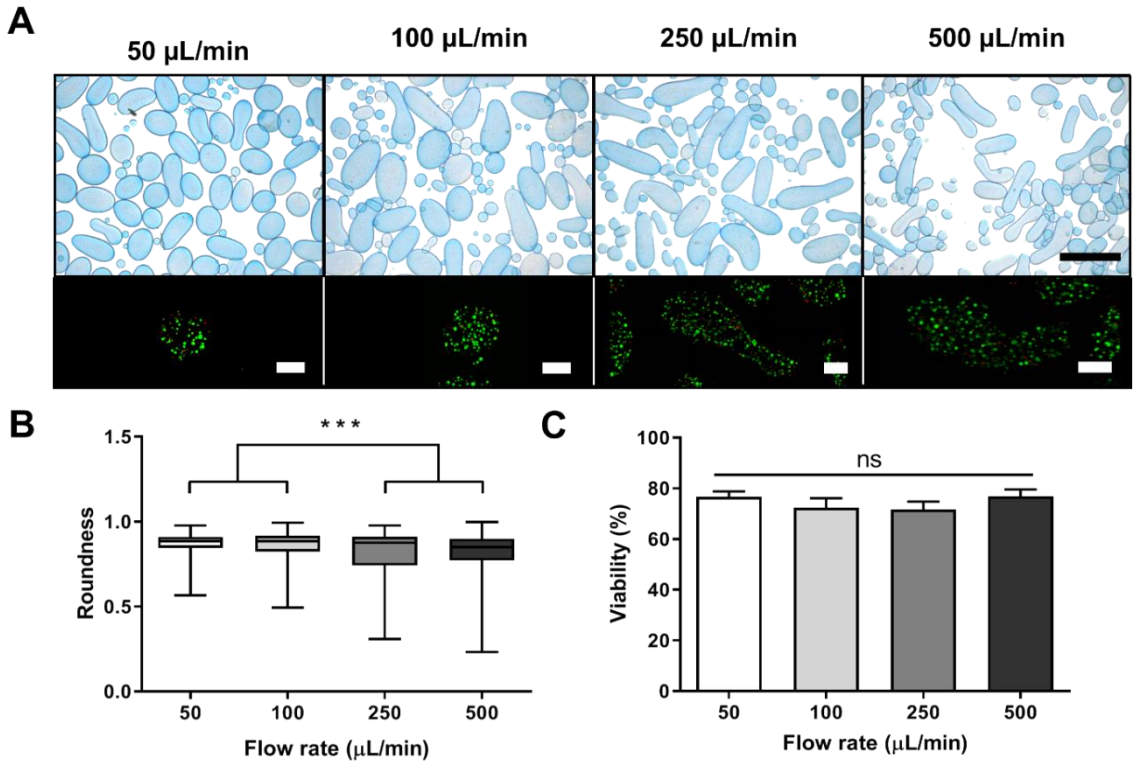

Figure 4-4: Change in shape with increasing flow rate (50, 100, 250 and 500 µL/min) (A) Visual assessment of change in shape and cell viability with increasing flow rate. Scale bar= 1 mm (acellular) and 200 µm (cellular). **(B)** Roundness of capsules sprayed using 3% alginate and different flow rates. *** ($p<0.0001$) indicates difference between groups. **(C)** Semi-quantitative image analysis of cell viability for **µCaps** formed using 3% alginate sprayed at different flow rates.

4.3.3 Higher concentrations/viscosities have a detrimental effect on cell viability which is exacerbated with smaller needle diameters

Live/Dead viability assessment was performed to investigate the effects of the EHDS process on chondrocytes for increasing alginate concentration (1, 2 and 3%) and needle gauge (21G, 26G and 30G) (Figure 4-5). A more well-defined Taylor cone formation was observed for

lower alginate concentrations (Figure 4-5 A). Cell viability was found to diminish with increasing concentration and thus a higher viscosity irrespective of needle size with significantly lower viability when using 3% alginate (Figure 4-5 B). Interestingly, there was partial recovery or an increase in cell viability after 7 days of culture for all experimental groups investigated (Figure 4-5 C). When comparing the effect of different applied voltages (5, 10 and 15 kV) after 7 days cell viability was not compromised at voltages up to 10 kV, with a minor detrimental effect observed at 15 kV (Figure 4-5 D, E).

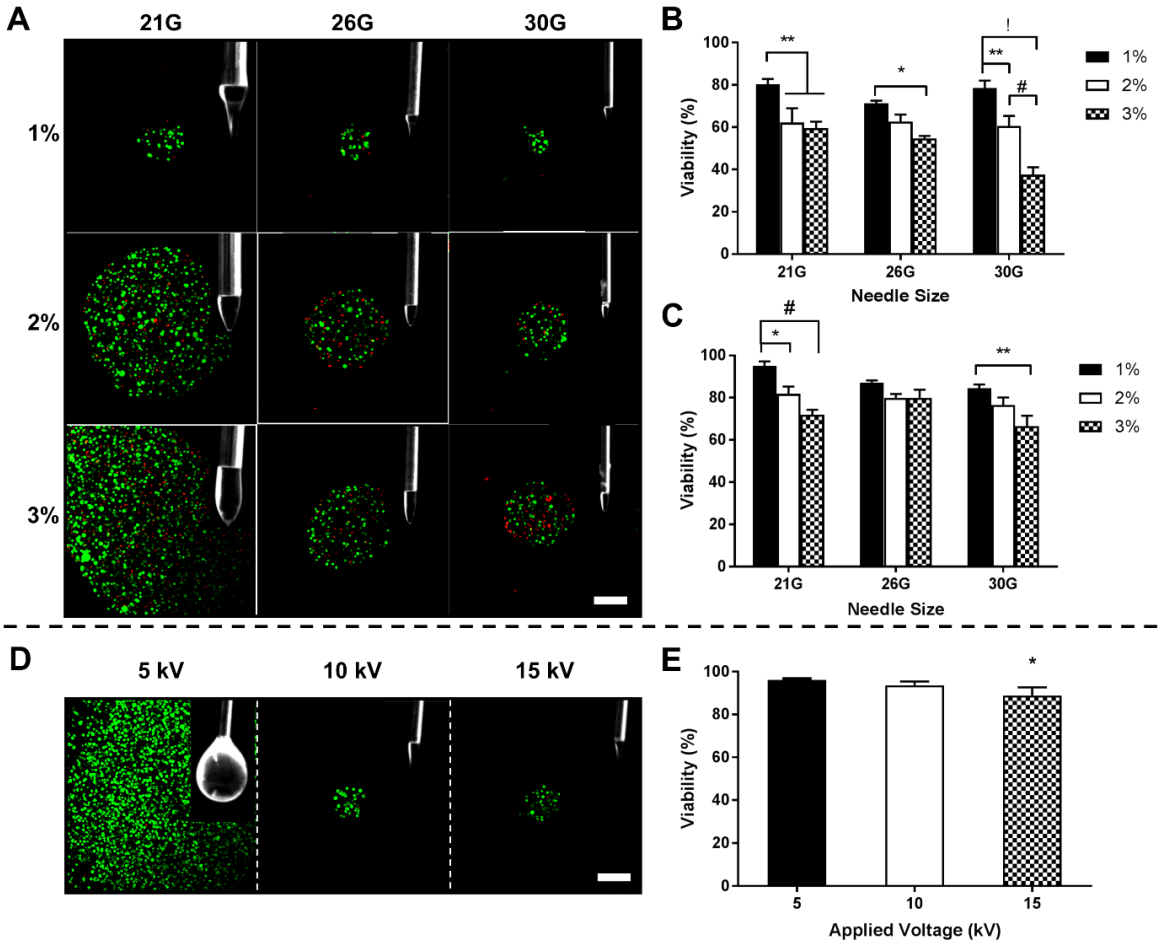

Figure 4-5: Effect of key processing parameters on cell viability (A) Live/Dead assessment of chondrocytes after spraying with varying needle size (21G, 26G and 30G) and alginate concentration (1, 2 and 3%) at day 0. Insets depict cone formation from needle tip. Scale bar =200 µm **(B)** Semi-quantitative image analysis of alginate concentration and needle size effects on cell viability at day 0 **(C)** Semi-quantitative image analysis of alginate concentration and needle size effects on cell viability at day 7. * ($p<0.05$), ** ($p<0.01$), # ($p<0.001$) and ! ($p<0.0001$) indicate differences between groups **(D)** Live/Dead images of ACs encapsulated in 1% alginate sprayed with 5, 10 and 15 kV respectively at day 7. Scale bar= 200 µm. **(E)** Semi quantitative image analysis of cell viability at day 7. * indicates significant difference between 5 and 15 kV, $p<0.05$.

4.3.4 Injection of capsules through a 25G needle has no detrimental effect on cell viability

To confirm the injectability of fabricated µCaps and subsequent potential for minimally invasive treatment for IVD degeneration, cellular µCaps produced with different needles were passed through a 25G needle (internal diameter 0.26 mm). Results show no significant difference in terms of cell viability post injection regardless of needle size (Figure 4-6). However, capsules sprayed with the larger 21G needle were too large in diameter and disrupted when passing through the 25G needle, resulting in bigger difference of cell viability of pre-and post-injection compared to all other groups (Figure 4-6 B).

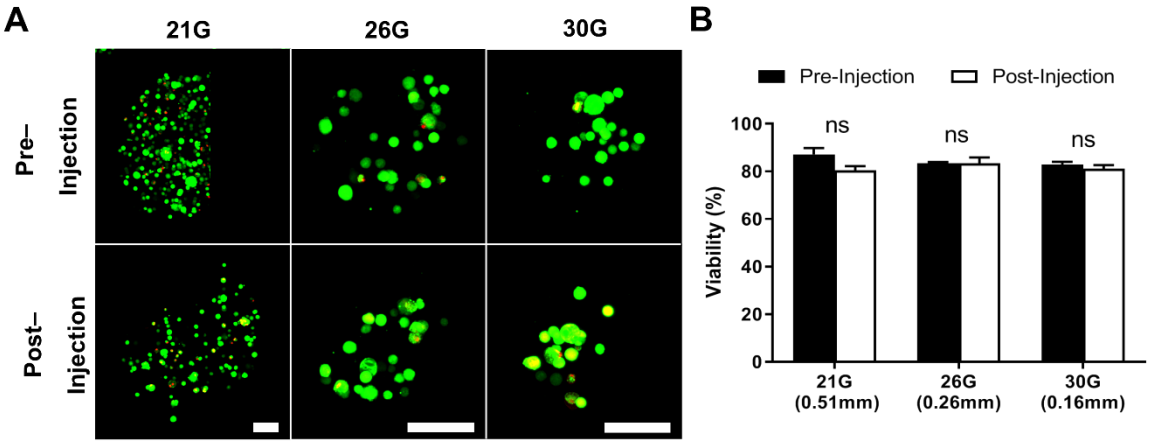

Figure 4-6: Microcapsules fabricated using 21G, 26G and 30G needles pre- and post-injection through a 25G needle (A) Live/Dead confocal images scale bar = 100 µm**. (B)** Semi-quantitative image analysis of cell viability (%) pre- and post- injection of different groups.

Based on these results, for the subsequent *in vitro* cell density culture experiments, a 30G needle operating at 10 kV with a flow rate of 100 µL/min was selected which yielded a population of µCaps of diameter, 151.6 ± 63 µm, with sufficient cell viability pre- and post- injection through a 25G needle.

4.3.5 Higher initial seeding density leads to diminished cell viability

Chondrocytes were encapsulated in 1% alginate at different densities (5, 10 and $20x10^6$ cells/mL). A trend for diminished cell viability was observed with increasing cell density immediately after encapsulation which became more pronounced after 28 days of culture (Figure 4-7 A). A change in cell morphology however was not observed, showing a rounded shape at day 0 and day 28 for all seeding densities investigated (Figure 4-7 A). Semi-quantitative image analysis revealed viability levels of 78 ±1.6%, 66.4 ± 6.8% and 66.2 ± 4.4% for 5, 10 and $20x10^6$ cells/mL initial seeding density respectively. After 28 days, elevated cell death was observed in all groups with decreased viability for increasing initial seeding density (Figure 4-7 B). For example, cell viability in the lowest seeding density ($5x10^6$ cells/mL) decreased by 16% from day 0 to day 28 whereas the viability of the medium ($10x10^6$ cells/mL) seeding density reduced by 33% and the highest seeding density group reduced by 50%. Biochemical data was found to correlate with Live/Dead staining, demonstrating decreasing total DNA content after 28 days with a significant difference relative to day 0 for an initial seeding density of $10x10^6$ and $20x10^6$ cells/mL (Figure 4-7 C).

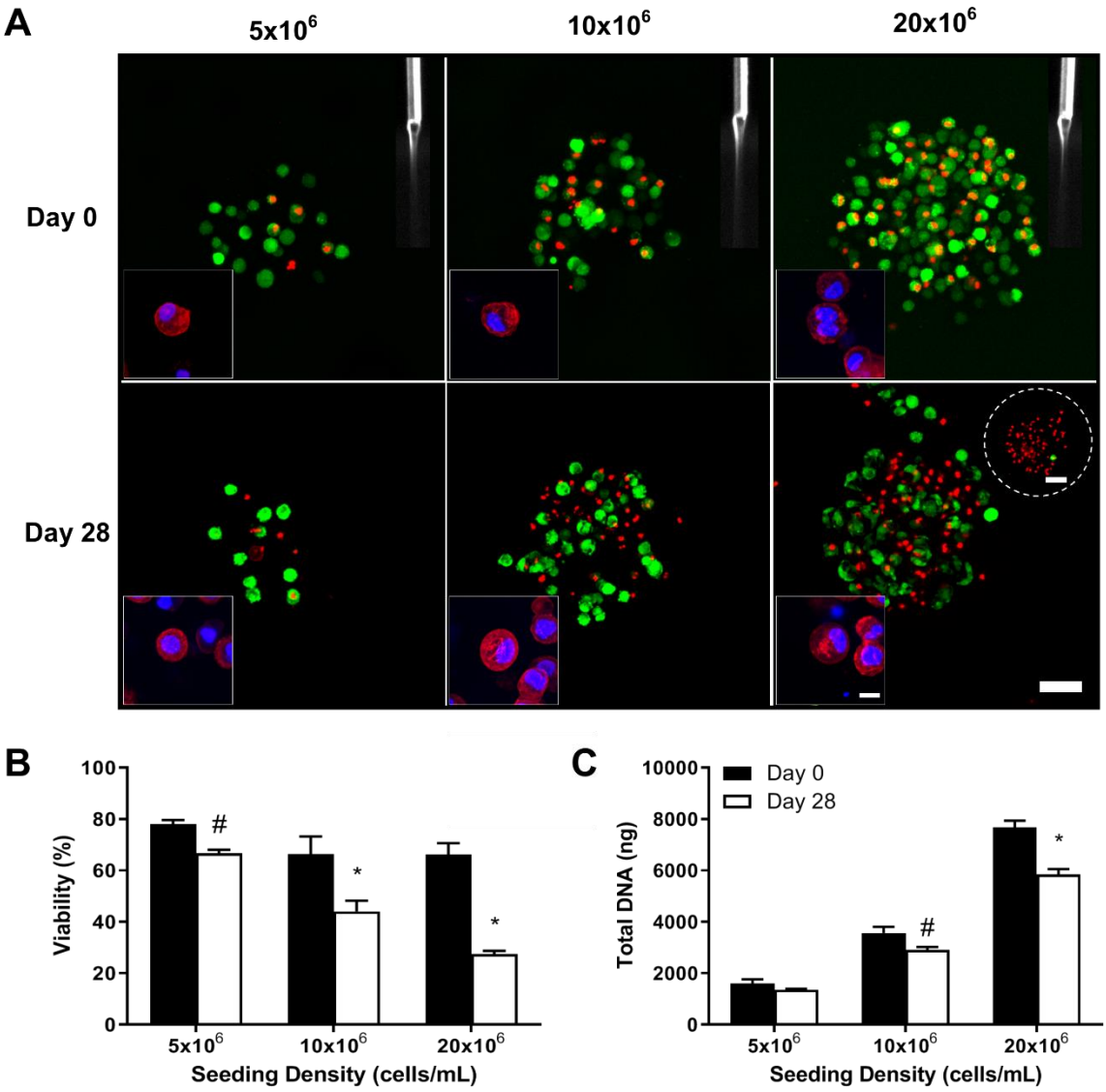

Figure 4-7: Cell proliferation and viability after 28 days in culture. (A) Live/Dead analysis showing increased cell death in higher cell density groups after 28 days. Scale bar=50 µm. Rounded cell morphology at day 0 and 28 (bottom left corner), scale bar= 10 µm **(B)** Semi-quantitative image analysis of cell viability at day 0 and day 28. **(C)** Total DNA content at day 0 (black bar) and day 28 (white bar) showing reduced DNA content in all groups after 28 days. # ($p<0.001$) and * ($p<0.0001$) indicating significant difference between day 0 and 28.

4.3.6 Increased initial seeding density resulted in higher levels of total sGAG and collagen accumulation whereas matrix accumulation on a per cell basis is enhanced at a lower seeding density

With increasing seeding density, the total amount of sGAG accumulation was enhanced (Figure 4-8 A). However, on a per cell basis, when normalising total sGAG per DNA, an opposite trend was observed with the highest sGAG per DNA content seen for an initial seeding desnity of $5x10^6$ cells/mL and an approximate decrease of 40% for an initial seeding density of $20x10^6$ cells relative to $5x10^6$ cells/mL (Figure 4-8 B). Similar trends were found for collagen accumulation with greater collagen deposition observed for increasing initial cell seeding density (Figure 4-8 C). Yet, when normalising to total DNA content, the lowest ($5x10^6$ cells/mL) and medium ($10x10^6$ cells/mL) seeding density groups exhibited similar amounts, which was significantly higher compared to the highest seeding density group (Figure 4-8 D). On evaluation of the sGAG:Collagen ratio, comparable values of approximately 4.5 were found for all seeding densties with no significant differences between groups (Figure 4-8 C).

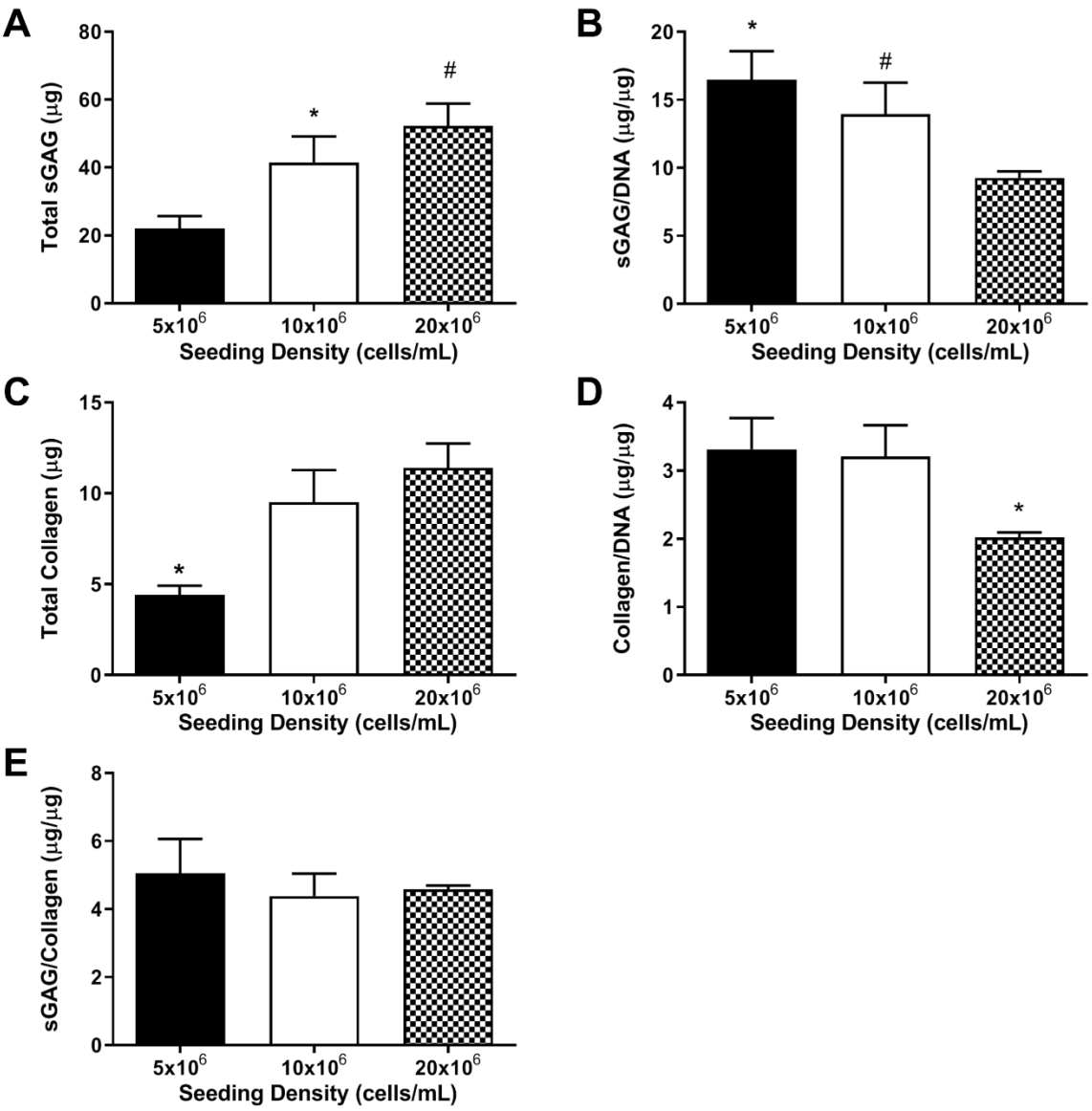

Figure 4-8: Biochemical quantification of matrix accumulation of chondrocytes in alginate µCaps **initially seeded at 5, 10 and 20x10^6 cells/mL (A)** Total amount of sGAG (µg). * ($p<0.01$) and # ($p<0.001$) indicates significant difference compared to 5x10^6 cells/mL initial seeding density **(B)** Normalized total sGAG per DNA (µg/µg). * ($p<0.001$) and # ($p<0.01$) indicates significant difference compared to 20x10^6 cells/mL initial seeding density **(C)** Total amount of collagen (µg). **(D)** Normalized total collagen per DNA (µg/µg). * indicates significant difference compared to all other groups ($p<0.001$) **(E)** sGAG: collagen (µg/µg) ratio.

Biochemical findings were found to correlate with histological observations with more intense staining of alcian blue/aldehyde fuchsin observed for 10 and $20x10^6$ cells/mL groups, indicating higher amounts of sGAG deposition (Figure 4-9 A) and more intense pericellular staining of picrosirius red after 28 days (Figure 4-9 B). Immunohistochemistry results revealed minimal amounts of Col1 deposition, with localised Col2accumulation observed in the pericellular region for all seeding density groups investigated (Figure 4-9 C and D).

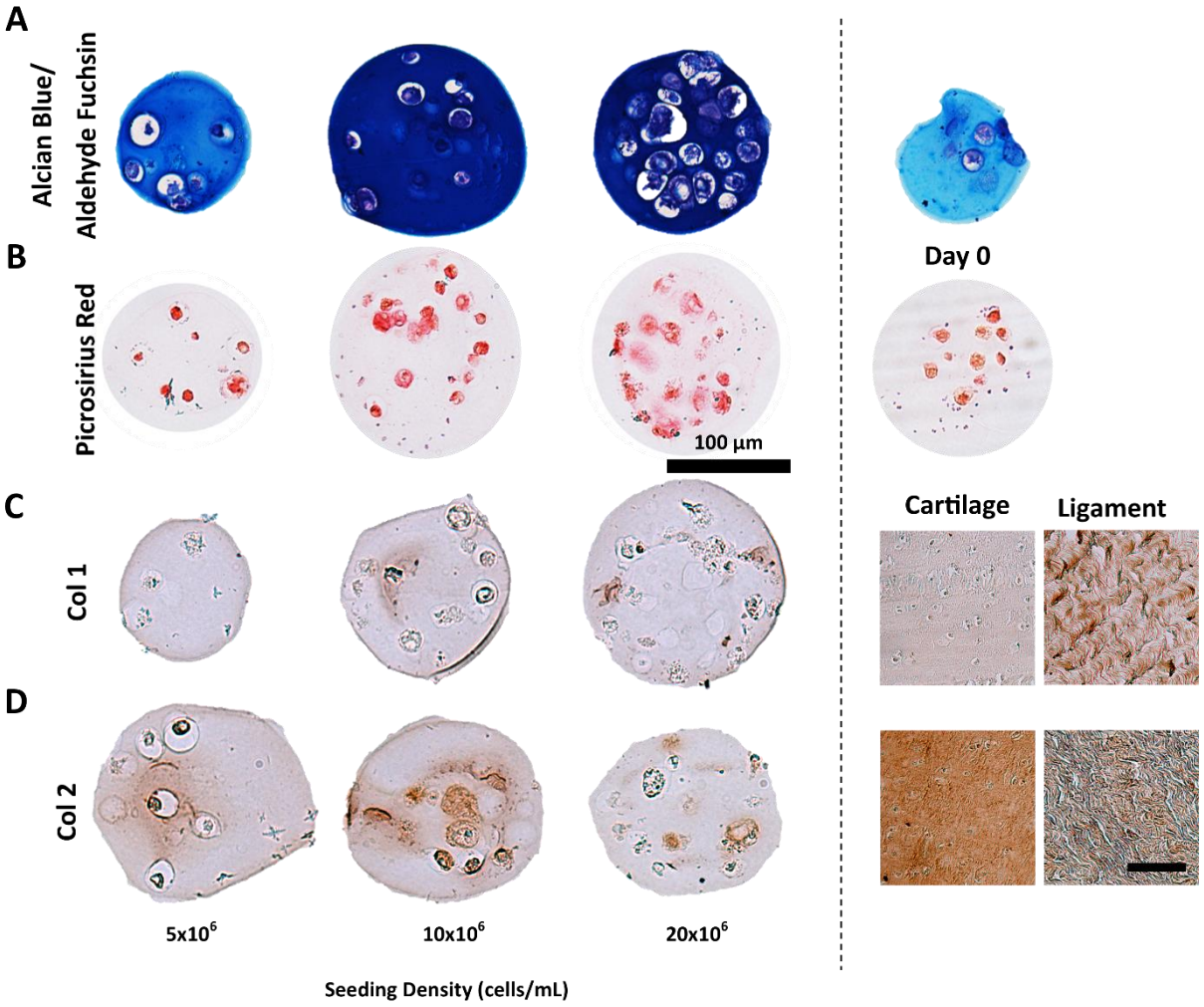

Figure 4-9: Histological straining for matrix deposition of ACs **in alginate** µCaps **initially seeded at 5, 10 and $20x10^6$ cells/mL (A)** alcian blue and aldehyde fuchsin showing enhanced sGAG deposition with higher initial cell number after 28 days and representative sample at Day 0 **(B)** Histological staining of collagen using picrosirius red staining showing collagen deposition after 28 days and representative sample at day 0. **(C)** Immunohistochemistry for Col1 and **(D)** Col2with control staining performed on ligament and cartilage. Scale bar =100µm.

4.3.7 Injection of µCaps into the highly pressurized IVD space

After having successfully established a system containing cellular capsules within the micron size range, their injectability into the IVD was assessed. Hereby a suspension of µCaps in a PBS solution was attempted to be introduced into the NP tissue using a 25G needle. However, a retention of capsules inside the syringe barrel was observed (Figure 4-10 A) with poor delivery into the IVD space (Figure 4-10 B) (µCaps in blue). When attempting the injection of µCaps suspended in a bulking gel, however, easier injection was observed (Figure 4-10 C) with improved µCaps delivery into the NP disc space (Figure 4-10 D).

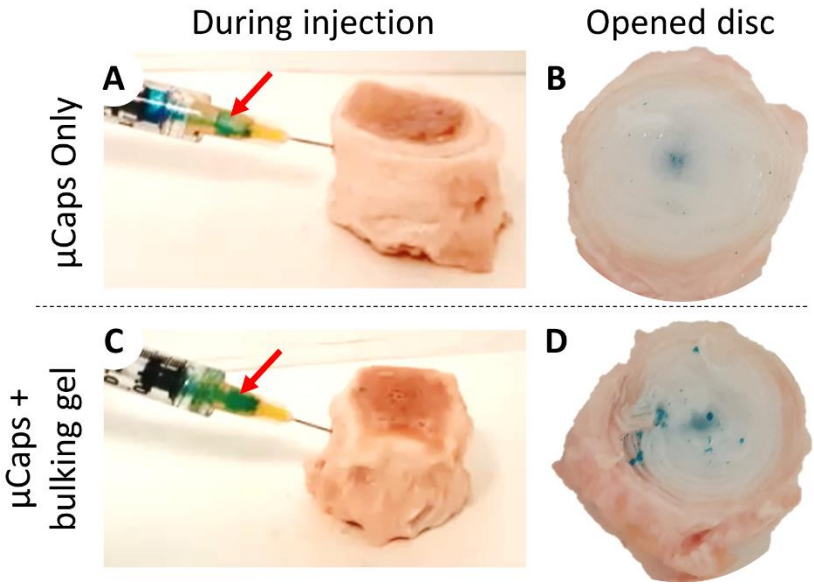

Figure 4-10: Injection of µCaps into bovine disc with and without bulking agent. µCaps without bulking agent remain within syringe barrel, while capsules injected with bulking agent pass through the needle hub (red arrow) into the IVD

4.4. Discussion

Microencapsulation of cells in a biomaterial address some of the challenges associated with current injectable cell-based therapies by providing a protective niche thereby preventing cell leakage, maintaining a stable phenotype, and providing protection during the injection delivery process. Thus, the use of EHDS for microencapsulation offers an attractive method in

terms of its efficiency and versatility. Cells and other targets such as drugs or bioactive molecules can be encapsulated under ambient conditions into a variety of different materials (Naqvi et al., 2016a). Additionally, cell-loaded µCaps have injectable properties (Nogués et al., 2013b, Wang et al., 2013) and therefore have the potential to be used for minimally invasive repair of tissues such as the intervertebral disc. The primary objective of this chapter was to characterise key processing parameters such as needle gauge, voltage, viscosity and flow rate to regulate the size and shape of alginate µCaps. The second objective was to assess cell viability when altering these parameters and finally to assess the effect of initial cell seeding density (5, 10 and $20x10^6$ cells/mL) on matrix accumulation of microencapsulated ACs after 28 days in disc-like culture conditions (i.e. low glucose, low oxygen, without exogenous growth factors).

Investigations of key processing parameters on the size and shape of µCaps fabricated using EHDS have been shown to be determined by both, physical properties of the polymeric solution (surface tension, density, electrical conductivity and viscosity) and hardware/operational parameters of the electrosprayer (applied flow rate, electric field strength, needle gauge and working distance in which the potential difference is formed) (Enayati et al., 2011b, Park et al., 2012, Gasperini et al., 2013b, Sahoo et al., 2010b). When varying the voltage, for instance, partial jetting can be observed at lower voltages. With increasing electric field strength transitioning to a sustained and stable jet (Taylor cone) occurs (Sahoo et al., 2010b, Gasperini et al., 2013b). Consistent with previous the average diameter of µCaps was found to decrease with increasing applied voltage and decreasing inner needle-diameter (Sahoo et al., 2010b, Braghirolli et al., 2013, Workman et al., 2014). For larger needle diameters, voltage appeared to influence µCaps size to a greater extent. Yet, there appears to be a threshold beyond which the impact of processing parameters diminishes. For instance, irrespective of applied voltage, a 30G needle could only regulate the size of the fabricated µCaps within a certain range. When analysed quantitatively, no significant difference in microcapsule size was found when using a 26G and 30G needle at 15 kV. However, µCaps produced using a 21G needle at the same voltage were significantly larger ($p<0.0001$). This is most likely due to the rate at which charge is transferred to the polymer

solution. Once the polymer solution becomes charged, it will move towards the uncharged plate and when using small needle diameters this charging process occurs rapidly. In our work, flow rate was not found to influence microcapsule size to any noticeable extent when operating with lower concentrations (Appendix 1, page xxiii). This is perhaps due to employing a small needle size and high voltage (10 kV), where microcapsule size is mainly governed by the needle diameter. However, when increasing alginate concentration and thus the viscosity of the solution, flow rate had more of an effect with larger (flow rate of 50 µL/min) and ellipsoidal shaped (flow rate of 250 µL/min) µCaps formed at a concentration 3%. This is perhaps due to the lower conductivity associated with viscous solutions which would otherwise require a higher electric field to overcome the surface tension and liquid viscosity to form an optimal Taylor cone (Enayati et al., 2010, Bock et al., 2012b). When spraying at higher flow rates (~250 µL/min) using 3% alginate solutions, ellipsoidal µCaps were formed, most likely due to the increased chain entanglement density of the alginate polymer solution akin to the electrospinning process (Bock et al., 2011).

Controlling the size of µCaps is important for several reasons; it facilitates control of the number of cells per microcapsule, regulates the degree of diffusion of nutrients and removal of waste by-products and perhaps most importantly determines the minimum needle gauge for injectable delivery. Microcapsule size also determines the packing density of concentrated sphere arrangements. Highly uniform microcapsule populations will have relatively large void spaces between spheres and conversely, spheres with a wider size distribution will pack together more closely creating higher density structures (Chen et al., 2011). Therefore, while controlling the microcapsule size and uniformity of distribution is important to a degree, a slight variation in sphere population sizes may be beneficial.

Investigating effect of key processing parameters on cell viability, no negative consequences of needle size was observed when operating with lower alginate concentrations (1% and 2%). However, with higher concentrations (e.g. 3%) and thus a higher viscosity, cell viability was observed to be diminished with decreasing needle diameter since higher viscosities

results in cells experiencing higher shear forces when passing through a needle. This may result in damage to the cell membrane leading to cell death. Overall, reduced cell viability was observed with increasing alginate concentration irrespective of needle size. After 7 days, part recovery with higher cell viability compared to day 0 was observed. The total number of analysed cells could not be kept consistent, which is a limitation of these results and needs to be considered. However, cell debris are more unlikely to be removed from an alginate hydrogel within 7 days, which suggests that the higher viability is due to proliferation of cells within the alginate gel and therefore a different cell number overall.

When comparing the effect of different applied voltages (5, 10 and 15kV), cell viability was not compromised at voltages up to 10kV, with a small compromised effect observed at 15kV. This is consistent with previous work performed on BMSCs which demonstrated that cells electrosprayed between 7.5-15 kV remained viable and proliferated at rates similar to native BMSC's while higher voltages (30 kV) reduced cell viability (Sahoo et al., 2010b). Similar studies have also demonstrated that stem cells do not exhibit any deleterious effects or cellular damage after spraying with electric field strengths between 1 and 15 kV (Braghirolli et al., 2013, Mongkoldhumrongkul et al., 2009). Based on these reasons, the 30G needle operating at 10 kV with a flow rate of 100 μL/min which yielded a population of μCaps of diameter (151.6 ± 63 μm) for the *in vitro* 28 day culture experiments were selected.

Results of seeding density effects demonstrated a decrease in cell viability and DNA content with increasing initial cell seeding density after 28 days in culture. This may be due to increased cell-cell contact at higher seeding densities which can cause local stress concentrations, altering cellular properties and eventually leading to cell-damage (Gasperini et al., 2013b). Previous work investigating different seeding densities (1, 5 and $10x10^6$ cells/mL) of encapsulated THP-1 cells (human monocytic cell line) demonstrated similar results, with lower cell viability observed at higher seeding densities four days post encapsulation(Workman et al., 2014). Conversely, Gasperini *et al.* did not observe any noticeable effects on cell viability when encapsulating B50 neuroblastoma rat cells at densities of $5x10^6$ and $10x10^6$ cells/mL (Gasperini

et al., 2013b). These conflicting observations could be due to the different cell types employed or most likely the differences in microcapsule size. For example, Workman *et al* fabricated µCaps using an applied voltage of ~7 kV resulting in µCaps with an average diameter of 885 µm (± 30 µm), which may result in diffusion limitations within the core (Workman et al., 2014). In contrast, Gasperini *et al*. fabricated much smaller µCaps using 1% alginate with diameters of 158 µm (± 42 µm) with a seeding density of $10x10^6$ cells/mL at 9 kV, which were of a similar size to those fabricated in our study. These differences in microcapsule size may result in nutrient deprivation (e.g. oxygen, glucose) or accumulation of metabolic waste products (e.g. lactic acid) which can affect cell viability. Importantly, in these experiments a low glucose (5.5 mM) media formulation was used to mimic native disc biochemical concentration which may be insufficient to sustain cell viability at higher seeding densities.

In the context of matrix deposition, the accumulation of ECM components such as glycosaminoglycan (sGAG) and collagen is highly dependent on the number of active cells and the accumulation rate of these active cells. For example, Kobayashi *et al*. investigated bovine NP cells and chondrocytes in 3D alginate culture with seeding densities of 4 and $25x10^6$ cells/mL and observed a two-to-four-fold increase in sGAG accumulation. However, the ability to accumulate matrix molecules on a per cell basis decreased by 50-60% (Kobayashi et al., 2008). Although sGAG accumulation can be increased to some extent by increasing cell density, the consequential demand for nutrients within 3D constructs slows metabolism and can lead to apoptosis and cell death, thereby limiting the rate that cells can produce matrix (Kobayashi et al., 2008). Similar results were observed in the current study showing higher levels of sGAG accumulated when increasing the initial cell number but with diminished cell viability possibly due to nutrient limitations. When normalizing the total sGAG to DNA content, the accumulation rate per cell decreased by approximately 40% for an initial seeding density of $20x10^6$ cells relative to $5x10^6$ cells/ml with similar trends were also observed for collagen.

Additionally, there is cell clustering evident in the highest seeding density group, which can lead to increased cell-cell contact between AC and consequentially intercellular

communication. Studies have demonstrated a direct correlation between cell-cell contact and chondrogenesis (de Windt et al., 2015, Cao et al., 2015), indicating its importance for ECM deposition. Therefore, it seems favourable to increase the cell density used to a certain level to enhance these connections and increase the amount of ECM being deposited.

Previous studies have demonstrated aggregation of µCaps when using other biomaterials such as collagen. For example, Wise *et al.* fabricated collagen-chitosan µCaps with marrow mononuclear cells or MSCs encapsulated using a water in oil emulsion method and demonstrated aggregation of these µCaps (Wise et al., 2014). In our study, no aggregation was observed. However, it is important to highlight that our cultures did not contain any exogenous growth factors to enhance matrix accumulation, which may otherwise have resulted in microcapsule aggregation.

As with any tissue regeneration strategy for IVD repair it is essential to verify that the matrix produced has the appropriate sGAG to collagen ratio as it is believed that this ratio may provide an appropriate metric for identifying NP-like tissue. Native disc tissue is characterised by its intrinsically high sGAG: collagen ratio which gives rise to its unique biomechanical properties and has been reported to be approximately 3.5:1 (Mwale et al., 2004, Naqvi and Buckley, 2015b). In this study, an sGAG:collagen ratio of approximately 4.5 was found for all groups with no significant differences between groups which closely matches that of native NP matrix. While this ratio may not help in determining whether cells have adopted a true NP-like phenotype, it provides an indication for the correct composition of the tissue that the cells produce.

This system was proposed for minimally invasive delivery of cells with improved deposition into the IVD. However, after injection of these µCaps within a PBS solution, into the IVD, poor delivery of µCaps was observed. The low viscosity of PBS and higher density of alginate µCaps resulted in inhomogeneous distribution of µCaps within the PBS liquid. Given the highly pressurized system of the IVD (intradiscal pressure between 0.5-1 MPa (Claus et al., 2008)), the liquid fluid of PBS was injected prior to the higher viscosity µCaps, which led to

accumulation of µCaps within the syringe barrel. However, this could be overcome using a more viscous bulking agent. Due to the higher viscosity of the bulking agent, more homogeneous distribution of µCaps was achieved with more efficient delivery of µCaps into the IVD space.

4.5. Conclusion

The potential of injectable delivery systems to enable clinicians to treat defects of the IVD in a minimally invasive manner is highly attractive and also offers significant potential in other areas of tissue regeneration. Taken together, this work demonstrates the effect of key individual processing parameters (voltage, needle diameter, polymer concentration and flow rate) to fabricate alginate microcapsules of different sizes using the EHDS process.

Altering the electric field strength and needle diameter was found to highly influence and regulate microcapsule size towards a smaller diameter with increasing voltage and smaller needle diameter. Increasing alginate concentration and thus viscosity increased overall microcapsule size but also affected the geometrical shape towards ellipsoidal-shaped gels. Importantly, increasing viscous solutions were found to be detrimental to cell viability for the parameters investigated in this work. Furthermore, an increased cell death with increasing seeding density was observed, which is perhaps due to increased nutrient demands. For microencapsulated chondrocytes, a seeding density of $10x10^6$ cells/mL showed a good compromise between cell viability and matrix accumulation. Furthermore, using a viscous bulking agent, more efficient µCaps delivery into the highly pressurized disc could be achieved. Overall, it was demonstrated that EHDS is a controllable, versatile approach to fabricate cellular µCaps, and may offer significant potential for minimally invasive repair strategies of the IVD.

CHAPTER 5
INCORPORATION OF COLLAGEN AND HYALURONIC ACID TO ENHANCE THE BIOACTIVITY OF FIBRIN-BASED HYDROGELS FOR NUCLEUS PULPOSUS REGENERATION

After discovering limited delivery of μCaps into the central NP space due to the natural high intradiscal pressure, which can be improved using a bulking agent with higher viscous properties, a bioactive bulking agent was explored for i) greater μCap deposition into the IVD and ii) enhanced matrix deposition capacities of cells. This addresses objective iii of this thesis.

5.1. Introduction

As described in Chapter 2, several strategies have been proposed to restore NP tissue using cell-based therapy and biomaterials.

This chapter focuses on the use of fibrin, which is perhaps one of the most clinically used hydrogels and has received particular attention as a sealant and adhesive in surgery (Eyrich et al., 2006a, MacGillivray, 2003a, Fattahi et al., 2004a). Fibrin is a viscoelastic polymer which crosslinks after an enzymatic reaction between fibrinogen and thrombin, facilitating *in situ* gelation. Previous work has demonstrated successful encapsulation of cells into fibrin hydrogels with cells, exhibiting good viability and proliferation (Acosta et al., 2011, Eyrich et al., 2007, Colombini et al., 2015, Bensaid et al., 2003, Cox et al., 2004). The primary components of fibrin, such as fibrinogen and thrombin, have been shown to modulate cell attachment, migration, and proliferation of stem cells and chondrocytes (Bensaid et al., 2003, Gille et al., 2005, Sporn et al., 1995). Chondrocytes have been shown to retain their rounded morphology in fibrin hydrogels, inhibiting dedifferentiation and promoting matrix production (Homminga et al., 1993). Also, the

effect of different parameters, such as pH, fibrinogen, and salt concentration, have been shown to influence long term fibrin gel stability (Eyrich et al., 2007).

In addition, incorporation of ECM constituents into fibrin gels, such as collagen and HA, have been shown to enhance matrix deposition by chondrocytes (Colombini et al., 2015, Li et al., 2014b). Collagen is the most abundant protein in mammalian ECM and supports tissue stability and structure. HA is a non-sulphated GAG, and is highly abundant in NP tissue, where its function is to maintain tissue hydration. Both materials have been used separately in various studies (Stern et al., 2004, Hegewald et al., 2011, Stern et al., 2000, Buser et al., 2014), with HA demonstrating a beneficial effect on matrix synthesis and proliferation. However, the benefits of incorporating collagen appear to be dependent on cell type. For example, Colombini et al. showed that collagen-enriched fibrin hydrogels were suitable for culturing of AF cells, but not NP cells (Colombini et al., 2015).

In the present study, fibrin hydrogels of different compositions were investigated in an attempt to create a bulking agent with two advantages: more efficient delivery of μCaps into the IVD and a suitable composition to promote NP-like ECM accumulation that would be compatible with commercial ventures. Therefore, the first objective explored the effects of fibrin concentration (12.5, 25, 37.5, and 50 mg/mL) on hydrogel stability and the viability and proliferation kinetics of ACs. Next, the bioactivity of this fibrin-based hydrogel was enhanced by incorporating key matrix components (Col and HA), and the effect on matrix formation by ACs was further investigated. Finally, the influence of incorporating different HA concentrations (2.5 and 5 mg/mL) into fibrin-based hydrogels was examined.

5.2. Methods

5.2.1 Study Design

This study consisted of three different stages (Figure 5-1). In all stages, ACs were isolated from porcine knee joints and expanded in monolayer until passage 1 or 2. In stage 1, different final fibrin concentrations (12.5, 25, 37.5, and 50 mg/mL) were investigated. Stage 2 involved

incorporation of collagen and HA into fibrin. Stage 3 examined the influence of increasing HA concentration on promoting matrix accumulation by articular-derived chondrocytes.

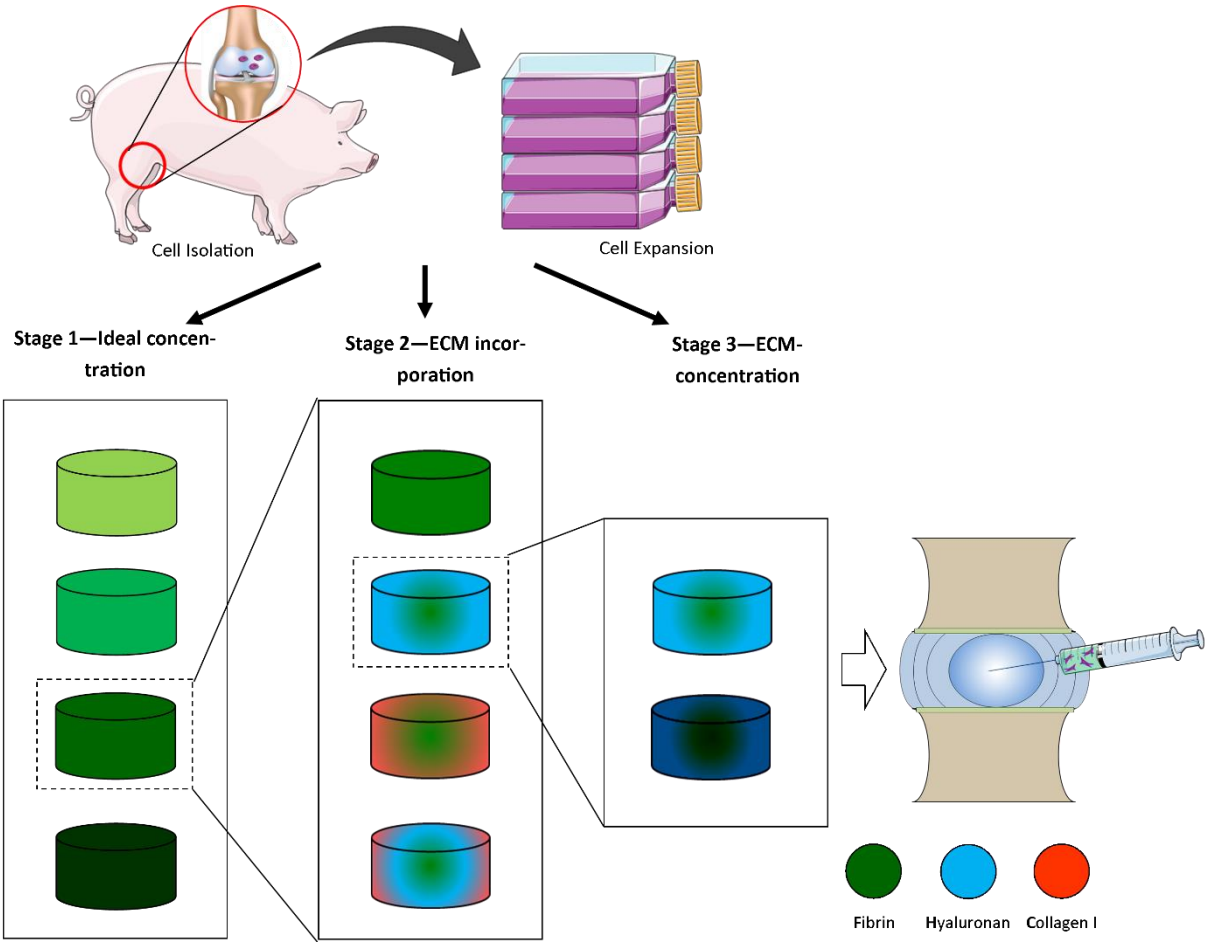

Figure 5-1: Schematic of experimental design of the fibrin study. In stage 1, different final fibrin concentrations (12.5, 25, 37.5, and 50 mg/mL) were investigated. Stage 2 involved incorporation of collagen and hyaluronic acid into fibrin. Stage 3 examined the influence of increasing HA concentrations (2.5, 5 mg/mL) on promoting matrix accumulation by articular-derived chondrocytes.

5.2.2 Hydrogel Fabrication

The following components were used for the fabrication of different hydrogel compositions: fibrinogen type I-S (60–85% protein, ~10% sodium citrate, and ~15% sodium chloride, Sigma-Aldrich F8630, Arklow, Ireland), thrombin from bovine plasma (Sigma-Aldrich, T4648, Arklow, Ireland), hyaluronic acid sodium salt from Streptococcus equi

(MW = 1.5 − 1.8 × 10^6 Da, Sigma-Aldrich 53747, Arklow, Ireland), and Col1, rat tail high concentration (Corning™ 354249, Corning, NY, USA)

5.2.2.1. Preparation of Fibrin Hydrogels with Various Concentrations of Fibrinogen

Fibrin hydrogels were produced by solubilising desired concentrations of fibrinogen type I-S (60–85% protein, ~10% sodium citrate, and ~15% sodium chloride, Sigma-Aldrich, Arklow, Ireland) in 10,000 KIU/mL aprotinin solution (Nordic Pharma, Sweden) containing 19 mg/mL sodium chloride at 37°C, and crosslinked using a pre-warmed thrombin solution (5 U/mL in 40 mM $CaCl_2$, pH 7) and allowed to gel (see Table 5-1). To allow gelation to proceed, hydrogels were incubated for 30 min at 37°C in a humidified atmosphere.

Table 5-1: Preparation of fibrin hydrogels with various concentrations (12.5, 25, 37.5, and 50 mg/mL).

Fibrinogen Concentration (mg/mL)	Fibrinogen: Thrombin ratio	Fibrinogen Concentration (mg/mL)
25	1:1	12.5
50	1:1	25
75	1:1	37.5
100	1:1	50

5.2.2.2. Fibrin Hydrogels Containing ECM Components (Collagen, Hyaluronic Acid)

Specific fibrin-based hydrogels (fibrin only, fibrin–HA, fibrin–Col, and fibrin–Col–HA) were fabricated at 37°C and allowed to crosslink for 60 min in a humidified atmosphere inside a 3% agarose mould (see Table 5-2). To create fibrin–HA hydrogels, HA (3 mg/mL) was dissolved in thrombin and combined with fibrinogen to yield a final concentration containing 1.5 mg/mL HA. To create fibrin–Col gels, Col1 (Corning, Corning, NY, USA) was incorporated at a final concentration of 1.33 mg/mL into a fibrinogen/thrombin mixture as follows: soluble collagen with an initial concentration of 6 mg/mL in 0.02 M acetic acid was neutralised using a buffer containing NaOH, $NaHCO_3$, HEPES, and 10× RPMI media, and combined with lg-DMEM

(1000 mg/mL D-glucose, Sigma, Arklow, Ireland). Thrombin (5 U/mL) was added and crosslinked using pre-warmed fibrinogen at a specified concentration to obtain a final concentration of 50 mg/mL fibrinogen. For fibrin–collagen–hyaluronic hydrogels, a thrombin–HA mix (5.2 mg/mL initial HA) was combined with neutralised collagen in a similar fashion as described for fibrin–collagen hydrogels and crosslinked using pre-warmed fibrinogen.

Table 5-2: Different materials investigated and their final concentrations.

	Abbreviation	Final Fibrin Conc. (mg/mL)	Col Conc. (mg/mL)	HA Conc. (mg/mL)
Fibrin	F	50		
Fibrin–HA	FH	50		1.5
Fibrin–COL	FC	50	1.33	
Fibrin–Col–HA	FCH	50	1.33	1.5

5.2.2.3. Fibrin-Based Hydrogels with Increasing Hyaluronic Acid Concentrations

Fibrin–HA hydrogels were created as described in the previous section (section 5.2.2.2. page 80) using an initial HA concentration of 5 mg/mL in thrombin (5 U/mL). Thrombin–HA solution was combined with fibrinogen (100 mg/mL) with and without the addition of 5 mg/mL HA at a ratio of 1:1 to obtain the desired final concentrations of 2.5 mg/mL or 5 mg/mL, respectively. Cells were combined with the fibrinogen solution prior to incorporation of thrombin. To ensure crosslinking, all hydrogels were incubated for 60 min at 37°C in a humidified atmosphere.

5.2.3 Cell Encapsulation

5.2.3.1. Varied Fibrin Concentration Hydrogels

For fibrin encapsulation, AC were suspended in fibrinogen solutions (Table 2-1) at a cell density of 8×10^6 cells/mL. This was combined with thrombin solution (1:1 ratio) and allowed to gel in an 3% agarose mould, pre-soaked in cell culture media to ensure nutrient supply for cells

for 30 min at 37°C to produce cylindrical constructs (Ø5 mm × 3 mm thickness), and a final cell seeding density of 4×10^6 cells/mL.

5.2.3.2. Fibrin–Collagen and Fibrin–Hyaluronic Acid–Collagen Hydrogels

For encapsulation, ACs were suspended in pre-warmed fibrinogen solution and combined with collagen–thrombin or collagen–HA–thrombin solution, respectively, to obtain a final cell seeding density of 4×10^6 cells/mL at matrix concentrations, described in Table 5-2. gelling took place in 3% agarose moulds soaked in media for 60 min at 37°C, producing cylindrical constructs (Ø5 mm × 3 mm thickness).

5.2.3.3. Fibrin–HA Hydrogels

For encapsulation of ACs into different concentrations of fibrin–HA hydrogels, cells were suspended in fibrinogen solution (100 mg/mL) with or without incorporation of 5 mg/mL HA. This was combined at a ratio of 1:1 with 5 U/mL thrombin–HA solution, to obtain a final cell seeding density of 4 x10^6 cells/mL and allowed to gel in a 3% agarose mould pre-soaked in media for 60 min at 37°C to produce cylindrical constructs (Ø 5 mm × 3 mm thickness). All samples were allowed to equilibrate overnight before initiation of experiments.

5.2.4 Culture of Chondrocyte Laden Fibrin-Based Constructs

All constructs were maintained at 37°C and 5% oxygen conditions in 2 mL of chemically defined medium (CDM) consisting of lg-DMEM supplemented with penicillin (100 U/mL)–streptomycin (100 µg/mL) (both GIBCO, Biosciences, Ireland), 0.25µg/mL AmpB, 40 µg/mL L-proline, 50 µg/mL L-ascorbic acid-2-phosphate, 1.5 mg/mL BSA, 1× insulin–transferrin–selenium, 100 nM dexamethasone (all from Sigma–Aldrich, Ireland), and 5% FBS. Medium was exchanged twice weekly for a total duration of 21 days.

5.2.5 Determination of Hydrogel Contraction

Hydrogel contraction kinetics were determined via image analysis using a digital camera (Canon Powershot SX240HS) at each feeding period (twice weekly). The average diameter of

three constructs was determined using image analysis software (ImageJ, National Institutes of Health, and Bethesda, Maryland).

5.2.6 Statistical Analysis

Statistical analyses were performed using GraphPad Prism (version 6, GraphPad Software, La Jolla, USA) software with 3–4 samples analysed for each experimental group of 3 individual experiments. The sGAG/collagen ratio was determined by dividing sGAG (µg) by collagen (µg). One-way ANOVA was used for analysis of variance with Tukey's multiple comparisons test to compare between groups. Results are displayed as mean ± SD, with significance accepted at a level of $p < 0.05$.

5.3. Results

5.3.1 Stage 1—Effect of Increasing Fibrinogen Concentration

5.3.1.1. A Minimum Concentration of 25 mg/mL Fibrinogen Is Required to Maintain Construct Stability over 21 days in Culture

At the initiation of culture, all constructs possessed an average diameter of 5.46 mm (±0.19 mm) (Figure 5-2 A, B). After four days in culture, constructs with the lowest fibrinogen concentration (12.5 mg/mL) underwent contraction (~27%, 3.99 ± 0.14 mm), whereas all other groups appeared to remain relatively stable. By day 21, the lowest concentration (12.5 mg/mL) had contracted by ~35%, with all other groups (25, 37.5, 50 mg/mL) exhibiting ~8% contraction relative to day 0.

5.3.1.2. Increasing Fibrinogen Concentration Enhances Cell Proliferation

Fibrinogen concentration was observed to significantly influence cell proliferation (Figure 5-2 C, D). For 12.5 mg/mL gels, DNA content was observed to decrease relative to day 0. At 25 mg/mL, no significant change was observed with time. However, for 37.5 mg/mL, a two-fold increase in DNA content was detected, which was enhanced further in 50 mg/mL gels (5-fold increase). Biochemical data was confirmed through live/dead staining (Figure 5-2 D), where

dead cells are represented in red, and viable cells in green. Significant cell death occurred at the lowest (12.5 mg/mL) concentration (top left image), with some cell death also observed for the two middle concentrations (25 and 37.5 mg/mL). By contrast, for 50 mg/mL gels, a high number of viable cells were noted (bottom right image).

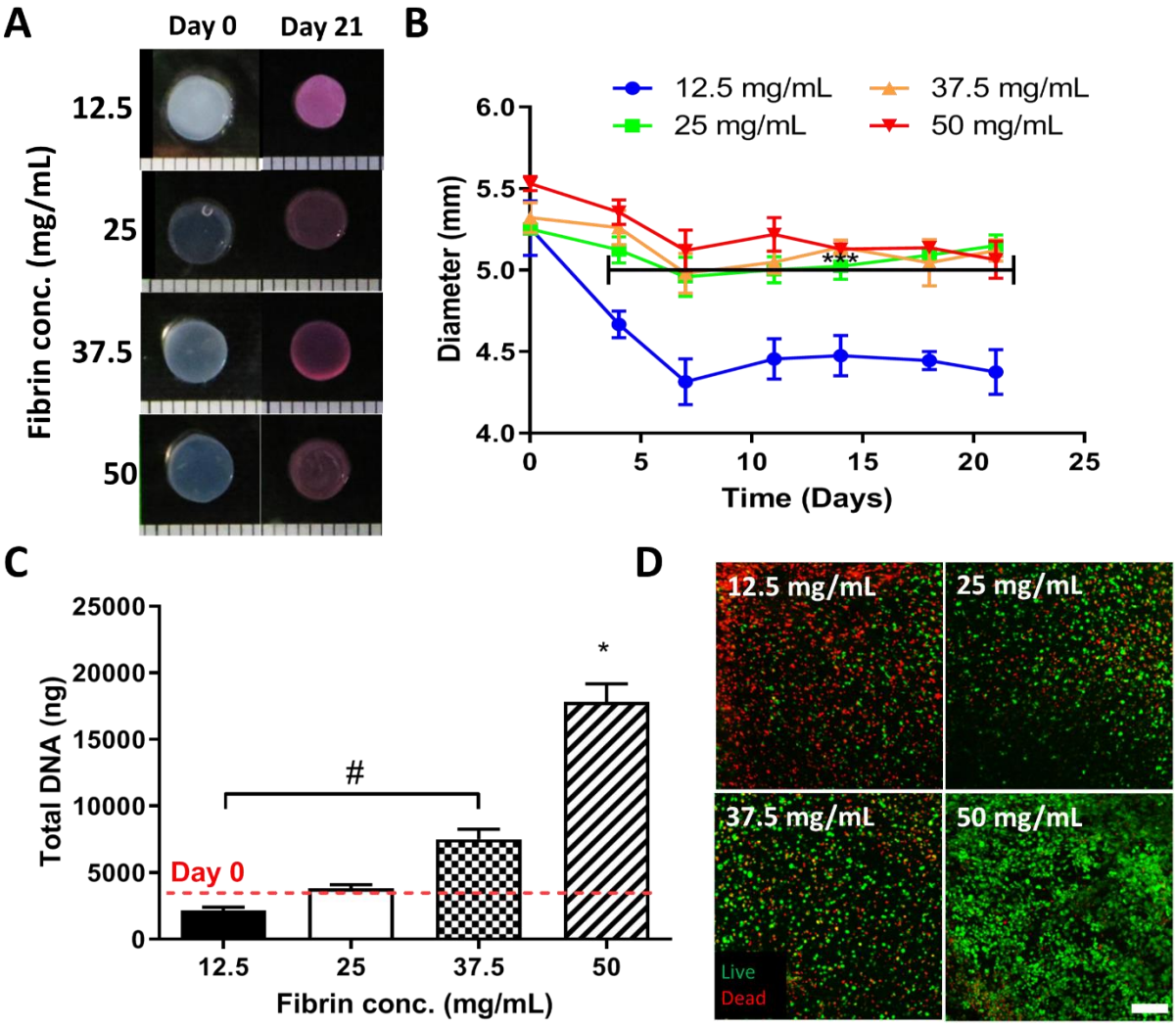

Figure 5-2: Effect of fibrinogen concentration on construct stability and cell proliferation (A) Macroscopic images before culture ("Day 0", left) and after three weeks in cell culture ("Day 21", right); **(B)** Contraction kinetics of constructs over time up to 21 days. Low concentration (12.5 mg/mL, blue) hydrogels contracted significantly over the first 7 days. *** indicates significant difference ($p < 0.001$); **(C)** Biochemical analysis of DNA content in constructs. # indicates significant difference between 12.5 and 37.5 mg/mL ($p < 0.01$) and * indicates a significant difference compared to all other groups ($p < 0.001$); **(D)** Live/dead analysis showing a high degree of cell death for the lowest concentration (12.5 mg/mL) and increased cell viability in the highest concentrations (50 mg/mL). Scale bar = 200 μm.

5.3.2 Stage 2—Incorporation of ECM into Fibrin-Based Hydrogels

5.3.2.1. Fibrin-ECM Acellular Hydrogels Remain Stable in Culture over 21 Days

To assess whether incorporation of ECM components was retained after encapsulation, acellular hydrogels were evaluated over 21 days. All hydrogel formulations maintained their shape (Figure 5-3 A) and initial size of 5 mm (± 0.2 mm) (Figure 5-3 B). Histological assessment for HA (using alcian blue at pH 2.5) and collagen in different gel formulations (Figure 5-3 C and D) revealed a stable amount of HA in Fibrin-HA (FH) groups after 21 days (arrowheads pointing at darker blue areas, indicating pockets of HA). However, less HA was detected in FCH after 21 days (Figure 5-3 C right). A homogeneous gel structure without darker blue staining was observed for groups without incorporation of HA (Figure 5-3 C) Picrosirius red staining of FC and FCH gels confirmed the incorporation and maintenance of collagen inside the gel over the entire culture period. Small fibres of collagen were observed to be homogeneously distributed within FC gels and in between HA pockets in FCH gels (Figure 5-3 D 40x images). No such Col fibres were seen in compositions without incorporated Col1.

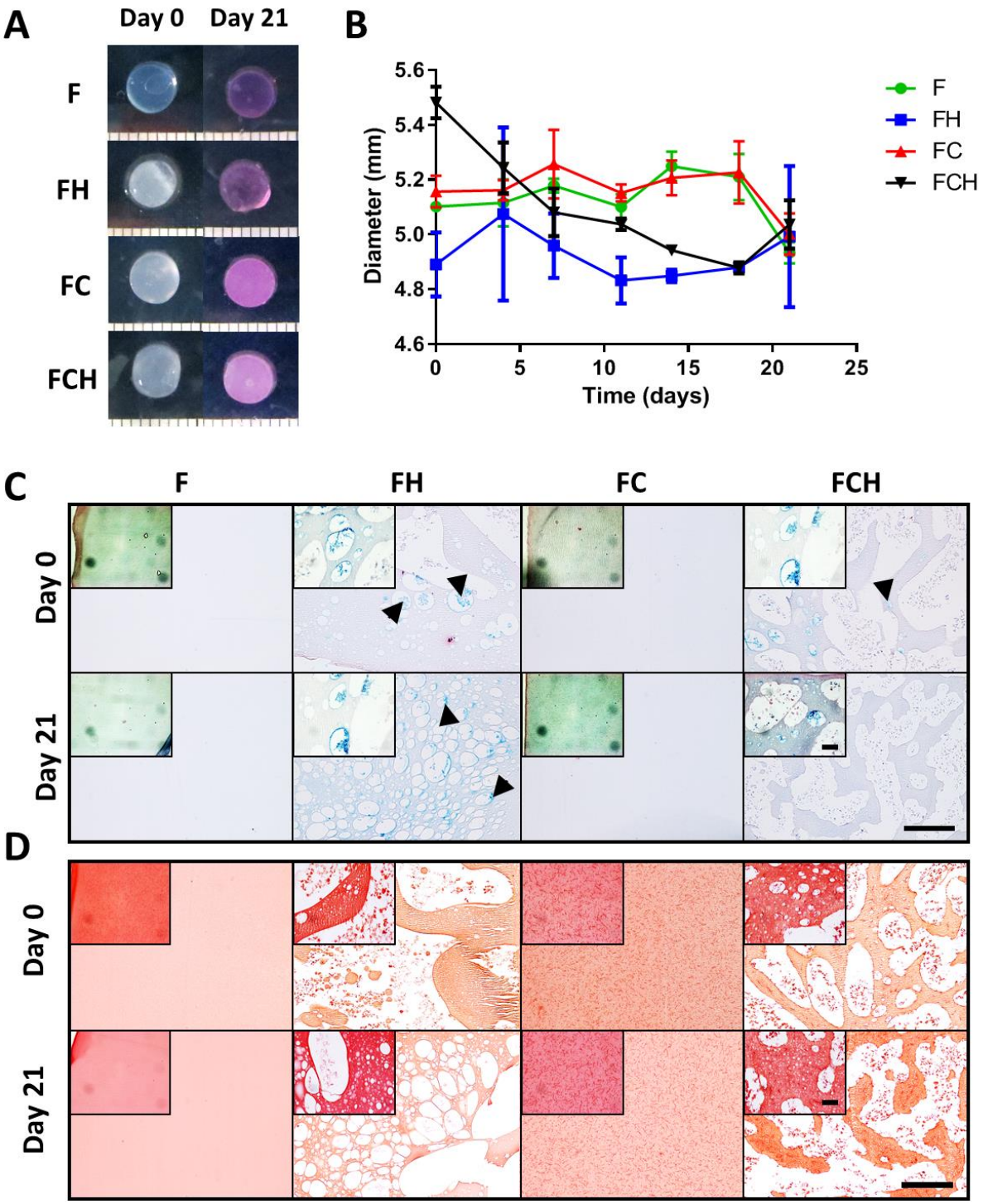

Figure 5-3: Assessment of geometry and composition stability for F, FH, FC and FCH acellular hydrogels over 21 days. (A) Macroscopic images of different gel formulations at day 0 and day 21; **(B)** Determination of diameter of hydrogel constructs**; (C)** Histological assessment of incorporated HA using alcian blue and **(D)** collagen using picrosirius red for all groups. Scale bar$_{10x}$ = 200 µm, scale bar$_{40x}$ = 50µm.

5.3.2.2. Fibrin-Based Hydrogels Incorporating Hyaluronic Acid Promote Chondrocyte Proliferation with Enhanced Cell Viability and Increased Cell Spreading

Cell viability and proliferation was investigated using a combination of semi-quantitative confocal image analysis and biochemical quantification of DNA content. From confocal images of live/dead staining (Figure 5-4 A), cell viability was determined to be 88.3% (± 4.6%) with no significant difference between hydrogel formulations (Figure 5-4 B). However, after 21 days of cell culture, reduced cell viability was observed in F and FC hydrogels compared to groups which contained HA (FH and FCH). DNA content increased from day 0 levels for all hydrogel formulations, with a four-fold increase observed for fibrin-only hydrogels and a five-fold increase in hydrogels containing HA (Figure 5-4 C).

Cell morphology was investigated using fluorescence staining of actin with phalloidin and nuclei staining with DAPI. Results revealed that incorporating HA promoted cell spreading immediately after cell encapsulation into the material (Figure 5-4 A—top). However, when combined with Col, cells did not spread as rapidly, and their appearance more closely resembled hydrogels without HA incorporation. After 21 days, cells in all hydrogel formulations exhibited a spread morphology (Figure 5-4 A—bottom) with the least degree of spreading observed in fibrin-only (F) hydrogels compared to all other groups containing ECM components (FH, FC, FCH).

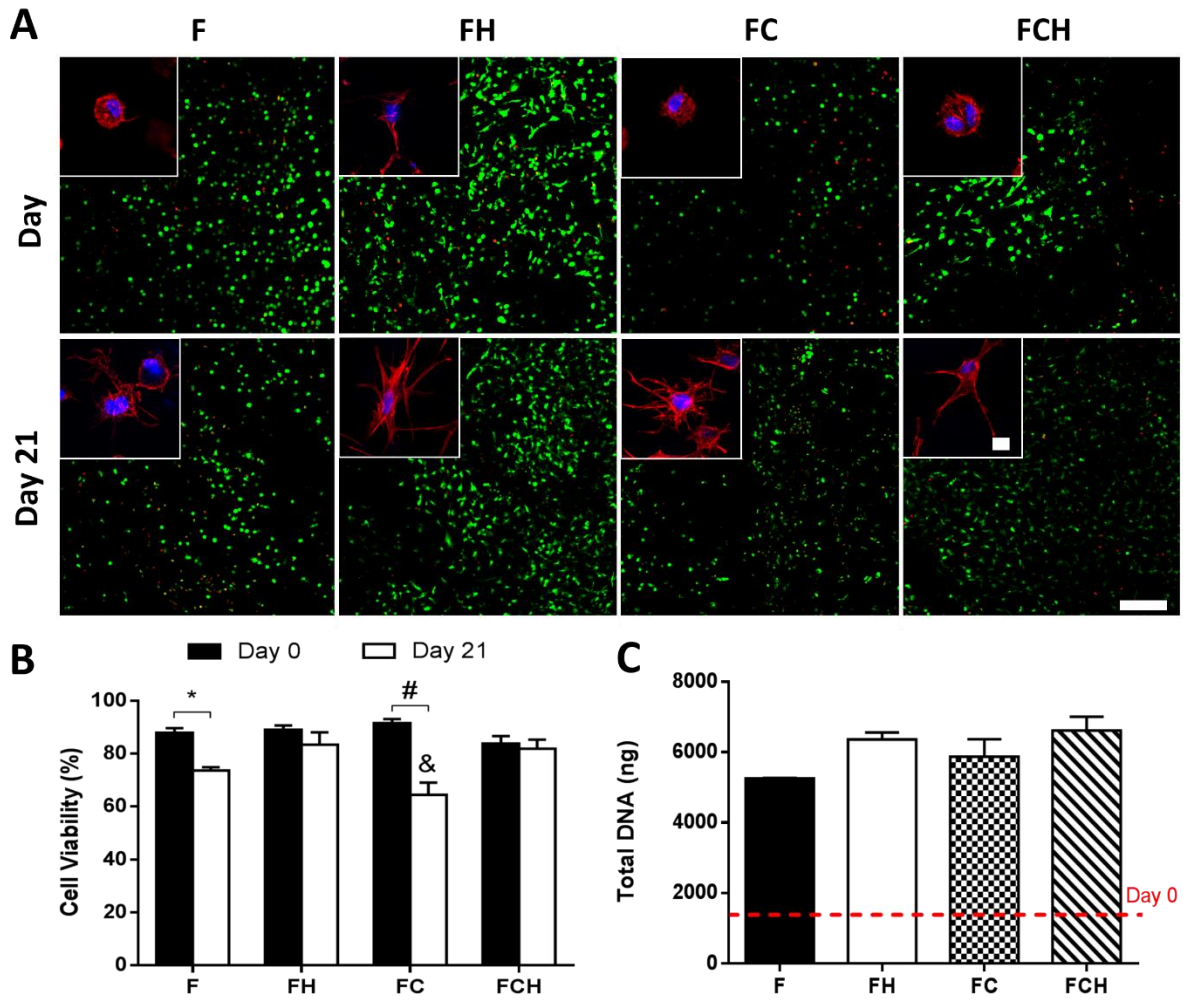

Figure 5-4: Cell viability, morphology and proliferation in F, FH, FC and FCH hydrogels over 21 days. (A) Live/dead imaging of different groups at day 0 (top row) and day 21 (bottom row). Scale bar = 200 µm with cell morphology (inset) for different hydrogel compositions; Scale bar = 10 µm; **(B)** Semi-quantitative analysis of cell viability (%). * ($p < 0.01$), # ($p < 0.0001$); & ($p < 0.001$) indicates statistical significance to day 21 values of FH and FCH; **(C)** Total DNA content (ng). Dashed line indicates day 0 levels.

5.3.2.3. HA Enhances sGAG Accumulation and Increases sGAG/Collagen Ratio

Matrix deposition was analysed through biochemical analysis and histological staining for sGAG and collagen. Total sGAG accumulation was higher in both FH (250.2 ± 23.5 µg) and FCH (233.8 ± 45.6 µg) hydrogels compared to materials without HA incorporation (169.9 ± 12.7 µg in F group and 182.4 ± 19.4 µg in FC group), (Figure 5-5 A). On a per cell basis, this trend was maintained, although no statistical difference was observed (Figure 5-5 B). More

intense staining for sGAG was observed in the periphery of constructs containing hyaluronic acid, while both F and FC hydrogels exhibited more homogenous staining (Figure 5-5 C).

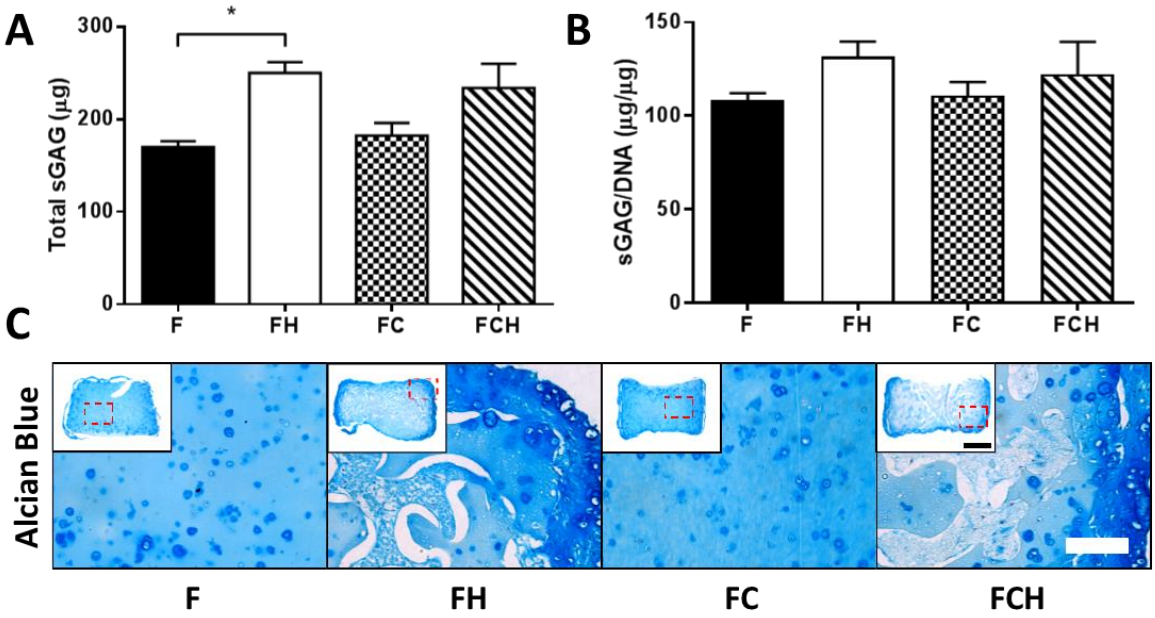

Figure 5-5: sGAG accumulation in F, FH, FC and FCH hydrogels over 21 days. (A) Total sGAG (µg); * indicates statistical significance ($p < 0.01$); **(B)** sGAG/DNA (µg/µg); **(C)** Histological staining using alcian blue for sGAG. Scale bar = 200 µm.

The highest amount of collagen was accumulated by cells encapsulated in an FC double matrix and found to be higher compared to the FCH triple matrix (initial amount of collagen was subtracted from day 21 values) (Figure 5-6 A). On a per cell basis, a similar result was observed (Figure 5-6 B). The highest sGAG/collagen ratio was found in FH hydrogels (Figure 5-6 C), which was calculated based on the total collagen (including baseline addition) contained in hydrogel constructs. From histological analysis, collagen deposition in F hydrogels was more homogenous, with higher peripheral collagen matrix observed in FH, FC, and FCH constructs (Figure 5-6 D). Immunohistochemical staining revealed elevated amounts of Col1 in the periphery of FC hydrogels, whereas Col2 was found in the periphery of constructs containing HA and in the pericellular matrix of chondrocytes within FC hydrogels (Figure 5-6 D).

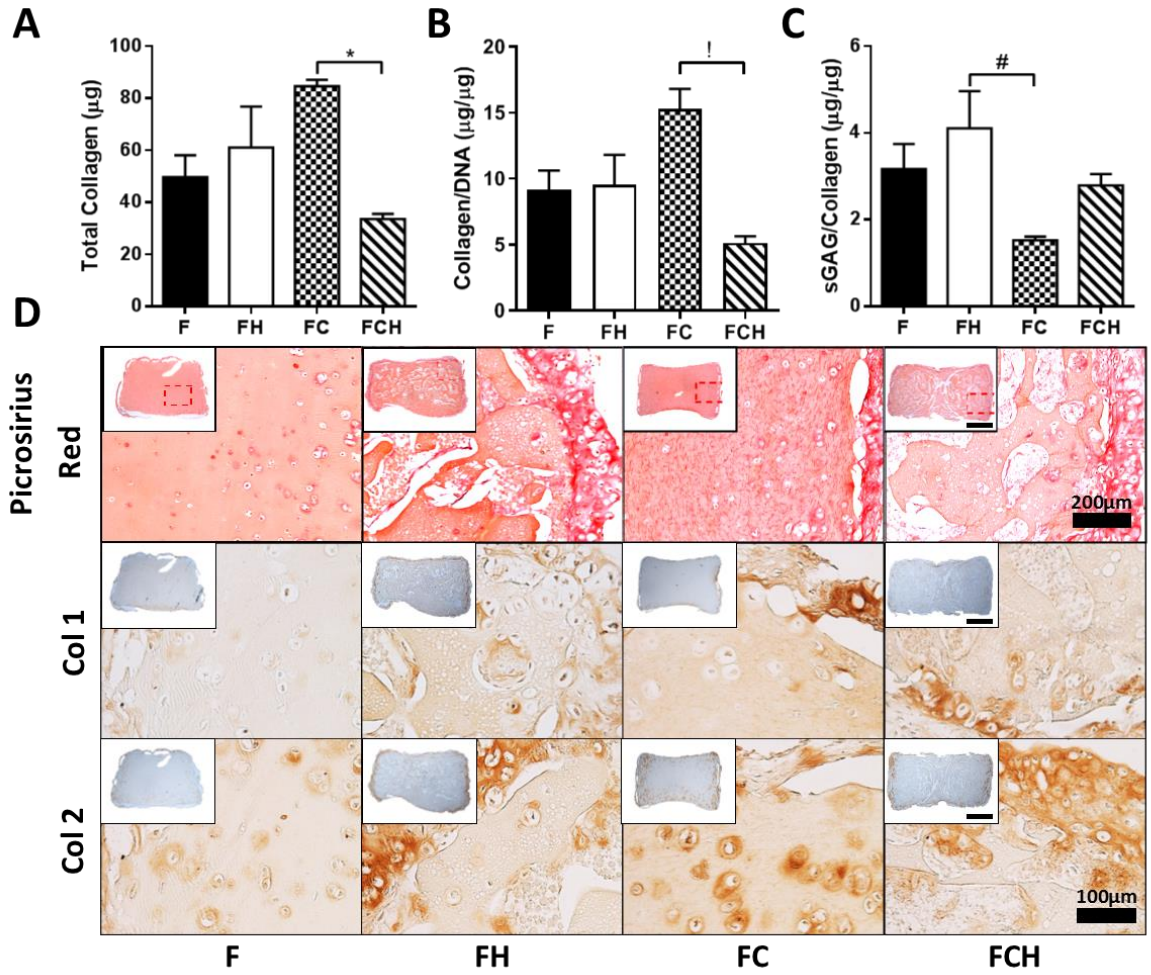

Figure 5-6: Collagen accumulation in F, FH, FC and FCH hydrogels over 21 days. (A) Total (net) Collagen (µg); * indicates significant difference ($p < 0.05$); **(B)** Total (net) collagen/DNA (µg/µg), ! indicates significant difference ($p < 0.01$). For both FC and FCH hydrogels, the initial amount of collagen was subtracted from day 21 values; **(C)** sGAG/total collagen ratio (µg/µg), calculated based on the total collagen (including baseline addition) contained in hydrogel constructs, # indicates significant difference ($p < 0.05$); **(D)** Histological staining with picrosirius red staining for collagen, scale bar = 200 µm, inset scale bar = 1000 µm and IHC staining for Col 1 and Col 2, scalebar = 100 µm, inset scale bar = 1000 µm.

5.3.3 Stage 3—Effect of Increasing HA Concentration in Fibrin-Based Hydrogels

5.3.3.1. Increasing Concentrations of HA do not Appear to Enhance Cell Viability or Proliferation

Live/dead images were captured at day 0 and day 21, showing good viability at the onset of culture, with increasing density of green fluorescent cells in FH-5 group after three weeks of

culture This group also exhibited the highest degree of contraction after 21 days (27.8 ± 3.7%) compared to both FH-2.5 (3.5 ± 3.1%) and F (3.3 ± 3.7%) groups (Figure 5-7 A). Semi quantitative image analysis revealed initial cell viabilities at day 0 of 87.7 ± 3.3% in F hydrogels, with the lowest viability observed for FH-2.5 hydrogels (75.8 ± 7.3%) (Figure 5-7 B). No significant changes in cell viability were observed over 21 days for any of the hydrogel formulations investigated. All groups exhibited an increase in DNA content (7-fold, 9.5-fold, and 5-fold increase in F, FH-2.5, and FH-5 respectively) relative to day 0 levels, with a significant difference between FH-2.5 and FH-5, showing a negative effect on cell proliferation with increasing HA concentration (Figure 5-7 C).

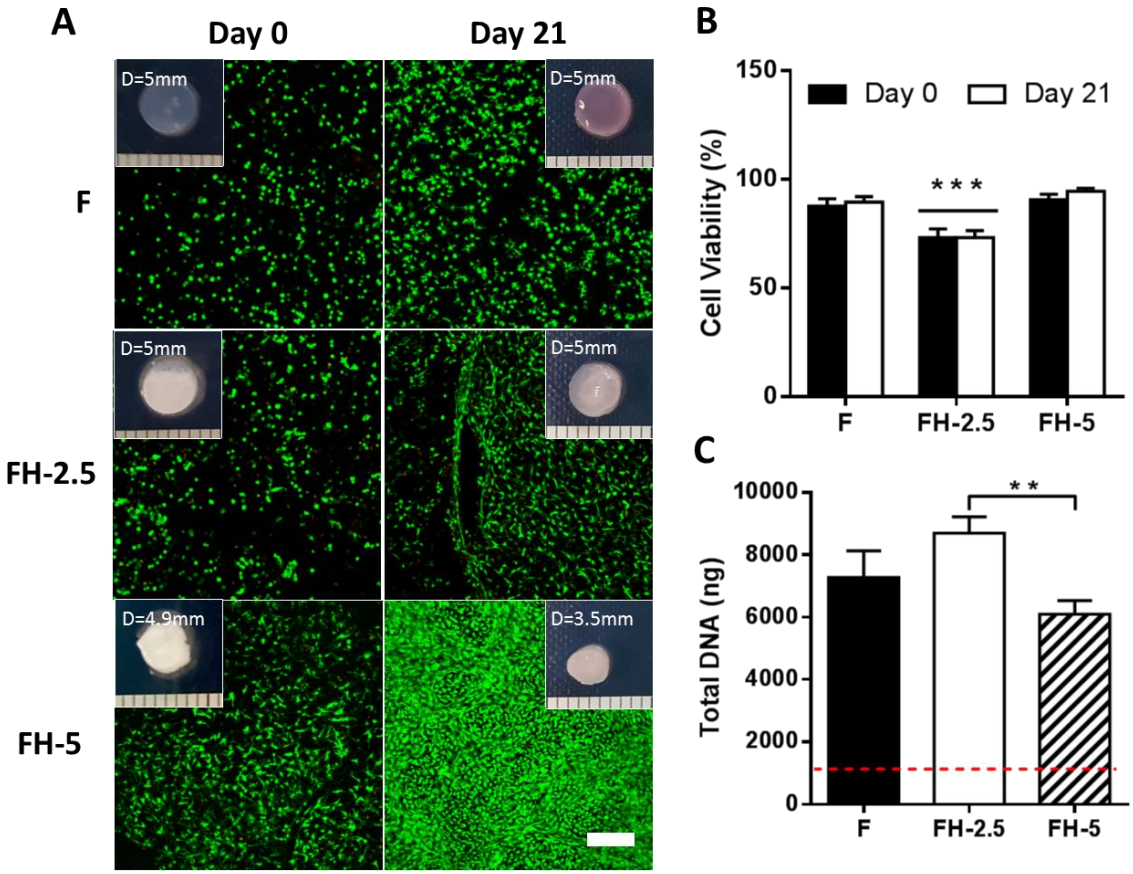

Figure 5-7: Effect of increasing concentration of HA (0, 2.5, and 5 mg/mL) on cell viability and proliferation in fibrin-based hydrogels over 21 days (A) Live/dead imaging at day 0 (left) and day 21 (right). Increased cell number was observed in groups with 5 mg/mL HA concentration. Scale bar = 200 µm; **(B)** Semi-quantitative analysis of cell viability (%). *** indicates statistical significance to all other groups ($p < 0.0001$); **(C)** Total DNA content (ng). ** indicates statistical significance ($p < 0.01$).

5.3.3.2. HA Enhances sGAG and Collagen Deposition in the Periphery of Constructs

There was an increase in total sGAG when increasing the concentration of incorporated HA with significantly higher levels of sGAG on a per cell basis with the highest amount of HA (FH-5), compared to all other groups ($p < 0.001$) (Figure 5-8 A, B). In addition, a significant difference was observed for total collagen between FH-2.5 and FH-5 ($p < 0.05$). However, no significant differences were detected between groups on a per cell basis when normalising the total collagen to DNA content (Figure 5-8 C, D). The highest ratio of sGAG/collagen was found for the highest FH matrix (3.3 ± 0.1) compared to all other groups ($p < 0.001$) (Figure 5-8 E).

Histology revealed higher sGAG content in the periphery of constructs containing HA (Figure 5-8 F—left). Of note, the staining in FH-5 hydrogels appears more homogeneously distributed, perhaps due to the contraction of constructs. On evaluation of picrosirius red staining, revealing collagen content, more profound staining was observed at the periphery of constructs after 21 days in all groups, similar to alcian blue staining (Figure 5-8 F).

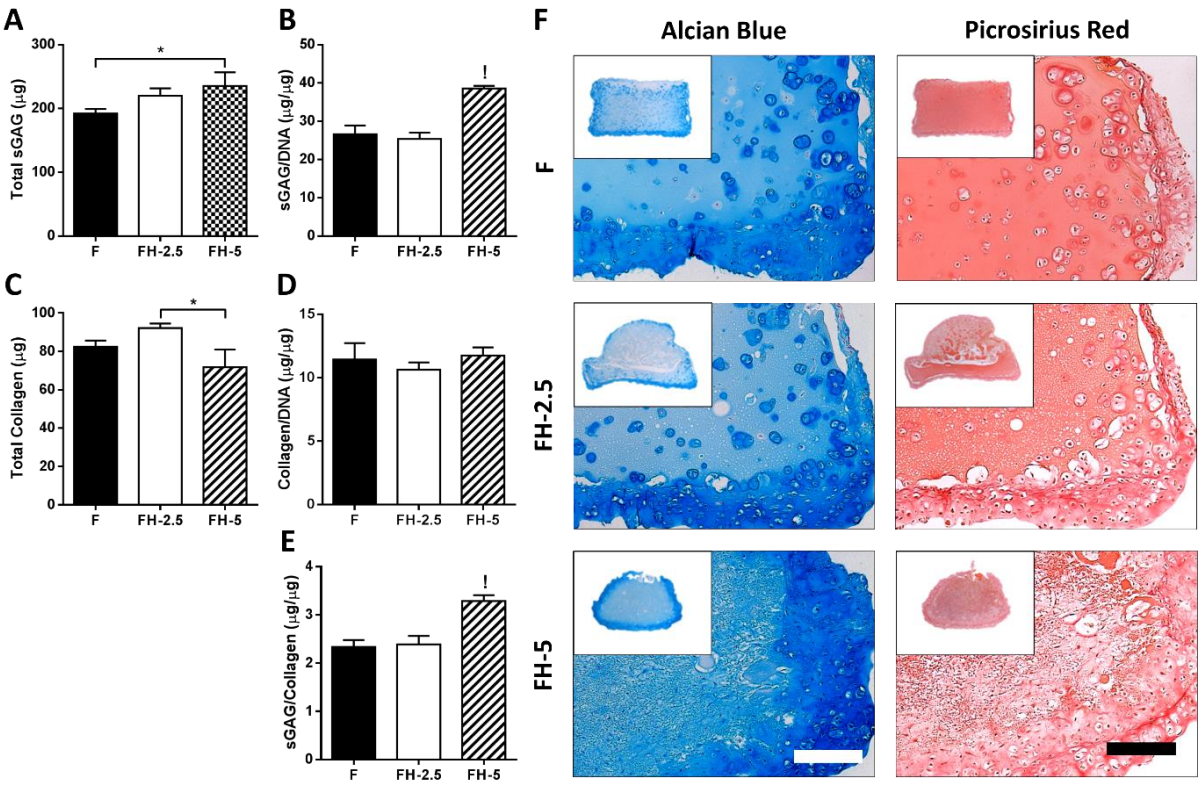

Figure 5-8: Effect of increasing concentration of HA (0, 2.5, and 5 mg/mL) on matrix accumulation of chondrocytes after 21 days of culture. (A) Total sGAG (µg) * indicates statistical difference ($p < 0.05$); **(B)** sGAG/DNA (µg/µg), ! indicates statistical difference compared to all other groups ($p < 0.001$); **(C)** Total Collagen (µg); * indicates significant difference ($p < 0.05$); **(D)** Collagen/DNA (µg/µg) **(E)** sGAG/Collagen ratio (µg/µg); ! indicates significant difference compared to all other groups ($p < 0.001$); **(F)** Histological staining using alcian blue for sGAG and picrosirius red for collagen. Scale bar = 200 µm.

5.4. Discussion

Various cell types have been successfully encapsulated into fibrin hydrogels, such as chondrocytes, human MSCs, and fibroblasts (Eyrich et al., 2007, Colombini et al., 2015, Cox et al., 2004, Hunter et al., 2004, Ho et al., 2006, Rowe et al., 2007). Fibrin is a viscoelastic material that has been used in different applications, such as a sealant and an adhesive in surgery for wound healing (Eyrich et al., 2006a, MacGillivray, 2003a, Fattahi et al., 2004a). However, further improvement can be made using ECM molecules incorporated into the fibrin matrix. It has been shown that ECM molecules, such as collagen and HA, have beneficial effects by promoting proliferation and matrix synthesis (Gorodetsky et al., 2011, Bertolo et al., 2012, Collins and

Birkinshaw, 2013). The overall aim of this work was, therefore, to identify a suitable composition of fibrin hydrogel to promote NP-like matrix formation, which is compatible with commercially available ventures. Fibrin concentration effects were first investigated, followed by determining the influence of ECM molecules, such as HA and Col1, on chondrocyte performance.

In a first instance it was found that lower fibrin concentrations (12.5 mg/mL) resulted in significant contraction, which was minimised for concentrations at or above 25 mg/mL. Similar observations have been reported by Eyrich et al., who found that a final fibrin concentration of 25 mg/mL or higher, a calcium concentration of 20 mM and pH between 6.8 and 9 produced a stable, transparent gel for up to three weeks (Eyrich et al., 2007). The contraction of lower fibrin concentrations could be due to the decreased fibre density, and therefore, different pore sizes between the fibres. At higher concentrations, the increasing fibre density leads to stiffer hydrogels, supporting the long-term stability of the hydrogel (Kotlarchyk et al., 2011, Duong et al., 2009). Kotlarchyk et al. used fluorescently labelled fibrin gels to analyse pore size and found smaller pore sizes for higher concentrations of fibrin (Kotlarchyk et al., 2011). Another study by Chiu et al. also found a correlation between smaller pore size in higher fibrinogen concentration gels with reduced diffusion and permeability through these gels (Chiu et al., 2012). These observations correlate with the findings of this work, and perhaps explain the lack of contraction with higher concentrations of fibrinogen, due to the presence of smaller pore sizes between the fibres which are more stable over time.

Further, cell proliferation was found to be enhanced for increasing fibrinogen concentrations. Previous work has reported reduced permeability with increasing concentration, which would be indicative of a diminished nutrient supply for encapsulated cells (Chiu et al., 2012) and may limit cell proliferation. For MSCs, Ho et al. observed increased proliferation with decreasing fibrinogen concentration (Chiu et al., 2012, Ho et al., 2006). These differences in proliferation kinetics could be due to the specific cell types utilised. Chondrocytes and MSCs are derived from different niches and have specific requirements in terms of nutrients such as glucose

and oxygen. The microenvironmental niche of chondrocytes comprises of low oxygen and low nutrient supply, due to it being an avascular tissue.

For lower fibrin concentrations, increased cell death was observed, which could be a result of the increased contraction due to lower fibre density (Kotlarchyk et al., 2011). Being softer gels, with larger pores, facilitates cells to exert a force on their surrounding matrix, resulting in contraction of hydrogels and smaller effective pore sizes. These smaller pores, and a higher cell density, may impact on nutrient availability, causing deprivation in the centre, where more cell death occurs.

The enhanced proliferation of chondrocytes in higher concentrated fibrin gels may also be due to increased cell–matrix interaction of fibrin with CD44 surface receptors (Alves et al., 2009, Alves et al., 2008). Cell–matrix interaction occurs through different surface proteins, and it is widely accepted that HA has a high affinity to the cell surface receptor CD44, which is present on different cell types such as chondrocytes, MSCs, and hemopoietic stem cells (Aguiar et al., 1999, Chow et al., 1995, Ramos et al., 2016, Zoller, 2015, Knudson and Knudson, 2004). Once CD44 is activated, an upregulation of the receptor occurs, resulting in reorganisation of the cytoskeleton proteins, clustering of CD44, covalent dimerisation, and binding of HA (Liu et al., 1998). High molecular weight (HMW) HAs are long molecules, which can bind to several CD44 receptors at a time, resulting in increased affinity. This binding can affect alignment of intracellular actin filaments, and thus influence the cell shape of chondrocytes (Underhill and Toole, 1980, Raja et al., 1988, Lesley et al., 2000), as observed in this work. It is also known that HA mediates both cell–cell and cell–matrix interactions (Aguiar et al., 1999, Chow et al., 1995). Chondrocytes have been shown to maintain their phenotype when cultured on HA compared to Col1 hydrogels, with enhanced proliferation and higher expression of chondrogenic markers such as Col2 and aggrecan (Park et al., 2014), illustrating the important role of ECM-derived molecules in regulating cellular phenotype. This is in agreement with our findings, whereby enhanced cell proliferation, sGAG, and Col2 accumulation was observed when HA was incorporated into the fibrin matrix.

In addition, incorporation of collagen into fibrin-based hydrogels enhanced total collagen accumulation after three weeks in culture, compared to all other groups. Specifically, enhanced levels of Col1 deposition were observed, predominantly at the periphery of hydrogels and greater levels of Col2 within the pericellular matrix (PCM) of chondrocytes. It has been shown that fibrin can interact with CD44 and the integrin αvβ3. αvβ3 is an integrin which has no intracellular effect on chondrocytes when present or knocked out, indicating no major role when attachment of chondrocytes occurs (Kurtis et al., 2003). The affinity to the integrin and the cell–matrix attachment using the RGD motifs of fibrin may be higher than the interaction with CD44, which explains the limited effect of fibrin gel on chondrocytes. Fibrin provides binding sites, which do not affect chondrocytes further through intracellular signalling. Previous work has shown higher levels of Col2 expression of NP cells in fibrin–collagen hydrogels both *in vitro* and *in vivo* (Colombini et al., 2015). It has also been shown that Col1 can specifically bind to fibrin, using the integrin αvβ3 connection as a functional interface matrix which could activate different intracellular pathways (Reyhani et al., 2014). Further, it has been shown that the combination of collagen and fibrin alters the mechanical properties (Cummings et al., 2004), which could also be responsible for phenotypic changes.

Exploring the effect of HA, it was observed that incorporation of HA into fibrin–collagen matrices appeared to suppress levels of total collagen and increased levels of sGAG, possibly due to the activation of CD44 receptors. Collagen–cell interactions mainly activate pathways involved with cell adhesion, cell migration, and stress fibre assembly in AF and NP cells, which are not primarily involved in matrix deposition (Sarath Babu et al., 2016). Mahapatra et al., examined the behaviour of chondrocytes in a triple matrix consisting of alginate, collagen, and HA (Alg–Col–HA), compared to a double matrix of alginate and HA only (Alg–HA) (Mahapatra et al., 2016). The authors found that the triple matrix supported proliferation significantly more than the double matrix after 21 days, with enhanced expression of chondrogenic markers. This contrasts with our findings, where the double matrix with HA and the triple matrix appear to have similar chondrogenic capacities. However, it should be noted that Mahapatra et al. utilised alginate as

the supporting gel, which does not provide binding sites, and may explain the different results observed.

In the final stage of this study, the effect of different amounts of HA incorporated into the fibrin matrix was investigated. Previous work has investigated the effect of different concentrations of HA (0.1–3.0 mg/mL) on chondrocytes in alginate hydrogels (Akmal et al., 2005). The authors observed a trend towards higher levels of DNA, sGAG, and collagen after 14 days with lower concentrations (0.1–1 mg/mL) of HA. However, at higher concentrations, diminished DNA and collagen contents were observed, similar to the present study. It has been shown that high molecular weight HA, as used in this work, can bind to several CD44 surface markers at a time (Raja et al., 1988, Lesley et al., 2000), indicating that saturation of CD44–HA interaction can occur even with a lower concentration of HMW HA molecules. This suggests a threshold exists beyond which increasing HA concentration will have no additional benefit.

Another possible explanation for the observed enhancement of sGAG with higher concentrations of HA is due to a physical change in hydrogel network, rather than a cellular activation alone. HA is inherently difficult to retain in hydrogel systems, and easily diffuses into the surrounding media (Lindenhayn et al., 1999), which was also evidenced in acellular hydrogel studies in the present work. Therefore, it is difficult to determine for what period lower HA concentrations are effective to elicit a beneficial response. At the highest HA concentration (FH-5), shrinkage of constructs was observed, which may have led to entrapment of HA within the fibrin matrix network, resulting in a higher degree of cell–cell contact and cellular condensation, thereby promoting chondrogenesis. Whether the beneficial effect of the highest concentration of HA is due to the binding of HA or due to the initiated condensation of the construct remains unclear and warrants further investigation. Overall, these findings suggest, despite increased contraction, a concentration of 5 mg/mL HA to be suitable for disc repair, due to the enhanced NP-like matrix accumulation of ACs within this network.

5.5. Conclusion

In this work, the incorporation of ECM molecules into fibrin-based hydrogels was explored in order to develop a suitable injectable system to facilitate μCaps delivery into the IVD and to take advantage of the use of a bioactive material for the host environment. Significant hydrogel contraction was observed using low (12.5 mg/mL) fibrin concentrations, with limited contraction for concentrations at or above 25 mg/mL. With the incorporation of ECM components, cell viability was seen to be maintained when HA was incorporated. HA also enhanced sGAG accumulation and tended to suppress collagen formation at higher concentrations. There did not appear to be any significant benefit of incorporating Col1 in the fibrin matrix. Lastly, an overall increase in the sGAG to collagen ratio was demonstrated when increasing HA concentration in the fibrin matrix to 5 mg/mL. Taken together, these results suggest that incorporation HA can enhance the bioactivity of fibrin-based hydrogels, which may help advance the clinical potential of commercial cell and biomaterial ventures in the treatment of IVD regeneration.

CHAPTER 6
PRIMING AS A MEANS TO MITIGATE ACIDIC PH EFFECTS ON BONE MARROW-DERIVED STEM CELLS AND ARTICULAR CHONDROCYTES CULTURED UNDER INTERVERTEBRAL DISC-LIKE CONDITIONS

Having addressed technical challenges associated with intradiscal injection to overcome limited cell delivery into the pressurized disc environment by proposing a combination of cellular µCaps within a biomimetic bulking agent, the following chapter focuses on objective iv and aims to establish a strategy to overcome the challenges of disc acidity and their effect on injected cells.

6.1. Introduction

As described previously, disc degeneration can be associated with a change in the harsh microenvironment found in the IVD. Especially the increased acidity has proven to be a major challenge for cell-based IVD regeneration strategies. Acidic microenvironments affect cells through different intracellular pathways. Transmembrane acid-sensing ion channels (ASIC) are proton-gated sensitive channels and are expressed in various cell types including ACs and NP cells (Zhou et al., 2015b, Rong et al., 2012, Gilbert et al., 2016a). Both ASIC-1 and ASIC-3 subunits have been found to be expressed in NP cells and ACs, which are permeable to Na^+ and Ca^{2+} ions (Cuesta et al., 2014, Zhou et al., 2015b). When activated, the influx of ions has been shown to trigger ion-dependent proteases, which can alter gene expression and induce apoptosis of cells (Yuan et al., 2016).

In the context of administration of cell-based therapies for the purpose of disc regeneration, it is important to consider the microenvironment and ability of transplanted cells to function normally. Various cell types such as disc-derived cells, bone marrow-derived stem cells

and chondrocytes have been investigated for disc regeneration (Gorensek et al., 2004, Illien-Junger et al., 2012). Commercial entities including DiscGenics Inc. (Salt Lake City, Utah) and Mesoblast Ltd. (Melbourne, Australia) are developing allogeneic cell-based products and are advancing with additional clinical trials (Smith et al., 2018). However, the impact of the harsh microenvironment of the degenerated intervertebral disc is an important factor that may affect the success of these approaches. Injected cells may experience limited nutrition or low pH conditions, resulting in compromised outcomes of the therapy. A further concern relates to the metabolism of cells, and whether the degenerated microenvironment can sustain increased metabolic demands upon delivery of cells to the targeted site.

Ideally, the injected cells should be capable of sustaining the acidic microenvironment of the disc as well as having a slow metabolic rate to avoid exacerbating nutrient deprivation effects. One approach to improve viability in low pH microenvironments may be through the formation of a protective ECM niche around the cells. In carcinogenic tissue, PCM has been shown to increase drug resistance indicating its protective features for cancerous cells (Noguera et al., 2012). Moreover, our previous studies have shown that priming of BMSCs using TGF-β3 promoted higher levels of sGAG and collagen deposition and supported cell survival of cryopreserved cells (Naqvi and Buckley, 2015a, Naqvi et al., 2018). Primed or pre-differentiated MSCs have been proposed in a number of other investigations for cartilage, bone and IVD regeneration (Lam et al., 2014), making this strategy a promising approach to overcome microenvironmental challenges for disc repair.

The overall objective of this study was to explore the effects of acidic microenvironments on BMSCs and ACs and to determine if priming can enhance cellular response in low pH conditions in terms of viability, metabolism and disc-like matrix accumulation.

6.2. Methods

6.2.1 Experimental design

This study investigated the effect of matrix acidity on BMSCs and ACs non-primed and primed using TGF-β3 (Figure 6-1). Cells were encapsulated in 1.5% alginate and cultured in different conditions: i) in low pH conditions for 3 weeks (non-primed) or ii) at standard pH (7.4) with growth factor supplementation for 2 weeks prior to an additional 3 weeks acidic conditions (primed), resulting in a total *in vitro* culture period of 5 weeks. All groups were maintained under low glucose (5.5 mM) and physioxic oxygen (5% O_2) conditions for the duration of the experiment.

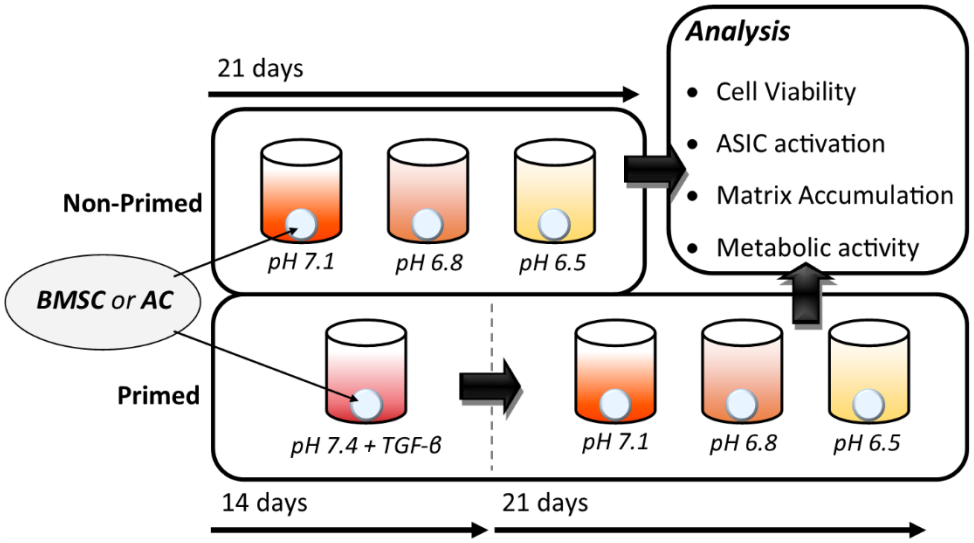

Figure 6-1: Study design. Alginate encapsulated BMSCs and ACs were cultured either in low pH conditions without growth factor supplementation for 21 days (top) or for 14 days with TGF-β3 supplementation prior to 21 days low pH culture (bottom). Analysis was performed in terms of cell viability, ASIC activation, matrix accumulation and metabolic activity.

6.2.2 pH stabilisation

Media with three different pH values were prepared by adding an appropriate amount of acid (LacA and hydrochloric acid) to supplemented lg-DMEM. Briefly, LacA was added to the media to obtain physiological levels (4 mM) normally found in the IVD (Bartels et al., 1998). Additionally, 3 M HCl was added to adjust pH levels (8 µL/mL, 9 µL/mL and 10 µL/mL for pH

7.1, 6.8 and 6.5 respectively). The pH-adjusted media was incubated overnight in a humidified incubator (5% CO_2) to allow buffer equilibrium (CO_2-dependent). The desired pH values were obtained after equilibration and were maintained for up to 72 hours.

6.2.3 Alginate encapsulation and culture

Culture expanded porcine cells were encapsulated in 1.5% alginate (w/v in PBS) (Pronova UP LVG, FMC NovaMatrix, Norway) at a density of $4x10^6$ cells/mL. The alginate/cell suspension was passed through a 12G needle (inner diameter = 2.16mm) and ionically crosslinked with 100 mM calcium chloride ($CaCl_2$, pH 7.2) for 15 min to form beads (Ø = 5 mm). Alginate beads were maintained in pH (7.4, 7.1, 6.8 and 6.5) adjusted supplemented chemically defined medium (SCDM) consisting of lg-DMEM, 100 U/mL penicillin, 100 µg/mL streptomycin, 1× ITS (all from GIBCO, Invitrogen, Dublin, Ireland), 0.25µg/mL AmpB, 40µg/mL L-proline, 1.5mg/mL BSA, 4.7 µg/mL linoleic acid, 50 µg/mL L- ascorbic acid-2-phosphate, 100nM dexamethasone (all Sigma-Aldrich, Ireland) and 10 ng/mL TGF- β3 (PeproTech, UK) for the primed group (pH 7.4). Alginate beads were cultured in standard 24-well plates with one bead per well and 2 mL of supplemented medium in physioxic (5% oxygen) conditions with complete medium exchanges performed twice weekly for the total culture duration of 21 and 35 days.

6.2.4 Immunofluorescence

ASIC-1 (ACCN2) and ASIC-3 were evaluated using an immunofluorescence staining technique. Briefly, 5 sections per sample for ASIC-1 were heat treated using a citrate buffer at pH 6, whereas 5 sections for ASIC-3 were treated with Pronase (Sigma-Aldrich) in a humidified environment at 37°C to enhance permeability of the ECM. All sections were incubated with goat serum to block non-specific sites and anti ACCN2 (ASIC-1) (1:50; 1 mg/mL, ab176203, rabbit monoclonal, Abcam, Cambridge, UK) and anti ASIC-3 (1:50; 1 mg/mL) primary antibodies (ab49333, rabbit monoclonal, Abcam, Cambridge, UK) were applied for 18 hr at 4°C. Next, the secondary antibody (ab15007 Goat Anti-Rabbit IgG H&L Alexa Fluor 488, 1:1000; 2.1 mg/mL, Abcam, Cambridge, UK) was added for 1 hr followed by incubation with DAPI (Vectastain PK-

400, Vector Labs, Peterborough, UK) for 10 min. 10 images per section were taken for image analysis.

6.2.5 Determination of metabolic consumption rates

Oxygen consumption of non-primed and primed alginate beads were monitored in air-tight glass vials for 3 days using PreSens SensorVials and the SDR Sensor Dish® Reader system. Low glucose (5.5 mM) CDM at specific acidity levels without growth factor supplementation was used. Glucose concentrations in media samples from day 0 to day 3 (non-primed) and day 14 to day 17 (primed) were quantitatively measured using a glucose meter (FreeStyle Optimum, abbot Diabetes Care, Ireland) (Naqvi and Buckley, 2015c). Lactate content was determined by measuring the reaction of lactate with NAD+ and lactate dehydrogenase and L-lactic acid as the standard as described previously (Heywood et al., 2006). All respiration rates (oxygen, glucose and lactate) were determined by normalizing to the number of viable cells at each time point examined.

6.2.6 Statistical analysis

Statistical analysis was performed using GraphPad Prism (version 8). Two different tests were carried out to determine statistical differences between groups: Firstly, Three-way ANOVA was used for the analysis of variance with Tukey's multiple comparison tests to compare between general groups (non-primed vs. primed, BMSC vs. AC and effect of pH). Secondly, Two-way ANOVA was applied to analyse variances with Tukey's multiple comparison tests to compare between individual experimental groups. Three samples were analysed for each experimental group of 3 individual experiments of different porcine donors. Numerical and graphical results are displayed as mean ± SD and significance was accepted at a level of $p < 0.05$.

6.3. Results

6.3.1 Priming Significantly improves cell viability of BMSC

Non-primed BMSCs exhibited low cell viability at all pH levels examined with average values of 27.3% and 20.7% at pH 7.1 and 6.8 respectively and a significant drop observed at pH 6.5 (2.2%, with $p<0.001$ and $p<0.01$ compared to pH 7.1 and 6.8 respectively) (Figure 6-2 A and C). AC, however, appeared to be less sensitive to different pH conditions maintaining approximately 62% viability across all pH levels investigated. After 14 days of priming using TGF-β3, cell viability of both cell types was improved with a significant increase to 76.3% and 73.5% of BMSC at pH 7.1 and 6.8 respectively ($p<0.0001$). Notably, BMSC at pH 6.5 showed a significant increase in cell viability of 62.0%, which is a 28-fold increase compared to non-primed (Figure 6-2 B and C). AC also demonstrated improved viabilities of 84.4%, 80.7% and 73.5% at pH 7.1, 6.8 and 6.5 respectively. Quantification of total DNA showed a decreased level of DNA over time for non-primed beads compared to Day 0, with constant lower levels of DNA across all pH levels and cell types examined. Priming enhanced cell proliferation initially with slightly higher levels observed for BMSC beads. DNA values were maintained during culture in low pH media for all groups (Figure 6-2 D).

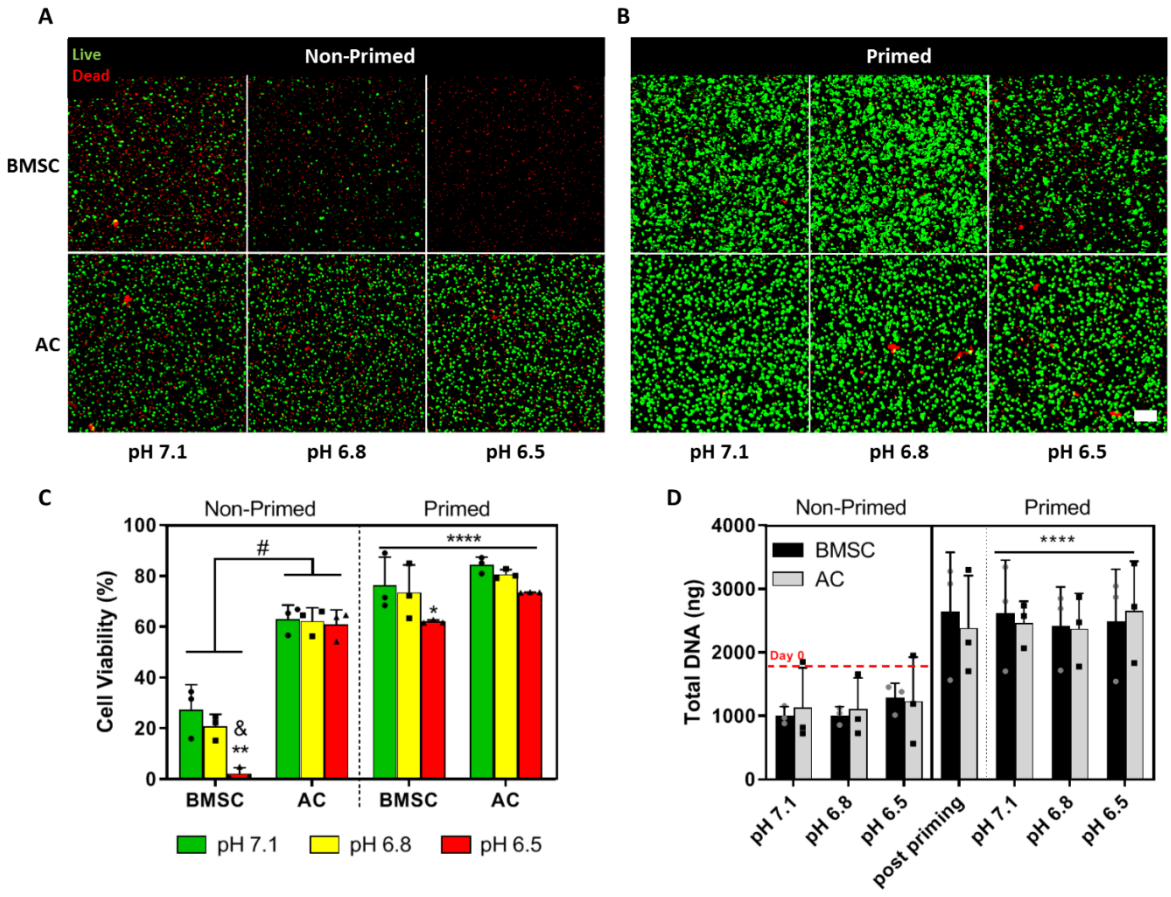

Figure 6-2: Cell viability and proliferation of BMSCs and ACs (A) Live/Dead analysis of BMSC and AC after culture in different pH conditions without priming and **(B)** with priming. Scale bar=150 µm. **(C)** Semi-quantitative analysis of cell viability without priming and with priming. **(D)** Biochemical quantification of DNA content of non-primed and primed beads. # indicates significant difference between non-primed BMSCs and ACs at all pH levels ($p<0.0001$), * indicates significant difference between primed BMSC at pH 6.5 and pH 7.1 ($p<0.05$), & and ** indicate significant difference between non-primed BMSC at pH 6.5 and non-primed BMSC at pH 7.1 ($p<0.001$) and pH 6.8 ($p<0.01$) respectively

6.3.2 Increasing expression of ASIC-1 after priming of BMSC

Expression of ASIC was determined using semi-quantitative image analysis. Results indicate that for BMSCs, ASIC-1 expression was significantly higher after priming compared to non-primed groups ($p<0.001$ at pH 7.1 and $p<0.0001$ at pH 6.8 and 6.5) and fluorescent images showed a larger cell body after priming of BMSCs. ACs exhibited a decrease in ASIC-1 expression at pH 7.1 after priming ($p<0.0001$), whereas expression increased for primed ACs at pH 6.8 ($p<0.0001$) (Figure 6-3 A and B). In contrast, ASIC-3 expression of BMSCs was not affected by pH or priming. However, its expression significantly increased in ACs after priming

and culturing at pH 6.8 and 6.5 ($p<0.0001$ and $p<0.001$ respectively). At pH 7.1, ASIC-3 expression was downregulated after priming and is significantly lower compared to pH 6.8 and 6.5 of primed AC ($p< 0.0001$) (Figure 6-3 A and C). Interestingly, ACs formed cell clusters in all acidic levels (2-5 cells per cluster) after priming (Figure 6-3 A).

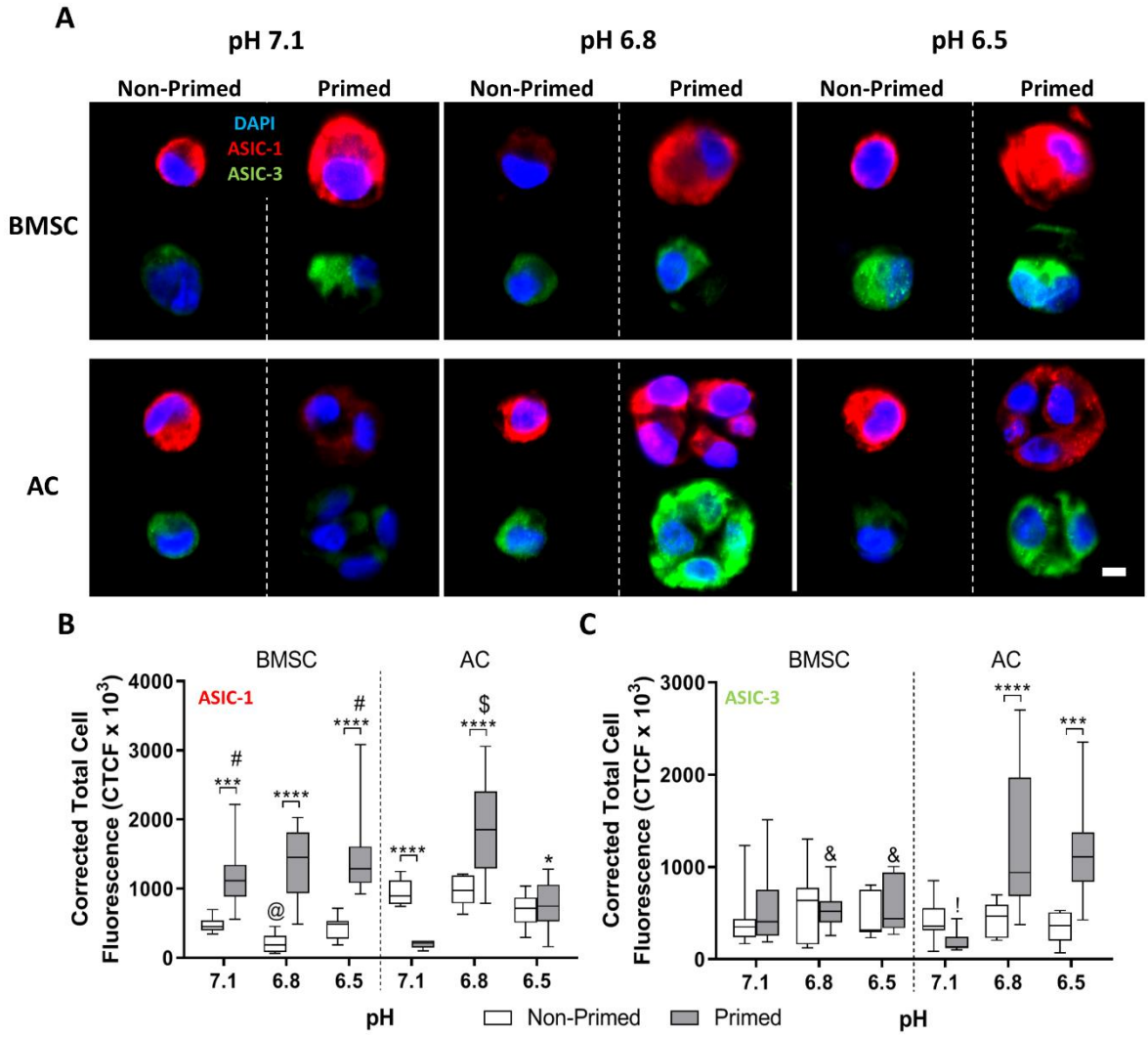

Figure 6-3: Expression of acid-sensitive ion channels of BMSCs and ACs. (A) Immunofluorescence of ASIC-1 (red) and ASIC-3 (green) of BMSCs (top) and ACs (bottom) before and after priming at different pH conditions (scale bar = 5 µm). **(B)** Semi-quantitative evaluation of the intensity of ASIC-1 expression. # indicates significant difference between primed BMSCs and ACs at same acidity ($p<0.001$), @ indicates significant difference between non primed BMSCs and non-primed ACs at pH 6.8 ($p<0.001$), $ indicates significant difference between primed ACs at pH 6.8 to all other pH conditions of this group ($p<0.0001$), * indicates significant difference between primed ACs at pH 6.5 to pH 7.1 ($p<0.05$), **** and *** indicate significant difference between specified groups ($p<0.0001$ and $p<0.001$ respectively), **(C)** Semi-quantitative evaluation of intensity of ASIC-3 expression; & indicates significant difference between BMSCs and ACs at same priming and pH conditions ($p<0.01$), ! indicates significant difference between primed ACs at pH 7.1 to pH 6.8 and pH 6.5 respectively ($p<0.0001$), **** and *** indicate significant difference between specified groups ($p<0.0001$ and $p<0.001$ respectively).

6.3.3 Matrix acidity inhibits sGAG accumulation, which can be mitigated by priming

Higher acidity was found to inhibit sGAG accumulation of non-primed ACs and was particularly pronounced at pH 6.5. Unsurprisingly, non-primed BMSCs did not accumulate sGAG regardless of pH level (Figure 6-4 A). After exposure to TGF-β3 for 14 days however, both BMSCs and ACs accumulated a baseline level of sGAG of 83.8 ± 49.2 µg and 78.8 ± 15.4 µg respectively, which increased 1.6-fold and 1.4-fold for BMSCs at pH 7.1 and 6.8. AC accumulated an additional 30% sGAG compared to post-priming baseline level throughout the low pH exposure (7.1 and 6.8) of 3 weeks (Figure 6-4 A). No change in sGAG deposition was observed after the 21 days culture at pH 6.5 for either BMSCs or ACs. Comparing the two different cell types it is evident that non-primed ACs have higher sGAG accumulation capacities than BMSCs, however, primed BMSCs produce similar levels across all groups (Figure 6-4 A and B). In terms of histology, non-primed BMSCs exhibited only background staining for alginate (light blue) but no staining for sGAG (dark blue/purple) similar to day 0 histology, which aligns the biochemical findings. Non-primed ACs exhibited pericellular deposition of sGAG at all pH levels, however at pH 6.5 the sGAG level deposited was below the detection limit of the assay (indicated with “nd”) but was still visible histologically (Figure 6-4 C left). After priming, more intense purple staining was observed indicating higher amounts of sGAG deposition in all groups. Histology images of post-priming shows sGAG deposition after TGF-β3 exposure but prior to low pH culture, demonstrating a great amount of sGAG deposition for both BMSC and AC respectively. In addition, BMSCs cultured at pH 7.1 and pH 6.8 exhibited intense staining after priming, which correlated with the biochemical quantification (Figure 6-4 C right).

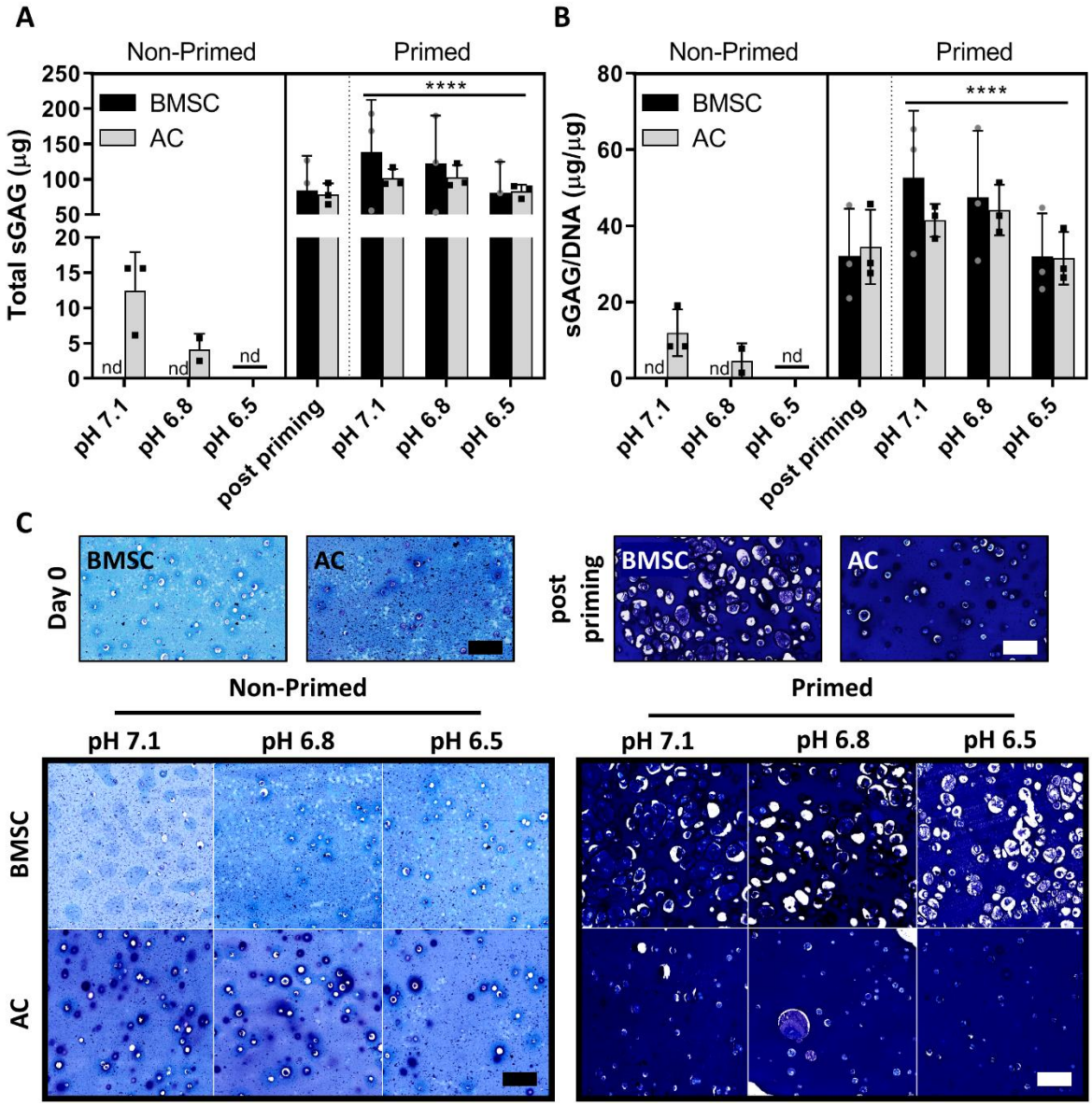

Figure 6-4: sGAG accumulation of non-primed and primed BMSCs and ACs at different pH levels. (A) Total sGAG (µg) accumulation of non-primed or primed BMSCs (black bar) and ACs (grey bar) after 21 days of exposure to low pH conditions. **(B)** normalised sGAG levels to total DNA (µg/µg), **** indicates significant difference between non-primed and primed groups ($p<0.0001$), "nd" indicates "not-detectable". **(C)** Alcian blue/aldehyde fuchsin staining indicating sGAG deposition (dark blue/purple) non-primed/primed cells before and after low pH exposure. Scale bar = 100 µm.

6.3.4 BMSC accumulate higher levels of collagen with greater amount of collagen 2 deposition

Having determined the amount of sGAG accumulated by cells under different conditions, quantification of collagen content and type was performed, another important constituent of the

ECM in NP-like tissue. Results indicated inhibition of collagen deposition for both non-primed BMSCs and ACs (Figure 6-5 A and D), which show similar negative staining for picrosirius red as at day 0 (Figure 6-5 D). However, priming had similar effects as observed for sGAG accumulation, showing a baseline total collagen-levels of 71.2 ± 15.5 µg and 60.0 ± 13.6 µg respectively for BMSCs and ACs post-priming (Figure 6-5 A). For ACs, these levels were maintained at all pH levels with no significant changes observed for either total collagen or collagen normalised by DNA content (Figure 6-5 A and B). These levels were lower in comparison to collagen levels accumulated by BMSCs. Moreover, BMSCs increased the total amount of collagen 1.5-fold when cultured for 21 days at pH 7.1 post-priming (Figure 6-5 A). However, newly synthesised collagen by BMSCs was inhibited with increasing matrix acidity, with a pH of 6.5 resulting in maintenance of basal levels. Overall, three-way ANOVA revealed a significant impact of pH on collagen/DNA level ($p<0.05$). Biochemical results were confirmed histologically, demonstrating more intense red staining of primed samples prior low pH culture and after culture at 7.1 and 6.8, indicating greater deposition of collagen matrix (Figure 6-5 D).

To evaluate matrix quality, the sGAG/collagen ratio was determined showing an average value of 1.5 ± 0.4 (Figure 6-5 C). Weak staining for Col1 was observed for both BMSC and AC for all pH levels after priming. Increased deposition of Col2 was found in the pericellular region of all AC cultures regardless of matrix acidity. More intense and obvious Col2 staining was detected throughout primed BMSC beads cultured at pH 7.1 and 6.8, which was diminished at pH 6.5 (Figure 6-5 D).

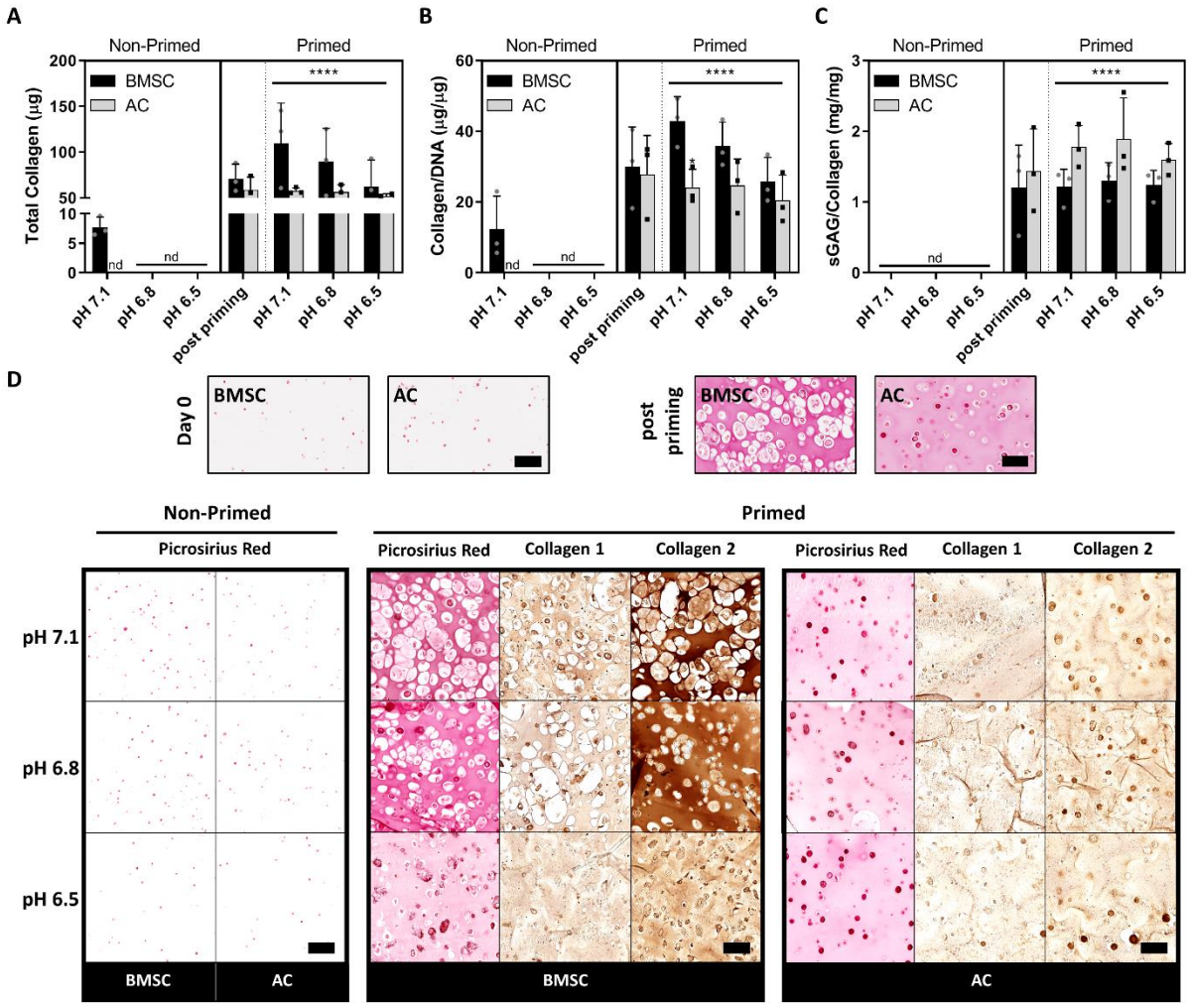

Figure 6-5: Collagen accumulation of non-primed and primed BMSCs and ACs at different pH levels. (A) Total collagen deposition (µg) of non-primed and primed BMSC (black bar) and AC (grey bar) after 21 days. **(B)** total collagen normalised to total DNA content (µg/µg). **(C)** sGAG per collagen ratio (mg/mg). * indicates significant difference of Primed BMSCs and ACs at pH 7.1 ($p<0.05$), **** indicates significant difference between non-primed and primed groups ($p<0.0001$), "nd" indicates "not-detectable". **(D)** Picrosirius Red staining was used to indicate total collagen deposition of cells at day 0, directly post-priming and non-primed (left) and primed (right) samples after low pH exposure. Further determination of the specific collagen type (Col1 and Col2) was performed using immunohistochemical analysis. Scale bar = 100 µm.

6.3.5 Priming alters the metabolic profile of BMSCs and ACs

Metabolic activity in terms of oxygen and glucose consumption as well as lactate production of non-primed and primed cells was investigated. Oxygen consumption rate (OCR) of BMSCs was found to be upregulated (2-fold) post-priming, whereas OCR of ACs tended to decrease post-priming, (Figure 6-6 A). Overall, ACs had significantly lower OCRs compared to

BMSCs ($p<0.01$). There was a trend in increased glucose consumption rates (GCR) of BMSCs after priming at all pH levels, however, the difference was not found to be statistically significant. ACs showed a trend towards decreased GCR with increasing matrix acidity post-priming (Figure 6-6 B). A similar profile was observed for lactate production rate (LPR), with a significant difference between non-primed and primed BMSC at pH 7.1 ($p<00.05$) and pH 6.8 ($p<0.001$) as well as a trend towards decreasing LPR with increasing acidity of ACs. Overall, non-primed cells showed lower lactate production compared to primed cells for both BMSCs and ACs (pH 7.1 and 6.8). Moreover, three-way ANOVA revealed a significant correlation between lactate production rate and pH ($p<0.01$) and priming had a significant effect on altering lactate metabolism ($p<0.0001$) (Figure 6-6 C). A significant increase in the ratio of lactate production to glucose consumption was found for primed BMSCs at pH 6.8 compared to non-primed BMSCs ($p<0.05$). In all other groups, a trend of decreasing ratio after priming was observed, with a decreasing ratio for non-primed AC with increasing acidity. Generally, it was found that priming had a significant influence on the lactate to glucose ratio ($p<0.05$) (Figure 6-6 D).

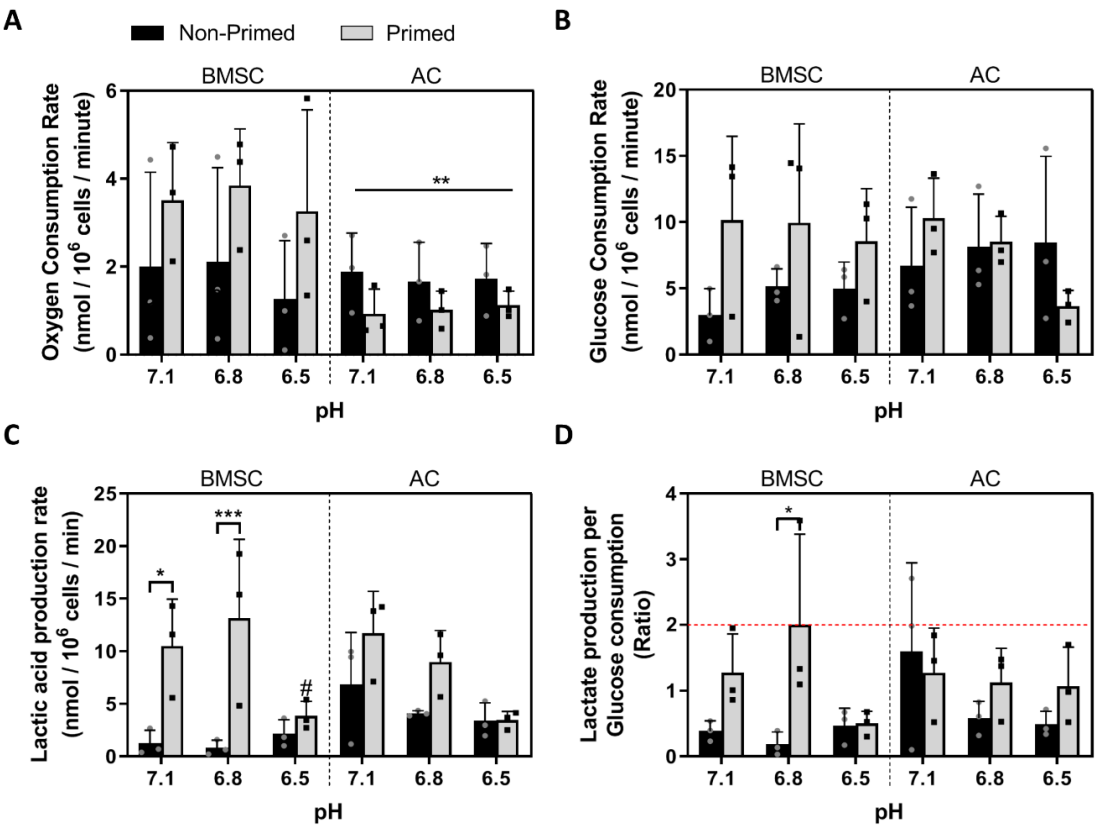

Figure 6-6: Metabolic activity of non-primed and primed BMSCs and ACs (A) Oxygen consumption rate **(B)** Glucose consumption rate and (C) Lactate production rate of BMSC and AC at different pH levels for non-primed (black bar) or primed (grey bar) in nmol/10^6 cells/minute. **(D)** Ratio of produced lactate per consumed glucose of cells either non-primed or primed at different media acidity. * indicates significant difference between non-primed and primed BMSCs of indicated group ($p<0.05$), ** indicates significant difference between BMSC and AC ($p<0.01$), *** indicates significant difference between non-primed and primed BMSCs of indicated groups ($p<0.001$) and # indicates significant difference between primed BMSC at pH 6.5 and pH 6.8.

6.4. Discussion

Disc degeneration is a widespread socio-economic problem affecting people of all ages globally. It is widely believed that degeneration originates in the NP of the IVD which is considered a harsh microenvironment and is believed to become more acidic with increasing degeneration due to changes in nutrient transport (Huang et al., 2014, Bibby et al., 2005b). If cell therapies are to become widespread as part of disc regeneration strategies, then it is important to ascertain if transplanted cells can sustain these acidic microenvironments and to develop culture techniques to enhance cellular responses. This study explored the effect of these challenging

acidic conditions on BMSCs and ACs and investigated if priming could enhance cellular response in terms of viability, disc-like matrix accumulation and metabolism.

It was found that low pH affects cell viability and matrix accumulation significantly, especially for BMSCs. This effect, however, can be overcome when cells are exposed to TGF-β3 priming prior to low pH culture. Cells that had been primed showed significantly higher viability and proliferation capacities and were capable of accumulating matrix molecules despite the low pH environment. Taken together these results demonstrate that priming of cells is a useful tool for cells that will be exposed to critical acidic conditions.

Investigations on the effects of pH on cell viability, have previously been explored for different cell types such as adipose-derived mesenchymal stem cells (ADSCs) (Han et al., 2014), BMSC (Naqvi and Buckley, 2016, Wuertz et al., 2009), Nucleus Pulposus Mesenchymal stem cells (NPMSC) (Han et al., 2014), NP cells (Hodson et al., 2018, Razaq et al., 2003) and ACs (Razaq et al., 2003). These studies demonstrated decreasing viability and proliferation with increasing matrix acidity, which correlates with our findings in the non-primed group. However, none of the previous studies attempted to pre-culture cells to improve their resistance to acidic environments. The primed groups in the present study showed significantly higher levels of viability after low pH culture, which may be due to the ECM being produced during the priming phase, providing a protective niche. It was demonstrated that non-primed cells accumulated an inadequate amount of ECM molecules when exposed to low pH media. After priming in normal pH conditions, cells subsequently produced a large amount of sGAG which increased for BMSC cultured at pH 7.1 and 6.8 and remained relatively constant for ACs after culturing in low pH media. In addition, cell viability and proliferation for both primed cell types increased, supporting the hypothesis that sGAG plays a key role in the success of the priming strategy. This correlates with previous findings by Naqvi *et al.*, who used priming to improve viability and matrix accumulation of cryopreserved BMSCs microencapsulated in alginate (Naqvi et al., 2018). One explanation for this effect may relate to the release of inflammatory factors (such as IL-1β and TNF-α) and protein degrading enzymes such as matrix metalloproteinases (MMPs). For instance,

Gilbert *et al.* and Han *et al.* observed a correlation between increasing MMP release with matrix acidity (Gilbert et al., 2016a, Han et al., 2014), whereas Razaq *et al.* and Wuertz *et al.* reported the opposite effect (Razaq et al., 2003, Wuertz et al., 2009). However, studies have shown elevated levels of IL-1β release with decreasing pH (Gilbert et al., 2016a). Moreover, it is known that MMP expression is increased in an inflamed environment (Flannery et al., 1999). MMPs are not only involved in matrix degradation and turnover but can also influence proteolysis and subsequent apoptosis (Mannello et al., 2005). It is evident that during low pH culture cells are affected by MMPs, which contribute to cell death whereas priming provides matrix molecules, which will be broken down prior to cell damage.

For a better understanding of the mechanism behind the pH effect, the activation of ASICs was investigated. ASICs have been found to be expressed in various cell types including neural cells, cancer cells, ACs and disc cells (Yuan et al., 2016, Zhou et al., 2015b, Gilbert et al., 2016a). It has been reported that the activation of ASICs correlates with an influx of calcium and sodium ions into the cellular cytoplasm, which activates intracellular pathways associated with apoptosis (Rong et al., 2012). In this study, however, no correlation between extracellular pH, acid channel activation and cell death could be observed. In contrast, an increase of ASIC-1 expression after priming was found, concomitant with enhanced cell viability. Previous studies demonstrated that the activation of this channel results in necrotic changes in rat cells, which is in disagreement with present findings (Zhou et al., 2015b). However, it needs to be noted that these previous experiments were performed in a 2D environment with an extracellular pH level of 6.0. This is an important difference compared to this study, where the cells were cultured in a 3D environment and at higher pH levels between 6.5 and 7.1, typically found in the disc. In previous investigations of ASIC activation it has been found that ASIC-1, ASIC-2 and ASIC-3 can also be activated at neutral pH (Yu et al., 2010, Gautschi et al., 2017), which implies that extracellular pH is not the only factor capable of activating these ion channels. This suggests that in the present study a different mechanism enhances ASIC expression. Due to a different activation mechanism, different intracellular pathways may also be activated by inflowing ions.

Calcium as a second messenger has been shown not only to be involved in inflammatory and apoptosis signalling but also in various different pathways, regulating cell division, mechanotransduction and actin-reorganization (Berridge et al., 1998, Erickson et al., 2003). Interestingly, a change in AC organization after priming was observed, which exhibited a cluster formation of 2-5 cells within a lacuna, which is typical for hyaline cartilage. It is known that the NP has large amounts of PGs and collagen, predominantly type 2, similar to hyaline cartilage tissue. In order to distinguish these two tissue types, Mwale *et al.* investigated differences in matrix composition of both and found that NP tissue contained a much higher sGAG per collagen ratio of 3.5:1 in comparison to a low ratio of 0.4:1 in hyaline cartilage (Mwale et al., 2004). In the present study, high levels of Col2 depositions of primed BMSC was found with a sGAG/collagen ratio of 1.5 ± 0.4 across all primed groups. This is not as high as native NP tissue but still 3.5-times higher than that of hyaline cartilage illustrating the potential of priming to enhance NP-like matrix accumulation.

Priming also had a considerable influence on the metabolic activity and respiration of cells. For instance, primed BMSCs tended to consume more oxygen compared to non-primed BMSC. High levels of oxygen consumption rate (OCR) have been reported by Pattappa *et al.* at an early stage of chondrogenic differentiation of BMSCs in low oxygen conditions (Pattappa et al., 2011). However, these levels significantly decreased after one day in pellet culture, suggesting that more aspects are involved in the high uptake-rate of oxygen after priming such as surrounding oxygen level, glucose availability, pH and different cell types (Bibby et al., 2005a, Huang et al., 2007). To compare with disc cells, it has been reported that NP cells of a degenerated disc have an OCR of 1.03-1.5 nmol/10^6 cells/min (Cisewski et al., 2018), which is similar to all non-primed samples. In addition to the altered kinetics of OCR, a change in GCR was observed in cells post priming. Work by Jackson *et al.* (Jackson, 2010) and Naqvi *et al.* (Naqvi and Buckley, 2015c) demonstrated a correlation between low oxygen availability (<5%) and raised glucose uptake. For instance, Naqvi et al. reported GCR of BMSC at 5% oxygen and 5mM glucose of 270 fmol/h/cell (which equals 4.5 nmol/10^6 cells/ min) (Naqvi and Buckley, 2015c), which was found

to be similar to non-primed BMSC at all pH levels of this work (7.1, 6.8 and 6.5). Post priming this level increased notably, but not significantly for BMSC cultured at all pH conditions. GCR of non-primed AC was found to be higher than that of non-primed BMSCs with an increasing tendency depending on acidity level. This trend reversed post priming with lower GCR in lower pH environment. Overall it appeared that the glucose demand differs depending on cell type and differentiation state. Interestingly, the higher levels of glucose consumption for primed cells correlated with higher levels of lactate production, except for primed BMSCs at pH 6.5, which showed only a small increase compared to non-primed. It has been shown that lactate production is highly influenced by surrounding pH, with decreasing levels at higher acidity (Bibby et al., 2005a). This is in agreement with the present findings for primed cells as well as for non-primed ACs. In addition, Pattappa *et al.* demonstrated increased lactate production of BMSCs during chondrogenic differentiation using TGF-β supplementation (Pattappa et al., 2011), which correlates with results of primed BMSCs in the present study. Non-primed cells, however, showed lower levels of lactate production for both cell types, which highlights the different metabolic activity of primed and non-primed cells. During anaerobic glycolysis, cells produce approximately 2 moles of lactate for every mole of glucose consumed (Dashty, 2013), emphasizing the challenges of cell nutrition within the intervertebral disc. In the current study, the lactate per glucose ratio was found to be below 2, except for primed BMSCs cultured at pH 6.8. This indicates that cells did not undergo anaerobic glycolysis and experienced sufficient level of extracellular oxygen within the time period investigated.

6.5. Conclusion

In conclusion, the results of the present study show that cells are negatively affected by low pH conditions in terms of cell viability and matrix accumulation, making them unsuitable for cell-based therapy of tissues exhibiting a challenging microenvironment. This effect can be overcome by priming using TGF-β3 prior to low pH exposure. Priming was observed to enhance cell viability and provided a baseline-level of ECM, offering a protective niche for successful tissue regeneration. Priming could therefore be used as a powerful tool for cell-based therapy of

the IVD to help injected cells withstand the typical harsh microenvironment, facilitate deposition of *de novo* ECM components and help ameliorate degenerative effects.

CHAPTER 7
ALTERING THE DEGENERATED ACIDIC DISC MICROENVIRONMENT USING ANTACID MICROCAPSULES

In this chapter, objective v and vi of this thesis was addressed and investigated different pH neutralizing antacids to improve the acidic microenvironment found in degenerated intervertebral discs.

7.1. Introduction

As described previously, the NP tissue is characterised by a harsh microenvironment with low levels of oxygen (5-10%), glucose (1-5 mM) and high levels of LacA (2-6 mM) (and thus an acidic pH) (Bartels et al., 1998, Selard et al., 2003, Nachemson, 1969), which even aggravates during degeneration (further details, see paragraph 2.2 “The Microenvironment of the Intervertebral Disc”, page 11). In the previous chapter it was demonstrated that priming of cells for cell-based therapy of the NP can overcome some of the detrimental effects of pH on cells, and on BMSCs in particular. However, priming alone is not capable of improving the low pH conditions, which remains a challenge for the resident NP cells. Antacids, which are compounds that can increase acidic pH have been long used to treat symptoms such as heartburn and dyspepsia, which are associated with hyper-acidic gastric fluids (Sontag, 1990). They are a group of multi-component salts whose active component is often based on aluminium hydroxide ($Al(OH)_3$), magnesium hydroxide ($Mg(OH)_2$), sodium bicarbonate ($NaHCO_3$), calcium carbonate ($CaCO_3$) or combinations thereof, and can impart effective pH neutralization properties. With regards to using them for microenvironmental changes, $CaCO_3$ has been previously used for its acid-sensitive properties in drug release vehicles for the manipulation of cancer microenvironments (Chen et al., 2012, Shi et al., 2015). Specifically, a drug is encapsulated into

a core of $CaCO_3$, which dissolves within the acidic carcinogenic environment and releases its content. For instance, Zhao *et al.* fabricated a vehicle of amorphous calcium carbonate/doxorubicin@Silica, which released doxorubicin in mildly acidic conditions (pH 6.5), resulting in cell death of cancer cells (Zhao et al., 2015). Besides these antacids, also HEPES (4-(2-hydroxyethyl)-1-piperazineethanesulfonic acid), a zwitterionic sulfonic agent has acid buffering capacities. It is commonly supplemented in cell culture media to maintain its pH within neutral range (pH 6.8 to 8.2). To investigate potential control over release of these pH altering agents, Chen *et al.*, encapsulated $Mg(OH)_2$ into alginate spheres to investigate different release kinetic patterns depending on sphere size and alginate concentration. They demonstrated a correlation of greater $Mg(OH)_2$ release in smaller alginate spheres as well as lower alginate concentration, indicating the ability to fine-tune the antacid delivery in low pH environments (Chen et al., 2018).

For a more suitable application in disc regeneration therapies, these salt-releasing capsules need to be injectable. Microencapsulation using EHDS is one such approach as described in previous chapters (paragraph 2.5.3 “Microencapsulation”, page 37 and Chapter 4, page 52).

To investigate the benefits of a proposed treatment, *in vitro* studies are highly limited. It lacks the 3D arrangement of cells as well as important cell-matrix interactions, which influences cell behaviour. For IVD regeneration, bovine tissue is widely used as it shows similar physical and biological properties to human IVDs (Demers et al., 2004, Rosenzweig et al., 2018, Illien-Junger et al., 2012, Grant et al., 2016, Lang et al., 2018, Peroglio et al., 2017, Hom et al., 2019). For a better understanding of specific aspects such as cell types, inflammatory factors or microenvironmental cues and their individual roles in tissue regeneration, explant models represent a useful alternative between insufficient *in vitro* experiments and *ex vivo* full organ culture, a common approach in IVD research. It maintains many of the inherent advantages of the full organ culture model such as the ability to conserve cells in their native tissue-structure environment, cellular composition and cell-cell configurations. For this reasons, the model has

been used for various tissue types including bone (Chan et al., 2009, Staines et al., 2019), cartilage (Sah et al., 1989, Vinardell et al., 2009, Secretan et al., 2010, Vainieri et al., 2018), meniscus (Steinert et al., 2007, Grogan et al., 2013) and cornea tissue engineering (Foreman et al., 1996, Sabater et al., 2013, Zhou et al., 2015a, Castro et al., 2019). The established disc explant model proposed in this work preserves connections of the disc cells with their surroundings, which is essential for their functionality and facilitates signal transmission with neighbouring cells. Many studies have demonstrated the positive paracrine effect MSCs have on disc cells, showing an increase of ECM deposition, cell viability and proliferation (Yamamoto et al., 2004, Richardson et al., 2006, Le Visage et al., 2006, Chen et al., 2017, Naqvi and Buckley, 2015a, Naqvi et al., 2019). Yet, the influence of each cell type within a more natural surrounding is still to be revealed.

Taken together, the overall objective of this chapter was to establish and characterize pH neutralizing µCaps and investigate their potential for disc regeneration by targeting its acidic microenvironment. Specifically, different antacids at different concentrations were compared in terms of their pH neutralization capacities as well as their size and release kinetics. Furthermore, their buffering effect on cell viability and matrix accumulation on NP cells and therapeutic cells was characterised. Lastly, using a disc explant model, the effect of these µCaps in combination with primed AC and BMSC µCap on pH neutralization and potential matrix deposition of surrounding cells was explored.

7.2. Methods

7.2.1 Experimental Design

A schematic overview of the experimental set up is illustrated in Figure 7-1. Overall, this study was divided into three phases. The first phase (Figure 7-1 - left) of this study investigates different properties of antacid µCaps. Hereby, different types of buffering salts and agents were assessed in terms of their pH neutralisation capacities using a pH sensor foil (PreSens, Germany), then the size of sprayed antacid µCaps with various concentrations were analysed and lastly, the release kinetics from µCaps into the local environment at low pH was investigated.

The second part of this study (Figure 7-1 - centre) focused on the effect the antacid µCaps have on therapeutic cells in terms of viability and matrix accumulation capacities as well as on viability on host cells (in this case: NP cells).

The third and final phase (Figure 7-1 – right) investigated a single antacid ($CaCO_3$) at a concentration of 500 mg/mL in combination with cellular µCap in a disc explant model. Here, 6 mm biopsies of the AF were taken from bovine IVDs and cored using a 3 mm biopsy and placed into a custom designed cage system for structural support and confinement (Appendix 2, page xxiv). A hydrogel containing $CaCO_3$ and cellular µCap were introduced into the disc-core and cultured for 21 days under simulated degenerative disc conditions (i.e. low pH, low oxygen, low glucose and high osmolarity). The evaluation was carried out in terms of pH (within the explant and the media), cell viability and matrix deposition.

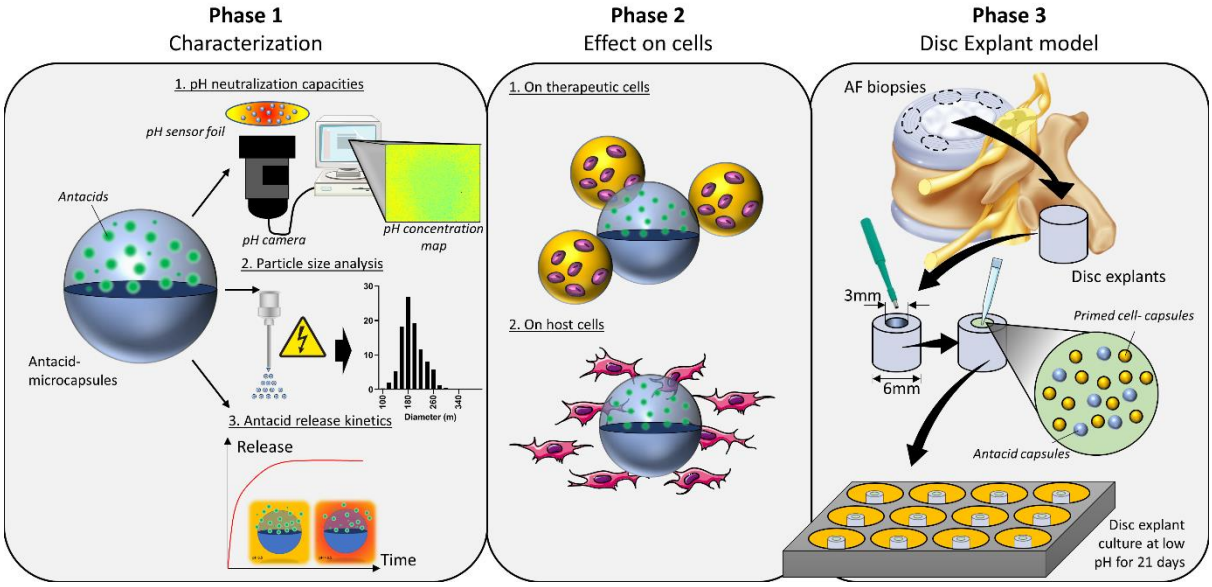

Figure 7-1: Experimantal design. Phase 1 investigated physical and chemical parameters of different antacids in terms of local pH change, size distribution and release kinetics. Phase 2 examined the effect of pH buffering µCaps on surrounding cells (therapeutic cells for cell therapy and host cells). Phase 3 explored antacid µCaps with cellular µCaps in a disc explant model.

7.2.2 Fabrication of antacid microcapsules

The desired amount of antacid ($Al(OH)_3$, $Mg(OH)_2$, $CaCO_3$ or HEPES) was mixed with 1% alginate (Pronova UP LVG, FMC NovaMatrix**,** Norway). For homogeneous distribution of the nanoparticles, the suspension was blended using a homogenizer in 2x 1 min cycles followed by 3x 1 min cycles of ultrasonication. The final solution was diluted using 1% alginate to obtain different concentrations (25-500 mg/mL).

For µCap fabrication, an in-house built EHD sprayer was used. The spraying parameters (voltage and needle size) were optimized depending on the antacid being used while the flow rate (50 µl/mL) and working distance (50 mm) were maintained constant. µCaps were collected in a dish containing 100 mM $CaCl_2$ for ionically crosslinking of the alginate polymer (protocol: Appendix 3, page xxv).

7.2.3 pH mapping

pH concentration maps were generated using a USB pH detector unit – microscope device and corresponding software (VisiSens; PreSens GmbH, Regensburg, Germany). Briefly, a pH sensor foil (Product code SF-HP5R, PreSens GmbH, Regensburg, Germany) was attached to the bottom of standard cell culture dish and antacid µCaps within a fibrin (50 mg/mL)- HA (5 mg/mL) hydrogel placed above. The construct was cultured in low pH media (pH 6.5) and images were taken from below at various time points to asses local pH change. The output file generated by the VisiSens™ AnalytiCal 2 Software (PreSens GmbH, Regensburg, Germany) was analysed using a custom written MatLab® code (MathWorks®, Version R2017a, Massachusetts, US)

7.2.4 Size analysis

For size analysis, ~350-1000 antacid-µCaps of each group were imaged using light microscopy and µCap diameters were determined using image analysis software (ImageJ, National Institutes of Health, and Bethesda, Maryland).

7.2.5 Release kinetics

At specific timepoints in culture, antacid μCaps were dissolved in 1 M HCl solution for 1 hour under constant rotation. Calcium and magnesium content of digests and corresponding media samples were quantified using Sentinel Calcium and Magnesium Liquid (Alpha Laboratories Ltd., UK) assay kits in accordance with the manufacturer's instructions.

7.2.6 Cellular microencapsulation

Cells were trypsinised and re-suspended in media and combined with sterile 2% alginate solution (Pronova UP LVG, FMC NovaMatrix, Norway) at a 1:1 ratio to yield a final alginate concentration of 1% and a seeding density of $10x10^6$ cells/mL. The alginate/cell solution was electrosprayed using an in-house built EHD sprayer with constant processing parameters (30G needle, 10 kV applied voltage, 100 μl/mL flow rate, 50 mm working distance). After ionically crosslinking for 5 minutes inside a 100 mM $CaCl_2$ bath (pH 7.2), μCaps were rinsed thoroughly with PBS before resuspension in the appropriate medium for culture.

7.2.7 In vitro priming of μCaps

Post-fabrication, cellular μCaps were transferred in a μCap: media ratio of 25 μL: 1 mL into a sterile container with lg-DMEM supplemented with penicillin (100 U/mL)-streptomycin (100 μg/mL) (GIBCO, Invitrogen, Dublin, Ireland), 0.25 μg/mL AmpB, 40 μg/mL L-proline, 100 nM dexamethasone, 50 μg/mL L-ascorbic acid 2-phosphate, 4.7 μg/mL linoleic acid (all Sigma-Aldrich, Arklow, Ireland) and 10 ng/mL TGF-β3 (PeproTech, UK). μCaps were cultured at 37°C and low oxygen (5% O_2) conditions for 14 days under constant agitation. Half media exchange was performed twice weekly.

7.2.8 Disc explant isolation and culture

Skeletally mature bovine tails were obtained from a local abattoir. Next discs were isolated with a custom-made guillotine and two attached blades with a distance of 4.5 mm between each other. From each obtained "disc slab", 3-5 6 mm biopsies were taken from the AF-region. The 6 mm AF-cylinders were cored using a 3 mm biopsy punch to generate a disc explant,

which was inserted into a custom made cage (Figure 7-2) and assigned to the following groups:, primed AC without $CaCO_3$ (AC -$CaCO_3$), primed BMSC without $CaCO_3$ (BM -$CaCO_3$), primed AC with $CaCO_3$ (AC +$CaCO_3$) and primed BMSC with $CaCO_3$ (BM +$CaCO_3$), and acellular gels with and without $CaCO_3$ served as controls. A 25 µL of hydrogel containing a fibrin (100 mg/mL)- HA (5 mg/mL) blend +/- $CaCO_3$ and +/- cellular µCaps samples were added into the 3 mm core of disc explants and cultured in low pH (pH 6.5), high osmolarity (~450 mOsm, adjusted using 150 mM sucrose), chondrogenic defined medium (CDM) containing lg-DMEM supplemented with 1 mg/mL Primocin (Invivogen, Toulouse, France), 5% FBS (GIBCO, Invitrogen, Dublin, Ireland), 100 KIU/ml aprotinin solution (Nordic Pharma, Limhamn, Sweden) 0.25 µg/mL AmpB, 1.5 mg/mL BSA, 1× ITS, 40 µg/mL L-proline, 100 nM dexamethasone, 50 µg/mL L-ascorbic acid 2-phosphate and 4.7 µg/mL linoleic acid (all Sigma-Aldrich, Ireland). The total culture period was 21 days at 37˚C in physioxic (5% oxygen) conditions, with medium exchanges performed twice weekly.

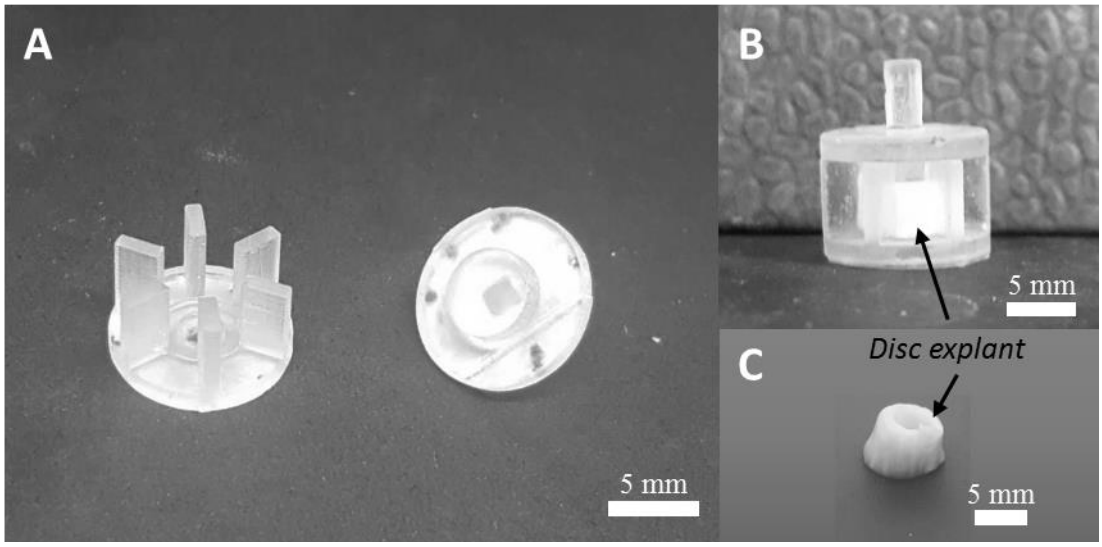

Figure 7-2: Disc explant cage (A) 3D printed cage using dental resin **(B)** assembled with disc explant scale bar = 5 mm **(C)** isolated disc explant from bovine IVD

7.2.9 Statistical analysis

Statistical analyses were performed using GraphPad Prism (version 8) software with 3-4 samples analysed for each experimental group. One- way ANOVA or Two-way ANOVA was used for the analysis of variance where appropriate, with Tukey post-tests to compare between groups. The results were displayed as mean ± SD and significance was accepted at a level of $p < 0.05$.

7.3. Results

7.3.1 Antacids µCaps can increase the local pH within an acidic environment

Different antacids, namely $Mg(OH)_2$, $CaCO_3$, the zwitterion HEPES and $Al(OH)_3$ at a concentration of 50 mg/mL were compared in terms of buffering capacities when exposed to low pH environment (pH 6.5) (Figure 7-3). Results revealed no difference of pH distribution in pH concentration maps between HEPES, $Al(OH)_3$ and the negative control group (pH 6.5 without pH changing µCaps).). $Mg(OH)_2$ and $CaCO_3$ however, increased the pH in the centre of the construct to 7.5 and 7.0 respectively (Figure 7-3 A). Comparing the pH alongside the x-axis of each construct, it is obvious, that the main effect of the buffering µCaps occurs in the centre with decreasing pH values towards the periphery (Figure 7-3 B). Comparing the acidity change over time of each group, it is evident that $Mg(OH)_2$ and $CaCO_3$ have the highest pH neutralization capacities. However, $Mg(OH)_2$ increases the pH level to a very basic level within the first 24 hours before plateauing towards neutral levels, which may be detrimental for cell viability (Figure 7-3 C). $CaCO_3$, on the other hand, is capable of increasing the local pH to a neutral level for the duration of the period investigated (Figure 7-3 C).

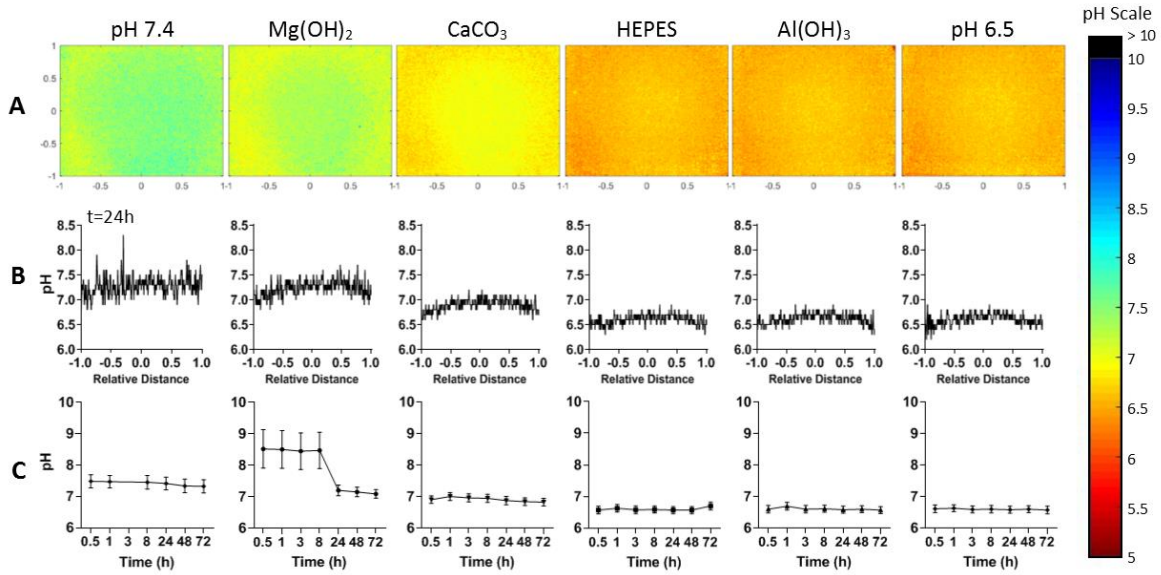

Figure 7-3: Local pH mapping of 50 mg/mL $Mg(OH)_2$, $CaCO_3$, HEPES and $Al(OH)_3$ µCaps exposed to low pH media in comparison to no µCaps with constant pH media (7.4 representing positive control and pH 6.5 representing negative control). (A) pH concentration maps of all groups at 24h. **(B)** pH across the x-axis after 24h and **(C)** change in local pH evaluated over 72 hours.

After doubling the antacid concentration for each group, no significant improved neutralisation was observed with remaining low pH levels using HEPES and $Al(OH)_3$ (Figure 7-4). $Mg(OH)_2$ and $CaCO_3$ still demonstrated neutralization of local pH for 72 hours.

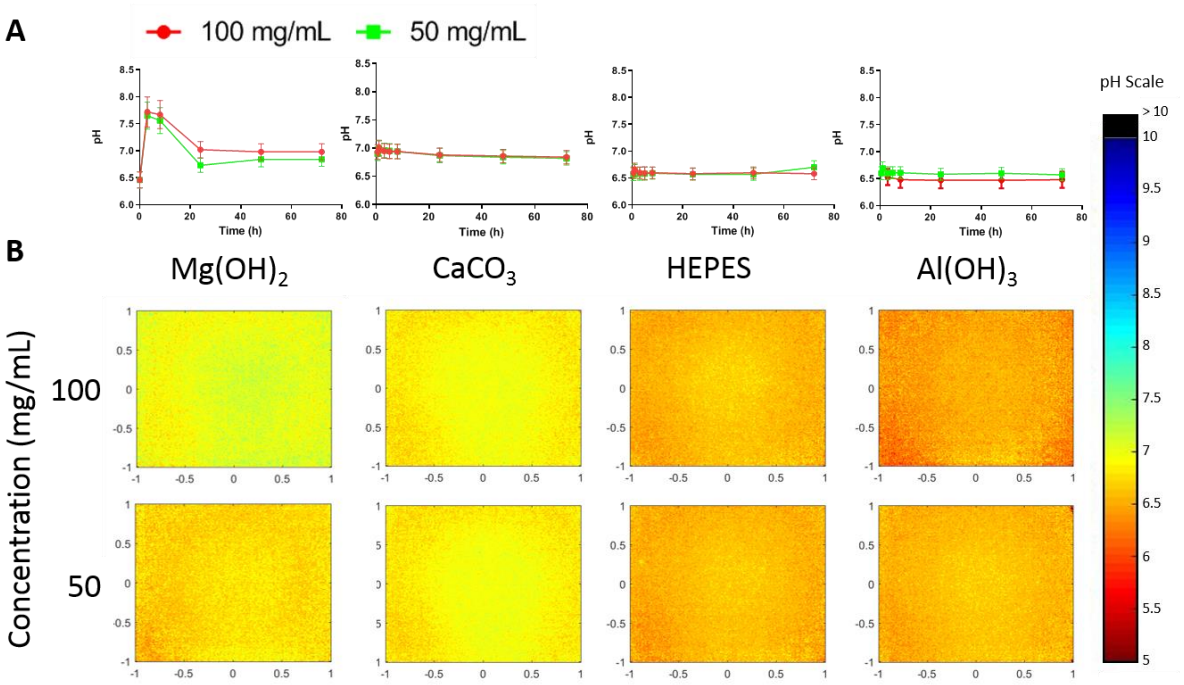

Figure 7-4: Local pH of 50 mg/mL and 100mg/mL of $Mg(OH)_2$, $CaCO_3$, HEPES and $Al(OH)_3$ µCaps exposed to low pH media (A) over 72 hours and **(B)** at 24h in a pH map

7.3.2 Increasing antacid concentration increases local pH levels

Following on from previous results (testing different pH buffering agents), $Mg(OH)_2$ and $CaCO_3$ was taken forward for further investigation on the impact of salt concentration. In Figure 7-5, the temporal effect of $Mg(OH)_2$ and $CaCO_3$ on the local environment within the construct and the surrounding media was evaluated for different initial concentrations (25, 50, 100, 250 and 500 mg/mL). $Mg(OH)_2$ was observed to change the pH of the acidic environment to a larger extent depending on the initial salt concentration (Figure 7-5 A). At the highest concentration (500 mg/mL), the local pH of the construct was found to exceed the range of the measuring limits (pH>10) and the pH of the media plateaued at pH 7.9 after 24 hours (Figure 7-5 A left). The local pH of the constructs showed an initial peak within the first 5 hours after acidic exposure but decreased towards a neutral pH over time (Figure 7-5 Ai solid line). Also, the media pH increased over time and reached values between 6.8 and 7.5 after 3 days depending on the initial $Mg(OH)_2$ concentration (Figure 7-5 A).

In contrast, changing the concentration of $CaCO_3$ did not exert such large variations on the surrounding pH compared to $Mg(OH)_2$ (Figure 7-5 B). Similar to $Mg(OH)_2$, the initial peak occurred within the first 5 hours of low pH exposure (Figure 7-5 Bi), but never exceeded levels above pH 8. The concentration of 500 mg/mL appeared to equilibrate at a neutral pH of 7 locally as well as within the culture media. The lowest concentration (25 mg/mL of $CaCO_3$) did not exert any significant effect on pH levels in either the construct or surrounding media (Figure 7-5 B – right).

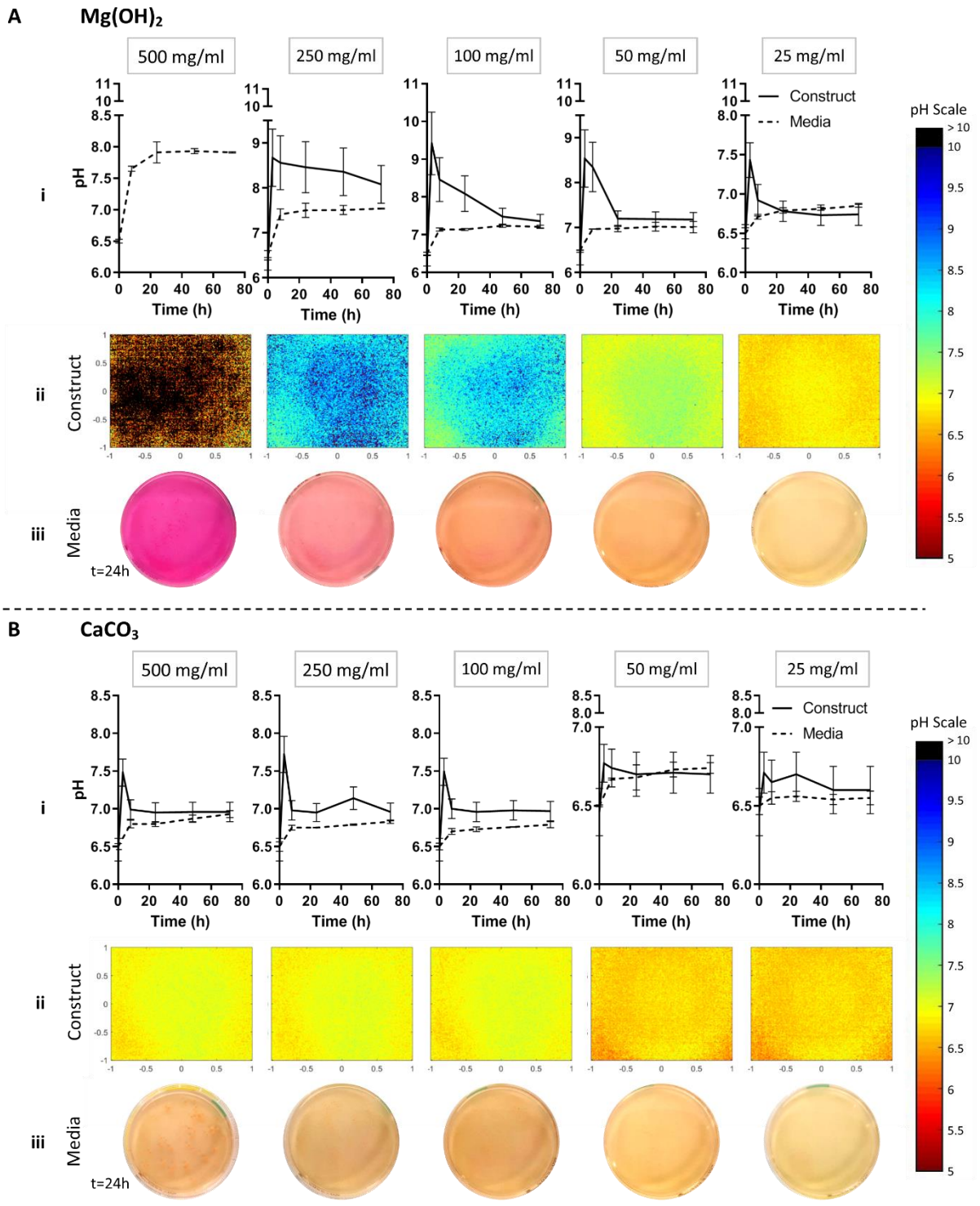

Figure 7-5: Different concentrations of $Mg(OH)_2$ and $CaCO_3$ and their buffering ability. (A) Effect of $Mg(OH)_2$ on pH level (i) over time locally and within the culture media. (ii) pH concentration map showing local pH distribution and (iii) media colour after 24h incubation. **(B)** Effect of $CaCO_3$ on pH level (i) over time locally and within the culture media. (ii) pH concentration map showing local pH distribution and (iii) media colour after 24h incubation.

7.3.3 $CaCO_3$ microcapsule size affects temporal neutralization capacity

After investigating different concentrations of $Mg(OH)_2$ and $CaCO_3$ in terms of pH neutralization limits, the highest $Mg(OH)_2$ group (500 mg/mL) was excluded as it exceeded the upper pH limit. Further characterisation of the concentrations 250, 100 and 50 mg/mL of $Mg(OH)_2$ and 500, 250 and 100 mg/mL of $CaCO_3$ in terms of µCap size and release kinetics was carried out. As seen in **Figure 7-6** A, $CaCO_3$ produced larger µCaps (size of 303.14 ± 48.16 µm), whereas $Mg(OH)_2$ exhibited significantly smaller sized µCaps (181.38 ± 11.07 µm, with $p<0.0001$). Moreover, comparing size distribution of both antacids at different concentrations reveals a homogeneous µCap size for all groups except the highest concentration of $CaCO_3$, which showed a wider range of µCap sizes (**Figure 7-6** B). Investigating the release of antacids from the µCaps into the media demonstrated a rapid drop of Mg^{2+} ions inside the µCaps within the first 24 hours, with a concomitant increase in Mg^{2+} concentration in the media (**Figure 7-6** C). With respect to Ca^{2+} release from µCaps into the surrounding media, a decrease of 12.3 ± 4.5% of Ca^{2+} within the µCaps was observed over the time investigated (72h) (**Figure 7-6** D). No significant difference in release kinetics of altered concentration was observed in both for the different initial concentrations of $Mg(OH)_2$ and $CaCO_3$ investigated.

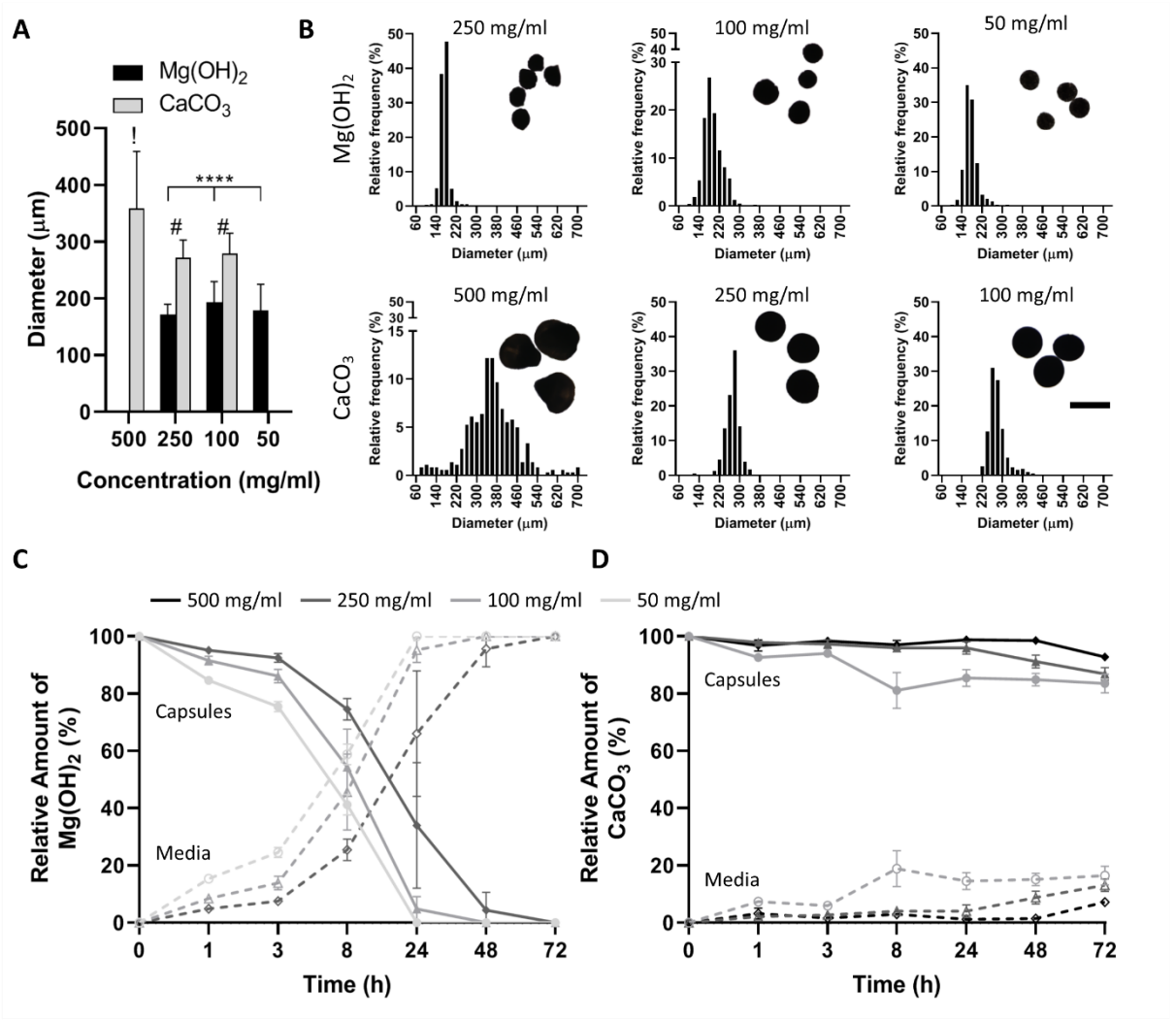

Figure 7-6: Characterization of $Mg(OH)_2$ and $CaCO_3$ µCaps of different initial concentrations, 50, 100, 250 mg/mL of $Mg(OH)_2$ and 100, 250 and 500 mg/mL of $CaCO_3$ (A) average diameter of $Mg(OH)_2$ µCaps (black bars) and $CaCO_3$ µCaps (grey bar). ! Indicates significant difference between 50 mg/mL $CaCO_3$ µCaps and all other $CaCO_3$ concentrations ($p<0.0001$), # indicates significant difference between $Mg(OH)_2$ and $CaCO_3$ for the same concentration ($p<0.0001$) and **** indicates significant difference between all concentrations of $Mg(OH)_2$ µCaps ($p<0.0001$) **(B)** Size distributions of $Mg(OH)_2$ µCaps (top row) and $CaCO_3$ µCaps (bottom row) at different concentrations. Scale bar = 400 µm. **(C)** Relative amount of Mg^{2+} release (%) over 72h from µCaps (solid line) into media (dashed line) for different initial concentrations **(D)** Relative amount of Ca^{2+} release (%) over 72h from µCaps (solid line) into media (dashed line) for different initial concentrations.

7.3.4 Altering the local pH using $Mg(OH)_2$ negatively affects NP cells

To evaluate the effect of local change of pH in a low pH environment on cell viability, two different aspects were investigated: the impact these pH-altering µCaps have on the potential therapeutic-cells (herein termed primed, microencapsulated AC) and on the host cells (NP cells) respectively. Results showed that culturing $Mg(OH)_2$ µCaps in the presence of primed AC µCaps

had no significant effect on cell viability with values as high as 92.9 ± 1.8% in all groups (Figure 7-7 Ai and B). In contrast, for NP cells, a significant decrease was observed for increasing concentration of $Mg(OH)_2$ with considerably lower cell viability at concentrations of 250 mg/mL (19.8 ± 12.4%) and 100 mg/mL (31.1 ± 26.5%) compared to AC ($p< 0.0001$) (Figure 7-7 Ai and B). In contrast, when culturing cells with $CaCO_3$ loaded µCaps, a high number (> 83%) of viable cells (AC and NP) could be observed (Figure 7-7 Aii). Quantification of cell viability revealed levels >80% in all groups with significantly higher cell viability of NP cells compared to AC in all groups ($p<0.001$ between NP and AC at 500 mg/mL and 250 mg/mL and $p< 0.0001$ between AC and NP at 100 mg/mL $CaCO_3$) (Figure 7-7 C). Despite cell viability of NP cells was found to be greater than 90% in all $CaCO_3$ groups, a significant decrease with increasing concentration was observed ($p< 0.05$) (Figure 7-7 C).

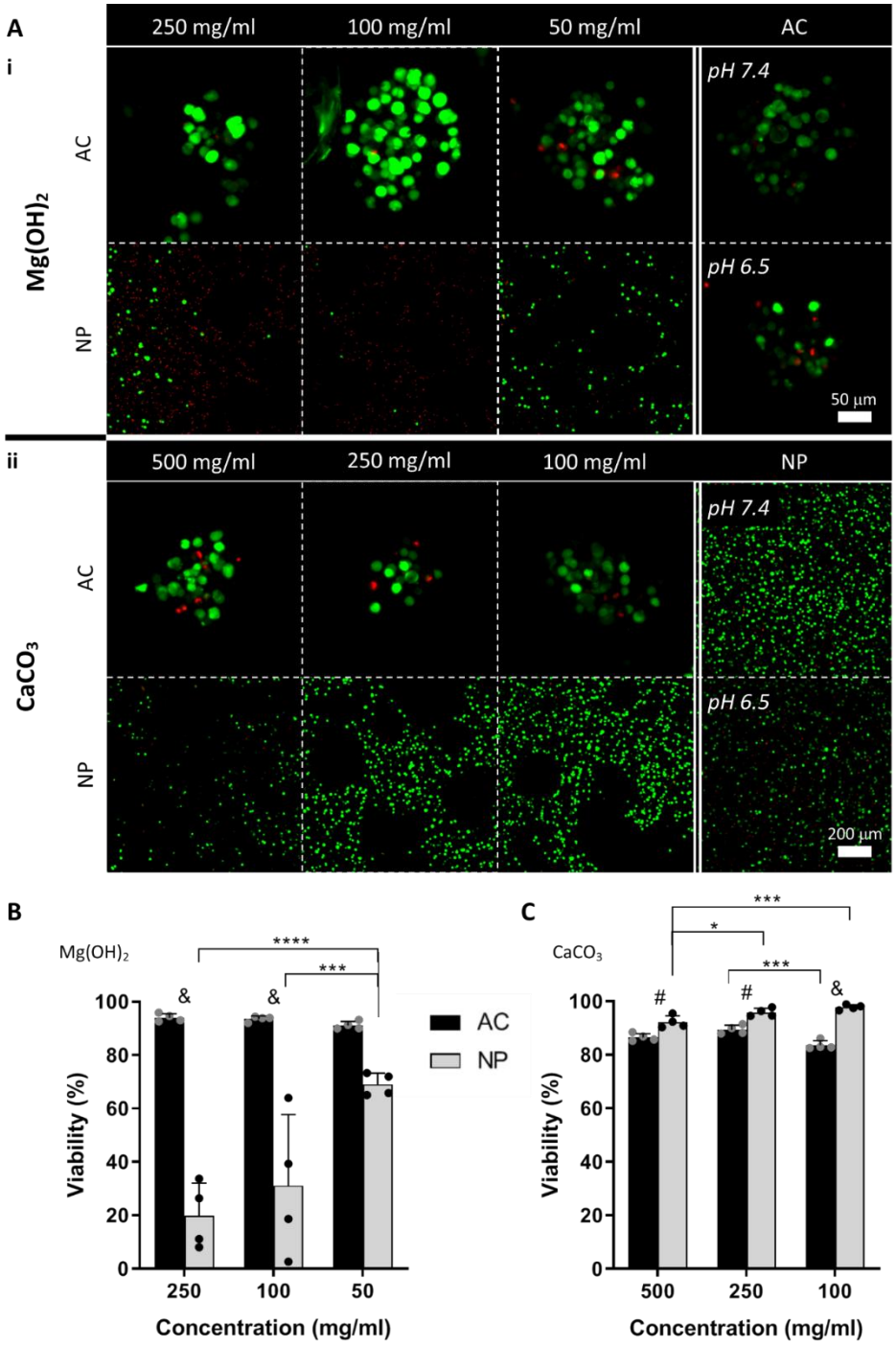

Figure 7-7: Concentration effects of $Mg(OH)_2$ and $CaCO_3$ buffering µCaps on AC (primed) and NP cells respectively. (A) Live/Dead assessment of cells after 24h exposure to $Mg(OH)_2$ (i) and $CaCO_3$ (ii) initial media pH of 6.5. AC and NP at pH 7.4 and pH 6.5 without antacid µCaps served as controls. Scale bar_{AC} = 50 µm, scale bar_{NP} = 200 µm **(B)** Semi-quantitative image analysis of cell viability when cultured at pH 6.5 alongside $Mg(OH)_2$ loaded µCaps at various concentrations (250, 100 and 50 mg/mL). & indicates significant difference between AC and NP at indicated concentration ($p<0.0001$). **** and *** indicate significant difference between indicated groups ($p<0.0001$ and $p<0.001$ respectively) **(C)** Semi-quantitative image analysis of cell viability when cultured at pH 6.5 alongside $CaCO_3$ loaded µCaps at various concentrations (500, 250 and 100 mg/mL). & and # indicate significant difference between AC and NP at indicated concentration ($p<0.0001$ and $p<0.001$ respectively). *** and * indicate significant difference between indicated groups ($p<0.001$ and $p<0.05$ respectively).

7.3.5 ECM content is not negatively influenced by $CaCO_3$ µCaps

Comparing primed AC and BMSC in low pH media conditions with and without exposure to $CaCO_3$ pH buffering µCaps revealed no significant difference in DNA content for any of the groups investigated (Figure 7-8 A). However, over three weeks without growth factor exposure, DNA level of AC dropped by 24.5%, 42.7% and 57.9% at media conditions with normal pH (7.4), low pH with $CaCO_3$ µCap supplementation and low pH without $CaCO_3$ µCaps respectively. BMSC, in contrast, increased DNA level by 150% compared to day 0 when cultured under standard pH conditions, whereas the level was maintained in acidic media culture (with and without $CaCO_3$ µCaps). Live-dead confocal imaging revealed good cell viability at day 0 with no detrimental effect after 21 days for all groups. Similar results were found in terms of sGAG accumulation (Figure 7-8 B). Biochemical analysis showed a decrease in sGAG content when ACs were cultured in pH 7.4 or with $CaCO_3$ µCaps, compared to day 0, whereas acidic media without $CaCO_3$ supplementation maintained baseline sGAG levels. However, differences were not found to be significant. BMSC showed a slight, but not significant, increase of sGAG levels compared to baseline in all groups. However, there was no significant difference found in sGAG content among the groups (pH 7.4, pH 6.5 +$CaCO_3$ and pH 6.5), which correlates with histological staining. Similar findings were made with regards to collagen deposition (Figure 7-8 C). µCaps containing AC demonstrated a reduction in the amount of collagen in all groups compared to day 0, yet no significant difference between groups (pH 7.4, pH 6.5 +$CaCO_3$ and pH 6.5) were observed. Collagen content within BMSC µCaps was generally found to be higher compared to AC, which was also observed histologically. A trend towards decreasing collagen levels with pH conditions was observed, however, the difference was not found to be significant.

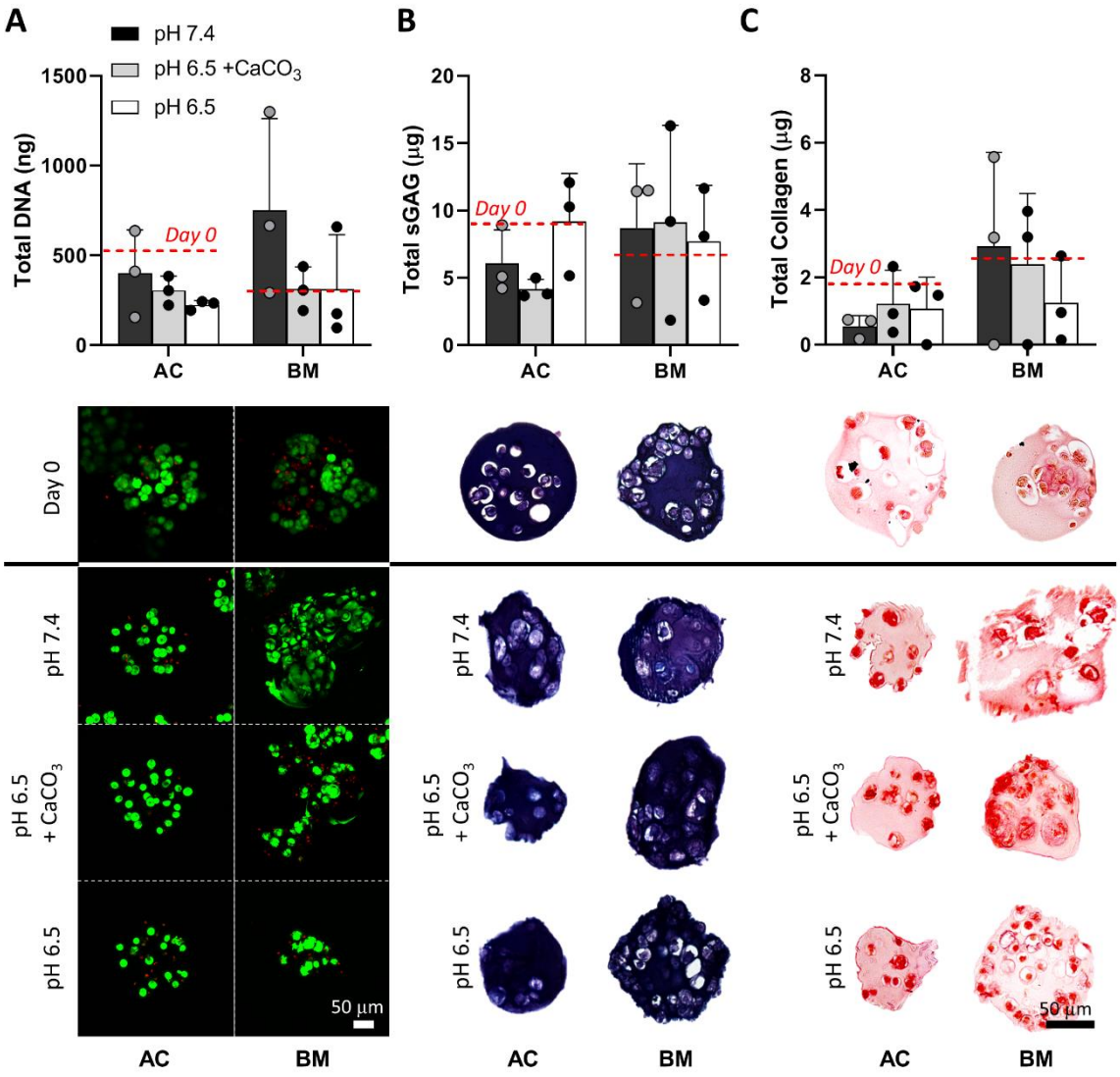

Figure 7-8: Effect of $CaCO_3$ on matrix deposition of primed cells after 21 days in acidic culture (A) Proliferation (Total DNA (ng)) and cell viability staining at day 0 and day 21. No significant difference between control groups (pH 7.4, black bar and pH 6.5-, white bar) and experimental group with $CaCO_3$ (6.5+, grey bar) was observed **(B)** Total sGAG amount (µg) and aldehyde fuchsin / alcian blue staining at day 0 and day 21. No significant difference between groups was detected **(C)** Total amount of collagen (µg) and picrosirius red staining at dat 0 and day 21. No significant difference between groups was observed. Scale bar = 50 µm

7.3.6 $CaCO_3$ significantly increases pH level within the core of a disc explant cultured under acidic conditions

Buffering capacities were further assessed in a disc explant study, whereby a ring explant from a bovine disc was taken and filled with a hybrid hydrogel containing different compositions of µCaps. After 21 days in culture under disc-like acidic conditions of pH 6.5, pH values within

the core and the surrounding culture media were investigated (see schematic displayed in Figure 7-9 A). Results showed a significantly higher pH level within the core when using primed cells and $CaCO_3$ µCaps in a hybrid gel compared to all other groups ($p< 0.0001$) (Figure 7-9 B). Measuring the acidity of the media, levels below pH 6.2 were measured in all groups, except for the constructs cultured with primed BMSC and $CaCO_3$ µCaps, which showed a significantly higher level of pH 6.29 ($p<0.0001$) (Figure 7-9 C).

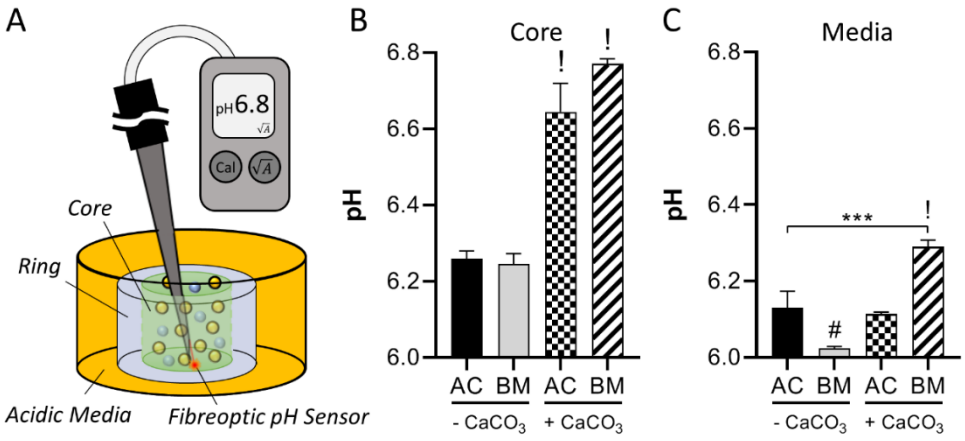

Figure 7-9: pH measurements after 21 days acidic culture of explants (A) schematic image of pH measurement procedure **(B)** pH values measured in core, ! Indicates significant difference compared to all other groups ($p<0.0001$) **(C)** pH values measured in media of explants. ! Indicates significant difference between BMSC +$CaCO_3$ and AC +$CaCO_3$ and BMSC –$CaCO_3$ ($p<0.0001$), # indicates significant difference BMSC –$CaCO_3$ and AC –$CaCO_3$ and AC +$CaCO_3$ ($p<0.01$), *** indicates significant difference between groups ($p<0.001$).

7.3.7 The antacid hybrid gel curtails DNA loss within the core while increasing DNA in the disc ring of explant cultures

The effects of $CaCO_3$ µCaps within the disc explants on cells was evaluated in terms of cell proliferation and viability. Within the core gel, the highest level of DNA was found in cellular groups (AC and BM) including $CaCO_3$ µCaps. However, compared to day 0 (dashed red line), the amount of DNA decreases over time. Overall, CaCO3 was found to have a significant impact on the level of total DNA within the core gel ($p<0.05$) (Figure 7-10 A). Within the disc ring, no significant difference between groups could be observed, yet, a slight increase in DNA content was detected in groups containing $CaCO_3$ µCaps compared to day 0 (dashed red line) irrespective

of cell type within the core (Figure 7-10 B). Evaluation of cell viability revealed a high percentage of living AC (92.8 ± 4.5%) in both: without and with $CaCO_3$ µCaps and showed significantly higher viability compared to BMSC. BMSC -$CaCO_3$ show 81 ± 9.1% viable cells ($p<0.05$ compared to AC -$CaCO_3$) and significantly low viability (36.2 ± 5.3%) when cultured with $CaCO_3$ ($p< 0.0001$) (Figure 7-10 C). Viability results were found to correlate with confocal images, displaying densely packed viable µCaps within the core of all groups except for BMSC + $CaCO_3$, where a large number of dead cells were observed (Figure 7-10 D) As the control groups were acellular, no cells could be observed and subsequently, no viability within the core of the explants was applicable (indicated n.a.).

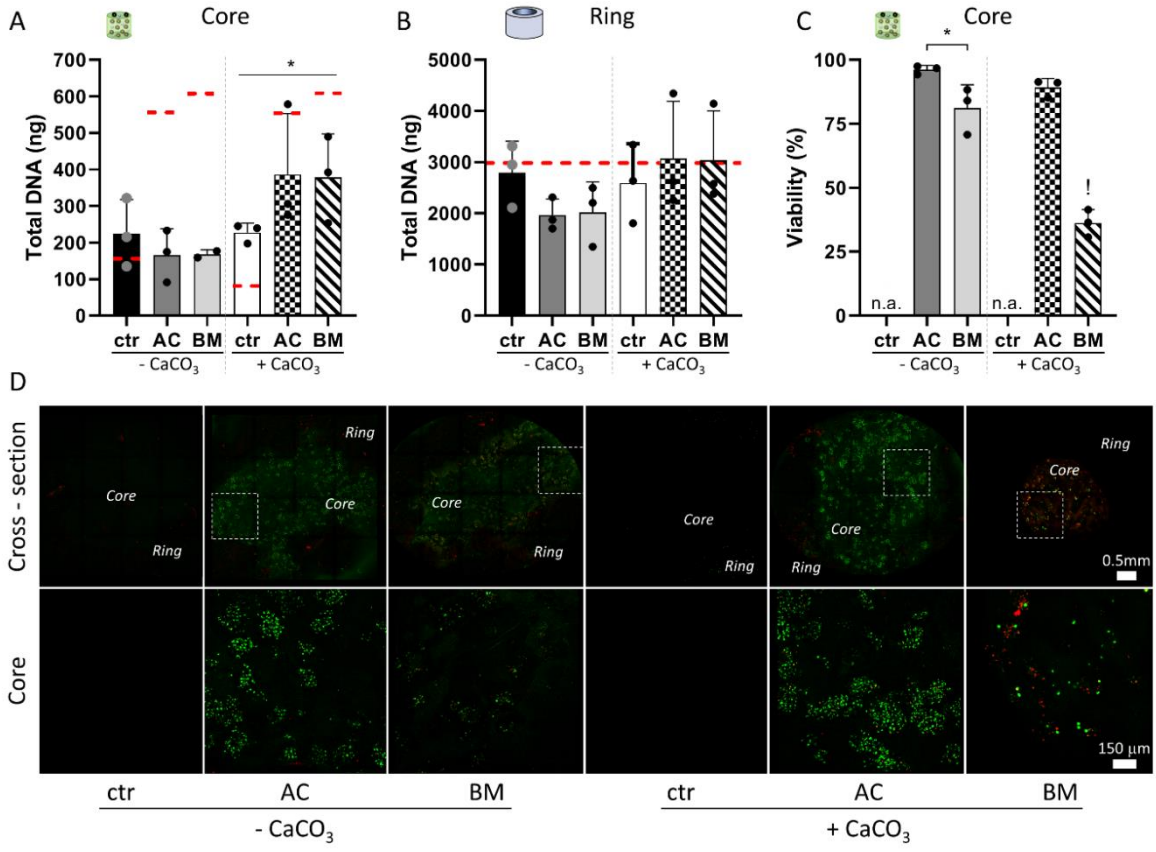

Figure 7-10: Proliferation and cell viability of explants (A) change in total DNA (ng) content within the core-gel, * indicates significant difference between groups with and without $CaCO_3$ ($p<0.05$) **(B)** change of total DNA (ng) in disc ring **(C)** viability of primed cells within the core hybrid gel; * indicates significant difference between groups ($p<0.05$), ! Indicates significant difference between BMSC + $CaCO_3$ and all other groups in terms of cell viability ($p<0.0001$), "n.a." indicates not applicable, dashed red line represents values at day 0 **(D)** Confocal images of viable (green) and dead (red) cells; macro scale (top) and magnified regions within the core (bottom row). Scale bar $_{\text{cross-section}}$ = 0.5 mm, scale bar $_{\text{core}}$ = 150 µm

7.3.8 Antacids curtail sGAG depletion within disc tissue

To evaluate the change of sGAG levels within the hybrid gel (core) and the disc tissue (ring), the two compartments were separated and analysed individually (Figure 7-11 A).. Results showed highest levels of sGAG within groups using CaCO3, which was found to have a significant impact on sGAG levels ($p<0.001$) (Figure 7-11 A). However, acellular groups (ctr) also showed elevated levels of sGAG within the core gel. A reduction of sGAG deposition in and the disc ring, compared to day 0 (red dashed line) was observed, with the highest total amount of sGAG in the ring using primed BMSC and $CaCO_3$ µCaps. The difference, however, was not found to be statistically significant (Figure 7-11 C)... Histologically the primed cellular µCaps were found in the core of the construct (Figure 7-11 D). A slightly less intense blue staining was observed in acellular control samples compared to cellular samples when comparing the cross-section images. However, these differences were not observed when comparing ring- groups at higher magnification.

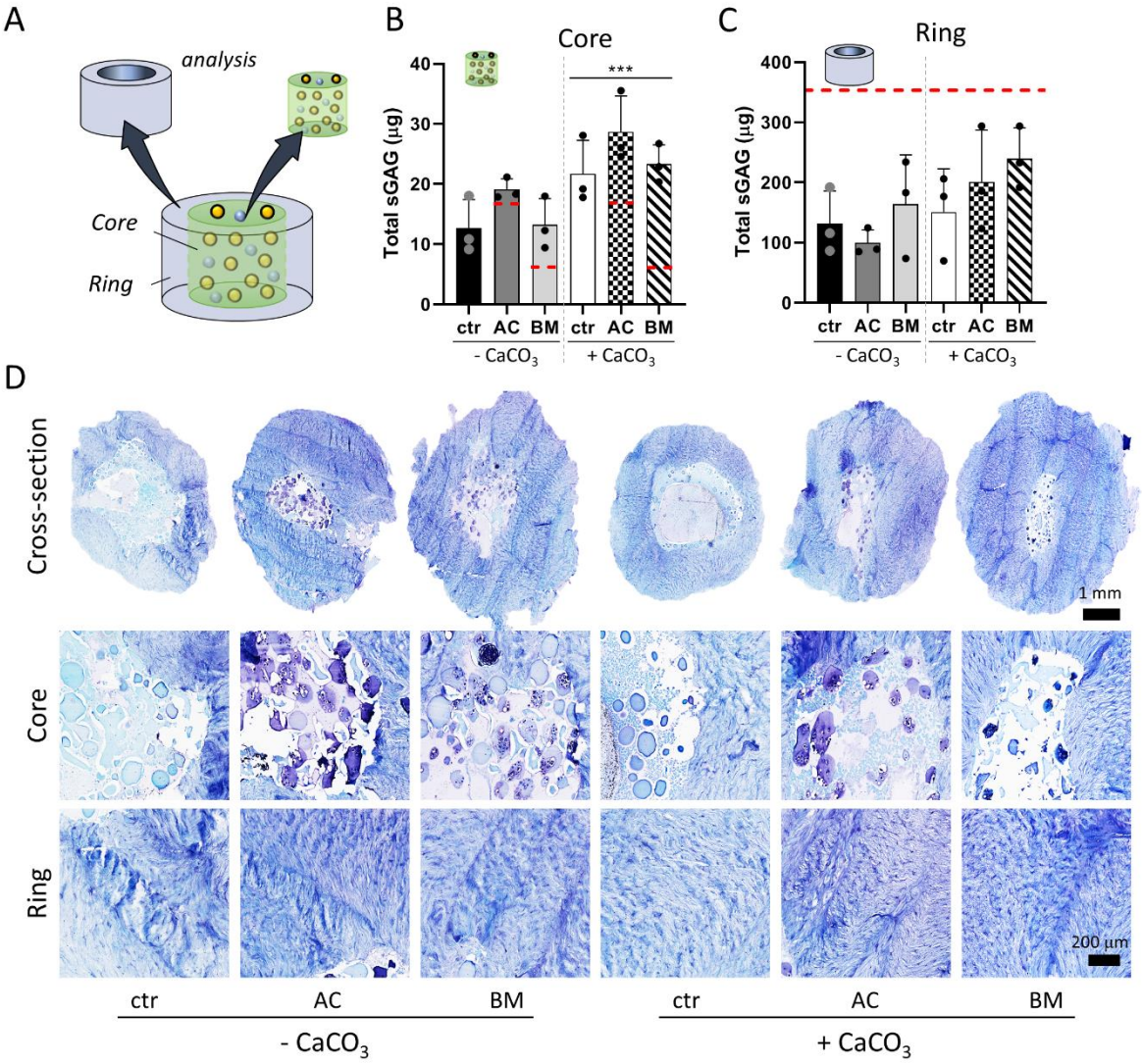

Figure 7-11: sGAG accumulation of explant cultures (A) schematic image of the different compartments analysed **(B)** total sGAG of acellular and primed AC and BMSC, with and without $CaCO_3$ in the core hydrogel after 21 days low pH exposure, *** indicates significant difference + $CaCO_3$ groups compared to -$CaCO_3$ groups ($p<0.001$) **(C)** total sGAG accumulation of disc explant ring after 21 days low pH exposure **(D)** Alcian Blue/Aldehyde Fuchsin staining indicating sGAG content of constructs. Top row showing a cross-section of the whole construct, middle row a close up of the core-hydrogel with cellular µCaps and bottom row, the disc ring. Scale $bar_{cross\text{-}section}$ = 1 mm Scale $bar_{close\text{-}up}$ = 200 µm

7.3.9 Primed cells promote collagen deposition in AF ring of disc explants

Comparing different groups in terms of total collagen content, results showed the highest amount of collagen being detected within the acellular control group without $CaCO_3$ after 21 days in low pH culture. A decrease of collagen was found in cellular groups compared to day 0 (red dashed line) (Figure 7-12 A). Interestingly, an increase of total collagen within the disc ring could be observed with up to 3400 ± 1300 µg higher levels when cultured with a core of BMSC + $CaCO_3$ compared to day 0. No significant difference in collagen content between groups was found (Figure 7-12 B). Evaluation of sGAG/collagen ratio within the core demonstrated values close to native NP tissue (3.5), with the closest match of BMSC + $CaCO_3$ (3.64 ± 1.1) Overall, using CaCO3 was found to have a significant impact on sGAG/collagen ratio of the core gel ($p<0.001$) (Figure 7-12 C). Histologically no difference in picrosirius red collagen staining was observed between any of the groups (core and ring), which also correlated with the biochemical quantification (Figure 7-12 D).

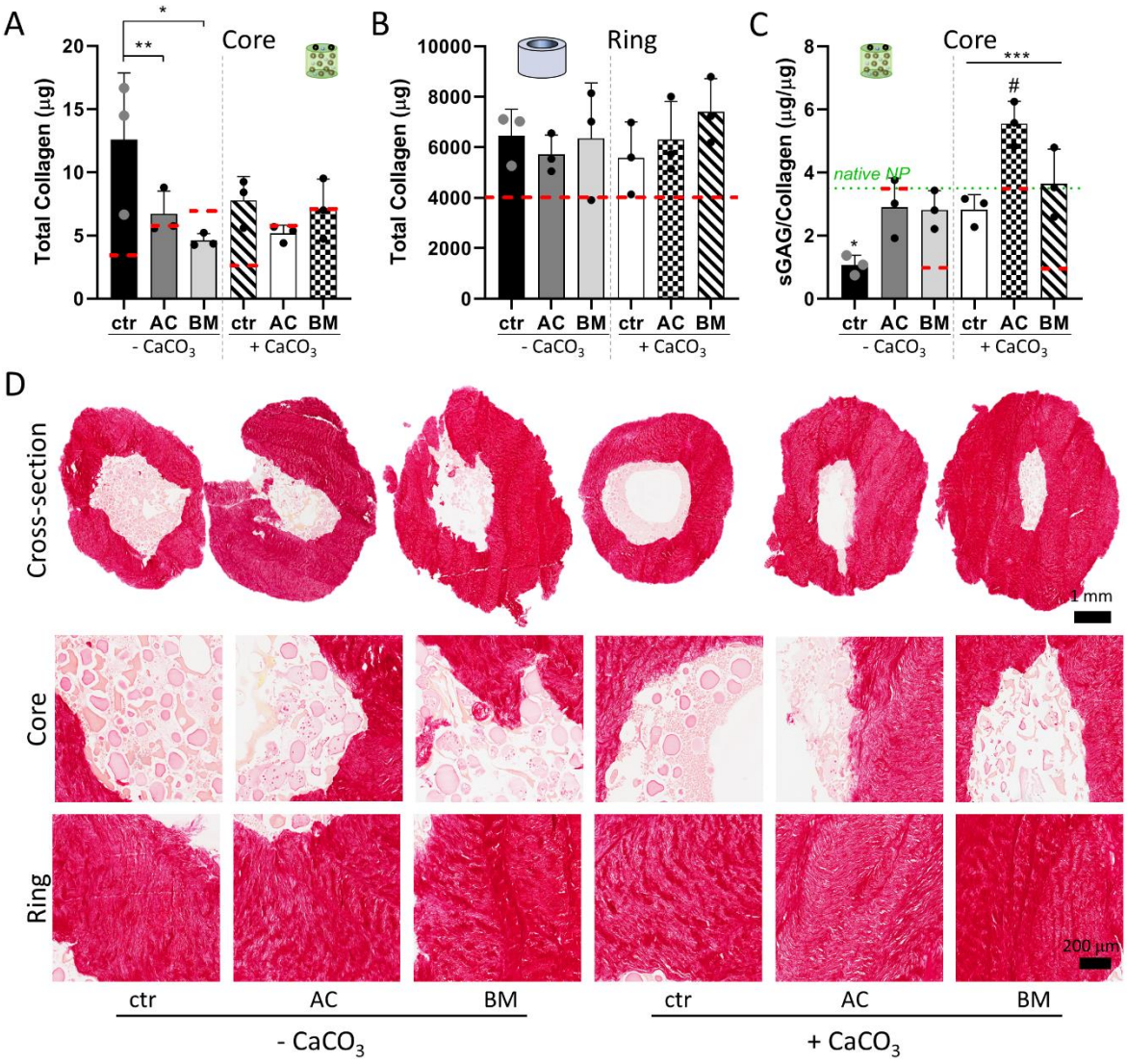

Figure 7-12: Collagen accumulation of explant cultures (A) total collagen of acellular and primed AC and BMSC, with and without $CaCO_3$ after 21 days low pH exposure in core hydrogel * and ** indicate significant difference between ctr -$CaCO_3$ and BM and AC -$CaCO_3$ respectively ($p<0.05$ and $p<0.01$) **(B)** total collagen accumulation (of disc explant ring after 21 days low pH exposure **(C)** sGAG/collagen ratios found in core gel green dashed line indicates values of native NP . * indicates significant difference of ctr-$CaCO_3$ to cellular groups -$CaCO_3$ ($p<0.05$), # indicates significant difference between AC+$CaCO_3$ to all other +$CaCO_3$-groups ($p<0.01$) and *** indicates significant impact of $CaCO_3$ on sGAG/collagen ratio ($p<0.001$) **(D)** Picrosirius red staining indicating collagen content of constructs. Top row shows a cross-section of the whole construct, middle row a close up of the core-hydrogel with cellular µCaps and bottom row the disc ring. Scale $bar_{cross\text{-}section}$ = 1 mm, Scale $bar_{close\text{-}up}$ = 200 µm

7.4. Discussion

The acidic microenvironment of the IVD plays a critical role in the imbalance of matrix anabolism and catabolism, which is believed to be a primary reason for the degeneration of the NP and subsequent LBP (Bibby et al., 2005b, Luoma et al., 2000). The overall aim of this study was to develop and characterize injectable, pH buffering µCaps to alter the low pH disc microenvironment and support host cells to either maintain or even regenerate disc tissue composition. Finally, these µCaps were evaluated *in vitro* as well as in a disc explant model to verify their potential when subjected to native-like microenvironmental conditions.

During the first phase of this study, investigations of different salts and buffering agents in terms of their pH neutralization capacities showed a limited potent effect of HEPES and $Al(OH)_3$ compared to $Mg(OH)_2$ and $CaCO_3$. HEPES is capable of maintain the pH within neutral range (pH 6.8 to 8.2), desired in standard cell culture media. A pH of 6.5 was used to represent degenerative disc conditions seemed to be too close to neutral pH to be affected by HEPES. The weak base $Al(OH)_3$ is mostly insoluble within a pH range of pH 6 to pH 8, hence the poor neutralization capacities.

In contrast, $Mg(OH)_2$ and $CaCO_3$, were found to raise the pH, even to an alkaline range in the case of $Mg(OH)_2$. $Mg(OH)_2$ is a strong base, which dissociates into $Mg^{2+}_{(aq)}$ and $2OH^-_{(aq)}$ under acidic conditions. The increase of OH^- ions within the surrounding solution creates an imbalance between H_3O^+ and OH^- causing a shift towards alkaline pH, which is accelerated due to the high diffusion coefficient of OH^- ($5.273x10^{-5}$ cm^2/s, (Vanysek, 2000)). $CaCO_3$ is a mostly insoluble weak base, which dissociates into $Ca^{2+}_{(aq)}$, $HCO_3^-{}_{(aq)}$ and $H_2O.CO_{2(aq)}$ within an acidic solution. The diffusion coefficient of HCO_3^- is 4.4 -times lower than that of OH^- explaining the slower increase of pH using $CaCO_3$ than $Mg(OH)_2$. µCap size and associated release kinetics also affect neutralization capacities of antacids. Evaluating different concentrations of $Mg(OH)_2$ and $CaCO_3$ entrapped in alginate µCaps revealed significantly bigger µCaps using $CaCO_3$ with the largest diameter when producing 500 mg/mL µCaps (358.6 ± 100.3 µm). An explanation may be two-fold: firstly, $CaCO_3$ nanoparticles used, are 2-3 times bigger than those of $Mg(OH)_2$ µCaps

and can influence the viscosity of alginate-antacid slurries. Secondly, $CaCO_3$ can induce partial crosslinking (Liu et al., 2002), which also increases the viscosity of the alginate solution. Both influence the rheologic properties and hence EHD spraying properties (Gansau et al., 2018). However, viscosity was not evaluated in this work to be certain about the statement. With respect to release kinetics a faster diffusion of Mg^{2+} ions from the µCaps into the media could be demonstrated compared to Ca^{2+} ions of all concentrations investigated. Both antacids are considered insoluble in water. However, as pH decreases, solubility increases with a 3-fold higher solubility of $CaCO_3$ at pH 6.0 compared to neutral pH (Plummer and Busenberg, 1982). However, Ca^{2+} ions have a higher affinity towards alginate compared to Mg^{2+} ions, retarding their rapid release from the alginate network while Mg^{2+} is more readily released into the media. Mg^{2+} ions were found to be fully released within 72 hours, whereas 80% of Ca^{2+} ions remained within the µCaps with a predicted completed release after several months. The mild buffering and the slower release kinetics of $CaCO_3$ are major advantages compared to $Mg(OH)_2$.

After excluding HEPES and $Al(OH)_3$ from further investigations due to poor neutralization capacities, the effect of $Mg(OH)_2$ and $CaCO_3$ on cell bioactivity was investigated. Examining cell viability of AC, no difference was observed between groups. A powerful resilience of primed AC when exposed to low pH conditions was demonstrated in the previous chapter (Chapter 6, page 99), which may be equally resilient exposed to a basic environment created by $Mg(OH)_2$. Yet, the effects of a basic environment on AC have been poorly covered in the literature. NP cells, on the other hand exhibit severe cell death within 24 hours using $Mg(OH)_2$ which amplifies with increasing concentration. This occurs predominantly peripherally of antacid µCaps, suggesting that the basic pH around the µCap boundaries is detrimental for these cells. Extreme extracellular pH conditions have been previously found to increase the expression of calcium-sensing receptors (CaSR) in some cells (Quinn et al., 2004). It has been found to bind Ca^{2+} and Mg^{2+} ions, activating intracellular pathways involved in apoptosis, cell proliferation, survival and cell maturation (Brennan and Conigrave, 2009, Zhang et al., 2016). Increased activation of this receptor due to basic pH and increased Mg^{2+} levels may overstimulate NP cells

resulting in cell death close to $Mg(OH)_2$ µCaps. CaSR has also been shown to be involved in calcification of the CEP of the IVD. Here, matrix deposition of CEP cells was inhibited due to high levels of Ca^{2+} ions (Grant et al., 2016). In this study, no significantly reduced matrix deposition of primed AC or BMSC was observed respectively when cultured with $CaCO_3$ µCaps. This is due to a five-times lower concentration of Ca^{2+} ions released into the media from $CaCO_3$ µCaps (0.08 mM) compared to the lowest concentration Grant *et al.* investigated (0.5 mM).

In phase 3 of this study the potential of a hybrid hydrogel containing $CaCO_3$ µCaps, primed AC or BMSC µCaps respectively within a fibrin-HA bulking gel was explored using a disc explant model. In the first instance, the neutralization capacities of $CaCO_3$ found *in vitro* were validated, demonstrating significantly higher pH levels within the core gel of the explants. Interestingly, the pH of the surrounding media was found to be below the initial set pH of 6.5. This may be due to the release of lactate during glycolysis of resident disc cells (Bibby et al., 2005b, Guehring et al., 2009) as well as primed AC and BMSC respectively (further details see paragraph 6.3.5, page 110 in previous chapter) which further acidifies the environment. After separating the core gel from the disc explant ring for individual analysis, highest DNA levels were found in groups with incorporated $CaCO_3$ µCaps inside the core. However, all DNA levels were below the DNA content detected at day 0, except for the acellular control groups, which showed a positive reading for DNA at day 0 as well as at day 21, indicating interference of the gels with the assay resulting in background noise. A migration of disc cells into the core gel may also explain the increase of DNA within acellular gels after 21 days, however, no cells were found within the core using cell viability staining. Therefore, an assay interference is the more likely explanation for these results. Surprisingly, high viability was found in all groups except for BMSC + $CaCO_3$. Perhaps these conflicting results are due to the degradation of the fibrin bulking gel. Studies by Kato *et al.* and Suzuki *et al.* demonstrated a correlation between acidity and MMP release which also have been shown to degrade fibrin (Ahmed et al., 2007, Kato et al., 2005, Suzuki et al., 2014, Bini et al., 1996). The remaining fractions of fibrin seem to interfere with analysis creating background noise during biochemical assays, confounding results, as mentioned

above. Moreover, due to the disrupted fibrin network, µCaps leaked from the fibrin gel into the surrounding environment hence were not considered for analysis. Yet, degradation of the bulking gel is favourable from a translational perspective. For translation, a bulking agent is required to facilitate injection of µCaps into the pressurized IVD while biodegrading over time facilitates good integration of cell µCaps into the tissue, and possibly enhancing paracrine cell-cell communication. For instance, resident cells from the disc explants showed increased DNA levels after 3 weeks culture with antacid µCaps, indicating a positive effect of $CaCO_3$ on proliferation, possibly due to improved pH conditions in combination with paracrine signalling of primed AC and BMSC respectively. Numerous studies have demonstrated an increase in disc cell proliferation in co-culture with BMSCs *in vitro* (Yamamoto et al., 2004, Naqvi and Buckley, 2015a, Le Visage et al., 2006, Naqvi et al., 2019). Surprisingly, primed BMSCs with $CaCO_3$ µCaps had significantly lower viability compared to all other groups. Potentially, elevated levels of extracellular Ca^{2+} aggravate detrimental effects of hypertonic media on BMSCs demonstrated by Wuertz *et al.* (Wuertz et al., 2008). For instance, CaSR within the cell membrane of BMSCs as well as extracellular Ca^{2+} is associated with osteogenesis (Caudarella et al., 2011, Xu et al., 2012, Cheng et al., 2013). Subsequentially, hypertonic media may induce an influx of Ca^{2+} similar as found in osteoblasts (Dascalu et al., 1995) resulting in elevated intracellular Ca^{2+} signalling, which is involved in matrix remodelling, proliferation and apoptosis (Berridge et al., 2003). Thus, excessive levels of intracellular Ca^{2+} due to high osmolarity and $CaCO_3$ µCaps may induce cell death of BMSCs.

Matrix metabolism is also a vital factor for disc regeneration. Quantification of sGAG within the core gel resulted in significantly higher levels when using $CaCO_3$ µCaps. However, acellular control gel also showed high sGAG reading using the DMMB assay, suggesting high background noise, as mentioned above. Nevertheless, matrix molecules were visible histologically within primed cellular µCaps of all groups. Within the disc ring, decreasing levels of sGAG after 21 days in simulated degenerative disc conditions (i.e. low pH, low glucose, high osmolarity) were demonstrated. Van Dijk *et al.* compared sucrose and polyethylene glycol (PEG)

to match osmotic pressure present in native disc tissue. They revealed increased osmolarity, tissue swelling and loss of PG from the tissue when using sucrose (van Dijk et al., 2011), which correlates with findings observed in this study. This depletion of PGs may be masking any paracrine signalling AC or BMSC may have on sGAG deposition of resident disc cells. Still, higher amounts of total sGAG were found in +$CaCO_3$ groups with primed cellular µCaps suggesting improved sGAG deposition of disc cells due to higher pH levels which have been reported previously (Naqvi and Buckley, 2016, Razaq et al., 2003, Wuertz et al., 2009). Comparing collagen levels found within the core gel, highest levels were detected in the acellular control group without $CaCO_3$, which may be explained the same way as above: interfering fractions of the fibrin hydrogel, which was degraded due to the acidic cell culture. The combination with calcium or the cells may partly prevent this degradation, by increased local pH or secretion of different factors from the cells, explaining why this extreme noise was not seen in other groups. However, these are speculations and need further investigations. Total collagen within the disc rings was found to increase in all groups. This supports the hypothesis that sGAG is lost due to depletion and not due to cellular anabolism. Groups with BMSC µCaps seem to increase the collagen levels within the disc tissue more than other groups, suggesting a potential paracrine effect on disc cells. However, the difference was not found to be significant. Many studies have investigated co-culture effects of BMSCs and NP cells, demonstrating better trans-cellular signalling when cell-cell contact occurs (Yamamoto et al., 2004, Richardson et al., 2006, Lehmann et al., 2018). In this study, however, primed cells are entrapped within alginate µCaps. Due to priming, cells deposit latent TGF-β3 into their surrounding matrix within the alginate µCaps, where it can bind to matrix molecules upon activation and release by factors including acidity and MMPs (Du et al., 2018, Engel et al., 1999, Khalil, 1999, Lyons et al., 1988). Under culture conditions used in this study, the latent TGF-β3 bound to matrix of primed µCaps gets activated and released, further promoting matrix synthesis of disc cells, which is seen here in increased collagen levels of disc rings.

Comparing AC and BMSCs as potential therapeutic cell types, it appears that AC can withstand the harsh environment of hypertonia and acidity in combination with $CaCO_3$ – pH neutralizing µCaps better than BMSCs despite priming. However, it has been found that BMSCs can differentiate towards a discogenic cell type (Steck et al., 2005, Richardson et al., 2006, Yamamoto et al., 2004), which is more favourable than a different cell type entirely. Moreover, better sGAG retention and higher collagen deposition were observed when co-culturing disc cells with BMSCs, suggesting slightly more effective paracrine signalling compared to AC. The differences between both cell types are not significant but considering translational aspects such as cell availability and progress on clinical trials, BMSCs may offer greater potency compared to AC.

Overall, this study aims to re-establish the pH microenvironment of a healthy IVD to restore the natural functions of resident cells in combination with cell-based therapy. However, disc degeneration is caused by multiple factors including inhibited nutrient diffusion and disc dehydration. Increasing the intracellular pH and introducing more cells may also cause a higher demand for nutrients, which cannot be satisfied without improved nutrient transportation.

7.5. Conclusion

In conclusion, this study developed and investigated pH buffering µCaps that can neutralize the acidic microenvironment of the degenerative IVD and improve matrix deposition capacities of resident disc cells. $CaCO_3$ has been found to be superior in terms of neutralization capacities, release kinetics and cellular response compared to all other antacids investigated. Using a disc explant model, it was demonstrated that $CaCO_3$ µCaps were capable of increasing the local pH within the core of a hybrid gel containing µCaps of $CaCO_3$ and cells. Primed cells were capable of increasing collagen deposition within the disc explant ring due to enhanced pH conditions as well as potentially paracrine signalling towards disc cells. However, little can be concluded regarding sGAG deposition due to depletion from the tissue. Overall this study aimed to improve the acidic microenvironment using a novel approach combining antacids and cell-

based therapy to subsequentially regenerate the intervertebral disc. With this approach, it was found that not only do injected cells deposit *de novo* matrix, but also the conditions of resident cells were improved by elevated pH levels and paracrine stimulation to encourage the deposition of new matrix molecules.

CHAPTER 8
DISCUSSION

8.1. Summary

The overall aim of this thesis was to develop and investigate a minimally invasive material for cell-based therapies of the degenerated IVD. Specifically, two key challenges associated with this approach were addressed: (i) technical obstacles related to cell delivery into the highly pressurized disc and (ii) microenvironmental challenges associated with the acidity of the degenerated (NP. The first challenge was resolved using microencapsulation of cells into alginate μCaps using EHDS technology - a process which can protect cells from shear forces during injection while also improving cell deposition into the NP matrix. The data presented here show that the size and shape of μCaps can be easily modified by changing operational parameters such as needle size, voltage and the flow rate of the polymer. Following optimization of these parameters to minimize capsule diameter for greater injectability (30G needle, 10 kV and 100 μL/min), different cell seeding densities were explored ($5x10^6$, $10x10^6$ and $20x10^6$ cells/mL). It was demonstrated that increasing cell seeding numbers resulted in both increased matrix deposition and cell death. Therefore, a medium cell density ($10x10^6$ cells/mL) was determined to be a good compromise between matrix accumulation and cell viability. Upon observing limited capsule deposition due to high intradiscal pressure, a viscous bulking agent based on fibrin was developed. In order to take advantage of both higher viscosity for better microcapsule delivery and improved material properties to enhance cellular response within the NP, a biomimetic fibrin composite containing HA was employed. This material showed improved cellular response in terms of cell viability and matrix deposition. After solving the question of cell delivery, the harsh intradiscal microenvironment was then addressed. Due to the acidic milieu observed within degenerative disc tissue (pH of 6.8 and 6.5 in mildly vs severely degenerated discs respectively), outcomes of cell-based therapy are often unfavourable. Therefore, AC and BMSC were primed using TGF-β3. This resulted in a dramatic increase in cell viability in low pH conditions and

enhanced matrix deposition, with sGAG and Col2 synthesis showing significant improvement. Lastly the microenvironment was addressed directly using antacid µCaps. By employing EHD spraying technology, micro-sized pH-neutralizing capsules containing $CaCO_3$ were fabricated. These were subsequently characterized and tested both *in vitro* and within a disc explant model., This process resulted in an increase in the local pH, thereby promoting matrix deposition and simultaneously enhancing positive paracrine signalling of primed cells. The material developed in this thesis is a hybrid hydrogel containing (i) TGF-β3-primed cell µCaps for cell-based therapies, (ii) antacid µCaps to alter the acidic microenvironment of the disc and (iii) a fibrin – HA bulking gel to facilitate capsule delivery and promote cellular response.

This thesis began by addressing technical issues involved in cell delivery into the intradiscal space for cell-based therapy. Firstly, microencapsulation of cells into ionically crosslinked alginate hydrogels using EHD spraying technology was explored and optimised (Chapter 4, page 52). Transplanted cells have been shown to stimulate proliferation and matrix deposition of residential disc cells through paracrine signalling while also possessing the ability to adopt a discogenic phenotype, thereby synthesizing the correct tissue composition (Richardson et al., 2006, Miyamoto et al., 2010). Intradiscal needle injection seems to be the most promising method as it is minimally invasive and can be image guided. Recurrent obstacles involve cell leakage and damage have been observed during this procedure (Vadala et al., 2012, Bertram et al., 2005, Li et al., 2014a, Moyer et al., 2010), but can be overcome using cellular microencapsulation. EHD spraying is a cost efficient, versatile, one-step technology for fabrication of cell-laden µCaps in a highly controllable fashion (Bock et al., 2012a). Consistent with previous studies, the average capsule size can be minimized by decreasing the inner needle diameter of the EHD sprayer and increasing the applied voltage (Sahoo et al., 2010b, Braghirolli et al., 2013, Workman et al., 2014), with optimal settings of 30G and 10 kV for fabrication of µCaps with an average diameter of 151.65 ± 62.9 µm. Exploring the effect on cell viability, high resistance towards applied voltage was found, whereas the combination of high viscosity alginate and a small needle size caused increased shear forces which resulted in more cell death.

Investigations of cell seeding density effects demonstrated greater total matrix deposition with higher encapsulated cell number. However, it appeared that closer cell-cell contact, and nutrient deprivation can diminish cell viability, resulting in decreased matrix production on a per cell basis with increasing cell seeding density, which was also found previously (Kobayashi et al., 2008, Gasperini et al., 2013a). After optimizing the EHD spraying settings for minimal μCaps size and maximum cell performance, initial intradiscal injection attempts of μCaps revealed poor delivery due to high pressure within the disc tissue, which causes retention of the higher density capsules which remain within the syringe barrel while the liquid solution passes into the NP (Appendix 2). Therefore, in Chapter 5, a viscous bulking agent was developed to overcome this limitation. Fibrin is a viscoelastic material which has been used in different applications such as a sealant and an adhesive in surgery for wound healing (Eyrich et al., 2006b, MacGillivray, 2003b, Fattahi et al., 2004b). It can be modified using ECM molecules such as collagen and HA, which have been shown to promote proliferation and matrix synthesis (Gorodetsky et al., 2011, Bertolo et al., 2012, Collins and Birkinshaw, 2013). Using this approach, the benefits of this material are two-fold: (i) facilitation of μCaps delivery and (ii) taking advantage of the superior properties of fibrin hydrogel and ECM molecules for tissue regeneration. Different concentrations of fibrinogen (12.5, 25, 37.5 and 50 mg/mL) were investigated and a better preservation of size and shape of fibrin hydrogels with increasing fibrinogen concentration was observed, which may be due to a higher fibre density and subsequentially smaller pore size within the hydrogel (Kotlarchyk et al., 2011, Duong et al., 2009). Improved cell viability was observed in hydrogels with higher concentrations of fibrin. Furthermore, the higher fibre density may lead to enhanced microcapsule distribution and retention within the gel and more efficient delivery into the NP tissue. Incorporation of Col1 and HA into the fibrin matrix aimed to create a biomimetic network for cells and hence increase their matrix deposition capacities. Following incorporation of Col1 into the fibrin matrix, more collagen was found to be deposited. Col1 has been demonstrated to bind to fibrin specifically using the integrin αvβ3 connection as a functional interface matrix which can activate different intracellular pathways (Reyhani et al., 2014) and subsequently promote collagen expression, as shown in NP cells encapsulated within a fibrin-collagen hydrogel

(Colombini et al., 2015). With NP being a highly hydrated tissue, amplification of sGAG accumulation is critical. It was demonstrated that this can be mediated by incorporating HA into the fibrin matrix, which has a high affinity to CD44 cell surface receptors. CD44 is expressed in various cell types including chondrocytes, MSCs and hemopoietic stem cells (Aguiar et al., 1999, Chow et al., 1995, T et al., 2016, Zoller, 2015, Knudson and Knudson, 2004), where it stimulates cell-cell and cell-matrix interactions (Aguiar et al., 1999, Chow et al., 1995) and can enhance the expression of chondrogenic markers such as Col2 and aggrecan in chondrocytes (Park et al., 2014). In this work the incorporation of HA into the fibrin gel resulted in suppression of collagen accumulation whereas sGAG deposition was increased. Exploring different concentrations of HA within the fibrin matrix revealed less cellular proliferation with high levels of HA (5 mg/mL), whilst deposition of sGAG was increased, thereby resulting in higher sGAG accumulation on a per cell base. Furthermore, using 5 mg/mL HA within fibrin hydrogels was found to diminish collagen deposition, resulting in the highest sGAG/collagen ratio which closer mimicked that of native NP tissue. Overall, in Chapter 4 and 5 critical aspects for cell delivery into the IVD were addressed and a combination of cellular µCaps and a fibrin - HA hybrid gel was developed and evaluated. This composite gel was proposed to be an efficient delivery vehicle with enhanced cellular µCaps deposition for cell-based therapy whilst further promoting positive cellular responses on injected cells as well as resident disc cells.

The local cellular environment within the degenerating disc has been shown to be harsh and is characterized by reduced O_2 (Bartels et al., 1998), diminished levels of glucose (Maroudas et al., 1975, Jackson et al., 2011), higher acidity (Bartels et al., 1998) and increased levels of proinflammatory cytokines (Altun, 2016). Nutrient supply into the disc occurs predominantly by diffusion through CEP and the AF (Jackson et al., 2011). During disc degeneration, however, CEPs tend to become calcified, resulting in limited nutrient transport into and out of the disc thereby affecting both resident cells and any potentially injected therapeutic cells which, as a result, display decreased viability and matrix accumulation capacity (Horner and Urban, 2001, Ohshima and Urban, 1992, Gilbert et al., 2016b). In chapter 6 and 7, the acidic microenvironment

was addressed with a view to enhancing the potential of cell-based therapies. In Chapter 6, AC and BMSC were cultured under three different pH-conditions, both with and without prior exposure to TGF-β3 (pH 7.1, 6.8 and 6.5 representing "healthy", "mildly degenerated" and "severely degenerated" discs respectively). The effect of acidity on cell viability has previously been explored for different cell types including ADSCs (Han et al., 2014), BMSC (Naqvi and Buckley, 2016, Wuertz et al., 2009), NPMSC (Han et al., 2014), NP cells (Hodson et al., 2018, Razaq et al., 2003) and ACs (Razaq et al., 2003). In each of these studies, decreasing cell viability with decreasing pH was observed. However, if cell therapies are to become widespread as part of disc regeneration strategies, then it is important to ascertain if transplanted cells can thrive within these acidic microenvironments and to develop cell culture techniques that enhance cellular responses. It was demonstrated that this can be achieved by pre-culturing cells in the presence of TGF-β3, resulting in significantly improved cell viability following low pH culture for both AC and BMSC cell types. This may be due to the development of a protective niche made of surrounding ECM, which correlates with previous findings by Naqvi *et al.* (Naqvi et al., 2018). Indeed, greater amounts of sGAG and collagen (type 2 in particular) and an elevated sGAG/collagen ratio were detected following TGF-β3 priming, implying improved NP-like matrix formation. Furthermore, a shift in metabolic activity was observed, demonstrating an overall higher activity of primed BMSCs compared to non-primed (i.e. higher OCR, GCR and LPR). AC on the contrary did not show significant metabolic changes. The change of metabolic activity of BMSC during differentiation was also seen by Pattappa *et al.*, who demonstrated increased lactate production of BMSCs during chondrogenesis using TGF-β supplementation (Pattappa et al., 2011), which suggests a phenotypical change of BMSCs during the priming stage that also contributes to the resistance against low pH environments.

After successfully providing therapeutic cells with the ability to withstand the acidic environment found in degenerative discs, the focus of Chapter 7 was to neutralize the environment and thereby provide better conditions for resident disc cells to promote tissue recovery. This can be achieved using antacids - a group of multi-component salts with pH

neutralizing properties. In this work, different antacids were encapsulated into alginate µCaps using the EHDS technology (as explored in Chapter 4). The results demonstrated that $Mg(OH)_2$ and $CaCO_3$, could successfully raise the pH, even to an alkaline range in the case of $Mg(OH)_2$ after 24 hours. $Mg(OH)_2$ and $CaCO_3$ are mostly insoluble in water but dissociate in acidic conditions into $Mg^{2+}_{(aq)}$ and $2OH^-_{(aq)}$, and $Ca^{2+}_{(aq)}$, $HCO_3^-{}_{(aq)}$ and $H_2O.CO_{2(aq)}$ respectively. With a 4.4-times higher diffusion coefficient of $OH^-_{(aq)}$ than $HCO_3^-{}_{(aq)}$, the pH increase is more rapid using the strong base $Mg(OH)_2$ than $CaCO_3$. The release kinetic of $Mg(OH)_2$ has been shown to be controlled by alginate concentration and capsule size (Chen et al., 2018). Here, the alginate concentration was kept consistent, but the antacid concentration was varied, which also resulted in change of µCap diameter. A rapid $Mg^{2+}_{(aq)}$ rate of release with a full release after 72h was observed, whereas 80% of $Ca^{2+}_{(aq)}$ ions remained within alginate µCaps after the same period. This may be due to a slow diffusion coefficient and a partial crosslinking of alginate, with a predicted total release after several months. Comparing the two antacids and their effect on cells, no adverse impact of $CaCO_3$ was observed on therapeutic or NP cells. $Mg(OH)_2$ on the other hand caused severe cell death of NP cells in close proximity to $Mg(OH)_2$ µCaps within 24 hours and this effect was amplified with higher concentration. This may be due to the pH induced activation of CaSR and its involvement in apoptosis, cell proliferation, survival and cell maturation (Brennan and Conigrave, 2009, Zhang et al., 2016, Quinn et al., 2004). Because of the superior properties of $CaCO_3$, this salt was selected for progression to the final phase. Therefore, 500 mg/mL $CaCO_3$ and cells (AC and BMSC) were microencapsulated using the EHDS technology as established in Chapter 4, cells were primed for 14 days as described in Chapter 6 and finally, both types of µCaps were combined within the fibrin-HA bulking gel developed in Chapter 5 and explored within a disc explant model using bovine disc tissue. Firstly, the neutralization capacities of $CaCO_3$ found *in vitro* were validated and were shown to result in significantly higher pH levels within the core gel of the explants.

Evaluation of the separate compartments (disc-ring and hybrid gel–core) revealed a decrease in DNA levels in the core in all cellular groups compared to day 0. As found by Ahmed

et al., fibrin hydrogel degrades in low pH environment due to MMPs released from cells (Ahmed et al., 2007). As a result, capsules were released into its surroundings which masks outcomes in this study but is also a big advantage from a translational perspective. However, positive reading for DNA was also seen in acellular control groups, which indicates background noise from the F-HA bulking gel. Nevertheless, high cell viability was observed within the core of all cellular groups except for primed BMSCs +$CaCO_3$. This may be due to an overstimulation of CaSR by $Ca^{2+}_{(aq)}$ ions as a result of the combination of hypertonic surrounding and increased levels of extracellular $Ca^{2+}_{(aq)}$ from $CaCO_3$ µCaps (Wuertz et al., 2008, Dascalu et al., 1995, Berridge et al., 2003). Analysing the disc ring, levels of DNA were found to be maintained when cultured with primed cells and $CaCO_3$ pH neutralizing µCaps. However, the differences were not found to be significant. Cellular groups without $CaCO_3$ on the other hand showed decreasing levels of DNA compared to day 0, which indicates that $CaCO_3$ in combination with paracrine signalling of primed AC and BMSC respectively nay have a positive effect on proliferation, which also has been demonstrated by numerous studies (Yamamoto et al., 2004, Naqvi and Buckley, 2015a, Le Visage et al., 2006, Naqvi et al., 2019). Acellular control group without $CaCO_3$ however, could also maintain DNA levels after low pH culture for 21 days, which suggests that disc cells are generally resilient against acidic cell culture. Depletion of sGAG from disc tissue was found in all groups (disc explants cultured with or without AC or BMSC and with or without $CaCO_3$, respectively) with the highest, yet not significantly, amount of sGAG being retained in groups containing $CaCO_3$, therefore suggesting that the sGAG deposition of disc cells can be positively influenced by higher pH levels, as it has been reported previously (Naqvi and Buckley, 2016, Razaq et al., 2003, Wuertz et al., 2009). In contrast, collagen accumulation was found to be increased in disc tissue for all groups investigated. Potential reasons for this phenomenon May be the effect of ECM molecules within the F-HA bulking gel, which is present in all groups, promoting matrix deposition of resident disc cells.

Chapter 6 and 7 not only focused on approaches to overcome the acidic microenvironment of the degenerative disc, but also compared AC and BMSC to find a suitable

cell type for disc cell-based therapy. Important criteria in this matter are cell survival and sustainability within the compromised environment. Additionally, a slow metabolism is favourable because of the limited nutrients available. Notochordal cells and NP cells have been proposed as suitable candidates as they are naturally adapted to the disc environment. However, isolation and 2D expansion of these cell types is challenging and tends to yield insufficient cell numbers for clinical translation. AC and BMSC on the other hand can be easily obtained and have the potential to accumulate disc-like matrix. BMSC have been shown to have limited capabilities to withstand the harsh environment of the IVD and while AC show better viability, the matrix accumulation capacities of AC are inadequate. Both can be overcome with priming, which may be costly and time consuming from a translational perspective. However, it appears that primed cells secrete paracrine factors to stimulate resident disc cells to enhance matrix deposition. Disc explants cultured with BMSCs demonstrated better sGAG retention and collagen deposition compared to explants cultured with AC. Yet, the difference was not found to be significant, which was demonstrated in Chapter 7. The metabolic activity of primed BMSC was found to be higher than that of AC, which could have a negative impact on resident cells, which are in competition over available nutrients. For clinical translation, a compromise must be made between cell harvest, cell processing prior implantation, matrix accumulation capacities of therapeutic cells and the paracrine effect these cells have on resident cells. BMSC have been tested in clinicals trials for IVD regeneration with some success (Yoshikawa et al., 2010, Orozco et al., 2011, Sakai and Schol, 2017, Pettine et al., 2015, Noriega et al., 2017, Pennicooke et al., 2016). This indicates that the higher metabolic activity is not necessarily a critical factor for the choice of cell type. Considering the ease of isolation of BMSC, the potential to drive them towards a discogenic cell type and the higher potency of paracrine signalling, BMSC seem to offer greater potential when compared to AC for IVD regeneration.

8.2. Limitations and Future Work

In this thesis, all cells were obtained from young (3 - 4-month-old) porcine donors. Although porcine cells are widely accepted to be suitable for investigation for use in cell-based

therapies for regenerative medicine, some differences remain compared to human cells (Noort et al., 2012, Bharti et al., 2016). Not only is there a difference in species, but also the age and health state of the cells are critical. For instance, the cells used in this thesis came from young and healthy donors, whereas clinically relevant cells would be typically derived from mature donors with diseased tissue. In a recent study by Maredziak et al., it was demonstrated that MSCs isolated from elderly human donors with compromised tissue showed limited proliferation rates, reduced chondrogenic and osteogenic differentiation capacities and increased senescence (Maredziak et al., 2016). Therefore, verification of the findings in this thesis using human cells is required. In addition, a bovine explant model was used to examine in vitro findings of this work. The use of porcine cells in a bovine explant model to correlate to human applications is debatable. However, it was chosen because of the similarities of both to human. As described above, porcine cells show many similarities to human cells and bovine disc tissue was reported to be similar to human discs in terms of aspect ratios, nutrient transport distances and biochemical composition (Demers et al., 2004). Despite mixing different species, it is believed to recapitulate human conditions sufficiently for initial evaluations. But it is clear that moving forward, cells and tissue should be derived from humans to make the experiments more representative for human applications.

In this work, an injectable hydrogel for minimally invasive treatment of DDD was established. Intradiscal injection through the AF, however, can cause localized cell death and altered disc mechanics when punctured with a needle (Korecki et al., 2008). A compromise between potential outcome and tissue damage needs to be made; otherwise a different delivery approach through the vertebral bodies must be considered, as proposed by Vadala *et al.* (Vadala et al., 2013). Additionally, it is still unclear how many cells and what volume would be suitable to be introduced into the IVD. Here, the natural cell density of healthy NP tissue was used as a guideline, but a different number might be more suitable for regeneration purposes. However, in this case, a trade-off also needs to be made between the amount of potential matrix being produced by injected cells and the risk of nutrient deprivation within the compromised environment of the disc following injection of too many cells. Computational modelling would

be a useful strategy to explore different variations and their effect on the disc environment without expensive and time-consuming cellular experiments. Regardless of which strategy is chosen for a tissue engineering approach to regenerate the IVD, damage of tissue will have to be made either via needle puncture or by replacing the entire disc with a tissue engineered implant. However, these methods have still higher potential to serve as a long-term solution compared to the current golden standard of invasive surgery techniques.

EHDS has proven to be an effective technology for efficiently of fabricating µCaps of small diameter without compromising cell fate. However, for µCaps smaller than 150 µm, this technology seems to be limited when using alginate polymer. Furthermore, the variety of polymers suitable for the set up proposed in this thesis is limited. UV induced crosslinked materials, polymers crosslinking under extreme temperature shifts or slow crosslinking materials would need additional components to be combined with EHDS. The use of alginate in this thesis has shown to possess many advantages, as it is compatible with EHDS and the cells retain a round phenotype as found in native NP tissue. However, it also prevents cell-cell contact between injected cells and resident cells, reducing the full potential of co-culture effects. Modifications of alginate using RGD peptides would likely promote cell spreading but could also improve cell migration within the polymer and consequently enhance trans-cellular signalling.

A major limitation using priming to improve cell performance from a translational perspective is time and expense. It is time-consuming and costly to expand cells and expose them to growth factors for the duration required to maximise their therapeutic potential. Therefore, further optimization is required. For example, despite the findings of TGF-β3 being an excellent mediator for promoting differentiation of BMSCs towards a discogenic phenotype, different intrinsic or extrinsic signals and extracellular cues such as an optimised combination of different growth factors and/or genetically modifications could further improve this process (Ding and Schultz, 2005, Song et al., 2012). In cartilage tissue engineering, it has been found that a combination of BMP with TGF-β can improve chondrogenesis (Weiss et al., 2010), while GDF-5 and GDF-6 can also promote differentiation towards a discogenic phenotype (Clarke et al.,

2014, Frauchiger et al., 2018). Furthermore, retinoic acid (a metabolite of vitamin A_1) has been found to induce differentiation of MSCs towards chondrocytes and osteoblasts, which would be an alternative to expensive growth factors (Dingwall et al., 2011, Henderson et al., 2011).

The complex microenvironment of the IVD is influenced by several factors including low oxygen, glucose and acidic pH. In this thesis, the main focused lay on improving the local acidic environment. However, all factors are interconnected and influenced by each other (Naqvi and Buckley, 2015c, Bibby et al., 2005b, Guehring et al., 2009, Holm et al., 1981, Huang et al., 2007). Increasing the local pH for better matrix deposition and viability may be hindered when the reduced glucose availability is not being simultaneously altered. Considering that calcification of the CEPs limits solute transport into and out of the NP, it is likely that metabolites such as lactate will continue to accumulate and cause a drop in pH level over time. Moreover, the quantity of $Ca^{2+}_{(aq)}$ ions released by $CaCO_3$ µCaps may increase above a threshold over years of therapy, initiate further CEP calcification and consequently reverse the original improvements. An approach to prevent this would be to attempt to induce vascularization of the CEPs, thereby enhancing nutrient transport.

Another aspect not considered in this thesis is the inflammatory environment of the degenerated disc. Proinflammatory cytokines such as TNF-α, IL-, IL-1, IL-17 and IFN-γ have been found to be upregulated during disc degeneration while anabolism inducing factors including IGF-1 and TGF-β appear to be downregulated (Risbud and Shapiro, 2014, Okuda et al., 2001, Matsunaga et al., 2003). The release of inflammatory factors is also dependent on microenvironmental factors such as pH (Erra Diaz et al., 2018) and can impact resident cells as well as therapeutic cells. To mimic the degenerative disc environment, inflammatory factors need to be included.

Using a reductionist explant model to evaluate specific aspects can be beneficial, yet the primary limitation is the lack of integrity of the full organ and mechanical stimulation. During Chapter 7, injected µCaps were lost due to fibrin degradation. Also, mechanical loading on the disc tissue impacts cellular response, which was not considered in this thesis. The IVD naturally

experiences complex biomechanical stimuli including compression, torsion, flexion and shear in different intensities and frequencies, which have differing effects on cell fate (Vergroesen et al., 2015). For instance, dynamic compression loading has been found to enhance nutrient transport, including growth factors such as TGF-β and FGF, which in turn affects NP cells (Fearing et al., 2018). Moreover, cyclic mechanical loading was demonstrated to induce chondrogenic differentiation of BMSC and enhance ECM deposition (Huang et al., 2013). These aspects were not considered in this work but are important aspects of NP tissue repair. Therefore, the next logical step would be the evaluation of the hybrid gel within an *ex vivo* organ culture in the presence of the relevant mechanical stimuli. This model will not be able to capture the impact of the individual cell type but will give insights into the matrix repair capacities of a more complex set up prior to moving towards more complex and ethically challenging models.

Finally, the sGAG depletion was also found to be a major limitation in this work. While the use of sucrose can increase the osmolarity of cell culture media, it does not prevent tissue swelling (van Dijk et al., 2011). Osmolarity is a critical aspect in NP homeostasis and affects resident cells in different ways, including impacting proliferation and matrix accumulation (Sadowska et al., 2018, Wuertz et al., 2007). Different supplements such as NaCl, KCl, PEG or urea have been previously used to increase osmolarity (van Dijk et al., 2011, Choi et al., 2018, Li et al., 2018, Dong et al., 2014, Mavrogonatou and Kletsas, 2012) and such approaches should be considered for the next experimental iteration. Furthermore, media analyses should be performed to account for any matrix molecules depleted from the tissue and to quantify intrinsic factors released from cells.

8.3. Concluding Remarks

- Using EHDS technology, injectable alginate µCaps could be produced with high control over size and shape by varying the processing. parameter of inner needle diameter, applied voltage, flow rate and alginate concentration. The optimised settings for cellular microencapsulation were found to be: using a **30G needle, subjected to 10 kV applied voltage with a flow rate of 100 µL/min and a 1% alginate solution**.
- Cells were successfully encapsulated inside alginate µCaps. A correlation between higher seeding density and both decreasing cell viability and amount of total matrix accumulation could be demonstrated. The optimal **seeding density was found to be $10x10^6$ cells/mL** which was a compromise between good cell viability and total ECM deposition.
- A biomimetic bulking gel composed of a fibrin-HA blend was developed which is capable of enhancing cellular response and promotes matrix deposition. Moreover, it facilitated delivery of µCaps into the highly pressurized IVD. **A blend of 50 mg/mL fibrin and 5 mg/mL HA** was found to give the best results.
- Exploring AC and BMSC in low pH conditions, representative for degenerative discs revealed compromised sustainability of BMSC with inhibited matrix accumulation capacities whereas **AC were maintained viable under acidity** with reduced matrix deposition capacities.
- Priming of cells for 14 days using TGF-β3 could significantly improve poor viability of BMSC and reduced ECM production of both cell types. **BMSCs were capable of creating a disc-like matrix network containing high levels of Col2 and elevated sGAG/Collagen ratios**.
- Exploring different antacids within EHD sprayed µCaps to restore healthy disc-pH environment demonstrated superior neutralization capacities in combination with slow release kinetics of $CaCO_3$ µCaps. A concentration of **500 mg/mL $CaCO_3$** encapsulated within the µCaps is capable of **sufficiently increasing the pH over a longer time** while no diminishing effects on cell viability or matrix accumulation capacities occur.
- Using the developed material containing EHD sprayed cellular capsules ($10x10^6$ cells/mL AC or BMSC respectively and 500 mg/mL $CaCO_3$) within a fibrin (50 mg/mL) – HA (5 mg/mL) bulking gel in a **disc explant model** under degenerative disc like conditions (i.e. low O_2, low glucose, high osmolarity and low pH), could **successfully increase local pH within its core**. Furthermore, collagen deposition within the disc ring could be increased, potentially due to paracrine signalling.
- Comparing **AC and BMSC, no significant benefit was found of one over the other** when cells were primed using TGF-β3. Yet, clinically BMSC seem to be more

attractive as they are easier to obtain and they have already passed through several clinical trials

BIBLIOGRAPHY

(ATSDR), A. F. T. S. A. D. R. 2008. Toxicological profile for Aluminum. *In:* DEPARTMENT OF HEALTH AND HUMAN SERVICES, P. H. S. (ed.). Atlanta, GA: U.S.

ACOSTA, F. L., METZ, L., ADKISSON, H. D., LIU, J., CARRUTHERS-LIEBENBERG, E., MILLIMAN, C., MALONEY, M. & LOTZ, J. C. 2011. Porcine Intervertebral Disc Repair Using Allogeneic Juvenile Articular Chondrocytes or Mesenchymal Stem Cells. *Tissue Engineering Part A.*

ADAMS, P. & MUIR, H. 1976. Qualitative changes with age of proteoglycans of human lumbar discs. *Ann Rheum Dis,* 35**,** 289-96.

AGRAWAL, A., GUTTAPALLI, A., NARAYAN, S., ALBERT, T. J., SHAPIRO, I. M. & RISBUD, M. V. 2007. Normoxic stabilization of HIF-1alpha drives glycolytic metabolism and regulates aggrecan gene expression in nucleus pulposus cells of the rat intervertebral disk. *Am J Physiol Cell Physiol,* 293**,** C621-31.

AGUIAR, D. J., KNUDSON, W. & KNUDSON, C. B. 1999. Internalization of the hyaluronan receptor CD44 by chondrocytes. *Exp Cell Res,* 252**,** 292-302.

AHMED, T. A., GRIFFITH, M. & HINCKE, M. 2007. Characterization and inhibition of fibrin hydrogel-degrading enzymes during development of tissue engineering scaffolds. *Tissue Eng,* 13**,** 1469-77.

AKMAL, M., SINGH, A., ANAND, A., KESANI, A., ASLAM, N., GOODSHIP, A. & BENTLEY, G. 2005. The effects of hyaluronic acid on articular chondrocytes. *J Bone Joint Surg Br,* 87**,** 1143-9.

ALBERTS, B., JOHNSON, A., LEWIS, J., RAFF, M., ROBERTS, K. & WALTER, P. 2008. *Molecular Biology of the Cell, 5th Edition,* New York, Garland Science.

ALTUN, I. 2016. Cytokine profile in degenerated painful intervertebral disc: variability with respect to duration of symptoms and type of disease. *Spine J,* 16**,** 857-61.

ALVES, C. S., BURDICK, M. M., THOMAS, S. N., PAWAR, P. & KONSTANTOPOULOS, K. 2008. The dual role of CD44 as a functional P-selectin ligand and fibrin receptor in colon carcinoma cell adhesion. *Am J Physiol Cell Physiol,* 294**,** C907-16.

ALVES, C. S., YAKOVLEV, S., MEDVED, L. & KONSTANTOPOULOS, K. 2009. Biomolecular characterization of CD44-fibrin(ogen) binding: distinct molecular requirements mediate binding of standard and variant isoforms of CD44 to immobilized fibrin(ogen). *J Biol Chem,* 284**,** 1177-89.

ANDERSEN, T., AUK-EMBLEM, P. & DORNISH, M. 2015. 3D Cell Culture in Alginate Hydrogels. *Microarrays (Basel),* 4**,** 133-61.

ANTOSIAK-IWARISKA, M., SITAREK, E., SABAT, M., GODLEWSKA, E., KINASIEWICZ, J. & WERYNSKI, A. 2009. Isolation, banking, encapsulation and transplantation of different types of Langerhans islets. *Polskie Archiwum Medycyny Wewnetrznej.*

ARIEFF, A. I., COOPER, J. D., ARMSTRONG, D. & LAZAROWITZ, V. C. 1979. Dementia, renal failure, and brain aluminum. *Ann Intern Med,* 90**,** 741-7.

ARINZEH, T. L. 2005. Mesenchymal stem cells for bone repair: preclinical studies and potential orthopedic applications. *Foot Ankle Clin,* 10**,** 651-65, viii.

AURICH, H., SGODDA, M., KALTWASSER, P., VETTER, M., WEISE, A., LIEHR, T., BRULPORT, M., HENGSTLER, J. G., DOLLINGER, M. M., FLEIG, W. E. & CHRIST, B. 2009. Hepatocyte

differentiation of mesenchymal stem cells from human adipose tissue in vitro promotes hepatic integration in vivo. *Gut,* 58**,** 570-81.

BAIMARK, Y. & SRISUWAN, Y. 2014. Preparation of alginate microspheres by water-in-oil emulsion method for drug delivery: Effect of Ca2+ post-cross-linking. *Advanced Powder Technology,* 25**,** 1541-1546.

BARBERO, A., GROGAN, S., SCHÄFER, D., HEBERER, M., MAINIL-VARLET, P. & MARTIN, I. 2004. Age related changes in human articular chondrocyte yield, proliferation and post-expansion chondrogenic capacity. *Osteoarthritis and Cartilage,* 12**,** 476-484.

BARTELS, E. M., FAIRBANK, J. C., WINLOVE, C. P. & URBAN, J. P. 1998. Oxygen and lactate concentrations measured in vivo in the intervertebral discs of patients with scoliosis and back pain. *Spine (Phila Pa 1976),* 23**,** 1-7; discussion 8.

BATTIE, M. C., VIDEMAN, T., KAPRIO, J., GIBBONS, L. E., GILL, K., MANNINEN, H., SAARELA, J. & PELTONEN, L. 2009. The Twin Spine Study: contributions to a changing view of disc degeneration. *Spine J,* 9**,** 47-59.

BAYOUSSEF, Z., DIXON, J. E., STOLNIK, S. & SHAKESHEFF, K. M. 2012. Aggregation promotes cell viability, proliferation, and differentiation in an in vitro model of injection cell therapy. *Journal of Tissue Engineering and Regenerative Medicine,* 6.

BENNEKER, L. M., HEINI, P. F., ALINI, M., ANDERSON, S. E. & ITO, K. 2005. 2004 Young Investigator Award Winner: vertebral endplate marrow contact channel occlusions and intervertebral disc degeneration. *Spine (Phila Pa 1976),* 30**,** 167-73.

BENSAID, W., TRIFFITT, J. T., BLANCHAT, C., OUDINA, K., SEDEL, L. & PETITE, H. 2003. A biodegradable fibrin scaffold for mesenchymal stem cell transplantation. *Biomaterials,* 24**,** 2497-502.

BENYA, P. D. & SHAFFER, J. D. 1982. Dedifferentiated chondrocytes reexpress the differentiated collagen phenotype when cultured in agarose gels. *Cell,* 30**,** 215-224.

BERRIDGE, M. J., BOOTMAN, M. D. & LIPP, P. 1998. Calcium--a life and death signal. *Nature,* 395**,** 645-8.

BERRIDGE, M. J., BOOTMAN, M. D. & RODERICK, H. L. 2003. Calcium signalling: dynamics, homeostasis and remodelling. *Nat Rev Mol Cell Biol,* 4**,** 517-29.

BERTOLO, A., HÄFNER, S., TADDEI, A. R., BAUR, M., PÖTZEL, T., STEFFEN, F. & STOYANOV, J. 2015. INJECTABLE MICROCARRIERS AS HUMAN MESENCHYMAL STEM CELL SUPPORT AND THEIR APPLICATION FOR CARTILAGE AND DEGENERATED INTERVERTEBRAL DISC REPAIR. 29**,** 70-81.

BERTOLO, A., MEHR, M., AEBLI, N., BAUR, M., FERGUSON, S. J. & STOYANOV, J. V. 2012. Influence of different commercial scaffolds on the in vitro differentiation of human mesenchymal stem cells to nucleus pulposus-like cells. *Eur Spine J,* 21 Suppl 6**,** S826-38.

BERTRAM, H., KROEBER, M., WANG, H., UNGLAUB, F., GUEHRING, T., CARSTENS, C. & RICHTER, W. 2005. Matrix-assisted cell transfer for intervertebral disc cell therapy. *Biochem Biophys Res Commun,* 331**,** 1185-92.

BHARTI, D., SHIVAKUMAR, S. B., SUBBARAO, R. B. & RHO, G. J. 2016. Research Advancements in Porcine Derived Mesenchymal Stem Cells. *Curr Stem Cell Res Ther,* 11**,** 78-93.

BIBBY, S. R., JONES, D. A., RIPLEY, R. M. & URBAN, J. P. 2005a. Metabolism of the intervertebral disc: effects of low levels of oxygen, glucose, and pH on rates of energy metabolism of bovine nucleus pulposus cells. *Spine (Phila Pa 1976),* 30**,** 487-96.

BIBBY, S. R. & URBAN, J. P. 2004. Effect of nutrient deprivation on the viability of intervertebral disc cells. *Eur Spine J,* 13**,** 695-701.

BIBBY, S. R. S., JONES, D. A., RIPLEY, R. M. & URBAN, J. P. G. 2005b. Metabolism of the intervertebral disc: effects of low levels of oxygen, glucose, and pH on rates of energy metabolism of bovine nucleus pulposus cells. *Spine,* 30**,** 487-496.

BINI, A., ITOH, Y., KUDRYK, B. J. & NAGASE, H. 1996. Degradation of cross-linked fibrin by matrix metalloproteinase 3 (stromelysin 1): hydrolysis of the gamma Gly 404-Ala 405 peptide bond. *Biochemistry,* 35**,** 13056-63.

BOBICK, B. E., CHEN, F. H., LE, A. M. & TUAN, R. S. 2009. Regulation of the chondrogenic phenotype in culture. *Birth Defects Research Part C - Embryo Today: Reviews.*

BOCK, N., DARGAVILLE, T. R. & WOODRUFF, M. A. 2012a. Electrospraying of polymers with therapeutic molecules: State of the art. *Progress in Polymer Science.*

BOCK, N., DARGAVILLE, T. R. & WOODRUFF, M. A. 2012b. Electrospraying of polymers with therapeutic molecules: State of the art. *Progress in Polymer Science,* 37**,** 1510-1551.

BOCK, N., WOODRUFF, M. A., HUTMACHER, D. W. & DARGAVILLE, T. R. 2011. Electrospraying, a Reproducible Method for Production of Polymeric Microspheres for Biomedical Applications. *Polymers,* 3**,** 131.

BOGDUK, N., APRILL, C. & DERBY, R. 2013. Lumbar discogenic pain: state-of-the-art review. *Pain Med,* 14**,** 813-36.

BOOS, N., WEISSBACH, S., ROHRBACH, H., WEILER, C., SPRATT, K. F. & NERLICH, A. G. 2002. Classification of age-related changes in lumbar intervertebral discs: 2002 Volvo Award in basic science. *Spine (Phila Pa 1976),* 27**,** 2631-44.

BOSNAKOVSKI, D., MIZUNO, M., KIM, G., TAKAGI, S., OKUMURA, M. & FUJINAGA, T. 2006. Chondrogenic differentiation of bovine bone marrow mesenchymal stem cells (MSCs) in different hydrogels: Influence of collagen type II extracellular matrix on MSC chondrogenesis. *Biotechnology and Bioengineering,* 93**,** 1152-1163.

BRAGHIROLLI, D. I., ZAMBONI, F., CHAGASTELLES, P. C., MOURA, D. J., SAFFI, J., HENRIQUES, J. A., PILGER, D. A. & PRANKE, P. 2013. Bio-electrospraying of human mesenchymal stem cells: An alternative for tissue engineering. *Biomicrofluidics,* 7**,** 44130.

BRENNAN, S. C. & CONIGRAVE, A. D. 2009. Regulation of cellular signal transduction pathways by the extracellular calcium-sensing receptor. *Curr Pharm Biotechnol,* 10**,** 270-81.

BRIDGEN, D., GILCHRIST, C., RICHARDSON, W., ISAACS, R., BROWN, C., YANG, K., CHEN, J. & SETTON, L. J. J. O. O. R. 2013. Integrin-mediated interactions with extracellular matrix proteins for nucleus pulposus cells of the human intervertebral disc. 31**,** 1661-1667.

BROCK, M., PATT, S. & MAYER, H. M. 1992. The form and structure of the extruded disc. *Spine (Phila Pa 1976),* 17**,** 1457-61.

BRUCHET, M. & MELMAN, A. 2015. Fabrication of patterned calcium cross-linked alginate hydrogel films and coatings through reductive cation exchange. *Carbohydrate Polymers,* 131**,** 57-64.

BUCKWALTER, J. A., PEDRINI-MILLE, A., PEDRINI, V. & TUDISCO, C. 1985. Proteoglycans of human infant intervertebral disc. Electron microscopic and biochemical studies. *J Bone Joint Surg Am,* 67**,** 284-94.

BUSER, Z., LIU, J., THORNE, K. J., COUGHLIN, D. & LOTZ, J. C. 2014. Inflammatory response of intervertebral disc cells is reduced by fibrin sealant scaffold in vitro. *J Tissue Eng Regen Med,* 8**,** 77-84.

CALDEIRA, J., SANTA, C., OSORIO, H., MOLINOS, M., MANADAS, B., GONCALVES, R. & BARBOSA, M. 2017. Matrisome Profiling During Intervertebral Disc Development And Ageing. *Sci Rep,* 7**,** 11629.

CAMPAGNOLI, C., ROBERTS, I. A. G., KUMAR, S., BENNETT, P. R., BELLANTUONO, I. & FISK, N. M. 2001. Identification of mesenchymal stem/progenitor cells in human first-trimester fetal blood, liver, and bone marrow. *Blood,* 98**,** 2396-2402.

CAO, B., LI, Z., PENG, R. & DING, J. 2015. Effects of cell-cell contact and oxygen tension on chondrogenic differentiation of stem cells. *Biomaterials,* 64**,** 21-32.

CAPLAN, A. I. 1991. Mesenchymal stem cells. *J Orthop Res,* 9**,** 641-50.

CAPLAN, A. I. 2009. Why are MSCs therapeutic? New data: new insight. *J Pathol,* 217**,** 318-24.

CARVALHO, J. L., BRAGA, V. B., MELO, M. B., CAMPOS, A. C., OLIVEIRA, M. S., GOMES, D. A., FERREIRA, A. J., SANTOS, R. A. & GOES, A. M. 2013. Priming mesenchymal stem cells boosts stem cell therapy to treat myocardial infarction. *J Cell Mol Med,* 17**,** 617-25.

CASTANO-IZQUIERDO, H., ALVAREZ-BARRETO, J., VAN DEN DOLDER, J., JANSEN, J. A., MIKOS, A. G. & SIKAVITSAS, V. I. 2007. Pre-culture period of mesenchymal stem cells in osteogenic media influences their in vivo bone forming potential. *J Biomed Mater Res A,* 82**,** 129-38.

CASTRO, N., GILLESPIE, S. R. & BERNSTEIN, A. M. 2019. Ex Vivo Corneal Organ Culture Model for Wound Healing Studies. *J Vis Exp*.

CAUDARELLA, R., VESCINI, F., BUFFA, A., RIZZOLI, E., CECCOLI, L. & FRANCUCCI, C. M. 2011. Role of calcium-sensing receptor in bone biology. *J Endocrinol Invest,* 34**,** 13-7.

CAVALLO, C., DESANDO, G., FACCHINI, A. & GRIGOLO, B. 2010. Chondrocytes from patients with osteoarthritis express typical extracellular matrix molecules once grown onto a three-dimensional hyaluronan-based scaffold. *Journal of Biomedical Materials Research - Part A,* 93**,** 86-95.

CHAN, M. E., LU, X. L., HUO, B., BAIK, A. D., CHIANG, V., GULDBERG, R. E., LU, H. H. & GUO, X. E. 2009. A Trabecular Bone Explant Model of Osteocyte-Osteoblast Co-Culture for Bone Mechanobiology. *Cell Mol Bioeng,* 2**,** 405-415.

CHEN, F., ZHANG, Z., DENG, Z., ZHANG, R., FAN, G., MA, D. & MCCLEMENTS, D. J. 2018. Controlled-release of antacids from biopolymer microgels under simulated gastric conditions: Impact of bead dimensions, pore size, and alginate/pectin ratio. *Food Res Int,* 106**,** 745-751.

CHEN, S., ZHAO, D., LI, F., ZHUO, R.-X. & CHENG, S.-X. 2012. Co-delivery of genes and drugs with nanostructured calcium carbonate for cancer therapy. *RSC Advances,* 2**,** 1820-1826.

CHEN, S., ZHAO, L., DENG, X., SHI, D., WU, F., LIANG, H., HUANG, D. & SHAO, Z. 2017. Mesenchymal Stem Cells Protect Nucleus Pulposus Cells from Compression-Induced Apoptosis by Inhibiting the Mitochondrial Pathway. *Stem Cells Int,* 2017**,** 9843120.

CHEN, Y., TENG, F. Y. & TANG, B. L. 2006. Coaxing bone marrow stromal mesenchymal stem cells towards neuronal differentiation: progress and uncertainties. *Cell Mol Life Sci,* 63**,** 1649-57.

CHEN, Z., WANG, L. & STEGEMANN, J. P. 2011. Phase-separated chitosan-fibrin microbeads for cell delivery. *J Microencapsul,* 28**,** 344-52.

CHENG, S., WANG, W., LIN, Z., ZHOU, P., ZHANG, X., ZHANG, W., CHEN, Q., KOU, D., YING, X., SHEN, Y., CHENG, X., YU, Z., PENG, L. & LU, C. 2013. Effects of extracellular calcium on viability and osteogenic differentiation of bone marrow stromal cells in vitro. *Hum Cell,* 26**,** 114-20.

CHEUNG, K. M. 2010. The relationship between disc degeneration, low back pain, and human pain genetics. *Spine J,* 10**,** 958-60.

CHIU, C. L., HECHT, V., DUONG, H., WU, B. & TAWIL, B. 2012. Permeability of three-dimensional fibrin constructs corresponds to fibrinogen and thrombin concentrations. *Biores Open Access,* 1**,** 34-40.

CHOI, H., CHAIYAMONGKOL, W., DOOLITTLE, A. C., JOHNSON, Z. I., GOGATE, S. S., SCHOEPFLIN, Z. R., SHAPIRO, I. M. & RISBUD, M. V. 2018. COX-2 expression mediated by calcium-TonEBP signaling axis under hyperosmotic conditions serves osmoprotective function in nucleus pulposus cells. *J Biol Chem,* 293**,** 8969-8981.

CHOW, G., KNUDSON, C. B., HOMANDBERG, G. & KNUDSON, W. 1995. Increased expression of CD44 in bovine articular chondrocytes by catabolic cellular mediators. *J Biol Chem,* 270**,** 27734-41.

CIAPETTI, G., GRANCHI, D., DEVESCOVI, V., LEONARDI, E., GREGGI, T., DI SILVESTRE, M. & BALDINI, N. 2012. Ex vivo observation of human intervertebral disc tissue and cells isolated from degenerated intervertebral discs. *Eur Spine J,* 21 Suppl 1**,** S10-9.

CISEWSKI, S. E., WU, Y., DAMON, B. J., SACHS, B. L., KERN, M. J. & YAO, H. 2018. Comparison of Oxygen Consumption Rates of Nondegenerate and Degenerate Human Intervertebral Disc Cells. *Spine (Phila Pa 1976),* 43**,** E60-E67.

CLARKE, L. E., MCCONNELL, J. C., SHERRATT, M. J., DERBY, B., RICHARDSON, S. M. & HOYLAND, J. A. 2014. Growth differentiation factor 6 and transforming growth factor-beta differentially mediate mesenchymal stem cell differentiation, composition, and micromechanical properties of nucleus pulposus constructs. *Arthritis Res Ther,* 16**,** R67.

CLAUS, A., HIDES, J., MOSELEY, G. L. & HODGES, P. 2008. Sitting versus standing: does the intradiscal pressure cause disc degeneration or low back pain? *J Electromyogr Kinesiol,* 18**,** 550-8.

COLLET, J. P., MOEN, J. L., VEKLICH, Y. I., GORKUN, O. V., LORD, S. T., MONTALESCOT, G. & WEISEL, J. W. 2005. The alphaC domains of fibrinogen affect the structure of the fibrin clot, its physical properties, and its susceptibility to fibrinolysis. *Blood,* 106**,** 3824-30.

COLLINS, M. N. & BIRKINSHAW, C. 2013. Hyaluronic acid based scaffolds for tissue engineering - A review. *Carbohydrate Polymers.*

COLOMBINI, A., LOPA, S., CERIANI, C., LOVATI, A. B., CROISET, S. J., DI GIANCAMILLO, A., LOMBARDI, G., BANFI, G. & MORETTI, M. 2015. In vitro characterization and in vivo behavior of human nucleus pulposus and annulus fibrosus cells in clinical-grade fibrin and collagen-enriched fibrin gels. *Tissue Eng Part A,* 21**,** 793-802.

COMELLA, K., SILBERT, R. & PARLO, M. 2017. Erratum to: Effects of the intradiscal implantation of stromal vascular fraction plus platelet rich plasma in patients with degenerative disc disease. *J Transl Med,* 15**,** 108.

COX, S., COLE, M. & TAWIL, B. 2004. Behavior of human dermal fibroblasts in three-dimensional fibrin clots: dependence on fibrinogen and thrombin concentration. *Tissue Eng,* 10**,** 942-54.

CUESTA, A., DEL VALLE, M. E., GARCIA-SUAREZ, O., VINA, E., CABO, R., VAZQUEZ, G., COBO, J. L., MURCIA, A., ALVAREZ-VEGA, M., GARCIA-COSAMALON, J. & VEGA, J. A. 2014. Acid-sensing ion channels in healthy and degenerated human intervertebral disc. *Connect Tissue Res,* 55**,** 197-204.

CUI, Y., YU, J., URBAN, J. P. & YOUNG, D. A. 2010. Differential gene expression profiling of metalloproteinases and their inhibitors: a comparison between bovine intervertebral disc nucleus pulposus cells and articular chondrocytes. *Spine (Phila Pa 1976),* 35**,** 1101-8.

CUMMINGS, C. L., GAWLITTA, D., NEREM, R. M. & STEGEMANN, J. P. 2004. Properties of engineered vascular constructs made from collagen, fibrin, and collagen-fibrin mixtures. *Biomaterials,* 25**,** 3699-706.

DARE, E. V., GRIFFITH, M., POITRAS, P., WANG, T., DERVIN, G. F., GIULIVI, A. & HINCKE, M. T. 2009. Fibrin sealants from fresh or fresh/frozen plasma as scaffolds for in vitro articular cartilage regeneration. *Tissue engineering. Part A,* 15**,** 2285-2297.

DASCALU, A., ORON, Y., NEVO, Z. & KORENSTEIN, R. 1995. Hyperosmotic modulation of the cytosolic calcium concentration in a rat osteoblast-like cell line. *J Physiol,* 486 (Pt 1)**,** 97-104.

DASHTDAR, H., ROTHAN, H. A., TAY, T., AHMAD, R. E., ALI, R., TAY, L. X., CHONG, P. P. & KAMARUL, T. 2011. A preliminary study comparing the use of allogenic chondrogenic pre-differentiated and undifferentiated mesenchymal stem cells for the repair of full thickness articular cartilage defects in rabbits. *J Orthop Res,* 29**,** 1336-42.

DASHTY, M. 2013. A quick look at biochemistry: carbohydrate metabolism. *Clin Biochem,* 46**,** 1339-52.

DE WINDT, T. S., SARIS, D. B., SLAPER-CORTENBACH, I. C., VAN RIJEN, M. H., GAWLITTA, D., CREEMERS, L. B., DE WEGER, R. A., DHERT, W. J. & VONK, L. A. 2015. Direct Cell-Cell Contact with Chondrocytes Is a Key Mechanism in Multipotent Mesenchymal Stromal Cell-Mediated Chondrogenesis. *Tissue Eng Part A,* 21**,** 2536-47.

DEMERS, C. N., ANTONIOU, J. & MWALE, F. 2004. Value and limitations of using the bovine tail as a model for the human lumbar spine. *Spine (Phila Pa 1976),* 29**,** 2793-9.

DESAI, K. G. H. & JIN PARK, H. 2005. Recent Developments in Microencapsulation of Food Ingredients. *Drying Technology,* 23**,** 1361-1394.

DEZAWA, M., ISHIKAWA, H., ITOKAZU, Y., YOSHIHARA, T., HOSHINO, M., TAKEDA, S.-I., IDE, C. & NABESHIMA, Y.-I. 2005. Bone marrow stromal cells generate muscle cells and repair muscle degeneration. *Science (New York, N.Y.),* 309**,** 314-317.

DIAMANT, B., KARLSSON, J. & NACHEMSON, A. 1968. Correlation between lactate levels and pH in discs of patients with lumbar rhizopathies. *Experientia,* 24**,** 1195-6.

DICKHUT, A., PELTTARI, K., JANICKI, P., WAGNER, W., ECKSTEIN, V., EGERMANN, M. & RICHTER, W. 2009. Calcification or dedifferentiation: Requirement to lock mesenchymal stem cells in a desired differentiation stage. *Journal of Cellular Physiology,* 219**,** 219-226.

DIELEMAN, J. L., BARAL, R., BIRGER, M., BUI, A. L., BULCHIS, A., CHAPIN, A., HAMAVID, H., HORST, C., JOHNSON, E. K., JOSEPH, J., LAVADO, R., LOMSADZE, L., REYNOLDS, A., SQUIRES, E., CAMPBELL, M., DECENSO, B., DICKER, D., FLAXMAN, A. D., GABERT, R.,

HIGHFILL, T., NAGHAVI, M., NIGHTINGALE, N., TEMPLIN, T., TOBIAS, M. I., VOS, T. & MURRAY, C. J. 2016. US Spending on Personal Health Care and Public Health, 1996-2013. *JAMA,* 316**,** 2627-2646.

DING, S. & SCHULTZ, P. G. 2005. Small molecules and future regenerative medicine. *Curr Top Med Chem,* 5**,** 383-95.

DINGWALL, M., MARCHILDON, F., GUNANAYAGAM, A., LOUIS, C. S. & WIPER-BERGERON, N. 2011. Retinoic acid-induced Smad3 expression is required for the induction of osteoblastogenesis of mesenchymal stem cells. *Differentiation,* 82**,** 57-65.

DONG, Z., FENG, L., ZHU, W., SUN, X., GAO, M., ZHAO, H., CHAO, Y. & LIU, Z. 2016. CaCO3 nanoparticles as an ultra-sensitive tumor-pH-responsive nanoplatform enabling real-time drug release monitoring and cancer combination therapy. *Biomaterials,* 110**,** 60-70.

DONG, Z. H., WANG, D. C., LIU, T. T., LI, F. H., LIU, R. L., WEI, J. W. & ZHOU, C. L. 2014. The roles of MAPKs in rabbit nucleus pulposus cell apoptosis induced by high osmolality. *Eur Rev Med Pharmacol Sci,* 18**,** 2835-45.

DU, L., ZHOU, T.-J., MA, Z.-J., TIAN, H.-J., QIN, A., ZHANG, K., ZHAO, C.-Q. & ZHAO, J. J. I. J. C. E. P. 2017. Integrin β1 overexpression protects nucleus pulposus cells from apoptosis and attenuates intervertebral disc degeneration. 10**,** 5285-5295.

DU, X., PAN, Z., LI, Q., LIU, H. & LI, Q. 2018. SMAD4 feedback regulates the canonical TGF-beta signaling pathway to control granulosa cell apoptosis. *Cell Death Dis,* 9**,** 151.

DUONG, H., WU, B. & TAWIL, B. 2009. Modulation of 3D fibrin matrix stiffness by intrinsic fibrinogen-thrombin compositions and by extrinsic cellular activity. *Tissue Eng Part A,* 15**,** 1865-76.

EAGLES, P. A. M., QURESHI, A. N. & JAYASINGHE, S. N. 2006. Electrohydrodynamic jetting of mouse neuronal cells. *The Biochemical journal,* 394**,** 375-378.

ENAYATI, M., AHMAD, Z., STRIDE, E. & EDIRISINGHE, M. 2010. Size mapping of electric field-assisted production of polycaprolactone particles. *J R Soc Interface,* 7 Suppl 4**,** S393-402.

ENAYATI, M., CHANG, M.-W., BRAGMAN, F., EDIRISINGHE, M. & STRIDE, E. 2011a. Electrohydrodynamic preparation of particles, capsules and bubbles for biomedical engineering applications. *Colloids and Surfaces A: Physicochemical and Engineering Aspects,* 382**,** 154-164.

ENAYATI, M., FAROOK, U., EDIRISINGHE, M. & STRIDE, E. 2011b. Electrohydrodynamic preparation of polymeric drug-carrier particles: mapping of the process. *Int J Pharm. 2011 Feb 14;404(1-2):110-5. doi: 10.1016/j.ijpharm.2010.11.014. Epub 2010 Nov 17.*

ENGEL, M. E., MCDONNELL, M. A., LAW, B. K. & MOSES, H. L. 1999. Interdependent SMAD and JNK signaling in transforming growth factor-beta-mediated transcription. *J Biol Chem,* 274**,** 37413-20.

ERICKSON, G. R., NORTHRUP, D. L. & GUILAK, F. 2003. Hypo-osmotic stress induces calcium-dependent actin reorganization in articular chondrocytes. *Osteoarthritis Cartilage,* 11**,** 187-97.

ERRA DIAZ, F., DANTAS, E. & GEFFNER, J. 2018. Unravelling the Interplay between Extracellular Acidosis and Immune Cells. *Mediators Inflamm,* 2018**,** 1218297.

ERWIN, W. M., DESOUZA, L., FUNABASHI, M., KAWCHUK, G., KARIM, M. Z., KIM, S., MDLER, S., MATTA, A., WANG, X. & MEHRKENS, K. A. 2015. The biological basis of degenerative disc

disease: proteomic and biomechanical analysis of the canine intervertebral disc. *Arthritis Res Ther,* 17**,** 240.

EYRE, D. R. 1979. Biochemistry of the intervertebral disc. *Int Rev Connect Tissue Res,* 8**,** 227-91.

EYRE, D. R. & MUIR, H. 1976. Types I and II collagens in intervertebral disc. Interchanging radial distributions in annulus fibrosus. *Biochem J,* 157**,** 267-70.

EYRICH, D., BRANDL, F., APPEL, B., WIESE, H., MAIER, G., WENZEL, M., STAUDENMAIER, R., GOEPFERICH, A. & BLUNK, T. 2007. Long-term stable fibrin gels for cartilage engineering. *Biomaterials,* 28**,** 55-65.

EYRICH, D., GOPFERICH, A. & BLUNK, T. 2006a. Fibrin in tissue engineering. *Adv Exp Med Biol,* 585**,** 379-92.

EYRICH, D., GÖPFERICH, A. & BLUNK, T. 2006b. Fibrin in tissue engineering. *Tissue Engineering.* Springer.

FARRELL, E., BOTH, S. K., ODÖRFER, K. I., KOEVOET, W., KOPS, N., O'BRIEN, F. J., DE JONG, R. J. B., VERHAAR, J. A., CUIJPERS, V., JANSEN, J., ERBEN, R. G. & VAN OSCH, G. J. V. M. 2011. In-vivo generation of bone via endochondral ossification by in-vitro chondrogenic priming of adult human and rat mesenchymal stem cells. *BMC musculoskeletal disorders,* 12**,** 31.

FATTAHI, T., MOHAN, M. & CALDWELL, G. T. 2004a. Clinical applications of fibrin sealants. *J Oral Maxillofac Surg,* 62**,** 218-24.

FATTAHI, T., MOHAN, M. & CALDWELL, G. T. 2004b. Clinical applications of fibrin sealants. *Journal of oral and maxillofacial surgery,* 62**,** 218-224.

FAVA, R. A. & MCCLURE, D. B. 1987. Fibronectin-associated transforming growth factor. *Journal of cellular physiology,* 131**,** 184-189.

FEARING, B. V., HERNANDEZ, P. A., SETTON, L. A. & CHAHINE, N. O. 2018. Mechanotransduction and cell biomechanics of the intervertebral disc. *JOR Spine,* 1.

FENG, G., ZHAO, X., LIU, H., ZHANG, H., CHEN, X., SHI, R., LIU, X., ZHAO, X., ZHANG, W. & WANG, B. 2011. Transplantation of mesenchymal stem cells and nucleus pulposus cells in a degenerative disc model in rabbits: a comparison of 2 cell types as potential candidates for disc regeneration. *J Neurosurg Spine,* 14**,** 322-9.

FENG, H., DANFELTER, M., STROMQVIST, B. & HEINEGARD, D. 2006. Extracellular matrix in disc degeneration. *J Bone Joint Surg Am,* 88 Suppl 2**,** 25-9.

FLANNERY, C. R., LITTLE, C. B., CATERSON, B. & HUGHES, C. E. 1999. Effects of culture conditions and exposure to catabolic stimulators (IL-1 and retinoic acid) on the expression of matrix metalloproteinases (MMPs) and disintegrin metalloproteinases (ADAMs) by articular cartilage chondrocytes. *Matrix Biol,* 18**,** 225-37.

FOREMAN, D. M., PANCHOLI, S., JARVIS-EVANS, J., MCLEOD, D. & BOULTON, M. E. 1996. A simple organ culture model for assessing the effects of growth factors on corneal re-epithelialization. *Exp Eye Res,* 62**,** 555-64.

FRANCO, C. L., PRICE, J. & WEST, J. L. 2011. Development and optimization of a dual-photoinitiator, emulsion-based technique for rapid generation of cell-laden hydrogel microspheres. *Acta Biomater,* 7**,** 3267-76.

FRAUCHIGER, D. A., HEEB, S. R., MAY, R. D., WOLTJE, M., BENNEKER, L. M. & GANTENBEIN, B. 2018. Differentiation of MSC and annulus fibrosus cells on genetically engineered silk

fleece-membrane-composites enriched for GDF-6 or TGF-beta3. *J Orthop Res,* 36**,** 1324-1333.

FREYRIA, A.-M. & MALLEIN-GERIN, F. 2012. Chondrocytes or adult stem cells for cartilage repair: The indisputable role of growth factors. *Injury.*

FRIESS, W. 1998. Collagen - Biomaterial for drug delivery. *European Journal of Pharmaceutics and Biopharmaceutics,* 45**,** 113-136.

GALOIS, L., HUTASSE, S., CORTIAL, D., ROUSSEAU, C. F., GROSSIN, L., RONZIERE, M. C., HERBAGE, D. & FREYRIA, A. M. 2006. Bovine chondrocyte behaviour in three-dimensional type I collagen gel in terms of gel contraction, proliferation and gene expression. *Biomaterials,* 27**,** 79-90.

GANEY, T., LIBERA, J., MOOS, V., ALASEVIC, O., FRITSCH, K. G., MEISEL, H. J. & HUTTON, W. C. 2003. Disc chondrocyte transplantation in a canine model: a treatment for degenerated or damaged intervertebral disc. *Spine (Phila Pa 1976),* 28**,** 2609-20.

GANSAU, J., KELLY, L. & BUCKLEY, C. T. 2018. Influence of key processing parameters and seeding density effects of microencapsulated chondrocytes fabricated using electrohydrodynamic spraying. *Biofabrication,* 10**,** 035011.

GARCIA, M. & KNIGHT, M. M. 2010. Cyclic loading opens hemichannels to release ATP as part of a chondrocyte mechanotransduction pathway. *Journal of Orthopaedic Research,* 28**,** 510-515.

GASPERINI, L., MANIGLIO, D. & MIGLIARESI, C. 2013a. Microencapsulation of cells in alginate through an electrohydrodynamic process. *Journal of Bioactive and Compatible Polymers,* 28**,** 413-425.

GASPERINI, L., MANIGLIO, D. & MIGLIARESI, C. 2013b. Microencapsulation of cells in alginate through an electrohydrodynamic process. *Journal of Bioactive and Compatible Polymers*.

GAUTSCHI, I., VAN BEMMELEN, M. X. & SCHILD, L. 2017. Proton and non-proton activation of ASIC channels. *PLoS One,* 12**,** e0175293.

GENNARO, A. R. & REMINGTON, J. P. 2000. Remington : the science and practice of pharmacy. 1219-1220.

GILBERT, H. T., HODSON, N., BAIRD, P., RICHARDSON, S. M. & HOYLAND, J. A. 2016a. Acidic pH promotes intervertebral disc degeneration: Acid-sensing ion channel -3 as a potential therapeutic target. *Sci Rep,* 6**,** 37360.

GILBERT, H. T., HOYLAND, J. A. & RICHARDSON, S. M. 2013. Stem cell regeneration of degenerated intervertebral discs: current status (update). *Curr Pain Headache Rep,* 17**,** 377.

GILBERT, H. T. J., HODSON, N., BAIRD, P., RICHARDSON, S. M. & HOYLAND, J. A. 2016b. Acidic pH promotes intervertebral disc degeneration: Acid-sensing ion channel -3 as a potential therapeutic target. *Sci Rep,* 6**,** 37360.

GILLE, J., MEISNER, U., EHLERS, E. M., MULLER, A., RUSSLIES, M. & BEHRENS, P. 2005. Migration pattern, morphology and viability of cells suspended in or sealed with fibrin glue: a histomorphologic study. *Tissue Cell,* 37**,** 339-48.

GOGATE, S. S., NASSER, R., SHAPIRO, I. M. & RISBUD, M. V. 2011. Hypoxic regulation of beta-1,3-glucuronyltransferase 1 expression in nucleus pulposus cells of the rat intervertebral disc: role of hypoxia-inducible factor proteins. *Arthritis Rheum,* 63**,** 1950-60.

GOLDSCHLAGER, T., GHOSH, P., ZANNETTINO, A., GRONTHOS, S., ROSENFELD, J. V., ITESCU, S. & JENKIN, G. 2010. Cervical motion preservation using mesenchymal progenitor cells and pentosan polysulfate, a novel chondrogenic agent: preliminary study in an ovine model. *Neurosurg Focus,* 28**,** E4.

GORENSEK, M., JAKSIMOVIC, C., KREGAR-VELIKONJA, N., GORENSEK, M., KNEZEVIC, M., JERAS, M., PAVLOVCIC, V. & COR, A. 2004. Nucleus pulposus repair with cultured autologous elastic cartilage derived chondrocytes. *Cell Mol Biol Lett,* 9**,** 363-73.

GORODETSKY, R., LEVDANSKY, L., GABERMAN, E., GUREVITCH, O., LUBZENS, E. & MCBRIDE, W. H. 2011. Fibrin microbeads loaded with mesenchymal cells support their long-term survival while sealed at room temperature. *Tissue Eng Part C Methods,* 17**,** 745-55.

GRANT, M. P., EPURE, L. M., BOKHARI, R., ROUGHLEY, P., ANTONIOU, J. & MWALE, F. 2016. Human cartilaginous endplate degeneration is induced by calcium and the extracellular calcium-sensing receptor in the intervertebral disc. *Eur Cell Mater,* 32**,** 137-51.

GRAYSON, W. L., BHUMIRATANA, S., GRACE CHAO, P. H., HUNG, C. T. & VUNJAK-NOVAKOVIC, G. 2010. Spatial regulation of human mesenchymal stem cell differentiation in engineered osteochondral constructs: effects of pre-differentiation, soluble factors and medium perfusion. *Osteoarthritis Cartilage,* 18**,** 714-23.

GREILING, D. & CLARK, R. A. 1997. Fibronectin provides a conduit for fibroblast transmigration from collagenous stroma into fibrin clot provisional matrix. *Journal of cell science,* 110 (Pt 7**,** 861-870.

GRIMSHAW, M. J. & MASON, R. M. 2000. Bovine articular chondrocyte function in vitro depends upon oxygen tension. *Osteoarthritis Cartilage,* 8**,** 386-92.

GRINSHPAN, D. D., NEVAR, T. N., SAVITSKAYA, T. A., BOIKO, A. V., KAPRALOV, N. V. & SHOLOMITSKAYA, I. A. J. P. C. J. 2008. Comparison of Acid-Neutralizing Properties of Anti-Acid Preparations of Various Compositions. 42**,** 400-404.

GROBOILLOT, A., BOADI, D., PONCELET, D. & NEUFELD, R. J. C. R. I. B. 1994. Immobilization of cells for application in the food industry. 14**,** 75-107.

GROGAN, S. P., CHUNG, P. H., SOMAN, P., CHEN, P., LOTZ, M. K., CHEN, S. & D'LIMA, D. D. 2013. Digital micromirror device projection printing system for meniscus tissue engineering. *Acta Biomater,* 9**,** 7218-26.

GRUBER, H. E. & HANLEY, E. N. 1998. Analysis of aging and degeneration of the human intervertebral disc. Comparison of surgical specimens with normal controls. *Spine,* 23**,** 751-757.

GRUBER, H. E. & HANLEY, E. N., JR. 2000. Human disc cells in monolayer vs 3D culture: cell shape, division and matrix formation. *BMC Musculoskelet Disord,* 1**,** 1.

GRUBER, H. E., INGRAM, J. A., NORTON, H. J. & HANLEY JR, E. N. 2007. Senescence in cells of the aging and degenerating intervertebral disc: immunolocalization of senescence-associated β-galactosidase in human and sand rat discs. *Spine,* 32**,** 321-327.

GRUBER, H. E., JOHNSON, T. L., LESLIE, K., INGRAM, J. A., MARTIN, D., HOELSCHER, G., BANKS, D., PHIEFFER, L., COLDHAM, G. & HANLEY, E. N. 2002. Autologous intervertebral disc cell implantation: a model using Psammomys obesus, the sand rat. *Spine,* 27**,** 1626-1633.

GRUNHAGEN, T., WILDE, G., SOUKANE, D. M., SHIRAZI-ADL, S. A. & URBAN, J. P. 2006. Nutrient supply and intervertebral disc metabolism. *J Bone Joint Surg Am,* 88 Suppl 2**,** 30-5.

GUEHRING, T., WILDE, G., SUMNER, M., GRUNHAGEN, T., KARNEY, G. B., TIRLAPUR, U. K. & URBAN, J. P. 2009. Notochordal intervertebral disc cells: sensitivity to nutrient deprivation. *Arthritis Rheum,* 60**,** 1026-34.

HALLORAN, D. O., GRAD, S., STODDART, M., DOCKERY, P., ALINI, M. & PANDIT, A. S. 2008. An injectable cross-linked scaffold for nucleus pulposus regeneration. *Biomaterials,* 29**,** 438-447.

HAN, B., WANG, H. C., LI, H., TAO, Y. Q., LIANG, C. Z., LI, F. C., CHEN, G. & CHEN, Q. X. 2014. Nucleus pulposus mesenchymal stem cells in acidic conditions mimicking degenerative intervertebral discs give better performance than adipose tissue-derived mesenchymal stem cells. *Cells Tissues Organs,* 199**,** 342-52.

HAUTIER, A., SALENTEY, V., AUBERT-FOUCHER, E., BOUGAULT, C., BEAUCHEF, G., RONZIÈRE, M.-C., DE SOBARNITSKY, S., PAUMIER, A., GALÉRA, P., PIPERNO, M., DAMOUR, O. & MALLEIN-GERIN, F. 2008. Bone morphogenetic protein-2 stimulates chondrogenic expression in human nasal chondrocytes expanded in vitro. *Growth factors (Chur, Switzerland),* 26**,** 201-211.

HEE, H. T., ISMAIL, H. D., LIM, C. T., GOH, J. C. & WONG, H. K. 2010. Effects of implantation of bone marrow mesenchymal stem cells, disc distraction and combined therapy on reversing degeneration of the intervertebral disc. *J Bone Joint Surg Br,* 92**,** 726-36.

HEGEWALD, A. A., ENZ, A., ENDRES, M., SITTINGER, M., WOICIECHOWSKY, C., THOME, C. & KAPS, C. 2011. Engineering of polymer-based grafts with cells derived from human nucleus pulposus tissue of the lumbar spine. *J Tissue Eng Regen Med,* 5**,** 275-82.

HENDERSON, S. E., SANTANGELO, K. S. & BERTONE, A. L. 2011. Chondrogenic effects of exogenous retinoic acid or a retinoic acid receptor antagonist (LE135) on equine chondrocytes and bone marrow-derived mesenchymal stem cells in monolayer culture. *Am J Vet Res,* 72**,** 884-92.

HERNÁNDEZ, R. M., ORIVE, G., MURUA, A. & PEDRAZ, J. L. 2010. Microcapsules and microcarriers for in situ cell delivery. *Advanced Drug Delivery Reviews.*

HERNIGOU, P., TROUSSELIER, M., ROUBINEAU, F., BOUTHORS, C., CHEVALLIER, N., ROUARD, H. & FLOUZAT-LACHANIETTE, C. H. 2016. Stem Cell Therapy for the Treatment of Hip Osteonecrosis: A 30-Year Review of Progress. *Clin Orthop Surg,* 8**,** 1-8.

HEYWOOD, H. K., BADER, D. L. & LEE, D. A. 2006. Rate of oxygen consumption by isolated articular chondrocytes is sensitive to medium glucose concentration. *J Cell Physiol,* 206**,** 402-10.

HILIBRAND, A. S. & ROBBINS, M. 2004. Adjacent segment degeneration and adjacent segment disease: the consequences of spinal fusion? *Spine J,* 4**,** 190S-194S.

HIRAISHI, S., SCHOL, J., SAKAI, D., NUKAGA, T., ERICKSON, I., SILVERMAN, L., FOLEY, K. & WATANABE, M. 2018. Discogenic cell transplantation directly from a cryopreserved state in an induced intervertebral disc degeneration canine model. *JOR Spine,* 1**,** e1013.

HO, W., TAWIL, B., DUNN, J. C. & WU, B. M. 2006. The behavior of human mesenchymal stem cells in 3D fibrin clots: dependence on fibrinogen concentration and clot structure. *Tissue Eng,* 12**,** 1587-95.

HODSON, N. W., PATEL, S., RICHARDSON, S. M., HOYLAND, J. A. & GILBERT, H. T. J. 2018. Degenerate intervertebral disc-like pH induces a catabolic mechanoresponse in human nucleus pulposus cells. *JOR SPINE,* 1**,** e1004.

HOHAUS, C., GANEY, T. M., MINKUS, Y. & MEISEL, H. J. 2008. Cell transplantation in lumbar spine disc degeneration disease. *Eur Spine J,* 17 Suppl 4**,** 492-503.

HOLM, S., MAROUDAS, A., URBAN, J. P., SELSTAM, G. & NACHEMSON, A. 1981. Nutrition of the intervertebral disc: solute transport and metabolism. *Connect Tissue Res,* 8**,** 101-19.

HOLZWARTH, C., VAEGLER, M., GIESEKE, F., PFISTER, S. M., HANDGRETINGER, R., KERST, G. & MULLER, I. 2010. Low physiologic oxygen tensions reduce proliferation and differentiation of human multipotent mesenchymal stromal cells. *BMC Cell Biol,* 11**,** 11.

HOM, W. W., TSCHOPP, M., LIN, H. A., NASSER, P., LAUDIER, D. M., HECHT, A. C., NICOLL, S. B. & IATRIDIS, J. C. 2019. Composite biomaterial repair strategy to restore biomechanical function and reduce herniation risk in an ex vivo large animal model of intervertebral disc herniation with varying injury severity. *PLoS One,* 14**,** e0217357.

HOMMINGA, G. N., BUMA, P., KOOT, H. W., VAN DER KRAAN, P. M. & VAN DEN BERG, W. B. 1993. Chondrocyte behavior in fibrin glue in vitro. *Acta Orthop Scand,* 64**,** 441-5.

HORBELT, D., DENKIS, A. & KNAUS, P. 2012. A portrait of Transforming Growth Factor beta superfamily signalling: Background matters. *Int J Biochem Cell Biol,* 44**,** 469-74.

HORNER, H. A. & URBAN, J. P. 2001. 2001 Volvo Award Winner in Basic Science Studies: Effect of nutrient supply on the viability of cells from the nucleus pulposus of the intervertebral disc. *Spine (Phila Pa 1976),* 26**,** 2543-9.

HUANG, A. H., FARRELL, M. J., KIM, M. & MAUCK, R. L. 2010. Long-term dynamic loading improves the mechanical properties of chondrogenic mesenchymal stem cell-laden hydrogel. *Eur Cell Mater,* 19**,** 72-85.

HUANG, C. Y., YUAN, T. Y., JACKSON, A. R., HAZBUN, L., FRAKER, C. & GU, W. Y. 2007. Effects of low glucose concentrations on oxygen consumption rates of intervertebral disc cells. *Spine (Phila Pa 1976),* 32**,** 2063-9.

HUANG, Y. C., LEUNG, V. Y., LU, W. W. & LUK, K. D. 2013. The effects of microenvironment in mesenchymal stem cell-based regeneration of intervertebral disc. *Spine J,* 13**,** 352-62.

HUANG, Y. C., URBAN, J. P. & LUK, K. D. 2014. Intervertebral disc regeneration: do nutrients lead the way? *Nat Rev Rheumatol,* 10**,** 561-6.

HUANG, Y. C., XIAO, J., LU, W. W., LEUNG, V. Y., HU, Y. & LUK, K. D. 2016. Lumbar intervertebral disc allograft transplantation: long-term mobility and impact on the adjacent segments. *Eur Spine J*.

HUNTER, C. J., MOUW, J. K. & LEVENSTON, M. E. 2004. Dynamic compression of chondrocyte-seeded fibrin gels: effects on matrix accumulation and mechanical stiffness. *Osteoarthritis Cartilage,* 12**,** 117-30.

IGNAT'EVA, N. Y., DANILOV, N., AVERKIEV, S., OBREZKOVA, M., LUNIN, V. & SOBOL,ÄÔ, E. 2007. Determination of hydroxyproline in tissues and the evaluation of the collagen content of the tissues. *Journal of Analytical Chemistry,* 62**,** 51-57.

ILLIEN-JUNGER, S., PATTAPPA, G., PEROGLIO, M., BENNEKER, L. M., STODDART, M. J., SAKAI, D., MOCHIDA, J., GRAD, S. & ALINI, M. 2012. Homing of mesenchymal stem cells in induced degenerative intervertebral discs in a whole organ culture system. *Spine (Phila Pa 1976),* 37**,** 1865-73.

INOUE, H. 1981. Three-dimensional architecture of lumbar intervertebral discs. *Spine (Phila Pa 1976),* 6**,** 139-46.

ISACKE, C. M. & YARWOOD, H. 2002. The hyaluronan receptor, CD44. *International Journal of Biochemistry and Cell Biology.*

ISHIHARA, H. & URBAN, J. P. 1999. Effects of low oxygen concentrations and metabolic inhibitors on proteoglycan and protein synthesis rates in the intervertebral disc. *J Orthop Res,* 17**,** 829-35.

JACKSON, A. R. 2010. *Transport and Metabolism of Glucose in Intervertebral Disc.* Doctor of Philosophy University of Miami.

JACKSON, A. R., HUANG, C. Y. & GU, W. Y. 2011. Effect of endplate calcification and mechanical deformation on the distribution of glucose in intervertebral disc: a 3D finite element study. *Comput Methods Biomech Biomed Engin,* 14**,** 195-204.

JACKSON, L. S. & LEE, K. J. L. W. T. 1991. Microencapsulation and the food industry. 24**,** 289-297.

JAKOB, M., DÉMARTEAU, O., SCHÄFER, D., HINTERMANN, B., DICK, W., HEBERER, M. & MARTIN, I. 2001. Specific growth factors during the expansion and redifferentiation of adult human articular chondrocytes enhance chondrogenesis and cartilaginous tissue formation in vitro. *Journal of Cellular Biochemistry,* 81**,** 368-377.

JOHNSON, W. E., EISENSTEIN, S. M. & ROBERTS, S. 2001. Cell cluster formation in degenerate lumbar intervertebral discs is associated with increased disc cell proliferation. *Connective tissue research,* 42**,** 197-207.

KADOW, T., SOWA, G., VO, N. & KANG, J. D. 2015. Molecular basis of intervertebral disc degeneration and herniations: what are the important translational questions? *Clin Orthop Relat Res,* 473**,** 1903-12.

KAFIENAH, W. & SIMS, T. J. 2004. Biochemical methods for the analysis of tissue-engineered cartilage. *Methods Mol Biol,* 238**,** 217-30.

KAFIENAH, W. E., JAKOB, M., DÉMARTEAU, O., FRAZER, A., BARKER, M. D., MARTIN, I. & HOLLANDER, A. P. 2002. Three-dimensional tissue engineering of hyaline cartilage: comparison of adult nasal and articular chondrocytes. *Tissue engineering,* 8**,** 817-826.

KANDEL, R., ROBERTS, S. & URBAN, J. P. 2008. Tissue engineering and the intervertebral disc: the challenges. *Eur Spine J,* 17 Suppl 4**,** 480-91.

KANG, A., PARK, J., JU, J., JEONG, G. S. & LEE, S. H. 2014. Cell encapsulation via microtechnologies. *Biomaterials,* 35**,** 2651-63.

KATO, Y., LAMBERT, C. A., COLIGE, A. C., MINEUR, P., NOEL, A., FRANKENNE, F., FOIDART, J. M., BABA, M., HATA, R., MIYAZAKI, K. & TSUKUDA, M. 2005. Acidic extracellular pH induces matrix metalloproteinase-9 expression in mouse metastatic melanoma cells through the phospholipase D-mitogen-activated protein kinase signaling. *J Biol Chem,* 280**,** 10938-44.

KATZ, M. M., HARGENS, A. R. & GARFIN, S. R. 1986. Intervertebral disc nutrition. Diffusion versus convection. *Clin Orthop Relat Res***,** 243-5.

KHALIL, N. 1999. TGF-beta: from latent to active. *Microbes Infect,* 1**,** 1255-63.

KIM, D. H., MARTIN, J. T., ELLIOTT, D. M., SMITH, L. J. & MAUCK, R. L. 2015. Phenotypic stability, matrix elaboration and functional maturation of nucleus pulposus cells encapsulated in photocrosslinkable hyaluronic acid hydrogels. *Acta Biomater,* 12**,** 21-9.

KITISIN, K., SAHA, T., BLAKE, T., GOLESTANEH, N., DENG, M., KIM, C., TANG, Y., SHETTY, K., MISHRA, B. & MISHRA, L. 2007. Tgf-Beta signaling in development. *Sci STKE,* 2007**,** cm1.

KLEINMAN, G. E., RODRIQUEZ, H., GOOD, M. C. & CAUDLE, M. R. 1991. Hypercalcemic crisis in pregnancy associated with excessive ingestion of calcium carbonate antacid (milk-alkali syndrome): successful treatment with hemodialysis. *Obstet Gynecol,* 78**,** 496-9.

KNUDSON, C. B. & KNUDSON, W. 2004. Hyaluronan and CD44: modulators of chondrocyte metabolism. *Clin Orthop Relat Res***,** S152-62.

KOBAYASHI, S., MEIR, A. & URBAN, J. 2008. Effect of cell density on the rate of glycosaminoglycan accumulation by disc and cartilage cells in vitro. *J Orthop Res,* 26**,** 493-503.

KONG, H. J., SMITH, M. K. & MOONEY, D. J. 2003. Designing alginate hydrogels to maintain viability of immobilized cells. *Biomaterials,* 24**,** 4023-4029.

KORECKI, C. L., COSTI, J. J. & IATRIDIS, J. C. 2008. Needle puncture injury affects intervertebral disc mechanics and biology in an organ culture model. *Spine (Phila Pa 1976),* 33**,** 235-41.

KOTLARCHYK, M. A., SHREIM, S. G., ALVAREZ-ELIZONDO, M. B., ESTRADA, L. C., SINGH, R., VALDEVIT, L., KNIAZEVA, E., GRATTON, E., PUTNAM, A. J. & BOTVINICK, E. L. 2011. Concentration independent modulation of local micromechanics in a fibrin gel. *PLoS One,* 6**,** e20201.

KREWSKI, D., YOKEL, R. A., NIEBOER, E., BORCHELT, D., COHEN, J., HARRY, J., KACEW, S., LINDSAY, J., MAHFOUZ, A. M. & RONDEAU, V. 2007. Human health risk assessment for aluminium, aluminium oxide, and aluminium hydroxide. *J Toxicol Environ Health B Crit Rev,* 10 Suppl 1**,** 1-269.

KUMAR, H., HA, D. H., LEE, E. J., PARK, J. H., SHIM, J. H., AHN, T. K., KIM, K. T., ROPPER, A. E., SOHN, S., KIM, C. H., THAKOR, D. K., LEE, S. H. & HAN, I. B. 2017. Safety and tolerability of intradiscal implantation of combined autologous adipose-derived mesenchymal stem cells and hyaluronic acid in patients with chronic discogenic low back pain: 1-year follow-up of a phase I study. *Stem Cell Res Ther,* 8**,** 262.

KURTIS, M. S., SCHMIDT, T. A., BUGBEE, W. D., LOESER, R. F. & SAH, R. L. 2003. Integrin-mediated adhesion of human articular chondrocytes to cartilage. *Arthritis Rheum,* 48**,** 110-8.

LAM, J., LU, S., LEE, E. J., TRACHTENBERG, J. E., MERETOJA, V. V., DAHLIN, R. L., VAN DEN BEUCKEN, J. J., TABATA, Y., WONG, M. E., JANSEN, J. A., MIKOS, A. G. & KASPER, F. K. 2014. Osteochondral defect repair using bilayered hydrogels encapsulating both chondrogenically and osteogenically pre-differentiated mesenchymal stem cells in a rabbit model. *Osteoarthritis Cartilage,* 22**,** 1291-300.

LAMBERS, H., PIESSENS, S., BLOEM, A., PRONK, H. & FINKEL, P. 2006. Natural skin surface pH is on average below 5, which is beneficial for its resident flora. *Int J Cosmet Sci,* 28**,** 359-70.

LANG, G., LIU, Y., GERIES, J., ZHOU, Z., KUBOSCH, D., SUDKAMP, N., RICHARDS, R. G., ALINI, M., GRAD, S. & LI, Z. 2018. An intervertebral disc whole organ culture system to investigate proinflammatory and degenerative disc disease condition. *J Tissue Eng Regen Med,* 12**,** e2051-e2061.

LE MAITRE, C. L., BAIRD, P., FREEMONT, A. J. & HOYLAND, J. A. 2009. An in vitro study investigating the survival and phenotype of mesenchymal stem cells following injection into nucleus pulposus tissue. *Arthritis research & therapy,* 11**,** R20.

LE MAITRE, C. L., FREEMONT, A. J. & HOYLAND, J. A. 2004a. Localization of degradative enzymes and their inhibitors in the degenerate human intervertebral disc. *J Pathol,* 204**,** 47-54.

LE MAITRE, C. L., HOYLAND, J. A. & FREEMONT, A. J. 2004b. Studies of human intervertebral disc cell function in a constrained in vitro tissue culture system. *Spine (Phila Pa 1976),* 29**,** 1187-95.

LE VISAGE, C., KIM, S. W., TATENO, K., SIEBER, A. N., KOSTUIK, J. P. & LEONG, K. W. 2006. Interaction of human mesenchymal stem cells with disc cells: changes in extracellular matrix biosynthesis. *Spine (Phila Pa 1976),* 31**,** 2036-42.

LEE, C. H., SINGLA, A. & LEE, Y. 2001. Biomedical applications of collagen. *International Journal of Pharmaceutics,* 221**,** 1-22.

LEE, C. R., SAKAI, D., NAKAI, T., TOYAMA, K., MOCHIDA, J., ALINI, M. & GRAD, S. 2007a. A phenotypic comparison of intervertebral disc and articular cartilage cells in the rat. *Eur Spine J,* 16**,** 2174-85.

LEE, D. W., CHOI, W. S., BYUN, M. W., PARK, H. J., YU, Y.-M. & LEE, C. M. 2003. Effect of gamma-irradiation on degradation of alginate. *Journal of agricultural and food chemistry,* 51**,** 4819-4823.

LEE, J., LEE, E., KIM, H. Y. & SON, Y. 2007b. Comparison of articular cartilage with costal cartilage in initial cell yield, degree of dedifferentiation during expansion and redifferentiation capacity. *Biotechnol Appl Biochem,* 48**,** 149-58.

LEE, J. C. & CHOI, S. W. 2015. Adjacent Segment Pathology after Lumbar Spinal Fusion. *Asian Spine J,* 9**,** 807-17.

LEHMANN, T. P., JAKUB, G., HARASYMCZUK, J. & JAGODZINSKI, P. P. 2018. Transforming growth factor beta mediates communication of co-cultured human nucleus pulposus cells and mesenchymal stem cells. *J Orthop Res,* 36**,** 3023-3032.

LESLEY, J., HASCALL, V. C., TAMMI, M. & HYMAN, R. 2000. Hyaluronan binding by cell surface CD44. *J Biol Chem,* 275**,** 26967-75.

LEVANT, J. A., WALSH, J. H. & ISENBERG, J. I. 1973. Stimulation of gastric secretion and gastrin release by single oral doses of calcium carbonate in man. *N Engl J Med,* 289**,** 555-8.

LI, H., WANG, J., LI, F., CHEN, G. & CHEN, Q. 2018. The Influence of Hyperosmolarity in the Intervertebral Disc on the Proliferation and Chondrogenic Differentiation of Nucleus Pulposus-Derived Mesenchymal Stem Cells. *Cells Tissues Organs,* 205**,** 178-188.

LI, Y. Y., DIAO, H. J., CHIK, T. K., CHOW, C. T., AN, X. M., LEUNG, V., CHEUNG, K. M. & CHAN, B. P. 2014a. Delivering mesenchymal stem cells in collagen microsphere carriers to rabbit degenerative disc: reduced risk of osteophyte formation. *Tissue Eng Part A,* 20**,** 1379-91.

LI, Z., KAPLAN, K. M., WERTZEL, A., PEROGLIO, M., AMIT, B., ALINI, M., GRAD, S. & YAYON, A. 2014b. Biomimetic fibrin-hyaluronan hydrogels for nucleus pulposus regeneration. *Regen Med,* 9**,** 309-26.

LIEBSCHER, T., HAEFELI, M., WUERTZ, K., NERLICH, A. G. & BOOS, N. 2011. Age-related variation in cell density of human lumbar intervertebral disc. *Spine (Phila Pa 1976),* 36**,** 153-9.

LINDENHAYN, K., PERKA, C., SPITZER, R., HEILMANN, H., POMMERENING, K., MENNICKE, J. & SITTINGER, M. 1999. Retention of hyaluronic acid in alginate beads: aspects for in vitro cartilage engineering. *J Biomed Mater Res,* 44**,** 149-55.

LIU, D., LIU, T., LI, R. & SY, M. S. 1998. Mechanisms regulating the binding activity of CD44 to hyaluronic acid. *Front Biosci,* 3**,** d631-6.

LIU, X. D., YU, W. Y., ZHANG, Y., XUE, W. M., YU, W. T., XIONG, Y., MA, X. J., CHEN, Y. & YUAN, Q. 2002. Characterization of structure and diffusion behaviour of Ca-alginate beads prepared with external or internal calcium sources. *J Microencapsul,* 19**,** 775-82.

LUOMA, K., RIIHIMAKI, H., LUUKKONEN, R., RAININKO, R., VIIKARI-JUNTURA, E. & LAMMINEN, A. 2000. Low back pain in relation to lumbar disc degeneration. *Spine (Phila Pa 1976),* 25**,** 487-92.

LYONS, G., EISENSTEIN, S. M. & SWEET, M. B. 1981. Biochemical changes in intervertebral disc degeneration. *Biochimica et biophysica acta,* 673**,** 443-453.

LYONS, R. M., KESKI-OJA, J. & MOSES, H. L. 1988. Proteolytic activation of latent transforming growth factor-beta from fibroblast-conditioned medium. *J Cell Biol,* 106**,** 1659-65.

MACGILLIVRAY, T. E. 2003a. Fibrin sealants and glues. *J Card Surg,* 18**,** 480-5.

MACGILLIVRAY, T. E. 2003b. Fibrin sealants and glues. *Journal of cardiac surgery,* 18**,** 480-485.

MAEDA, M., TANI, S., SANO, A. & FUJIOKA, K. 1999. Microstructure and release characteristics of the minipellet, a collagen-based drug delivery system for controlled release of protein drugs. *Journal of Controlled Release,* 62**,** 313-324.

MAHAPATRA, C., JIN, G. Z. & KIM, H. W. 2016. Alginate-hyaluronic acid-collagen composite hydrogel favorable for the culture of chondrocytes and their phenotype maintenance. *Tissue Eng Regen Med,* 13**,** 538-546.

MAJUMDAR, M. K., THIEDE, M. A., MOSCA, J. D., MOORMAN, M. & GERSON, S. L. 1998. Phenotypic and functional comparison of cultures of marrow-derived mesenchymal stem cells (MSCs) and stromal cells. *Journal of cellular physiology,* 176**,** 57-66.

MAKOGONENKO, E., TSURUPA, G., INGHAM, K. & MEDVED, L. 2002. Interaction of fibrin(ogen) with fibronectin: Further characterization and localization of the fibronectin-binding site. *Biochemistry,* 41**,** 7907-7913.

MALDA, J., MARTENS, D. E., TRAMPER, J., VAN BLITTERSWIJK, C. A. & RIESLE, J. 2003. Cartilage tissue engineering: controversy in the effect of oxygen. *Crit Rev Biotechnol,* 23**,** 175-94.

MALDA, J., VAN BLITTERSWIJK, C. A., VAN GEFFEN, M., MARTENS, D. E., TRAMPER, J. & RIESLE, J. 2004. Low oxygen tension stimulates the redifferentiation of dedifferentiated adult human nasal chondrocytes. *Osteoarthritis Cartilage,* 12**,** 306-13.

MALONZO, C., CHAN, S. C., KABIRI, A., EGLIN, D., GRAD, S., BONEL, H. M., BENNEKER, L. M. & GANTENBEIN-RITTER, B. 2015. A papain-induced disc degeneration model for the assessment of thermo-reversible hydrogel-cells therapeutic approach. *J Tissue Eng Regen Med,* 9**,** E167-76.

MANIADAKIS, N. & GRAY, A. 2000. The economic burden of back pain in the UK. *Pain,* 84**,** 95-103.

MANNELLO, F., LUCHETTI, F., FALCIERI, E. & PAPA, S. 2005. Multiple roles of matrix metalloproteinases during apoptosis. *Apoptosis,* 10**,** 19-24.

MAREDZIAK, M., MARYCZ, K., TOMASZEWSKI, K. A., KORNICKA, K. & HENRY, B. M. 2016. The Influence of Aging on the Regenerative Potential of Human Adipose Derived Mesenchymal Stem Cells. *Stem Cells Int,* 2016**,** 2152435.

MARIADI, BANGUN, H. & KARSONO 2015. *Formulation and in vitro evaluation of gastroretentive drug delivery system of antacids using alginate-chitosan films*.

MARIEB, E. N. & HOEHN, K. 2008. *Human Anatomy and Physiology with Interactive Physiology 10-System Suite*, CUMMINGS.

MAROUDAS, A., STOCKWELL, R. A., NACHEMSON, A. & URBAN, J. 1975. Factors involved in the nutrition of the human lumbar intervertebral disc: cellularity and diffusion of glucose in vitro. *J Anat,* 120**,** 113-30.

MATSUNAGA, S., NAGANO, S., ONISHI, T., MORIMOTO, N., SUZUKI, S. & KOMIYA, S. 2003. Age-related changes in expression of transforming growth factor-beta and receptors in cells of intervertebral discs. *J Neurosurg,* 98**,** 63-7.

MAVROGONATOU, E. & KLETSAS, D. 2012. Differential response of nucleus pulposus intervertebral disc cells to high salt, sorbitol, and urea. *J Cell Physiol,* 227**,** 1179-87.

MAZZITELLI, S., TOSI, A., BALESTRA, C., NASTRUZZI, C., LUCA, G., MANCUSO, F., CALAFIORE, R. & CALVITTI, M. 2008. Production and characterization of alginate microcapsules produced by a vibrational encapsulation device. *J Biomater Appl,* 23**,** 123-45.

MEISEL, H. J., GANEY, T., HUTTON, W. C., LIBERA, J., MINKUS, Y. & ALASEVIC, O. 2006. Clinical experience in cell-based therapeutics: intervention and outcome. *Eur Spine J,* 15 Suppl 3**,** S397-405.

MEISEL, H. J., SIODLA, V., GANEY, T., MINKUS, Y., HUTTON, W. C. & ALASEVIC, O. J. 2007. Clinical experience in cell-based therapeutics: disc chondrocyte transplantation A treatment for degenerated or damaged intervertebral disc. *Biomol Eng,* 24**,** 5-21.

MICHALEK, A. J., FUNABASHI, K. L. & IATRIDIS, J. C. 2010. Needle puncture injury of the rat intervertebral disc affects torsional and compressive biomechanics differently. *Eur Spine J,* 19**,** 2110-6.

MINOGUE, B. M., RICHARDSON, S. M., ZEEF, L. A., FREEMONT, A. J. & HOYLAND, J. A. 2010a. Characterization of the human nucleus pulposus cell phenotype and evaluation of novel marker gene expression to define adult stem cell differentiation. *Arthritis Rheum,* 62**,** 3695-705.

MINOGUE, B. M., RICHARDSON, S. M., ZEEF, L. A., FREEMONT, A. J. & HOYLAND, J. A. 2010b. Transcriptional profiling of bovine intervertebral disc cells: implications for identification of normal and degenerate human intervertebral disc cell phenotypes. *Arthritis Res Ther,* 12**,** R22.

MITTERMAYR, R., WASSERMANN, E., THURNHER, M., SIMUNEK, M. & REDL, H. 2006. Skin graft fixation by slow clotting fibrin sealant applied as a thin layer. *Burns,* 32**,** 305-311.

MIYAMOTO, T., MUNETA, T., TABUCHI, T., MATSUMOTO, K., SAITO, H., TSUJI, K. & SEKIYA, I. 2010. Intradiscal transplantation of synovial mesenchymal stem cells prevents intervertebral disc degeneration through suppression of matrix metalloproteinase-related genes in nucleus pulposus cells in rabbits. *Arthritis Res Ther,* 12**,** R206.

MOCHIDA, J., SAKAI, D., NAKAMURA, Y., WATANABE, T., YAMAMOTO, Y. & KATO, S. 2015. Intervertebral disc repair with activated nucleus pulposus cell transplantation: a three-year, prospective clinical study of its safety. *Eur Cell Mater,* 29**,** 202-12; discussion 212.

MONGKOLDHUMRONGKUL, N., FLANAGAN, J. M. & JAYASINGHE, S. N. 2009. Direct jetting approaches for handling stem cells. *Biomed Mater,* 4**,** 015018.

MOYER, H. R., KINNEY, R. C., SINGH, K. A., WILLIAMS, J. K., SCHWARTZ, Z. & BOYAN, B. D. 2010. Alginate microencapsulation technology for the percutaneous delivery of adipose-derived stem cells. *Ann Plast Surg,* 65**,** 497-503.

MUELLER, M. B., FISCHER, M., ZELLNER, J., BERNER, A., DIENSTKNECHT, T., PRANTL, L., KUJAT, R., NERLICH, M., TUAN, R. S. & ANGELE, P. 2010. Hypertrophy in mesenchymal stem cell

chondrogenesis: effect of TGF-beta isoforms and chondrogenic conditioning. *Cells Tissues Organs,* 192**,** 158-66.

MURPHY, M. B., MONCIVAIS, K. & CAPLAN, A. I. 2013. Mesenchymal stem cells: environmentally responsive therapeutics for regenerative medicine. *Experimental &Amp; Molecular Medicine,* 45**,** e54.

MURUA, A., PORTERO, A., ORIVE, G., HERNÁNDEZ, R. M., DE CASTRO, M. & PEDRAZ, J. L. 2008. Cell microencapsulation technology: Towards clinical application. *Journal of Controlled Release.*

MWALE, F., CIOBANU, I., GIANNITSIOS, D., ROUGHLEY, P., STEFFEN, T. & ANTONIOU, J. 2011. Effect of oxygen levels on proteoglycan synthesis by intervertebral disc cells. *Spine (Phila Pa 1976),* 36**,** E131-8.

MWALE, F., ROUGHLEY, P. & ANTONIOU, J. 2004. Distinction between the extracellular matrix of the nucleus pulposus and hyaline cartilage: a requisite for tissue engineering of intervertebral disc. *Eur Cell Mater,* 8**,** 58-63; discussion 63-4.

NACHEMSON, A. 1969. Intradiscal measurements of pH in patients with lumbar rhizopathies. *Acta Orthop Scand,* 40**,** 23-42.

NAQVI, S. M. & BUCKLEY, C. T. 2014. Differential Response of Encapsulated Nucleus Pulposus and Bone Marrow Stem Cells in Isolation and Coculture in Alginate and Chitosan Hydrogels. *Tissue Eng Part A,* (In Press).

NAQVI, S. M. & BUCKLEY, C. T. 2015a. Differential response of encapsulated nucleus pulposus and bone marrow stem cells in isolation and coculture in alginate and chitosan hydrogels. *Tissue Eng Part A,* 21**,** 288-99.

NAQVI, S. M. & BUCKLEY, C. T. 2015b. Differential Response of Encapsulated Nucleus Pulposus and Bone Marrow Stem Cells in Isolation and Coculture in Alginate and Chitosan Hydrogels. *Tissue Eng Part A,* 21**,** 288-99.

NAQVI, S. M. & BUCKLEY, C. T. 2015c. Extracellular matrix production by nucleus pulposus and bone marrow stem cells in response to altered oxygen and glucose microenvironments. *J Anat,* 227**,** 757-66.

NAQVI, S. M. & BUCKLEY, C. T. 2016. Bone Marrow Stem Cells in Response to Intervertebral Disc-Like Matrix Acidity and Oxygen Concentration: Implications for Cell-based Regenerative Therapy. *Spine (Phila Pa 1976),* 41**,** 743-50.

NAQVI, S. M., GANSAU, J. & BUCKLEY, C. T. 2018. Priming and cryopreservation of microencapsulated marrow stromal cells as a strategy for intervertebral disc regeneration. *Biomed Mater,* 13**,** 034106.

NAQVI, S. M., GANSAU, J., GIBBONS, D. & BUCKLEY, C. T. 2019. In vitro co-culture and ex vivo organ culture assessment of primed and cryopreserved stromal cell microcapsules for intervertebral disc regeneration. *Eur Cell Mater,* 37**,** 134-152.

NAQVI, S. M., VEDICHERLA, S., GANSAU, J., MCINTYRE, T., DOHERTY, M. & BUCKLEY, C. T. 2016a. Living Cell Factories - Electrosprayed Microcapsules and Microcarriers for Minimally Invasive Delivery. *Advanced Materials,* 28**,** 5662-5671.

NAQVI, S. M., VEDICHERLA, S., GANSAU, J., MCINTYRE, T., DOHERTY, M. & BUCKLEY, C. T. 2016b. Living Cell Factories - Electrosprayed Microcapsules and Microcarriers for Minimally Invasive Delivery. *Adv Mater,* 28**,** 5662-71.

NEDRESKY, D. & SINGH, G. 2020. Anatomy, Back, Nucleus Pulposus. *StatPearls.* Treasure Island (FL).

NISHIDA, K., KANG, J. D., GILBERTSON, L. G., MOON, S. H., SUH, J. K., VOGT, M. T., ROBBINS, P. D. & EVANS, C. H. 1999. Modulation of the biologic activity of the rabbit intervertebral disc by gene therapy: an in vivo study of adenovirus-mediated transfer of the human transforming growth factor beta 1 encoding gene. *Spine,* 24**,** 2419-2425.

NOGUERA, R., NIETO, O. A., TADEO, I., FARINAS, F. & ALVARO, T. 2012. Extracellular matrix, biotensegrity and tumor microenvironment. An update and overview. *Histol Histopathol,* 27**,** 693-705.

NOGUÉS, C., THOMAS, D., PANDIT, A. & O?BRIEN, T. 2013a. Stem Cell Microencapsulation for Therapeutic Angiogenesis. *Biomaterials for Stem Cell Therapy.* CRC Press.

NOGUÉS, C. S., THOMAS, D., PANDIT, A. & O'BRIEN, T. 2013b. Stem Cell Microencapsulation for Therapeutic Angiogenesis. *Biomaterials for Stem Cell Therapy.* CRC Press.

NOMURA, T., MOCHIDA, J., OKUMA, M., NISHIMURA, K. & SAKABE, K. 2001. Nucleus pulposus allograft retards intervertebral disc degeneration. *Clin Orthop Relat Res***,** 94-101.

NOORT, W. A., OERLEMANS, M. I., ROZEMULLER, H., FEYEN, D., JAKSANI, S., STECHER, D., NAAIJKENS, B., MARTENS, A. C., BUHRING, H. J., DOEVENDANS, P. A. & SLUIJTER, J. P. 2012. Human versus porcine mesenchymal stromal cells: phenotype, differentiation potential, immunomodulation and cardiac improvement after transplantation. *J Cell Mol Med,* 16**,** 1827-39.

NORIEGA, D. C., ARDURA, F., HERNANDEZ-RAMAJO, R., MARTIN-FERRERO, M. A., SANCHEZ-LITE, I., TORIBIO, B., ALBERCA, M., GARCIA, V., MORALEDA, J. M., SANCHEZ, A. & GARCIA-SANCHO, J. 2017. Intervertebral Disc Repair by Allogeneic Mesenchymal Bone Marrow Cells: A Randomized Controlled Trial. *Transplantation,* 101**,** 1945-1951.

NOTH, U., RACKWITZ, L., HEYMER, A., WEBER, M., BAUMANN, B., STEINERT, A., SCHUTZE, N., JAKOB, F. & EULERT, J. 2007. Chondrogenic differentiation of human mesenchymal stem cells in collagen type I hydrogels. *J Biomed Mater Res A,* 83**,** 626-35.

O'RIORDAN, K., ANDREWS, D., BUCKLE, K. & CONWAY, P. J. J. O. A. M. 2001. Evaluation of microencapsulation of a Bifidobacterium strain with starch as an approach to prolonging viability during storage. 91**,** 1059-1066.

OEGEMA, T. R., JR. 1993. Biochemistry of the intervertebral disc. *Clin Sports Med,* 12**,** 419-39.

OHSHIMA, H. & URBAN, J. P. 1992. The effect of lactate and pH on proteoglycan and protein synthesis rates in the intervertebral disc. *Spine (Phila Pa 1976),* 17**,** 1079-82.

OHSHIMA, K., NAKAYA, T., INOUE, A. K., HATAYA, T., HAYASHI, Y. & SHIKATA, E. 1992. Production and characteristics of strain common antibodies against a synthetic polypeptide corresponding to the C-terminal region of potato virus Y coat protein. *J Virol Methods,* 40**,** 265-73.

OKUDA, S., MYOUI, A., ARIGA, K., NAKASE, T., YONENOBU, K. & YOSHIKAWA, H. 2001. Mechanisms of age-related decline in insulin-like growth factor-I dependent proteoglycan synthesis in rat intervertebral disc cells. *Spine (Phila Pa 1976),* 26**,** 2421-6.

OKUMA, M., MOCHIDA, J., NISHIMURA, K., SAKABE, K. & SEIKI, K. 2000. Reinsertion of stimulated nucleus pulposus cells retards intervertebral disc degeneration: An in vitro and in vivo experimental study. *Journal of Orthopaedic Research,* 18**,** 988-997.

OROZCO, L., SOLER, R., MORERA, C., ALBERCA, M., SANCHEZ, A. & GARCIA-SANCHO, J. 2011. Intervertebral disc repair by autologous mesenchymal bone marrow cells: a pilot study. *Transplantation,* 92**,** 822-8.

OSADA, R., OHSHIMA, H., ISHIHARA, H., YUDOH, K., SAKAI, K., MATSUI, H. & TSUJI, H. 1996. Autocrine/paracrine mechanism of insulin-like growth factor-1 secretion, and the effect of insulin-like growth factor-1 on proteoglycan synthesis in bovine intervertebral discs. *Journal of Orthopaedic Research,* 14**,** 690-699.

PARK, H., KIM, P. H., HWANG, T., KWON, O. J., PARK, T. J., CHOI, S. W., YUN, C. O. & KIM, J. H. 2012. Fabrication of cross-linked alginate beads using electrospraying for adenovirus delivery. *Int J Pharm,* 427**,** 417-25.

PARK, J. B., CHANG, H. & KIM, K. W. 2001. Expression of Fas ligand and apoptosis of disc cells in herniated lumbar disc tissue. *Spine (Phila Pa 1976),* 26**,** 618-21.

PARK, J. Y., CHOI, J. C., SHIM, J. H., LEE, J. S., PARK, H., KIM, S. W., DOH, J. & CHO, D. W. 2014. A comparative study on collagen type I and hyaluronic acid dependent cell behavior for osteochondral tissue bioprinting. *Biofabrication,* 6**,** 035004.

PARK, S. H., PARK, S. R., CHUNG, S. I., PAI, K. S. & MIN, B. H. 2005. Tissue-engineered cartilage using fibrin/hyaluronan composite gel and its in vivo implantation. *Artif Organs,* 29**,** 838-45.

PARK, Y. B., HA, C. W., RHIM, J. H. & LEE, H. J. 2018. Stem Cell Therapy for Articular Cartilage Repair: Review of the Entity of Cell Populations Used and the Result of the Clinical Application of Each Entity. *Am J Sports Med,* 46**,** 2540-2552.

PATTAPPA, G., HEYWOOD, H. K., DE BRUIJN, J. D. & LEE, D. A. 2011. The metabolism of human mesenchymal stem cells during proliferation and differentiation. *J Cell Physiol,* 226**,** 2562-70.

PAUL, A., GE, Y., PRAKASH, S. & SHUM-TIM, D. 2009. Microencapsulated stem cells for tissue repairing: implications in cell-based myocardial therapy. *Regenerative medicine,* 4**,** 733-745.

PENNICOOKE, B., MORIGUCHI, Y., HUSSAIN, I., BONSSAR, L. & HÄRTL, R. 2016. Biological Treatment Approaches for Degenerative Disc Disease: A Review of Clinical Trials and Future Directions. *Cureus,* 8**,** e892-e892.

PEROGLIO, M., DOUMA, L. S., CAPREZ, T. S., JANKI, M., BENNEKER, L. M., ALINI, M. & GRAD, S. 2017. Intervertebral disc response to stem cell treatment is conditioned by disc state and cell carrier: An ex vivo study. *J Orthop Translat,* 9**,** 43-51.

PETTINE, K. A., MURPHY, M. B., SUZUKI, R. K. & SAND, T. T. 2015. Percutaneous Injection of Autologous Bone Marrow Concentrate Cells Significantly Reduces Lumbar Discogenic Pain Through 12 Months. *STEM CELLS,* 33**,** 146-156.

PLUMMER, L. N. & BUSENBERG, E. J. G. E. C. A. 1982. The solubilities of calcite, aragonite and vaterite in CO2-H2O solutions between 0 and 90 C, and an evaluation of the aqueous model for the system CaCO3-CO2-H2O. 46**,** 1011-1040.

POWER, K. A., GRAD, S., RUTGES, J. P., CREEMERS, L. B., VAN RIJEN, M. H., O'GAORA, P., WALL, J. G., ALINI, M., PANDIT, A. & GALLAGHER, W. M. 2011. Identification of cell surface-specific markers to target human nucleus pulposus cells: expression of carbonic anhydrase XII varies with age and degeneration. *Arthritis Rheum,* 63**,** 3876-86.

QUINN, S. J., BAI, M. & BROWN, E. M. 2004. pH Sensing by the calcium-sensing receptor. *J Biol Chem,* 279**,** 37241-9.

RAJ, P. P. 2008. Intervertebral disc: anatomy-physiology-pathophysiology-treatment. *Pain Pract,* 8**,** 18-44.

RAJA, R. H., MCGARY, C. T. & WEIGEL, P. H. 1988. Affinity and distribution of surface and intracellular hyaluronic acid receptors in isolated rat liver endothelial cells. *J Biol Chem,* 263**,** 16661-8.

RAMOS, B. R., MENDES, N. D., TANIKAWA, A. A., AMADOR, M. A., DOS SANTOS, N. P., DOS SANTOS, S. E., CASTELLI, E. C., WITKIN, S. S. & DA SILVA, M. G. 2016. Ancestry informative markers and selected single nucleotide polymorphisms in immunoregulatory genes on preterm labor and preterm premature rupture of membranes: a case control study. *BMC Pregnancy Childbirth,* 16**,** 30.

RAZAQ, S., WILKINS, R. J. & URBAN, J. P. 2003. The effect of extracellular pH on matrix turnover by cells of the bovine nucleus pulposus. *Eur Spine J,* 12**,** 341-9.

RENKEN A., H. D. 1998. Microencapsulation: a review of polymers and technologies with a focus on bioartificial organs. *Polimery,* T. 43, nr 530-540.

REYHANI, V., SEDDIGH, P., GUSS, B., GUSTAFSSON, R., RASK, L. & RUBIN, K. 2014. Fibrin binds to collagen and provides a bridge for alphaVbeta3 integrin-dependent contraction of collagen gels. *Biochem J,* 462**,** 113-23.

RICHARDSON, S. M. & HOYLAND, J. A. 2008. Stem cell regeneration of degenerated intervertebral discs: current status. *Curr Pain Headache Rep,* 12**,** 83-8.

RICHARDSON, S. M., KNOWLES, R., TYLER, J., MOBASHERI, A. & HOYLAND, J. A. 2008. Expression of glucose transporters GLUT-1, GLUT-3, GLUT-9 and HIF-1alpha in normal and degenerate human intervertebral disc. *Histochem Cell Biol,* 129**,** 503-11.

RICHARDSON, S. M., WALKER, R. V., PARKER, S., RHODES, N. P., HUNT, J. A., FREEMONT, A. J. & HOYLAND, J. A. 2006. Intervertebral disc cell-mediated mesenchymal stem cell differentiation. *Stem Cells,* 24**,** 707-16.

RINGEISEN, B. R., OTHON, C. M., BARRON, J. A., YOUNG, D. & SPARGO, B. J. 2006. Jet-based methods to print living cells. *Biotechnology Journal.*

RISBUD, M. V., ALBERT, T. J., GUTTAPALLI, A., VRESILOVIC, E. J., HILLIBRAND, A. S., VACCARO, A. R. & SHAPIRO, I. M. 2004. Differentiation of mesenchymal stem cells towards a nucleus pulposus-like phenotype in vitro: implications for cell-based transplantation therapy. *Spine,* 29**,** 2627-2632.

RISBUD, M. V., GUTTAPALLI, A., STOKES, D. G., HAWKINS, D., DANIELSON, K. G., SCHAER, T. P., ALBERT, T. J. & SHAPIRO, I. M. 2006. Nucleus pulposus cells express HIF-1 alpha under normoxic culture conditions: a metabolic adaptation to the intervertebral disc microenvironment. *J Cell Biochem,* 98**,** 152-9.

RISBUD, M. V., SCHIPANI, E. & SHAPIRO, I. M. 2010. Hypoxic regulation of nucleus pulposus cell survival: from niche to notch. *Am J Pathol,* 176**,** 1577-83.

RISBUD, M. V. & SHAPIRO, I. M. 2014. Role of cytokines in intervertebral disc degeneration: pain and disc content. *Nat Rev Rheumatol,* 10**,** 44-56.

ROBERTS, S., EVANS, E. H., KLETSAS, D., JAFFRAY, D. C. & EISENSTEIN, S. M. 2006. Senescence in human intervertebral discs. *Eur Spine J,* 15 Suppl 3**,** S312-6.

ROCHE, S., RONZIÈRE, M. C., HERBAGE, D. & FREYRIA, A. M. 2001. Native and DPPA cross-linked collagen sponges seeded with fetal bovine epiphyseal chondrocytes used for cartilage tissue engineering. *Biomaterials.* Elsevier Science Ltd.

RONG, C., CHEN, F. H., JIANG, S., HU, W., WU, F. R., CHEN, T. Y. & YUAN, F. L. 2012. Inhibition of acid-sensing ion channels by amiloride protects rat articular chondrocytes from acid-induced apoptosis via a mitochondrial-mediated pathway. *Cell Biol Int,* 36**,** 635-41.

ROSENZWEIG, D. H., FAIRAG, R., MATHIEU, A. P., LI, L., EGLIN, D., D'ESTE, M., STEFFEN, T., WEBER, M. H., OUELLET, J. A. & HAGLUND, L. 2018. Thermoreversible hyaluronan-hydrogel and autologous nucleus pulposus cell delivery regenerates human intervertebral discs in an ex vivo, physiological organ culture model. *Eur Cell Mater,* 36**,** 200-217.

ROUGHLEY, P. J. 2004. Biology of intervertebral disc aging and degeneration: involvement of the extracellular matrix. *Spine (Phila Pa 1976),* 29**,** 2691-9.

ROWE, S. L., LEE, S. & STEGEMANN, J. P. 2007. Influence of thrombin concentration on the mechanical and morphological properties of cell-seeded fibrin hydrogels. *Acta Biomater,* 3**,** 59-67.

ROWLAND, C. R., LENNON, D. P., CAPLAN, A. I. & GUILAK, F. 2013. The effects of crosslinking of scaffolds engineered from cartilage ECM on the chondrogenic differentiation of MSCs. *Biomaterials,* 34**,** 5802-12.

ROWLEY, J. A., MADLAMBAYAN, G. & MOONEY, D. J. 1999. Alginate hydrogels as synthetic extracellular matrix materials. *Biomaterials,* 20**,** 45-53.

RUTGES, J., CREEMERS, L. B., DHERT, W., MILZ, S., SAKAI, D., MOCHIDA, J., ALINI, M. & GRAD, S. 2010. Variations in gene and protein expression in human nucleus pulposus in comparison with annulus fibrosus and cartilage cells: potential associations with aging and degeneration. *Osteoarthritis Cartilage,* 18**,** 416-23.

SABATER, A. L., GUARNIERI, A., ESPANA, E. M., LI, W., PROSPER, F. & MORENO-MONTANES, J. 2013. Strategies of human corneal endothelial tissue regeneration. *Regen Med,* 8**,** 183-95.

SADOWSKA, A., KAMEDA, T., KRUPKOVA, O. & WUERTZ-KOZAK, K. 2018. Osmosensing, osmosignalling and inflammation: how intervertebral disc cells respond to altered osmolarity. *Eur Cell Mater,* 36**,** 231-250.

SAH, R. L., KIM, Y. J., DOONG, J. Y., GRODZINSKY, A. J., PLAAS, A. H. & SANDY, J. D. 1989. Biosynthetic response of cartilage explants to dynamic compression. *J Orthop Res,* 7**,** 619-36.

SAHNI, A., ODRLJIN, T. & FRANCIS, C. W. 1998. Binding of basic fibroblast growth factor to fibrinogen and fibrin. *The Journal of biological chemistry,* 273**,** 7554-7559.

SAHOO, S., LEE, W. C., GOH, J. C. & TOH, S. L. 2010a. Bio-electrospraying: A potentially safe technique for delivering progenitor cells. *Biotechnol Bioeng,* 106**,** 690-8.

SAHOO, S., LEE, W. C., GOH, J. C. H. & TOH, S. L. 2010b. Bio-electrospraying: A potentially safe technique for delivering progenitor cells. *Biotechnology and Bioengineering,* 106**,** 690-698.

SAKAI, D. 2008. Future perspectives of cell-based therapy for intervertebral disc disease. *Eur Spine J,* 17 Suppl 4**,** 452-8.

SAKAI, D. & SCHOL, J. 2017. Cell therapy for intervertebral disc repair: Clinical perspective. *Journal of orthopaedic translation,* 9**,** 8-18.

SAKAI, S., MU, C., KAWABATA, K., HASHIMOTO, I. & KAWAKAMI, K. 2006. Biocompatibility of subsieve-size capsules versus conventional-size microcapsules. *Journal of Biomedical Materials Research - Part A,* 78**,** 394-398.

SANTORO, E., AGRESTA, F., BUSCAGLIA, F., MULIERI, G., MAZZAROLO, G., BEDIN, N. & MULIERI, M. 2007. Preliminary experience using fibrin glue for mesh fixation in 250 patients

undergoing minilaparoscopic transabdominal preperitoneal hernia repair. *Journal of laparoendoscopic & advanced surgical techniques. Part A,* 17**,** 12-15.

SARATH BABU, N., KRISHNAN, S., BRAHMENDRA SWAMY, C. V., VENKATA SUBBAIAH, G. P., GURAVA REDDY, A. V. & IDRIS, M. M. 2016. Quantitative proteomic analysis of normal and degenerated human intervertebral disc. *Spine J,* 16**,** 989-1000.

SCHIPANI, E., RYAN, H. E., DIDRICKSON, S., KOBAYASHI, T., KNIGHT, M. & JOHNSON, R. S. 2001. Hypoxia in cartilage: HIF-1alpha is essential for chondrocyte growth arrest and survival. *Genes Dev,* 15**,** 2865-76.

SCHLAMEUS, W. 1995. Centrifugal Extrusion Encapsulation. *Encapsulation and Controlled Release of Food Ingredients.* American Chemical Society.

SCHMID, G., WITTELER, A., WILLBURGER, R., KUHNEN, C., JERGAS, M. & KOESTER, O. 2004. Lumbar disk herniation: correlation of histologic findings with marrow signal intensity changes in vertebral endplates at MR imaging. *Radiology,* 231**,** 352-8.

SCHMIERER, B. & HILL, C. S. 2007. TGFbeta-SMAD signal transduction: molecular specificity and functional flexibility. *Nat Rev Mol Cell Biol,* 8**,** 970-82.

SCHUCKER, J. J. & WARD, K. E. 2005. Hyperphosphatemia and phosphate binders. *Am J Health Syst Pharm,* 62**,** 2355-61.

SCOTTI, C., OSMOKROVIC, A., WOLF, F., MIOT, S., PERETTI, G. M., BARBERO, A. & MARTIN, I. 2012. Response of human engineered cartilage based on articular or nasal chondrocytes to interleukin-1beta and low oxygen. *Tissue Eng Part A,* 18**,** 362-72.

SECRETAN, C., BAGNALL, K. M. & JOMHA, N. M. 2010. Effects of introducing cultured human chondrocytes into a human articular cartilage explant model. *Cell Tissue Res,* 339**,** 421-7.

SELARD, E., SHIRAZI-ADL, A. & URBAN, J. P. 2003. Finite element study of nutrient diffusion in the human intervertebral disc. *Spine (Phila Pa 1976),* 28**,** 1945-53; discussion 1953.

SEMENZA, G. L. 1994. Transcriptional regulation of gene expression: mechanisms and pathophysiology. *Hum Mutat,* 3**,** 180-99.

SHAFIU KAMBA, A., ISMAIL, M., TENGKU IBRAHIM, T. A. & ZAKARIA, Z. A. B. 2013. A pH-Sensitive, Biobased Calcium Carbonate Aragonite Nanocrystal as a Novel Anticancer Delivery System %J BioMed Research International. 2013**,** 10.

SHI, H., LI, L., ZHANG, L., WANG, T., WANG, C., ZHU, D. & SU, Z. 2015. Designed preparation of polyacrylic acid/calcium carbonate nanoparticles with high doxorubicin payload for liver cancer chemotherapy. *CrystEngComm,* 17**,** 4768-4773.

SHIM, W. S., JIANG, S., WONG, P., TAN, J., CHUA, Y. L., TAN, Y. S., SIN, Y. K., LIM, C. H., CHUA, T., TEH, M., LIU, T. C. & SIM, E. 2004. Ex vivo differentiation of human adult bone marrow stem cells into cardiomyocyte-like cells. *Biochem Biophys Res Commun,* 324**,** 481-8.

SINGH, K., MASUDA, K., THONAR, E. J., AN, H. S. & CS-SZABO, G. 2009. Age-related changes in the extracellular matrix of nucleus pulposus and anulus fibrosus of human intervertebral disc. *Spine (Phila Pa 1976),* 34**,** 10-6.

SMITH, L. J., NERURKAR, N. L., CHOI, K. S., HARFE, B. D. & ELLIOTT, D. M. 2011. Degeneration and regeneration of the intervertebral disc: lessons from development. *Dis Model Mech,* 4**,** 31-41.

SMITH, L. J., SILVERMAN, L., SAKAI, D., LE MAITRE, C. L., MAUCK, R. L., MALHOTRA, N. R., LOTZ, J. C. & BUCKLEY, C. T. 2018. Advancing cell therapies for intervertebral disc regeneration

from the lab to the clinic: Recommendations of the ORS spine section. *JOR Spine,* 1**,** e1036.

SONG, H., CHANG, W., SONG, B. W. & HWANG, K. C. 2012. Specific differentiation of mesenchymal stem cells by small molecules. *Am J Stem Cells,* 1**,** 22-30.

SONTAG, S. J. 1990. The medical management of reflux esophagitis. Role of antacids and acid inhibition. *Gastroenterol Clin North Am,* 19**,** 683-712.

SPORN, L. A., BUNCE, L. A. & FRANCIS, C. W. 1995. Cell proliferation on fibrin: modulation by fibrinopeptide cleavage. *Blood,* 86**,** 1802-10.

STAINES, K. A., BROWN, G. & FARQUHARSON, C. 2019. The Ex Vivo Organ Culture of Bone. *Methods Mol Biol,* 1914**,** 199-215.

STECK, E., BERTRAM, H., ABEL, R., CHEN, B., WINTER, A. & RICHTER, W. 2005. Induction of intervertebral disc-like cells from adult mesenchymal stem cells. *Stem Cells,* 23**,** 403-11.

STEINERT, A. F., PALMER, G. D., CAPITO, R., HOFSTAETTER, J. G., PILAPIL, C., GHIVIZZANI, S. C., SPECTOR, M. & EVANS, C. H. 2007. Genetically enhanced engineering of meniscus tissue using ex vivo delivery of transforming growth factor-beta 1 complementary deoxyribonucleic acid. *Tissue Eng,* 13**,** 2227-37.

STEPHAN, S., JOHNSON, W. E. & ROBERTS, S. 2011. The influence of nutrient supply and cell density on the growth and survival of intervertebral disc cells in 3D culture. *Eur Cell Mater,* 22**,** 97-108.

STERN, S., LINDENHAYN, K. & PERKA, C. 2004. Human intervertebral disc cell culture for disc disorders. *Clin Orthop Relat Res***,** 238-44.

STERN, S., LINDENHAYN, K., SCHULTZ, O. & PERKA, C. 2000. Cultivation of porcine cells from the nucleus pulposus in a fibrin/hyaluronic acid matrix. *Acta Orthop Scand,* 71**,** 496-502.

STOYANOV, J. V., GANTENBEIN-RITTER, B., BERTOLO, A., AEBLI, N., BAUR, M., ALINI, M. & GRAD, S. 2011. Role of hypoxia and growth and differentiation factor-5 on differentiation of human mesenchymal stem cells towards intervertebral nucleus pulposus-like cells. *Eur Cell Mater,* 21**,** 533-47.

SUGIURA, S., ODA, T., IZUMIDA, Y., AOYAGI, Y., SATAKE, M., OCHIAI, A., OHKOHCHI, N. & NAKAJIMA, M. 2005. Size control of calcium alginate beads containing living cells using micro-nozzle array. *Biomaterials,* 26**,** 3327-3331.

SUN, X., ZHAO, D., LI, Y. L., SUN, Y., LEI, X. H., ZHANG, J. N., WU, M. M., LI, R. Y., ZHAO, Z. F., ZHANG, Z. R. & JIANG, C. L. 2013. Regulation of ASIC1 by Ca2+/calmodulin-dependent protein kinase II in human glioblastoma multiforme. *Oncol Rep,* 30**,** 2852-8.

SUZUKI, A., MAEDA, T., BABA, Y., SHIMAMURA, K. & KATO, Y. 2014. Acidic extracellular pH promotes epithelial mesenchymal transition in Lewis lung carcinoma model. *Cancer Cell Int,* 14**,** 129.

T, L. R., SANCHEZ-ABARCA, L. I., MUNTION, S., PRECIADO, S., PUIG, N., LOPEZ-RUANO, G., HERNANDEZ-HERNANDEZ, A., REDONDO, A., ORTEGA, R., RODRIGUEZ, C., SANCHEZ-GUIJO, F. & DEL CANIZO, C. 2016. MSC surface markers (CD44, CD73, and CD90) can identify human MSC-derived extracellular vesicles by conventional flow cytometry. *Cell Commun Signal,* 14**,** 2.

TAKAHASHI, I., NUCKOLLS, G. H., TAKAHASHI, K., TANAKA, O., SEMBA, I., DASHNER, R., SHUM, L. & SLAVKIN, H. C. 1998. Compressive force promotes sox9, type II collagen and aggrecan and inhibits IL-1beta expression resulting in chondrogenesis in mouse embryonic limb bud mesenchymal cells. *J Cell Sci,* 111 (Pt 14)**,** 2067-76.

TARNAWSKI, A., TANOUE, K., SANTOS, A. M. & SARFEH, I. J. 1995. Cellular and molecular mechanisms of gastric ulcer healing. Is the quality of mucosal scar affected by treatment? *Scand J Gastroenterol Suppl,* 210**,** 9-14.

TAVAKOLI, J., ELLIOTT, D. M. & COSTI, J. J. 2017. The ultra-structural organization of the elastic network in the intra- and inter-lamellar matrix of the intervertebral disc. *Acta Biomater,* 58**,** 269-277.

THIRUMALA, S., GIMBLE, J. M. & DEVIREDDY, R. V. 2013. Methylcellulose based thermally reversible hydrogel system for tissue engineering applications. *Cells,* 2**,** 460-75.

THOMPSON, J. P., OEGEMA, T. R. & BRADFORD, D. S. 1991. Stimulation of mature canine intervertebral disc by growth factors. *Spine,* 16**,** 253-260.

THORPE, A. A., DOUGILL, G., VICKERS, L., REEVES, N. D., SAMMON, C., COOPER, G. & LE MAITRE, C. L. 2017. Thermally triggered hydrogel injection into bovine intervertebral disc tissue explants induces differentiation of mesenchymal stem cells and restores mechanical function. *Acta Biomater,* 54**,** 212-226.

TSAI, T. T., DANIELSON, K. G., GUTTAPALLI, A., OGUZ, E., ALBERT, T. J., SHAPIRO, I. M. & RISBUD, M. V. 2006. TonEBP/OREBP is a regulator of nucleus pulposus cell function and survival in the intervertebral disc. *J Biol Chem,* 281**,** 25416-24.

TSCHUGG, A., MICHNACS, F., STROWITZKI, M., MEISEL, H. J. & THOME, C. 2016. A prospective multicenter phase I/II clinical trial to evaluate safety and efficacy of NOVOCART Disc plus autologous disc chondrocyte transplantation in the treatment of nucleotomized and degenerative lumbar disc to avoid secondary disease: study protocol for a randomized controlled trial. *Trials,* 17**,** 108.

UCHIYAMA, Y., CHENG, C. C., DANIELSON, K. G., MOCHIDA, J., ALBERT, T. J., SHAPIRO, I. M. & RISBUD, M. V. 2007. Expression of acid-sensing ion channel 3 (ASIC3) in nucleus pulposus cells of the intervertebral disc is regulated by p75NTR and ERK signaling. *J Bone Miner Res,* 22**,** 1996-2006.

ULUDAG, H., DE VOS, P. & TRESCO, P. A. 2000. Technology of mammalian cell encapsulation. *Advanced drug delivery reviews,* 42**,** 29-64.

UNDERHILL, C. B. & TOOLE, B. P. 1980. Physical characteristics of hyaluronate binding to the surface of simian virus 40-transformed 3T3 cells. *J Biol Chem,* 255**,** 4544-9.

URBAN, J. P. 2002. The role of the physicochemical environment in determining disc cell behaviour. *Biochem Soc Trans,* 30**,** 858-64.

URBAN, J. P., HOLM, S., MAROUDAS, A. & NACHEMSON, A. 1982. Nutrition of the intervertebral disc: effect of fluid flow on solute transport. *Clin Orthop Relat Res***,** 296-302.

URBAN, J. P., SMITH, S. & FAIRBANK, J. C. 2004. Nutrition of the intervertebral disc. *Spine (Phila Pa 1976),* 29**,** 2700-9.

URITS, I., CAPUCO, A., SHARMA, M., KAYE, A. D., VISWANATH, O., CORNETT, E. M. & ORHURHU, V. 2019. Stem Cell Therapies for Treatment of Discogenic Low Back Pain: a Comprehensive Review. *Curr Pain Headache Rep,* 23**,** 65.

VADALA, G., RUSSO, F., PATTAPPA, G., SCHIUMA, D., PEROGLIO, M., BENNEKER, L. M., GRAD, S., ALINI, M. & DENARO, V. 2013. The transpedicular approach as an alternative route for intervertebral disc regeneration. *Spine (Phila Pa 1976),* 38**,** E319-24.

VADALA, G., SOWA, G., HUBERT, M., GILBERTSON, L. G., DENARO, V. & KANG, J. D. 2012. Mesenchymal stem cells injection in degenerated intervertebral disc: cell leakage may induce osteophyte formation. *J Tissue Eng Regen Med,* 6**,** 348-55.

VAINIERI, M. L., WAHL, D., ALINI, M., VAN OSCH, G. & GRAD, S. 2018. Mechanically stimulated osteochondral organ culture for evaluation of biomaterials in cartilage repair studies. *Acta Biomater,* 81**,** 256-266.

VAN DIJK, B., POTIER, E. & ITO, K. 2011. Culturing bovine nucleus pulposus explants by balancing medium osmolarity. *Tissue Eng Part C Methods,* 17**,** 1089-96.

VAN OSCH, G. J., VAN DER VEEN, S. W. & VERWOERD-VERHOEF, H. L. 2001. In vitro redifferentiation of culture-expanded rabbit and human auricular chondrocytes for cartilage reconstruction. *Plastic and reconstructive surgery,* 107**,** 433-440.

VANYSEK, P. 2000. Ionic conductivity and diffusion at infinite dilution. 83**,** 76-78.

VEDICHERLA, S. & BUCKLEY, C. T. 2017a. In vitro extracellular matrix accumulation of nasal and articular chondrocytes for intervertebral disc repair. *Tissue Cell,* 49**,** 503-513.

VEDICHERLA, S. & BUCKLEY, C. T. 2017b. Rapid Chondrocyte Isolation for Tissue Engineering Applications: The Effect of Enzyme Concentration and Temporal Exposure on the Matrix Forming Capacity of Nasal Derived Chondrocytes. *Biomed Res Int,* 2017**,** 2395138.

VELIKONJA, N. K., WOZNIAK, G., MALICEV, E., KNEZEVIC, M. & JERAS, M. 2001. Protein synthesis of human articular chondrocytes cultured in vitro for autologous transplantation. *Pflugers Arch,* 442**,** R169-70.

VERGROESEN, P. P., KINGMA, I., EMANUEL, K. S., HOOGENDOORN, R. J., WELTING, T. J., VAN ROYEN, B. J., VAN DIEEN, J. H. & SMIT, T. H. 2015. Mechanics and biology in intervertebral disc degeneration: a vicious circle. *Osteoarthritis Cartilage,* 23**,** 1057-70.

VERMONDEN, T., FEDOROVICH, N. E., VAN GEEMEN, D., ALBLAS, J., VAN NOSTRUM, C. F., DHERT, W. J. & HENNINK, W. E. 2008. Photopolymerized thermosensitive hydrogels: synthesis, degradation, and cytocompatibility. *Biomacromolecules,* 9**,** 919-26.

VINARDELL, T., THORPE, S. D., BUCKLEY, C. T. & KELLY, D. J. 2009. Chondrogenesis and integration of mesenchymal stem cells within an in vitro cartilage defect repair model. *Ann Biomed Eng,* 37**,** 2556-65.

VOS, P. D., ANDERSSON, A., TAM, S. K., FAAS, M. M. & HALLE, J. P. 2006. Advances and Barriers in Mammalian Cell Encapsulation for Treatment of Diabetes. *Immunology, Endocrine & Metabolic Agents - Medicinal Chemistry (Formerly Current Medicinal Chemistry - Immunology, Endocrine & Metabolic Agents).*

WALDMAN, S. D., GRYNPAS, M. D., PILLIAR, R. M. & KANDEL, R. A. 2003. The use of specific chondrocyte populations to modulate the properties of tissue-engineered cartilage. *Journal of Orthopaedic Research,* 21**,** 132-138.

WANG, C. Q., WU, J. L., ZHUO, R. X. & CHENG, S. X. 2014. Protamine sulfate-calcium carbonate-plasmid DNA ternary nanoparticles for efficient gene delivery. *Mol Biosyst,* 10**,** 672-8.

WANG, G. L., JIANG, B. H., RUE, E. A. & SEMENZA, G. L. 1995. Hypoxia-inducible factor 1 is a basic-helix-loop-helix-PAS heterodimer regulated by cellular O2 tension. *Proc Natl Acad Sci U S A,* 92**,** 5510-4.

WANG, L., RAO, R. R. & STEGEMANN, J. P. 2013. Delivery of mesenchymal stem cells in chitosan/collagen microbeads for orthopedic tissue repair. *Cells Tissues Organs,* 197**,** 333-43.

WANG, L., SHANSKY, J., BORSELLI, C., MOONEY, D. & VANDENBURGH, H. 2012. Design and Fabrication of a Biodegradable, Covalently Crosslinked Shape-Memory Alginate Scaffold for Cell and Growth Factor Delivery. *Tissue Engineering Part A.*

WANG, L. & STEGEMANN, J. P. 2011. Glyoxal crosslinking of cell-seeded chitosan/collagen hydrogels for bone regeneration. *Acta Biomater,* 7**,** 2410-7.

WEILER, C., NERLICH, A. G., ZIPPERER, J., BACHMEIER, B. E. & BOOS, N. 2002. 2002 SSE Award Competition in Basic Science: expression of major matrix metalloproteinases is associated with intervertebral disc degradation and resorption. *Eur Spine J,* 11**,** 308-20.

WEISS, A. & ATTISANO, L. 2013. The TGFbeta superfamily signaling pathway. *Wiley Interdiscip Rev Dev Biol,* 2**,** 47-63.

WEISS, S., HENNIG, T., BOCK, R., STECK, E. & RICHTER, W. 2010. Impact of growth factors and PTHrP on early and late chondrogenic differentiation of human mesenchymal stem cells. *J Cell Physiol,* 223**,** 84-93.

WHATLEY, B. R. & WEN, X. 2012. Intervertebral disc (IVD): Structure, degeneration, repair and regeneration. *Materials Science and Engineering: C,* 32**,** 61 - 77.

WILKE, H. J., KETTLER, A., WENGER, K. H. & CLAES, L. E. 1997. Anatomy of the sheep spine and its comparison to the human spine. *Anat Rec,* 247**,** 542-55.

WILKENS, P., SCHEEL, I. B., GRUNDNES, O., HELLUM, C. & STORHEIM, K. 2013. Prognostic factors of prolonged disability in patients with chronic low back pain and lumbar degeneration in primary care: a cohort study. *Spine (Phila Pa 1976),* 38**,** 65-74.

WISE, J. K., ALFORD, A. I., GOLDSTEIN, S. A. & STEGEMANN, J. P. 2014. Comparison of uncultured marrow mononuclear cells and culture-expanded mesenchymal stem cells in 3D collagen-chitosan microbeads for orthopedic tissue engineering. *Tissue Eng Part A,* 20**,** 210-24.

WORKMAN, V. L., TEZERA, L. B., ELKINGTON, P. T. & JAYASINGHE, S. N. 2014. Controlled Generation of Microspheres Incorporating Extracellular Matrix Fibrils for Three-Dimensional Cell Culture. *Advanced Functional Materials,* 24**,** 2648-2657.

WU, J., WANG, D., RUAN, D., HE, Q., ZHANG, Y., WANG, C., XIN, H., XU, C. & LIU, Y. 2014. Prolonged expansion of human nucleus pulposus cells expressing human telomerase reverse transcriptase mediated by lentiviral vector. *J Orthop Res,* 32**,** 159-66.

WUERTZ, K., GODBURN, K. & IATRIDIS, J. C. 2009. MSC response to pH levels found in degenerating intervertebral discs. *Biochem Biophys Res Commun,* 379**,** 824-9.

WUERTZ, K., GODBURN, K., NEIDLINGER-WILKE, C., URBAN, J. & IATRIDIS, J. C. 2008. Behavior of mesenchymal stem cells in the chemical microenvironment of the intervertebral disc. *Spine (Phila Pa 1976),* 33**,** 1843-9.

WUERTZ, K., URBAN, J. P., KLASEN, J., IGNATIUS, A., WILKE, H. J., CLAES, L. & NEIDLINGER-WILKE, C. 2007. Influence of extracellular osmolarity and mechanical stimulation on gene expression of intervertebral disc cells. *J Orthop Res,* 25**,** 1513-22.

XU, Y. & HANNA, M. A. 2008. Morphological and structural properties of two-phase coaxial jet electrosprayed BSA-PLA capsules. *Journal of microencapsulation,* 25**,** 469-477.

XU, Z., YAN, L., GE, Y., ZHANG, Q., YANG, N., ZHANG, M., ZHAO, Y., SUN, P., GAO, J., TAO, Z. & YANG, Z. 2012. Effect of the calcium sensing receptor on rat bone marrow-derived mesenchymal stem cell proliferation through the ERK1/2 pathway. *Mol Biol Rep,* 39**,** 7271-9.

YAMAMOTO, Y., MOCHIDA, J., SAKAI, D., NAKAI, T., NISHIMURA, K., KAWADA, H. & HOTTA, T. 2004. Upregulation of the viability of nucleus pulposus cells by bone marrow-derived stromal cells: significance of direct cell-to-cell contact in coculture system. *Spine (Phila Pa 1976),* 29**,** 1508-14.

YANG, J.-A., YEOM, J., HWANG, B. W., HOFFMAN, A. S. & HAHN, S. K. 2014. In situ-forming injectable hydrogels for regenerative medicine. *Progress in Polymer Science,* 39**,** 1973-1986.

YANG, X. & LI, X. 2009. Nucleus pulposus tissue engineering: a brief review. *Eur Spine J,* 18**,** 1564-72.

YASUMA, T., ARAI, K. & YAMAUCHI, Y. 1993. The histology of lumbar intervertebral disc herniation. The significance of small blood vessels in the extruded tissue. *Spine (Phila Pa 1976),* 18**,** 1761-5.

YOSHIKAWA, T., UEDA, Y., MIYAZAKI, K., KOIZUMI, M. & TAKAKURA, Y. 2010. Disc Regeneration Therapy Using Marrow Mesenchymal Cell Transplantation: A Report of Two Case Studies. 35**,** E475-E480.

YU, Y., CHEN, Z., LI, W. G., CAO, H., FENG, E. G., YU, F., LIU, H., JIANG, H. & XU, T. L. 2010. A nonproton ligand sensor in the acid-sensing ion channel. *Neuron,* 68**,** 61-72.

YUAN, F. L., ZHAO, M. D., JIANG, D. L., JIN, C., LIU, H. F., XU, M. H., HU, W. & LI, X. 2016. Involvement of acid-sensing ion channel 1a in matrix metabolism of endplate chondrocytes under extracellular acidic conditions through NF-kappaB transcriptional activity. *Cell Stress Chaperones,* 21**,** 97-104.

ZENG, Y., CHEN, C., LIU, W., FU, Q., HAN, Z., LI, Y., FENG, S., LI, X., QI, C., WU, J., WANG, D., CORBETT, C., CHAN, B. P., RUAN, D. & DU, Y. 2015. Injectable microcryogels reinforced alginate encapsulation of mesenchymal stromal cells for leak-proof delivery and alleviation of canine disc degeneration. *Biomaterials,* 59**,** 53-65.

ZHANG, C., ZHANG, T., ZOU, J., MILLER, C. L., GORKHALI, R., YANG, J. Y., SCHILMILLER, A., WANG, S., HUANG, K., BROWN, E. M., MOREMEN, K. W., HU, J. & YANG, J. J. 2016. Structural basis for regulation of human calcium-sensing receptor by magnesium ions and an unexpected tryptophan derivative co-agonist. *Sci Adv,* 2**,** e1600241.

ZHANG, Y., PHILLIPS, F. M., THONAR, E. J., OEGEMA, T., AN, H. S., ROMAN-BLAS, J. A., HE, T. C. & ANDERSON, D. G. 2008. Cell therapy using articular chondrocytes overexpressing BMP-7 or BMP-10 in a rabbit disc organ culture model. *Spine (Phila Pa 1976),* 33**,** 831-8.

ZHAO, Y., LUO, Z., LI, M., QU, Q., MA, X., YU, S. H. & ZHAO, Y. 2015. A preloaded amorphous calcium carbonate/doxorubicin@silica nanoreactor for pH-responsive delivery of an anticancer drug. *Angew Chem Int Ed Engl,* 54**,** 919-22.

ZHOU, Q., LIU, Z., WU, Z., WANG, X., WANG, B., LI, C., LIU, Y., LI, L., WAN, P., HUANG, Z. & WANG, Z. 2015a. Reconstruction of Highly Proliferative Auto-Tissue-Engineered Lamellar Cornea Enhanced by Embryonic Stem Cell. *Tissue Eng Part C Methods,* 21**,** 639-48.

ZHOU, R., WU, X., WANG, Z., GE, J. & CHEN, F. 2015b. Interleukin-6 enhances acid-induced apoptosis via upregulating acid-sensing ion channel 1a expression and function in rat articular chondrocytes. *Int Immunopharmacol,* 29**,** 748-760.

ZIGLER, J., DELAMARTER, R., SPIVAK, J. M., LINOVITZ, R. J., DANIELSON, G. O., 3RD, HAIDER, T. T., CAMMISA, F., ZUCHERMANN, J., BALDERSTON, R., KITCHEL, S., FOLEY, K., WATKINS, R., BRADFORD, D., YUE, J., YUAN, H., HERKOWITZ, H., GEIGER, D., BENDO, J., PEPPERS, T., SACHS, B., GIRARDI, F., KROPF, M. & GOLDSTEIN, J. 2007. Results of the prospective, randomized, multicenter Food and Drug Administration investigational device exemption study of the ProDisc-L total disc replacement versus circumferential fusion for the treatment of 1-level degenerative disc disease. *Spine (Phila Pa 1976),* 32**,** 1155-62; discussion 1163.

ZOLLER, M. 2015. CD44, Hyaluronan, the Hematopoietic Stem Cell, and Leukemia-Initiating Cells. *Front Immunol,* 6**,** 235.

ZSCHARNACK, M., HEPP, P., RICHTER, R., AIGNER, T., SCHULZ, R., SOMERSON, J., JOSTEN, C., BADER, A. & MARQUASS, B. 2010. Repair of chronic osteochondral defects using predifferentiated mesenchymal stem cells in an ovine model. *Am J Sports Med,* 38**,** 1857-69.

ZWETSLOOT, P. P., VEGH, A. M., JANSEN OF LORKEERS, S. J., VAN HOUT, G. P., CURRIE, G. L., SENA, E. S., GREMMELS, H., BUIKEMA, J. W., GOUMANS, M. J., MACLEOD, M. R., DOEVENDANS, P. A., CHAMULEAU, S. A. & SLUIJTER, J. P. 2016. Cardiac Stem Cell Treatment in Myocardial Infarction: A Systematic Review and Meta-Analysis of Preclinical Studies. *Circ Res,* 118**,** 1223-32.

APPENDICES

Appendix 1

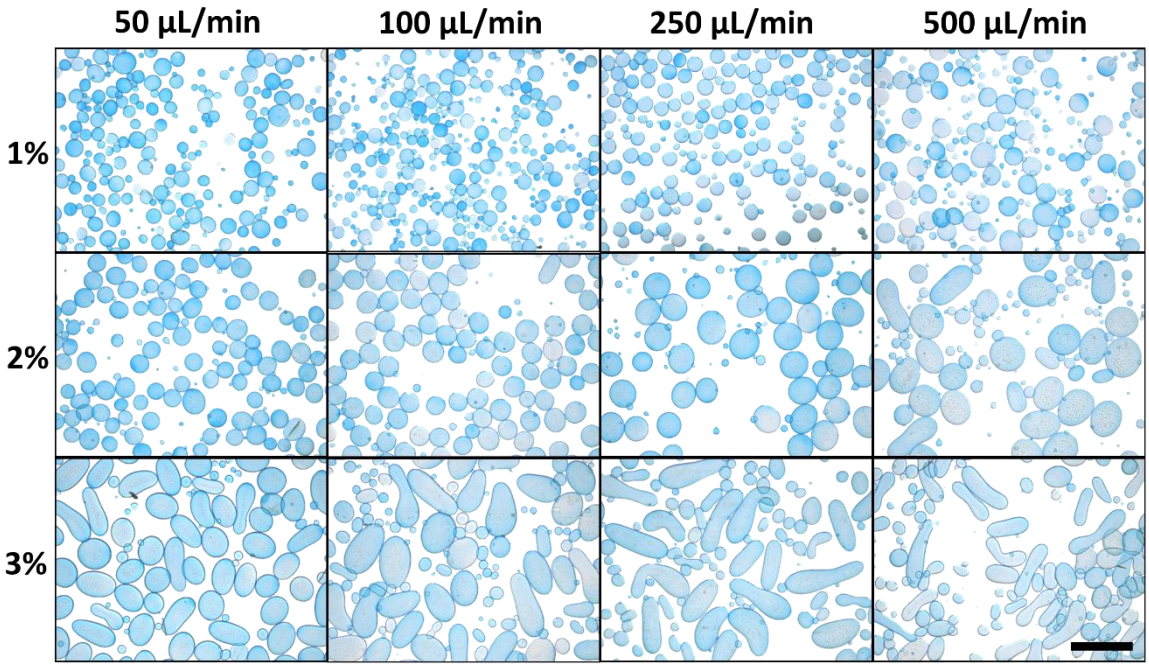

Figure A 1: Effect of key processing parameters of alginate concentrations at different flow rates. Scale Bar= 1000 µm

Appendix 2

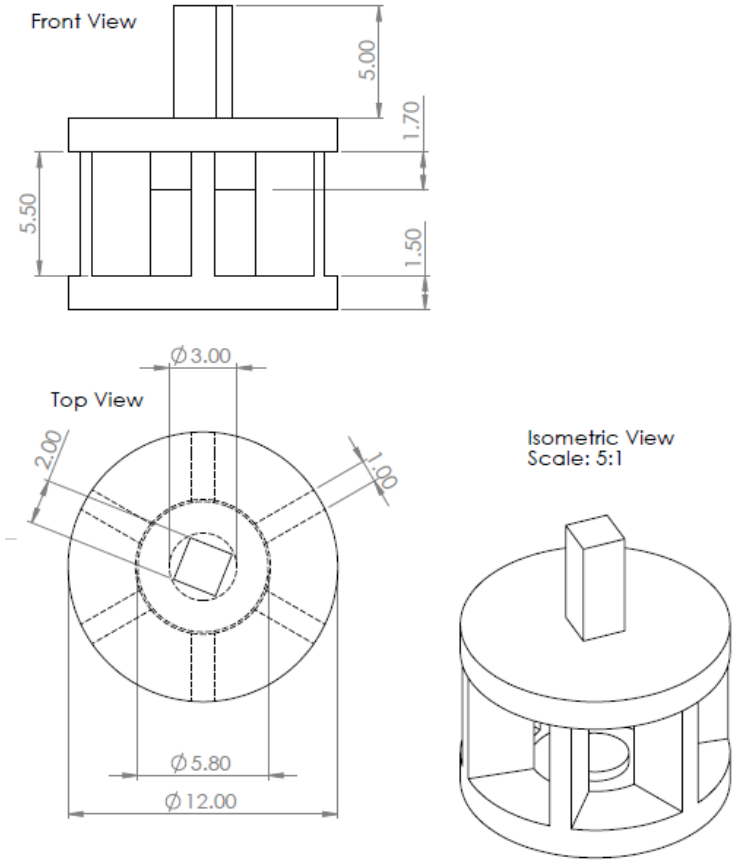

Figure A 2: Disc explant cage – technical drawing of cage design

Appendix 3

Fabrication of antacid microcapsules

Preparations in advance

- Prepare a 1% alginate solution
- Sterilize the small blade of the IKA homogenizer using the autoclave
- Sterilize ultrasonication probe by
    - Soaking in virkon (10min)
    - Soaking in 70% IMS (10min)
    - UV (20min)
- autoclave needles for electrosprayer
- autoclave metal collector dish for EHDS
- sterilize tubing for EHDS using the EtO sterilizer

Preparation procedure

Work sterile in hood

1. Weigh antacid powder for desired concentration (between 50 mg/mL to 500 mg/mL)
    a. Use a sterile 5 mL tube or 30 mL tube
2. Add appropriate amount of 1% alginate
3. Use the sterile small blade of homogenizer
    a. On ice: 2x 1 min with 30 sec break in between
4. Ultrasonication
    a. on ice: 3x 1min with 30 sec breaks between cycles
5. Keep solution at 37^{o}C until use
6. Other, store at 4^{o}C
   (if re-used: ultrasonicate once again before spray)

Spraying procedure

- Use sterilized electrosprayer
  Settings:

- Needle (ideally 19G or smaller)
- Flow Rate: 50 uL/min
- Voltage: 7-10 kV
  Into 100 mM $CaCl_2$